

Cranfield University
College of Aeronautics

Ph.D Thesis

Academic Year 1995/1996

S. M. Al-Ahmed

Integrating Combat Effectiveness Disciplines
into the Aircraft Conceptual/Preliminary Design
Phase

Supervisor

Professor John P. Fielding

Abstract

An assessment methodology has been developed for use during the conceptual/preliminary design phase to quantify the effectiveness of newly designed aircraft. The effectiveness is measured by a squadron Sortie Generation Rate (SGR). Key elements of this methodology were the establishment of link parameters between design synthesis and the main effectiveness disciplines. These were Reliability and Maintainability (R&M), Survivability / Vulnerability and Acquisition Cost. A programmable solid modeller was used to create a solid CAD assembly of the aircraft critical components. A ray tracing technique has been used to develop an interactive vulnerability assessment tool. A Mission Simulation Model (MSM) has been developed which typically simulates the operation of a squadron of aircraft and gives the operational activities such as flying sorties and maintenance actions. The methodology has been validated based on real data from recent conflicts. The application aspects of the methodology have been demonstrated by quantifying the effectiveness of two recent combat aircraft.

Table of Contents

ABSTRACT..... i

ACKNOWLEDGEMENT..... ii

DEDICATION..... iii

LIST OF FIGURES.....iv

NOTATION.....vii

ABBREVIATION..... xiii

CHAPTER ONE: INTRODUCTION1

1.1 GENERAL.....1

1.2 EFFECTIVENESS OF A COMBAT AIRCRAFT.....1

1.3 RESEARCH OBJECTIVES AND THESIS OUTLINE4

1.4 BACKGROUND.....6

CHAPTER TWO.....10

2.1 SYNTHESIS INTRODUCTION10

2.2 INITIAL CONCEPTUAL DESIGN AND SIZING10

2.2.1 CONFIGURATION LAYOUT10

2.2.2 THRUST AND WEIGHT RATIOS11

2.2.3 TAKEOFF WEIGHT BUILD-UP16

2.2.4 EMPTY WEIGHT ESTIMATION17

2.2.5 FUEL FRACTION ESTIMATION17

2.2.6 TAKEOFF WEIGHT CALCULATIONS.....17

2.3 BASIC ITEMS SIZING.....18

2.3.1 RADOME.....19

2.3.2 COCKPIT.....19

2.3.3 UNDERCARRIAGE.....19

2.3.4 ENGINE19

2.3.5 INTAKE DUCTS19

2.4 GEOMETRY-BASED ITEMS.....20

2.4.1 FUSELAGE DESIGN20

2.4.2 WING DESIGN.....20

2.4.3 EMPENNAGE DESIGN.....20

2.5 ACQUISITION COST ESTIMATION.....21

2.6 CASE STUDY21

2.6.1 DESIGN REQUIREMENTS FOR THE F-1622

2.6.2 DESIGN INPUT DATA22

2.6.3 TEST CASE RESULTS23

CHAPTER THREE: RELIABILITY AND MAINTAINABILITY ESTIMATION.....25

3.1 INTRODUCTION TO R&M25

3.2 DATA COLLECTION AND COMPILATION25

3.2.1 R&M DATA COLLECTION EFFORT.....25

3.2.2 DATA COMPILATION26

3.3 THE APPROACH USED IN DATA ANALYSIS; PARETO PRINCIPLE27

3.3.1 PARETO PRINCIPLE.....28

3.3.2 RELIABILITY DATA TRENDS28

3.3.3 PARETO’S CURVE PARAMETERS.....29

3.4 AIRCRAFT MAINTAINABILITY ESTIMATION.....31

CHAPTER FOUR: INTERACTIVE SURVIVABILITY/VULNERABILITY ASSESSMENT41

4.1 INTRODUCTION TO AIRCRAFT SURVIVABILITY41

4.2 AIRCRAFT VULNERABILITY.....42

**4.3 IDENTIFICATION OF THE CRITICAL COMPONENTS AND THEIR DAMAGE-
CAUSED FAILURE MODES42**

4.3.1 AIRCRAFT KILL LEVELS42

4.3.2 CRITICAL COMPONENT ANALYSIS.....43

4.3.3 AIRCRAFT DAMAGE-CAUSED KILL MODES.....44

4.4 VULNERABILITY ASSESSMENT.....44

4.4.1 VULNERABILITY MEASURES45

4.4.2 NONREDUNDANT COMPONENTS WITHOUT OVERLAP46

4.4.3 NONREDUNDANT COMPONENTS WITH OVERLAP47

4.4.4 SOME REDUNDANT COMPONENTS WITHOUT OVERLAP48

4.4.5 REDUNDANT COMPONENTS WITH OVERLAP49

4.4.6 MULTIPLE HIT VULNERABILITY50

4.4.7 KILL TREE DIAGRAM51

4.5 VULNERABILITY RESULTS PRESENTATION52

4.6 THE INTERACTIVE VULNERABILITY ASSESSMENT.....54

4.7 SOLID MODELLING.....54

4.7.1 THE EVOLUTION OF SOLID MODELLING54

4.7.2 SOLID MODELLING TECHNIQUES57

4.8 PARASOLID SOLID MODELLER62

4.8.1 ABOUT PARASOLID63

4.8.2 INTERFACES TO PARASOLID63

4.8.3 PARASOLID PROGRAMMING CONCEPTS64

4.8.4 BUILDING ASSEMBLIES.....66

4.9 MODEL BUILDING66

4.9.1 ASSEMBLY REFERENCE POINT AND REFERENCE VECTOR67

4.9.2 MODEL-BUILDING METHODOLOGY67

4.10 AIRCRAFT’S COMPONENTS MODELLING68

4.10.1 AIRCRAFT RADOME.....70

4.10.2 COCKPIT.....70

4.10.3 FUSELAGE	70
4.10.4 WINGS	70
4.10.5 EMPENNAGE.....	71
4.10.6 ENGINES.....	71
4.10.7 INTAKE DUCTS.....	71
4.11 SHOTLINES ASSESSMENT TECHNIQUE	71
4.11.1 SHOTLINE ASSESSMENT	72
4.11.2 RAY TRACING.....	72
4.11.3 COMPONENT'S NAME DEFINITION	74
4.11.4 COMPONENT'S PROBABILITY OF KILL	74
4.11.5 INTERNAL KILL TREE ANALYSIS	75
4.12 VULNERABLE AREA ASSESSMENT.....	75
CHAPTER FIVE: THE MISSION SIMULATION MODEL.....	77
5.1 INTRODUCTION	77
5.2 SIMULATIONS, TECHNIQUES AND LANGUAGES	77
5.3 THE MSM	78
5.3.1 PURPOSE OF THE MODEL	78
5.3.2 THE SCENARIO TO SIMULATE	79
5.3.3 AIRCRAFT STATES	79
5.4 EVENTS SEQUENCE.....	81
5.5 MSM OUTPUT.....	85
5.6 MSM LIMITATIONS	85
CHAPTER SIX: METHODOLOGY APPLICATIONS AND VALIDATIONS	91
6.1 APPLICATION INTRODUCTION.....	91
6.2 MODULE'S DATA FLOW.....	91
6.3 DESERT STORM OPERATION.....	92
6.3.1 F-15E OPERATION.....	92
6.3.2 F-16 OPERATION	95
6.4 USE OF THE METHODOLOGY TO INVESTIGATE AIRCRAFT CHARACTERISTICS AND THEIR EFFECTIVENESS	96
6.4.1 NUMBER OF ENGINES	96
6.4.2 PAYLOAD AND RANGE.....	99
6.4.3 THREAT DIRECTION	100
6.5 USE OF THE METHODOLOGY FOR AIRCRAFT EVALUATION.....	101
CHAPTER SEVEN: DISCUSSION	107
7.1 INTRODUCTION	107
7.2 RESEARCH DEVELOPMENT AND EVOLUTION	107
7.3 THE DESIGN SYNTHESIS.....	108

7.4 ESTIMATION OF R&M109

7.5 THE MSM110

7.6 SOLID MODELLING VULNERABILITY ASSESSMENT.....110

7.7 EFFECTIVENESS STUDIES.....112

CHAPTER EIGHT: CONCLUSIONS AND RECOMMENDATIONS114

8.1 CONCLUSIONS114

8.2 RECOMMENDATIONS115

REFERENCES116

APPENDIX A121

A.1 INTRODUCTION.....121

A.2 INITIAL SIZING AND CONCEPTUAL DESIGN.....121

A.2.1 TAKEOFF-WEIGHT BUILD-UP121

A.2.2 MISSION SEGMENT WEIGHT FRACTION122

A.3 SIZING OF BASIC ITEMS.....124

A.3.1 RADOME.....124

A.3.2 COCKPIT.....125

A.4. GEOMETRY SIZING OF THE MAIN COMPONENTS.....126

A.4.1 ENGINE SIZING126

A.4.2 LANDING GEAR SIZING.....127

A.4.3 FUSELAGE SIZING.....127

A.4.4 WING130

A.4.5 EMPENNAGE134

 A.4.5.1 Vertical Stabiliser.....134

 A.4.5.2 Horizontal Stabiliser.....136

A.5 AIRCRAFT ACQUISITION UNIT COST137

A.5.1 DEFINITIONS.....137

A.6 TEST CASE RESULTS.....147

APPENDIX B.....159

B.1 INTRODUCTION.....159

B.2 FAILURE RATE DATA AND ANALYSIS159

B.3 METHOD OF CALCULATING FAILURE RATE.159

B.3 MAINTAINABILITY DATA AND ANALYSIS.....166

APPENDIX C170

C.1 INTRODUCTION.....170

C.2 INTERACTIVE SOLID MODELLING170

C.2.1 RADOME PART170

C.2.2 CREW172

C.2.3 WING174

C.2.4 FUSELAGE.....180

C.2.5 LANDING GEAR.....183

C.2.6 ENGINE.....184

C.2.7 AIRCRAFT SYSTEMS185

C.3 STANDARD VULNERABILITY ASSESSMENT TECHNIQUES187

C.3.2 VULNERABLE AREA ROUTINE187

C.3.3 SHOTLINE ASSESSMENT.....193

APPENDIX D195

D.1 INTRODUCTION.....195

D.2 VARIABLES LIST195

D.3 SUBROUTINES.....196

D.4 PROGRAM INPUTS AND OUTPUTS198

D.5 SOURCE CODE200

Acknowledgement

This project would not have been possible without the help of many people. I would like to express my sincere thanks to all of them including:

My supervisor ***Professor John Fielding*** for his supervision of the project and for providing me with the much needed guidance.

His Highness General Mohammed Bin Abdullah Al-Saud, former King Faisal Air Academy Commandant, and all the KFAA staff for their support of my study.

General Abdulaziz Al-Henaidi, Commander RSAF Logistic and Supply, for his personal support of the data gathering visit to MDA at St. Louis.

Mr. Edgar Jackson of the RSAF HQ R&D for his invaluable assistance in liaising with the companies who provided the required data.

Mr. Earl Godby and Richard Darcy of New Business Group of MDA St Louis, ***Mr. Jerry Null and George Compton*** of the MDA Customer Survive and ***Mr. Loren Timm and Dave Wright*** of Lockheed Fort Worth for their cooperation in providing the required material.

Mr. Mark Bass, Peace Sun program manger at St Louis and ***Mr. Carl Count***, of MDA Riyadh Office, for their nice hospitality during my visit to MDA St Louis.

Professor Robert Ball of the Naval Postgraduate School for his invitation to Monterey and his invaluable advice and suggestions.

Mr. Paul Alonze of British Aerospace Warton, for his technical advise.

Mr. Frank Siegers for his technical assistance and proof reading the manuscript.

My friends ***Abdulrazak Al-Mahmoud*** for the time we spent in the past three years in Cranfield and ***Mohammed Al-Anezi*** for his moral support. And Finally for His wonderful children ***Talaal, Atlaal, Muhanad and Manaaf***.

Dedication

To My Mother

List of Figures

Fig. 1.1	Typical mission scenario
Fig. 1.2	Combat aircraft effectiveness disciplines
Fig. 1.3	Effectiveness disciplines integration.
Fig. 2.1	Some layouts of a combat aircraft.
Fig. 2.2	Maximum lift coefficient.
Fig. 2.3	Takeoff parameter.
Fig. 2.4	Initial sizing design process.
Fig. 2.5	Elements of aircraft life cycle cost.
Fig. 2.6	Test case mission profile.
Fig. 2.7	Test case results.
Fig. 2.8	Acquisition unit cost of the Gripen JAS-39
Fig. 3.1	Reliability data trend for aircraft F
Fig. 3.2	Reliability data trend for aircraft H
Fig. 3.3	Reliability data trend for aircraft E
Fig. 3.4	Reliability data trend for aircraft T
Fig. 3.5	Pareto distribution of old and new aircraft.
Fig. 3.6	Sample of Pareto Analysis.
Fig. 3.7	Pareto chart and equation of aircraft (F)
Fig. 3.8	Pareto chart and equation of aircraft (H)
Fig. 3.9	Pareto chart and equation of aircraft (E)
Fig. 3.10	Pareto chart and equation of aircraft (T)
Fig. 3.11	Pareto chart and equation of aircraft (P)
Fig. 3.12	Parameters that defines Pareto distribution curve.
Fig. 3.13	Number of systems
Fig. 3.14	Actual and estimated values of FR(1)
Fig. 3.15	Actual and estimated values of FR(8)
Fig. 4.1	Nonredundant components without overlap
Fig. 4.2	Nonredundant components with overlap

Fig. 4.3	Some redundant components without overlap
Fig. 4.4	Redundant components with overlap
Fig. 4.5	Critical components tree.
Fig. 4.6	The six aircraft aspects
Fig. 4.7	The 26 aircraft aspects
Fig. 4.8	Wireframe ambiguity
Fig. 4.9	A wireframe aircraft model
Fig. 4.10	Surface model topological relationships.
Fig. 4.11	Surface model of an aircraft.
Fig. 4.12	Geometrical definition of an ellipsoid
Fig. 4.13	Geometrical definition of a cone
Fig. 4.14	Geometrical definition of a torus.
Fig. 4.15	Geometrical definition of a box.
Fig. 4.16	Boolean operations on solid bodies
Fig. 4.17	Swinging and sweeping.
Fig. 4.18	Lofting of curve segments
Fig. 4.18	Lofting of curve segments
Fig. 4.20	General assembly structure
Fig. 4.21	Modelling reference point and reference vector
Fig. 4.22	Vulnerability assessment methodology
Fig. 4.23	Shotline grid over an aircraft model
Fig. 4.24	Ray tracing concept.
Fig. 4.25	Shotline assessment modules.
Fig. 4.26	Vulnerable area computation
Fig. 5.1	Aircraft State and Logic Flags.
Fig. 5.2	Time clocks for each aircraft.
Fig. 5.3	MSM Event Sequence.
Fig. 5.4	MSM Program Flow Chart.
Fig. 6.1	Main modules and files
Fig. 6.2	F-15E's SGR

Fig. 6.3	F15E Mission Capable Rate
Fig. 6.4	Mission capable rates at Desert Storm.
Fig. 6.5	F15E's sorties per aircraft.
Fig. 6.6	F-16 Mission Capable Rate
Fig. 6.7	Sorties flown per aircraft
Fig. 6.8	SGR of the F16
Fig. 6.9	Aircraft Pk at different hits
Fig. 6.10	SGR of a single and twin-engine aircraft
Fig. 6.11	SGR of single and twin-engine aircraft
Fig. 6.12	Aircraft size effect on its Pk
Fig. 6.13	Pk from different directions
Fig. 6.14	Target and threat interaction
Fig. 6.15	The F-15E .
Fig. 6.16	The F-22
Fig. 6.17.	Top view of the F-15 from the solid modeller.
Fig. 6.18	Pk due to 50 random shots in the 20m rectangle
Fig. 6.19	Pk of the two aircraft.
Fig. 6.20	Effect of R&M
Fig. 6.21	Effect of RCS.

Notation

The following notations are those used in CONCEPT program as follows:

- C means it is computed followed by its units within practise and D means it has no unit (Dimensionless),
- I means it is an input value, followed by the value - if it is an empirical constant- or DES if a design requirement.

A. Initial Sizing

Symbol	Description	Type (units)
σ	Density ratio	I, DES, (D)
ψ°	Turn rate	C (rad/sec)
(L/D)	Lift-to-drag ratio	C (D)
$(T/W)_{to}$	Takeoff thrust ratio	C (D)
$(W/S)_{cruise}$	Cruise wing loading	C (lb/ft ²)
$(W/S)_{stall}$	Stall wing loading	C (lb/ft ²)
$(W/S)_{to}$	Takeoff wing loading	C (lb/ft ²)
A	Aspect ratio	C (D)
C	Specific fuel consumption	I, DES, (1/sec)
C_{D0}	Zero-lift drag coefficient	C (D)
$C_{L\max}$	Maximum lift coefficient	C (D)
$C_{L\ to}$	Takeoff lift coefficient	C (D)
d	Combat time	I, DES, (sec)
e	Oswald efficiency factor	C (D)
E	Loiter time	I, DES, (sec)
M_{\max}	Maximum Mach number	I, DES,(D)
n	Load factor	I, DES, (D)
q_{stall}	Dynamic pressure at stall	I, DES, (lb/ft ³)
R	Segment range	I,DES, (ft)
S	Wing surface area	C (ft ²)
S_a	Obstacle clearance distance	I, DES, (ft)
$S_{landing}$	Landing ground roll	I, DES, (ft)
TOP	Takeoff parameter	C (lb/ft ²)
V	Aircraft velocity	I, DES, (ft/sec)
W_0	Takeoff weight	C (lb)

W_c	Crew weight	I, DES, (lb)
W_e	Empty weight	C (lb)
W_f	Fuel weight	C (lb)
W_w	Weight in wheel	C,(lb)
W_p	Payload weight	I,DES, (lb)
W_x	Aircraft weight at end of mission	C,(lb)

B. Geometry Based Synthesis

AEFN	wing 1/4 chord-point	I,1.75,(D)
AETN	tailplane aspect ratio	I,3.5,(D)
AW	Gross-wing aspect ratio	C,(m)
AWN	Nett-wing aspect ratio	C,(D)
BETN	Tailplane nett-span	C,(m)
BFA	Width of fuselage cross-section at station A	C,(m ²)
BFE	Width fuselage at section E	C,(m)
BFF	Width of fuselage at station F	C,(m)
BIDD	Intake width at section D	C,(m)
BUMW	Main landing gear width	C,(m)
BW	Gross-wing span	C,(m)
BWBB	Span of centre-section of wing box	C(m)
BWN	Nett-wing span	C(m)
BWNF	Span of fuel tank in wing-box external to the fuselage	C,(m)
CEFB	Fin chord at body side	C,(m)
CEFM	Fin mean aerodynamic chord	C,(m)
CETB	Tailplane chord at body side	C,(m)
CWBB	Wing-box chord at body sides	C,(m)
CWCB	Nett-wing root chord	C,(m)
CWCC	Centre-line chord of the gross-wing	C,(m)
CWCT	Wing-tip chord	C(m)
CWMA	Wing mean aerodynamic chord	C,(m)
CWMA	wing aerodynamic mean chord	C(m)
CWMG	Geometric mean-chord of the wing	C(m)

CWMN	Mean chord of the nett-wing	C,(m)
DAR	Radar scanner diameter	I,0.6,(m)
DP1	Diameter of engine section 1	C,(m)
DP3	Diameter of engine section 3	C,(m)
DUMW	Main landing gear wheel diameter	C, (m)
EBP1	Engine bay width clearance at section 1	C,(m)
EBP3	Engine bay width clearance at section 3	C,(m)
EDAR	Clearance between radar scanner and structure	I,0.06,(m)
EHCS	Distance between the seat back and the rear bulkhead	I,0.3,(m)
EHP1	Engine bay height clearance at section 1	C,(m)
EHP3	Engine bay height clearance at section 3	C,(m)
ELUP	Distance from landing-gear pintle point and rear of gear bay	I,0.25,(m)
FBUMW	Factor to allow for main gear width clearance	I,1.5,(D)
FBWNF	Fractional span of the nett-wing box containing fuel tank	I,1.0,(D)
FCWD	Front-spar position as a fraction of local wing chord	I,0.15,(m)
FCWR	Rear-spar position as a fraction of local wing chord	I,0.6,(m)
FDUMW	Factor to allow main landing gear clearance	I,1.1,(D)
FOFDK	Area factor for fuselage section D	I,0.85,(D)
GOFI	Area gradient of radome section	I,0.3442,(m)
HC1	Distance between thigh point and eye point in standard cockpit	I,0.745,(m)
HC2	Distance between thigh point and heel point in standard cockpit	I,0.694,(m)
HC3	Distance between thigh point and seat back in standard cockpit	I,0.33,(m)
HC5	Front bulkhead height above floor	C,(m)
HCEYE	Height of the pilot's eye point above the cockpit floor	C,(m)
HCSEAT	Pilot's seating point height above floor measured along seat back	I,0.222,(m)
HFA	Height of fuselage cross-section at station A	C,(m ²)
HFA1	Underfloor depth at fuselage section A	C,(m)
HFB	Height of fuselage cross-section at station B	C,(m)
HFB1	Underfloor depth at fuselage section B	C,(m)
HFD	Height of fuselage at section D	C,(m)
HFDS	Minimum height of fuselage height at section D	C,(m)
HFE	Height of fuselage at section E	C,(m)
HFF	Height of fuselage at station F	C,(m)
HIDD	Intake height at section D	C,(m)
LAR	Length of radar avionics bay	I,0.6,(m)

LAX1	Length of forward electronics bay	I,1.2,(m)
LCEYE	Horizontal distance between cockpit front bulkhead and the eye point	C,(m)
LCFL	Length of cockpit floor	C,(m)
LCFOOT	Horizontal distance between cockpit front bulkhead and heel point	I,0.127,(m)
LCFTE	Distance from nett-wing mean 1/4 point to fin trailing-edge	C,(m)
LCTTE	Distance of mean 1/4 chord point of tailplane from its trailing-edge	C,(m)
LEFCQM	Fin moment arm measured from wing mean 1/4 chord point	C,(m)
LETCQM	tailplane moment arm measured from wing mean 1/4 chord point	C,(m)
LIDG	Intake diffuser length	C,(m)
NFIN	Number of fins (1 or 2)	I,(1 or 2)
OFA	Fuselage cross-section area of section A	I,(m ²)
OFDS	Minimum cross-section area at section D	C,(m ²)
OFI	Fuselage cross-section area at radar station.	C (m ²)
OIDD	Duct area at fuselage cross-section D	C, (m)
OIE	Duct cross-section area at section E	C,(m)
OII	Intake cross-section area	C,(m)
OWBB	Cross-sectional area of the centre-section of the wing-box	C,(m)
QCEYE	Pilot's forward and downward viewing angle	I,17.0,(deg)
QCFOOT	Angle between the line joining the thigh-heel points and horizontal	C (deg)
QCSEAT	Angle of back of ejection seat	I,25.0,(deg)
QEF	Fin cant angle	I,(deg)
QEFL	Fin leading-edge sweep	I,45.0,(deg)
QETL	Tailplane leading-edge sweep	I,40.0,(deg)
QW2	Wing mid-chord sweep	C(deg)
QW4	Wing 1/4 chord sweep	C(deg)
QWL	Wing leading-edge sweep	C(deg)
RADFA	Radius of fuselage corner for section A	C,(m)
RAHB	Ratio of length of sides of fuselage section A	I,(1.0162),(D)
RAR	Fuselage cross-section radius at radar station	C (m)
RCCAN	Canopy radius at fuselage station B	I,0.4,(m)
REFFC	Fin volume ratio	I,2.0,(D)
RETSW	Tailplane volume ratio	I,0.3,(D)
RFSA	Ratio of fuselage corner radius to fuselage width of section A	I,0.48,(D)
RLUPCW	Landing-gear pintle position from wing mean aerodynamic chord	I,(0.1,(m)
ROFDN	Scaling factor section D	C,(D)

RXFLEN	Ratio of XFLEN to fuselage length	I,0-0.8,(D)
RXWCQM	Distance of wing 1/4 chord-point point aft of nose / XFN	I,0.6,(D)
SEFN	Fin area	C,(m)
SEFNV	Projection of the fin planform area into the vertical plane	C,(m²)
SETN	Tailplane area	C,(m²)
SW	Gross-wing area	C,(m²)
SWN	Nett-wing area	C(m²)
UEFN	Fin taper ratio	I,0.3,(D)
UETN	Tailplane taper ratio	I,0.3,(D)
UW	Taper ratio of the gross wing	C(D)
UWBCF	Factor for utilisation of centre-section of wing-box for fuel storage	I,0.9,(D)
UWCN	Nett-wing taper ratio	C,(D)
UWCNF	Taper-ratio of wing fuel tank	C,(D)
VWBB	Volume of centre-section of the wing-box	C,(m³)
VWBCF	Fuel volume at centre-section of the wing-box	C,(m³)
VWBEF	Volume available at wing-box for fuel tanakage	C,(m³)
VWF	Total fuel volume in wing structure	C,(m³)
XA	Distance from aircraft nose to front bulkhead	C (m)
XD	Distance from aircraft nose to station D	C,(m)
XFLEN	Distance from fin trailing-edge and engine exit plane	C,(m)
XFR	Radome length	C (m)
XII	Distance of intake inlet from aircraft nose	I,(m)
XUMB	Distance of main-gear bay from aircraft nose	C,(m)
XWCQM	Distance of wing 1/4 chord-point from aircraft nose	C,(m)

C. Aircraft Cost

Symbol	Description
A	AMPR (airframe unit weight) in pounds.
A_{TF}	Judgement factor for advanced technology features.
A_{TT}	Advanced technology testing judgement factor (1.0 to 2.0)
C_{ABE}	Cost of after-burning engines.
C_{AED}	Development engineering cost.
C_{AEP}	Production engineering cost.
C_{AMC}	Advanced materials cost factor.
C_{AV}	Avionics cost.
C_{DDTE}	Development Cost.
C_{DSC}	Development support cost.
C_E	Engine cost.
C_{FTAR}	Cost of flight test operations.
C_{LO}	Low observable materials judgement factor (1.0 to 1.3)
C_{MD}	Development manufacturing labour cost.
C_{MMD}	Development manufacturing materials cost.
C_{MMP}	Production manufacturing materials cost.
C_{MP}	Production manufacturing labour cost.
C_{PI}	Cost escalation factor (ratio of the consumer price index for
C_{PROD}	Total Production cost.
C_{QD}	Development quality control cost.
C_{QP}	Production quality control cost.
C_S	Judgement cost factor for program security requirements.
C_{TD}	Development tooling cost.
C_{TP}	Production tooling cost.
C_{UA}	Acquisition unit cost.
E_{RATE}	Engineering hourly rate.
N_E	Number of engines per aircraft.
Q	Quantity of aircraft to be produced (subscript D for development
Q_D	Quantity of development aircraft.
Q_P	Quantity of production aircraft.
R	Production rate (aircraft per month).
S	Maximum speed (knots at best altitude)
T_{HD}	Tooling hours for development.

T_{HP}	Tooling hours for production.
T_{SL}	Sea level maximum thrust (lb)
W_{AV}	Avionics weight (lb)
WE_{AT}	Weight empty of advanced fighter attack aircraft.
WE_{CFA}	Weight empty of conventional fighter/attack aircraft.

D. Survivability

P_d	Probability of detection
P_s	Probability of survival
P_H	Probability of hit
$P_{K/H}$	Probability of kill given a hit on the aircraft.
A_P	Presented area of the aircraft
A_V	Vulnerable area of the aircraft
A_{pi}	Presented area of the i th component.
A_{vi}	Vulnerable area of the i th component.
$P_{k/hi}$	Probability of killing the i th component given a hit on it.
$P_{k/Hi}$	Probability of killing the i th component given a hit on the aircraft.
$P_{h/Hi}$	Probability of hitting the i th component given a hit on the aircraft.

Abbreviation

ACSYNT	AirCRAFT SYNThesis.
AFOTEC	Air Force Operational Test and Evaluation Centre (US)
ASTOVL	Advanced Short Takeoff and Vertical Landing.
CAD	Computer Aided Design
CSG	Constructive Solid Geometry
DES	Discrete Event Simulation
DRA	Defence Research Agency (UK)
FMEA	Failure Mode and Effect Analysis
FTA	Fault Tree Analysis
GO	Graphical Output
KI	Kernel Interface
KTA	Kill Tree Analysis
MCR	Mission Capable Rate
MH/FH	Maintenance Man-Hour per Flight Hour.
MTOM	Mission Trade-Off Model
MTTR	Mean Time To Repair
MVO	Multi-Variate Optimiser.
Pk	Probability of Kill
R&M	Reliability and Maintainability.
RAE	Royal Aircraft Establishment (UK)
RAF	Royal Air Force
RCS	Radar Cross Section
RSAF	Royal Saudi Air Force
SGR	Sortie Generation Rate.
SM	Solid Modelling
WUC	Work Unit Code

Chapter One

Introduction

1.1 General

A new aircraft progresses through three main phases of design before the start of production . In the first phase, conceptual design, the basic questions of configuration arrangement, size and weight, and performance are answered. The feasibility of the design to accomplish a given mission is established. The second phase, preliminary design, begins when the major changes are over. During this phase specialists in areas such as structures, landing gear, and control systems will design and analyse their portion of the aircraft. Finally, detail design contributes to the tasks necessary for production, such as production design and tooling/fabrication process set-up. It is during the conceptual phase that decisions are made to evaluate innovative integration schemes and feasible technologies that can lead to an effective aircraft design, which meets the requirements. In current fighter aircraft projects, mission effectiveness analysis has been a key factor in developing the most important design parameters. Although traditional trade-offs between design parameters such as lift, drag, propulsion and weight are still important, the design process has been expanded to include new disciplines that are more related to the operational environment of the aircraft. Recent conflicts have demonstrated that combat aircraft are the key to victory and places fighter aircraft at the top of a weapon system arsenal.

1.2 Effectiveness of a Combat Aircraft

Combat aircraft effectiveness is a wide term and can be quantified in many ways depending on the aircraft/mission type. The effectiveness of a combat aircraft reflects the degree of success when conducting an assigned mission. This effectiveness is influenced by many factors, of which some are related to the aircraft itself, some are related to its armament package, some are related to the encountered threat and some to the operational environment. For a typical combat aircraft mission-scenario, as shown in Fig.

1.1, an aircraft takes-off and flies as fast as possible to the target area, locates the assigned target, delivers its weapons on the target, and returns to its base.

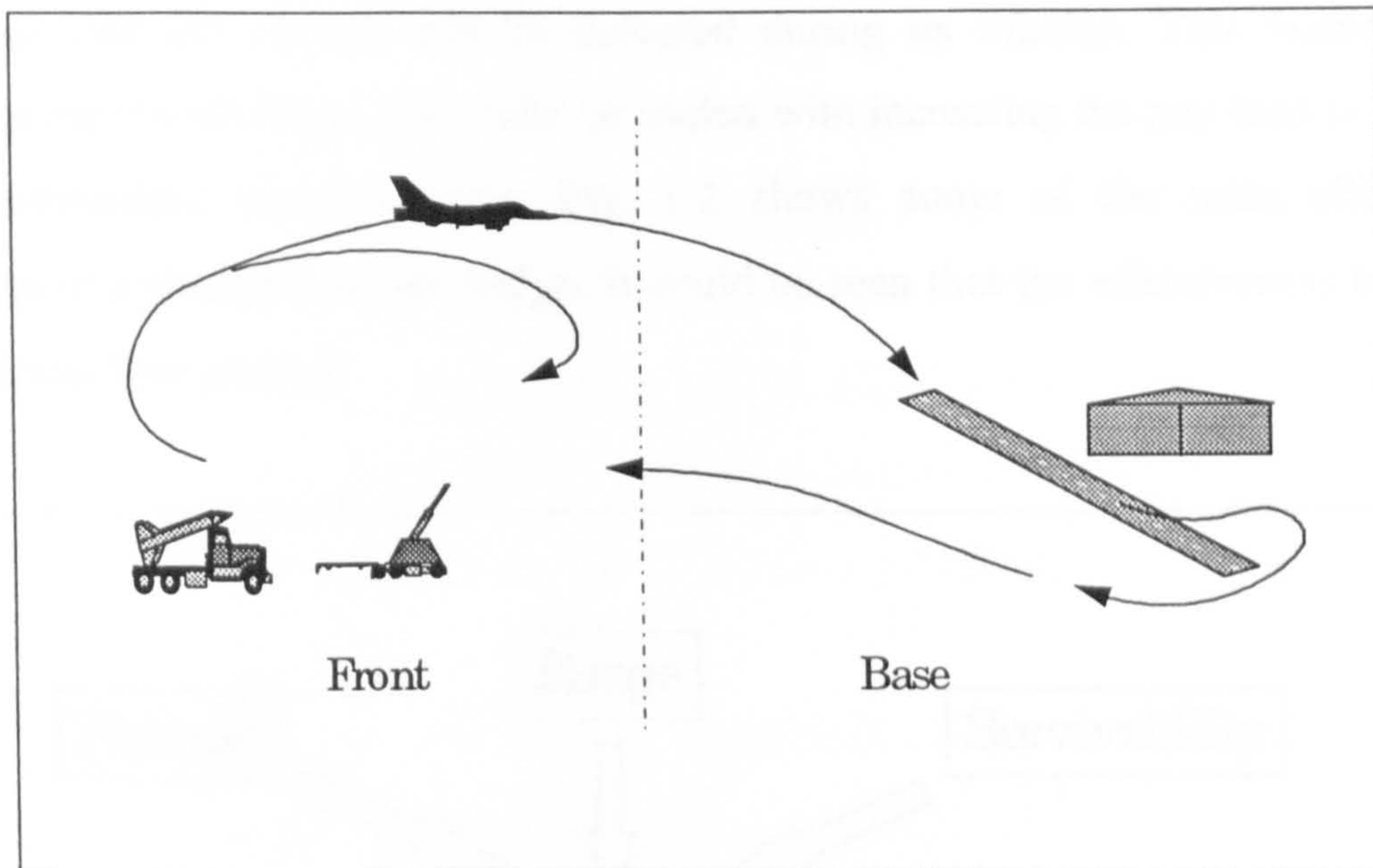


Fig. 1.1: Typical mission scenario

An analysis of this scenario reveals that the degree of success of this mission depends on:

1. The aircraft availability to conduct the mission.
2. The performance characteristics of the aircraft.
3. Target location and identification capability.
3. Effectiveness of the aircraft weapon's package.
4. The aircraft survivability characteristics.

The availability of the aircraft affects its effectiveness because the more aircraft are available, the higher the probability that the target is killed. Availability is affected by the aircraft Reliability and Maintainability (R&M) and logistics factors such as maintenance personnel, damage battle repair and spare parts availability. The effectiveness of the mission is always affected by aircraft survivability. Aircraft with more survivability will return from a mission more often, and hence more aircraft will be available for subsequent missions. Aircraft payload affects the mission effectiveness because the more payload carried the more targets are likely to be killed. Also the higher the payload the fewer sorties will be required to kill a target and hence the less probability of losing an

aircraft. Aircraft performance capabilities affect effectiveness by allowing the aircraft to get in and out of the target area in a short time and allowing more effective tactical flying manoeuvres as well as affecting survivability. Aircraft radar signature influences the probability that the aircraft will be detected during its mission. This feature greatly influences the effectiveness and could be traded with increasing the pay-load in favour of some performance characteristics. Fig. 1.2 shows some of the main effectiveness disciplines of a combat aircraft design. It could be seen that the effectiveness factors are different and inter-related.

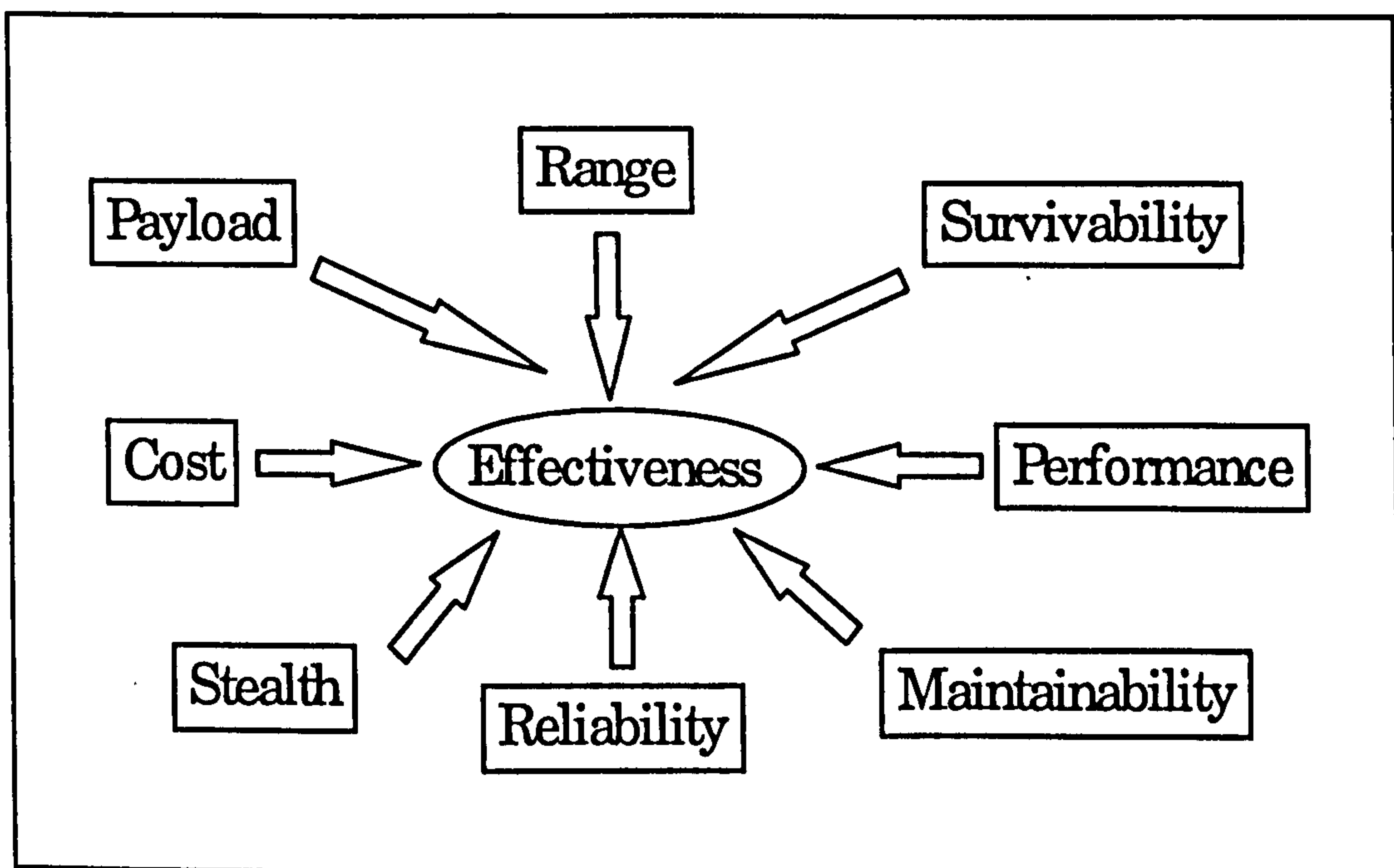


Fig. 1.2: Combat aircraft effectiveness disciplines

The following measures are the most widely used by Air Force analysts to evaluate the effectiveness of a fighter aircraft:

- Percent bombs in target area.
- Cost per target kill (Bangs per Buck).
- Payload per sortie.
- Payload-range.
- Kill ratio.
- Sorties per day or Sortie Generation Rate (SGR)

The SGR was selected in this study to be the measure of aircraft effectiveness. This was because the SGR reflects more of the design-related effectiveness disciplines than other definitions as follows:

- If the aircraft speed (performance) is high it will get to the target area and back home in a shorter time, which means a higher SGR.
- If the aircraft is reliable, it means that less failures are likely to occur, hence high availability and finally a higher SGR.
- If the aircraft has good maintainability design features, the shorter the failure repair time will be and hence there will be more availability and finally a higher SGR.
- If the aircraft is survivable there will be a lower probability of combat loss, hence a higher SGR.

The SGR is not the only, or even the best, measure of effectiveness but has been adopted for the progress of the thesis as a convenient comparator. The other effectiveness measures, such as percent bombs on target and cost per target kill rely more on classified data unavailable to the author.

1.3 Research Objectives and Thesis Outline

The objective of this thesis is to:

1. Establish a methodology which can be used in the conceptual/preliminary design phase to quantify the effectiveness of the newly designed aircraft in terms of its SGR.
2. Find a link by which the R&M could be integrated with the conceptual design phase.
3. Develop an interactive methodology to perform standard vulnerability assessment while in the conceptual/preliminary design phase.
4. Integrate the above design disciplines into a methodology that makes it possible to be driven by the conceptual / preliminary design process. It is to be modular, for ease of future enhancement or expansion by means of integrating future disciplines.
5. Test the methodology on existing aircraft for which relevant data are available.

6. Exercise the methodology to investigate its potential.

Fig. 1.3 gives an outline of the main elements required to produce the methodology.

The Thesis chapters are as follows:

Chapter Two illustrates a simple method to approach a design synthesis of a combat aircraft. The design synthesis is intended to reflect the impact of the main design requirements on the aircraft's size.

Chapter Three investigates an approach to estimate the R&M of a combat aircraft.

Chapter Four Discusses survivability and contains the fundamentals of combat aircraft vulnerability and the approach developed to quantify an aircraft vulnerability.

Chapter Five contains a Mission Simulation Model (MSM). The MSM simulates a squadron of aircraft in a wartime scenario. The model is used to link the effectiveness disciplines and to give a single measure of merit, which is the aircraft SGR.

Chapter Six illustrates the use of the methodology, and some validation tests.

Chapter Seven discusses the main research aspects.

Chapter Eight contains some concluding remarks, and suggestions for future work.

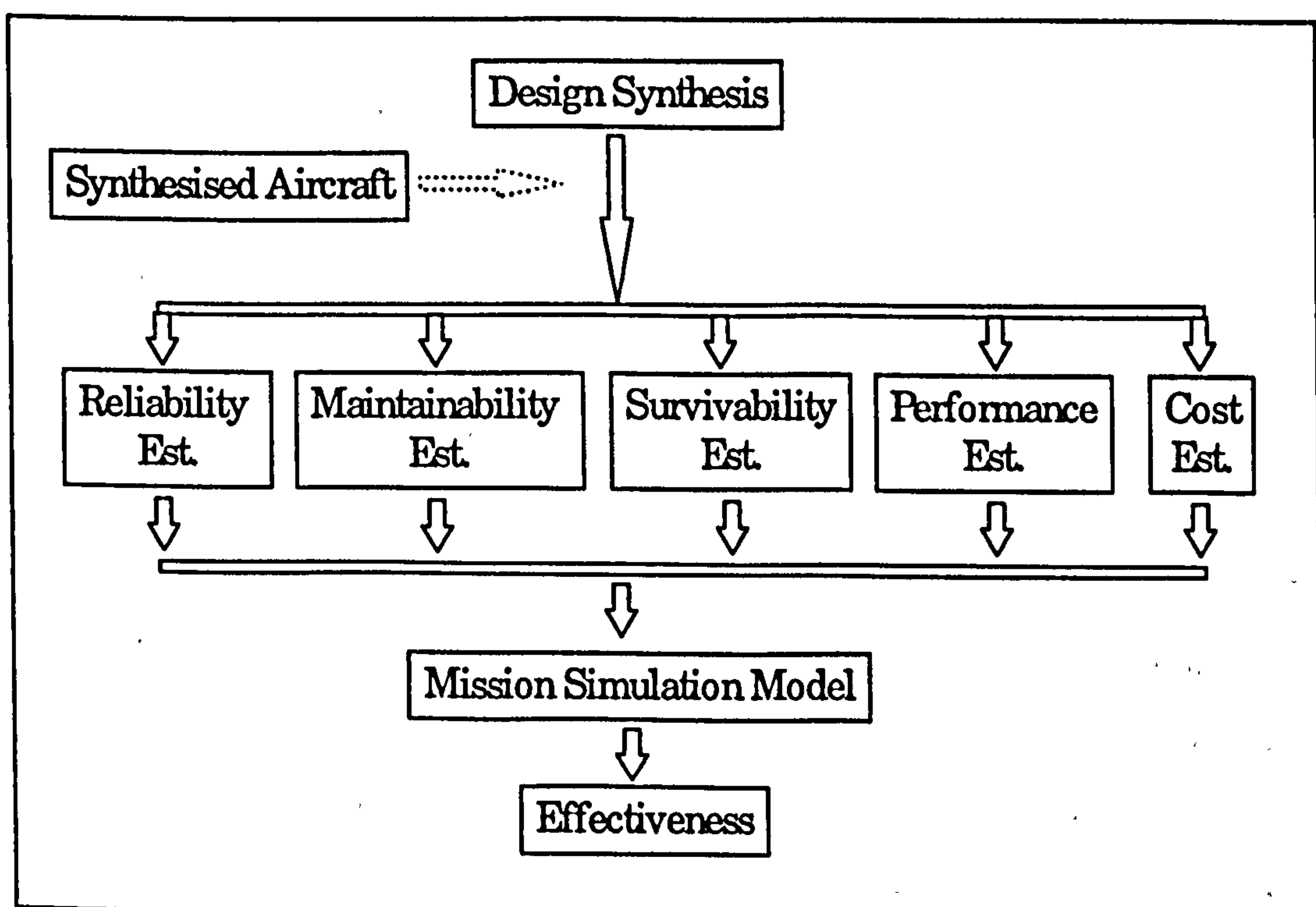


Fig. 1.3 Effectiveness disciplines integration

1.4 Background

Due to the nature of this research, it was expected at the early days of the research that few materials in this area could be found in the academic literature. The literature survey started by gathering and studying related research works through the university library and UK university libraries through the Inter-library-loan system. Searching through the international scientific databases such as NTIS and Compendex helped in locating international academic and industrial organisations conducting researches of similar type. The literature survey could be divided according to the effectiveness discipline research main subjects.

Combat Design Synthesis

For the past two decades, much effort has been expended on developing computerised design synthesis methods. Most of this being spent on design synthesis of transport aircraft. In 1971 the Royal Aeronautical Establishment (RAE) developed a design synthesis of a transport airliner which can be linked to a Multi Variate Optimiser (MVO). The design synthesis was for a conventional transport aircraft with rear-mounted engines. The Defence Research Agency (DRA), formerly RAE, developed this design synthesis for a combat aircraft with side intakes and conventional tail arrangement called SWEPT (Ref. 1). Cranfield University was the main contractor, through research grants, to modify the SWEPT-MVO design synthesis to include a canard-delta configuration (Ref. 2), Advanced Supersonic Takeoff and Vertical Landing (Ref. 3) and currently a design synthesis of future combat aircraft (Ref. 4). A design synthesis for a general combat aircraft is still a research challenge because of the different layouts, classes, and shapes of combat aircraft. Commercial computerised design synthesis became available alongside text books in aircraft design. The RDS system was developed from the design algorithms of (Ref. 5) to be an aircraft design teaching tool. The RDS is a PC-Based initial sizing and performance program, and has the capabilities of providing weight and cost analysis as well as simple graphical presentation of the design aircraft (Ref. 6). Another program, ACSYNT (Ref. 7) is probably the most sophisticated and complete computerised design synthesis available at the moment. ACSYNT (AirCraft SYNThesis) capabilities reflect the efforts of an institute formed by a group consisting of eight US

aerospace companies and several NASA and Navy agencies, together with NASA Ames Research centre. ACSYNT is a fully parametric 3D conceptual design tool for aircraft. NASA Ames Research Centre pioneered the development of ACSYNT over twenty-five years ago, with constrained parameter optimisation as a fundamental element of the program. Ames Research Centre has continuously improved ACSYNT during this period. Since 1986, NASA and Virginia Polytechnic Institute have worked together to develop a computer aided design version of ACSYNT which uses a graphical user interface and generates 3-D surface models. These efforts follow international graphics and programming standards, making the program machine and graphics device-independent. ACSYNT has been successfully used in many aircraft systems studies in government, industry, and academia and is recognised as especially valuable in the design of high-performance aircraft. It should be noted that ACSYNT is only available to the US government and industry members of the ACSYNT Institute.

Combat Aircraft Mission Simulation

Few studies have been published for combat aircraft operation simulation. Studies of this type are not widely published in the academic literature, because of the sensitivity of the data used in the simulation, and also on the simulation results and verification. In 1977 the American Joint Technical Co-ordination Group on Aircraft Survivability (JTTCG/AS) published a report titled Mission Trade-Off Model (MTOM). The MTOM is a simulation program that was specially developed to assess the impact of survivability enhancement features activities (Ref. 8). The MTOM does not go into the aircraft system level, instead expected-value calculations are made for the simulated aircraft. Burleigh, (Ref. 9), established a simple attrition simulation model of a defined number of aircraft. The model treats the aircraft as one system, failure rates and maintenance times are calculated using redefined probability functions. In this model, the related simultaneous events such as sorties and repairs are independent of the time of the day, instead a counter-index is used. The US Air Force Operational Test and Evaluation Centre (AFOTEC) conducted a series of simulation studies of combat aircraft. Most of these studies are classified. Captain Letitia of AFOTEC, (Ref. 10), presented results of the F-15E mission reliability

and availability through simulating the operational environment of a squadron of 24 aircraft.

R&M Estimation of a Combat Aircraft

R&M is usually believed to be out of the hands of the conceptual designers because it largely depends upon detail design of the aircraft components. R&M's growing importance as a dominant factor of the cost effectiveness of any aerospace vehicle, has led to a growing research effort undergoing to estimate the R&M figure at the early design stage. R&M contributes to more than 70% of the cost-related driving factors which are defined at the conceptual/preliminary design phase. The generally-accepted procedure to estimate a new aircraft R&M figures is to compare the new aircraft to a similar existing aircraft then allowing percentages for technology improvements. The use of historical data as a basis for estimating aircraft R&M is a widely accepted procedure in the aircraft industry. In the transport aircraft industry, aircraft R&M prediction was improved dramatically by the continuous feedback from aircraft operators and aircraft manufacturers, and the perceived effect of R&M on airlines' revenues and flight scheduling. The first study to establish a link between R&M and aircraft design was conducted by Harmon et al (Ref. 11). The approach was based on correlation analysis to develop a model which relates historical maintenance data to design/performance parameters. The maintainability model consists of statistical linear equations relating each aircraft system maintenance index, maintenance Man-Hour per Flight Hour (MH/FH), to a design parameter which is more related to that system. Serghides, (Ref. 12), used this method to develop reliability as well as maintainability equations to combat and transport aircraft.

Combat Aircraft Survivability

Combat aircraft survivability (susceptibility and vulnerability) is a newly-evolving design discipline that was for some time limited to Defence analysts. Recently, a text-book has been published which contains the fundamentals of combat aircraft survivability (Ref. 13). This book presents survivability as an important subject, and contains more useful

information than those found in the MIL-STD for combat aircraft survivability (Ref. 14). Radar Cross Section (RCS) is a major quantified factor for stealth design, and hence its susceptibility. Because of the classified nature of these researches as well as the difficulty of modelling or estimating the RCS of a design, almost no literature was found that could provide a reliable methodology to estimate the RCS of an aircraft design, although limited data are available from (Ref. 43). In the vulnerability side, a growing interest is developing in different areas to build and enhance methodologies that assess aircraft vulnerability. Unfortunately most of the results are not available in academia, and have been conducted by US government subcontractors. Reference (15) present an interactive, PC-Based, vulnerability assessment tool that has its own simple modelling capabilities and performs some of the standard vulnerability assessment requirements. Like ACSYNT this program is only available for the US industrial and academic organisations.

Discipline Integration

Very recent researches outlined the integration of some effectiveness disciplines by some combat aircraft manufacturers, General Dynamics and Northrop corporations. Kitowski (Ref. 16) of General Dynamics Corporation outlined a methodology to reflect the incorporation of thrust-vectoring and cost on a single measure of merit. That was the number of kills, in an air-to-air mission type. Wheelock (Ref. 17) of Northrop Corporation outlined the company's involvement in advanced low observable aircraft development programs. Wheelock outlined the integration of range, payload, runway, performance, availability, reliability, survivability and accuracy into the design optimisation process. He also stated that the methodology's quantitative contractual specification requirement remain classified.

It can be seen from the above that there is considerable information about conceptual design in the open literature. Security considerations considerably limited the information available on mission simulation, R&M and survivability, but there is sufficient information available to attempt a development of a methodology to incorporate combat effectiveness into the conceptual /preliminary design process. Some information became available during the study and has been incorporated.

Chapter Two

Design Synthesis of a Combat Aircraft (CONCEPT)

2.1 Synthesis Introduction

For the last two decades much attention has been given to developing computerised procedures for aircraft design synthesis. Most of these programs are devoted to civil aircraft design and analysis. This chapter discusses the design synthesis which has been specially developed to be able to be linked to the subsequently-developed effectiveness modules. The design synthesis can be considered to be composed of two parts; the first for the initial sizing part and then the part for the sizing of basic items.

2.2 Initial Conceptual Design and Sizing

Aircraft sizing is the process of determining the takeoff gross weight and fuel weight required for an aircraft concept to perform its design mission. Since the design synthesis developed is to be used for a wide spectrum of aircraft sizes, the initial sizing is relatively crude and is dependent on existing aircraft data. The main target of the initial sizing design process is to estimate the takeoff weight, empty weight and the fuel weight required to fly the mission.

2.2.1 Configuration Layout

The selection of the general layout of a new combat aircraft is based on the analysis of the design specifications and the degree of new technologies to be incorporated in the design. The operational requirements, such as superior manoeuvrability, affects the configuration layout by, perhaps, incorporating canard lifting surfaces. Unlike transport aircraft, combat aircraft may have a wide range of layouts and configurations. The main configuration layout aspects of combat aircraft major components are:

- Fuselage layout and cross section (semi-circular, semi-rectangular, chin etc.)

- Wing layout (trapezoidal, delta, diamond) and vertical position (low, mid, high)
- Engines layout and position (one or two)
- Tail layout (one fin, two, with/without a horizontal stabiliser)
- Intake layout and shape (one intake or two, rectangular, semi-circular, side mounted, nose, chin, etc.)
- Landing gear layout.

The combination of these different layouts of major items gives many different designs.

Fig. 2.1 illustrates some of the current designs of different configurations.

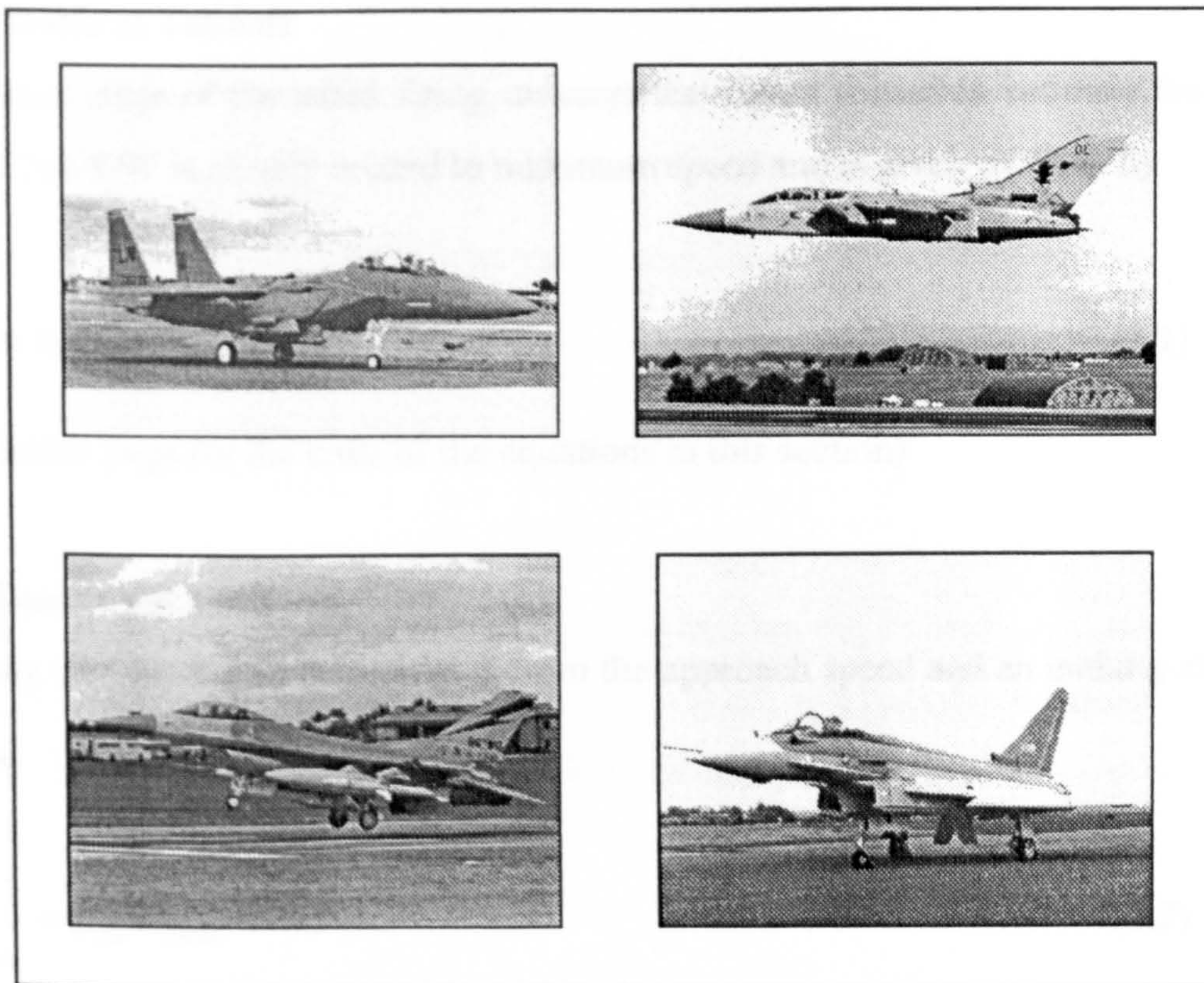


Fig. 2.1 Some layouts of a combat aircraft

2.2.2 Thrust and Weight Ratios

Thrust-to-weight ratio (thrust ratio) T/W directly affects the performance of the aircraft. An aircraft with a higher T/W will accelerate more quickly, climb more rapidly, reach a higher maximum speed, and sustain higher turn rates. T/W is not a constant, the weight

of the aircraft varies during flight as fuel is burned. Also, the engine thrust varies with altitude, velocity and cycle. The wing loading (weight ratio) is the weight of the aircraft divided by the area of the reference wing, W/S . As with the thrust ratio, the term weight ratio normally refers to the takeoff wing loading, but can also refer to combat and other flight conditions. Wing loading affects stall speed, climb rate, takeoff and landing distances, and turn performance. Wing loading has a marked effect upon a sized aircraft's takeoff gross weight. If the wing loading is reduced, the wing becomes larger. Wing loading and thrust ratio must be optimised together.

Thrust Ratio at Takeoff

At this start stage of the initial sizing, an empirical figure is used to estimate the T/W at takeoff. The T/W is closely related to maximum speed and is given by (Ref. 5):

$$\left(\frac{T}{W}\right)_{to} = 0.648 M_{\max}^{0.594} \quad (2.1)$$

(see notation page for the units of the equations in this section)

Wing Loading at Stall

The wing loading at stall is calculated from the approach speed and an initial guess value of $C_{L\max}$.

$$\left(\frac{W}{S}\right)_{stall} = q_{stall} C_{L\max} \quad (2.2)$$

For an initial estimate of maximum lift coefficient, it is necessary to resort to test results and historical data. (Refs. 5 and 18) provide data of maximum lift trends vs wing 1/4 chord sweep angle for aspect ratios 3-8 as shown in Fig. 2.2.

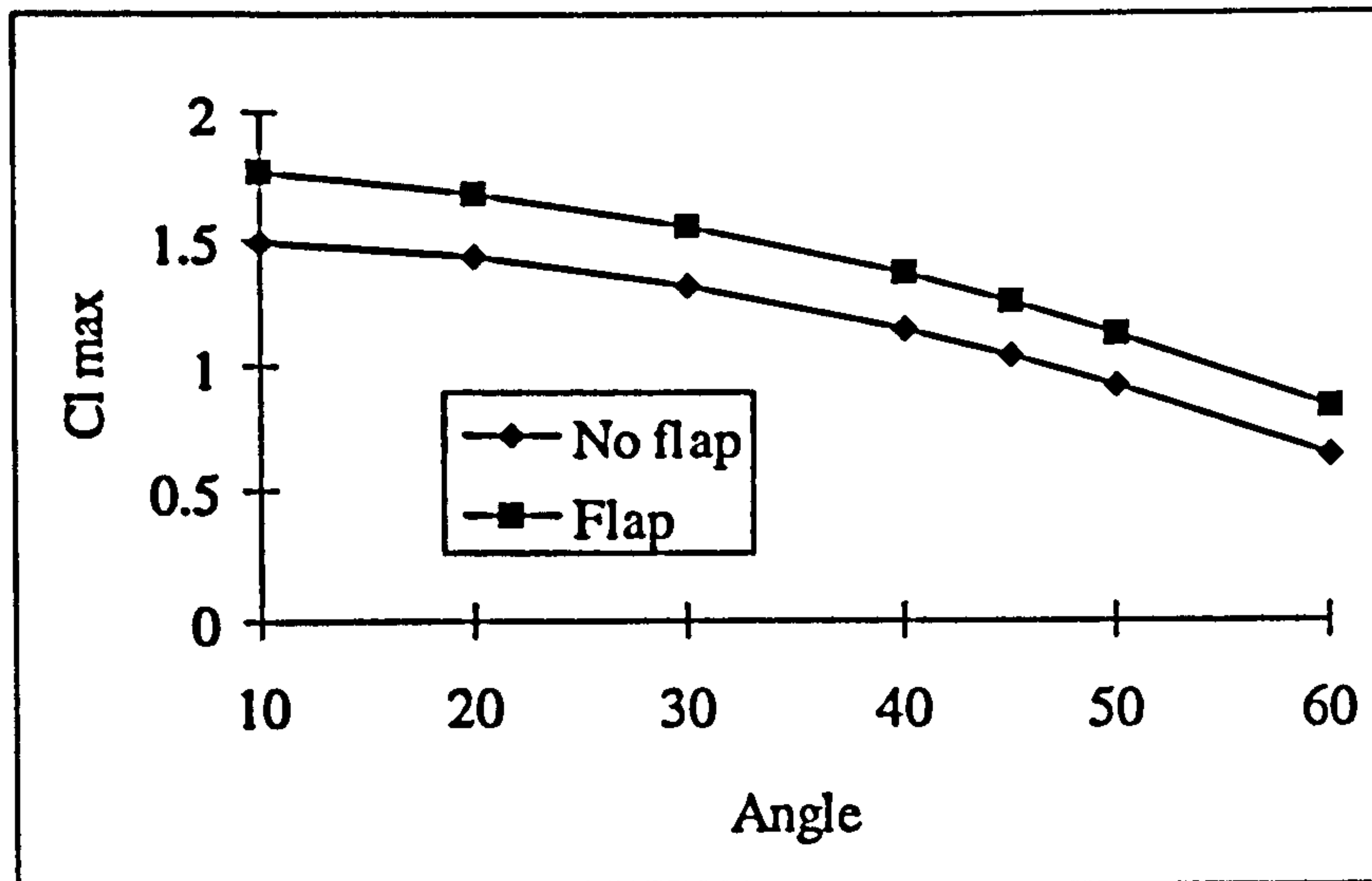


Fig. 2.2 Maximum lift coefficient

Wing Loading at Landing

The landing wing loading is calculated by the equation

$$S_{\text{landing}} = 80 \left(\frac{W}{S} \right) \left(\frac{1}{\sigma C_{L\max}} \right) + S_a \quad (2.3)$$

Landing distance is largely determined by wing loading. The above equation provides a good approximation of the landing distance, which can be used to estimate the maximum landing wing loading. The first term represents the ground roll to absorb the kinetic energy at touch down speed. The constant term S_a , represents the obstacle-clearance distance.

Wing Loading at Takeoff

Both thrust ratio, and weight ratio contribute to the takeoff distance. The equation below assumes that the thrust ratio at takeoff has been selected and can be used to determine the required wing loading to attain some required takeoff distance.

$$\left(\frac{W}{S} \right)_{to} = (TOP) \sigma C_{L_{to}} \left(\frac{T}{W} \right)_{to} \quad (2.4)$$

For initial estimate of the required wing loading a statistical approach for estimation of takeoff distance can be used. Fig. 2.3 permits estimation of the takeoff parameter (TOP) for different categories of aircraft.

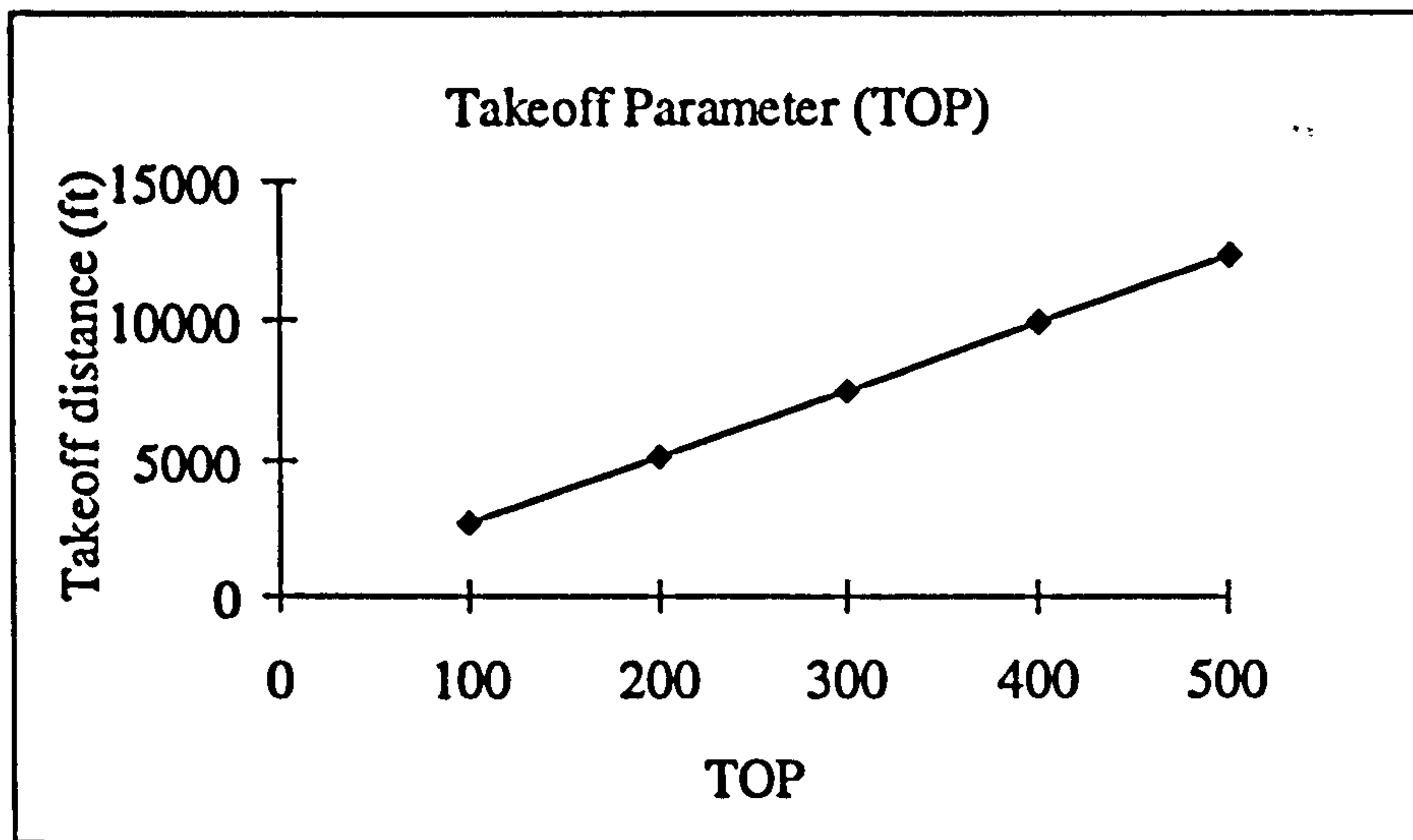


Fig. 2.3 Takeoff parameter

Wing Loading at Cruise

To maximise range during cruise, the wing loading should be selected to provide a high L/D at the cruise conditions. A jet aircraft will obtain maximum range by flying at a wing loading such that the parasite drag is three times the induced drag (Ref. 5). This yields the following formula for wing loading selection for range optimisation of jet aircraft.

$$\left(\frac{W}{S}\right)_{cruise} = q \sqrt{\frac{\pi A e C_{D0}}{3}} \quad (2.5)$$

An initial value for the drag at zero lift was used and equals to 0.015 for jet fighter-type aircraft. The Oswald efficiency factor (e) is a measure of drag due to lift efficiency, and equals approximately 0.6 for a fighter.

Wing Loading For Turn Performance

There are two important turn rates. The “sustained” turn rate for flight conditions is the turn rate at which the thrust of the aircraft is just approximately opposite to the flight direction, then the thrust must equal the drag for a sustained turn. If the aircraft turns at a quicker rate, the drag becomes greater than the available thrust, so the aircraft begins to slow down or lose altitude. The “instantaneous” turn rate is the highest turn rate possible, ignoring the fact that the aircraft will slow down or lose altitude and is limited by the wing’s lifting capability. Turn rate is equal to the radial acceleration divided by the velocity,

$$\psi^{\bullet} = \frac{g\sqrt{n^2 - 1}}{V} \quad (2.6)$$

where (n) is the load factor or g-loading and is given by

$$n = \frac{qC_L}{\left(\frac{W}{S}\right)} \quad (2.7)$$

Equation (2.6) can be solved for the load factor at the required turn rate as follows:

$$n = \sqrt{\left(\frac{\psi^{\bullet} V}{g}\right)^2 + 1} \quad (2.8)$$

The required wing loading can be solved for in equation (2.7) as follows:

$$\left(\frac{W}{S}\right) = \frac{qC_{L_{\max}}}{n} \quad (2.9)$$

The only unknown is the maximum lift-coefficient at combat conditions. This is not the same as the maximum lift coefficient for landing. During combat, use of full flap setting

is not usually possible. For initial design purposes, a combat maximum lift coefficient of about 0.6-0.8 should be assumed for a fighter with only a simple trailing-edge flap for combat. Equation (2.9) may then be solved to derive the wing-loading for the maximum instantaneous turn rate.

Wing Loading For Sustained Turn Performance

The wing loading to attain a required sustained load factor (n) using all of the available thrust can be determined by equating the thrust and drag, and using the fact that since lift equals weight times (n), the lift coefficient during manoeuvre equals the wing loading times (n), divided by the dynamic pressure. This yields

$$T = qSC_{D0} + qS\left(\frac{C_L^2}{\pi Ae}\right) = qSC_{D0} + \frac{n^2 W^2}{qS\pi Ae} \quad (2.10)$$

or

$$\frac{T}{W} = \frac{qC_{D0}}{\left(\frac{W}{S}\right)} + \frac{W}{S} \left(\frac{n^2}{q\pi Ae} \right) \quad (2.11)$$

Equation (2.11) can be solved for W/S to yield the wing loading that attains a required sustained load factor (n) as follows:

$$\left(\frac{W}{S}\right) = \frac{\left(\frac{T}{W}\right) \pm \sqrt{\left(\frac{T}{W}\right)^2 - \left(\frac{4n^2 C_{D0}}{\pi Ae}\right)}}{\frac{2n^2}{q\pi Ae}} \quad (2.12)$$

2.2.3 Takeoff Weight Build-up

The takeoff weight is divided into crew weight, payload weight, fuel weight, and the remaining empty weight. The takeoff weight is then expressed as a function of the known

weights (payload and crew) and two dimensionless terms, the ratios of fuel and empty weights to the takeoff weight, i.e.

$$W_0 = \frac{W_c + W_p}{1 - \left(\frac{W_{fuel}}{W_0} \right) - \left(\frac{W_e}{W_0} \right)} \quad (2.13)$$

2.2.4 Empty Weight Estimation

Statistical data are used to estimate the empty weight fraction (W_e / W_0). (Ref. 5) gives empirical trends of the empty weight fraction for different categories of aircraft. For jet fighters it is given by:

$$\frac{W_e}{W_0} = 2.34 W_0^{-0.13} \quad (2.14)$$

2.2.5 Fuel Fraction Estimation

The fuel fraction is determined as the ratio between the weight at the end of the mission and the takeoff weight (W_x / W_0). Fuel fraction is estimated based on the mission profile with the use of approximate calculations of fuel consumption and aerodynamics. Appendix A contains the method used to estimate the fuel fraction based on the mission profile.

2.2.6 Takeoff Weight Calculations

The takeoff weight is found by the iterative method illustrated by Fig. 2.4 The iteration process starts by guessing the takeoff weight, calculating the statistical empty weight fraction and then calculating the takeoff weight. If the result does not match the guess value, a value between the two is used as the next guess. The iterative process usually converges in just a few iterations.

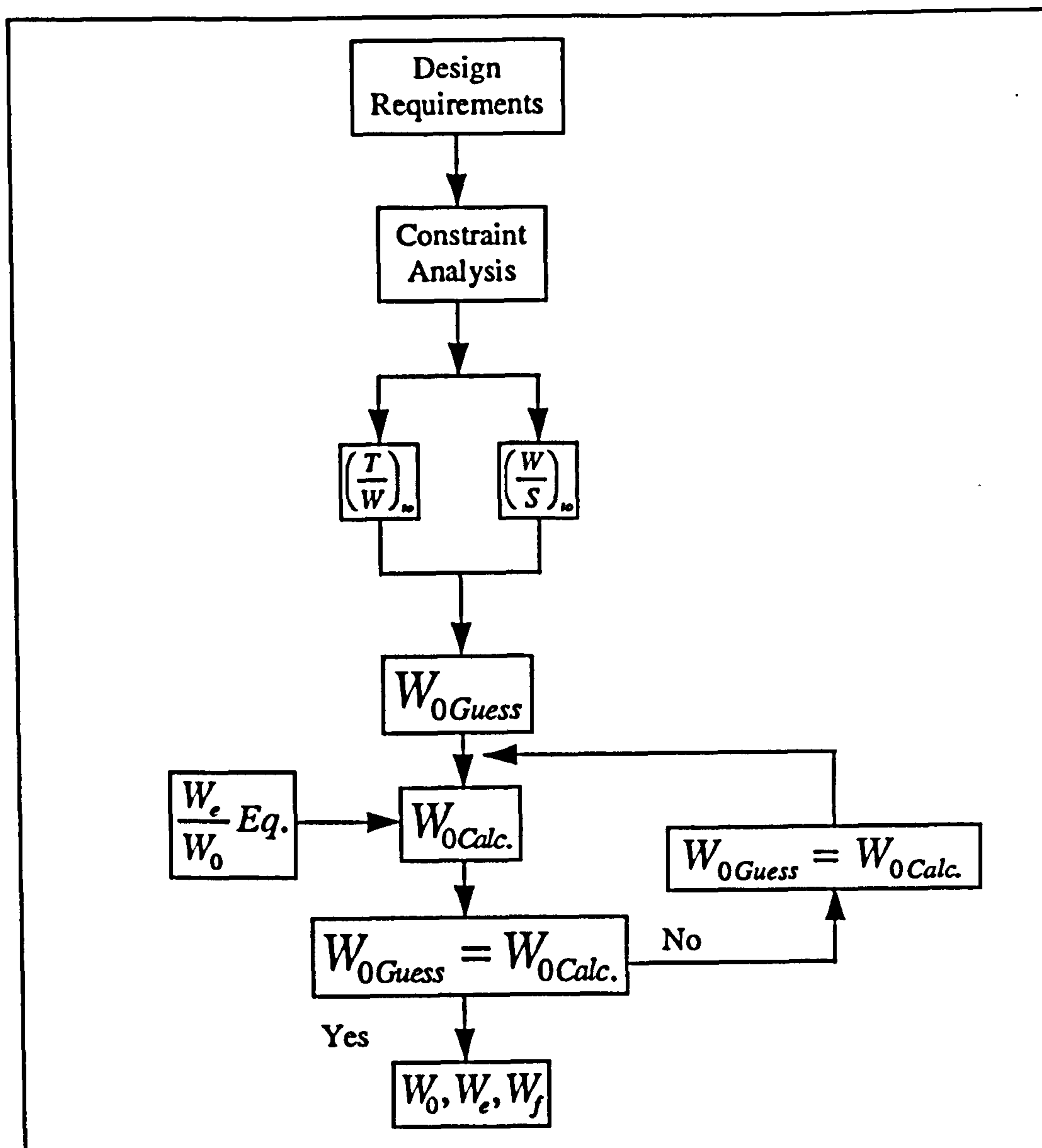


Fig. 2.4 Initial sizing design process

2.3 Basic Items Sizing

The basic items are the main parts of the aircraft and they are contained within the fuselage. Their size is estimated from the initial sizing process and the definition of the aircraft configuration. The detailed fuselage and aircraft dimensions are then derived from the sizes of the basic items.

2.3.1 Radome

The radome is defined by the radar dish diameter. In addition a linear variation of cross-sectional area with the axial distance is assumed.

2.3.2 Cockpit

The geometry of a standard single-seat cockpit for combat aircraft is defined in (Ref. 1) The cockpit dimensions are calculated using input data related to the cockpit type specifications.

2.3.3 Undercarriage

The geometry of the nose and main undercarriage is derived from a correlation with the takeoff weight. The undercarriage bays are evaluated as the sum of the leg and tyre volumes. The leg length is used to define the leg volume and the tyre diameter and width the tyre volume.

2.3.4 Engine

The engine size is found by a set of first-order statistical jet-engine models based upon data from existing engines. These equations are functions of max. Mach number, takeoff thrust and bypass ratio.

2.3.5 Intake Ducts

The intake diffusers are assumed to have a given fixed area ratio with reference to the inlet area of the engine. The intake diffuser(s) rectangular inlet is then calculated using a given aspect ratio (ratio of height to width). A minimum length for the intake diffusers is then described, which is a function of their width or height.

2.4 Geometry-Based Items

The geometry based items are the main aircraft components that give the aircraft external shape.

2.4.1 Fuselage Design

The fuselage length is computed by adding the length of the main non-overlapping components. A number of fuselage stations are defined along the fuselage length. These stations are set to coincide with the main aircraft equipment locations such as the radar dish position and the main undercarriage position. The distance and the shape of these stations is arbitrary and depends on the design and the size of the fixed items.

2.4.2 Wing Design

The gross wing area is calculated after determining the takeoff wing loading and the takeoff weight. The wing geometry is calculated from user-defined input design data such as the aspect ratio and the taper ratio. From these the unknown wing parameters such as the wing span and the trailing-edge angle are then found. Following these gross wing calculations, and using a first estimate of the fuselage width at the wing position, the nett-wing geometry is derived. This includes the wing box, the wing fuel tanks, the ailerons and the flaps.

2.4.3 Empennage Design

The geometrical dimensions of the fin and tailplane are determined similarly to the wing ones, but volume coefficients are used instead. The volume coefficients are supplied as input data. Other input data provided is the nett aspect ratio, the nett taper ratio, the sweep angles of leading and trailing edges and the thickness-to-chord ratios. Equally the distance between wing quarter-chord and fin and tailplane quarter-chord, given as a fraction of the fuselage length, are provided as input data. Hence, the nett surface areas of the fin and tailplane are calculated.

2.5 Acquisition Cost Estimation

A major factor in combat aircraft effectiveness is its acquisition cost. Acquisition cost includes all costs incurred to place an aircraft on the flight line. This include the cost of research, development, production tooling, assembly, military construction, spare parts and training. Fig. 2.5 shows the elements which make up aircraft acquisition cost. The aircraft acquisition cost method of (Ref. 19) has been modified to be programmed in FORTRAN and linked as a subroutine in the design synthesis.

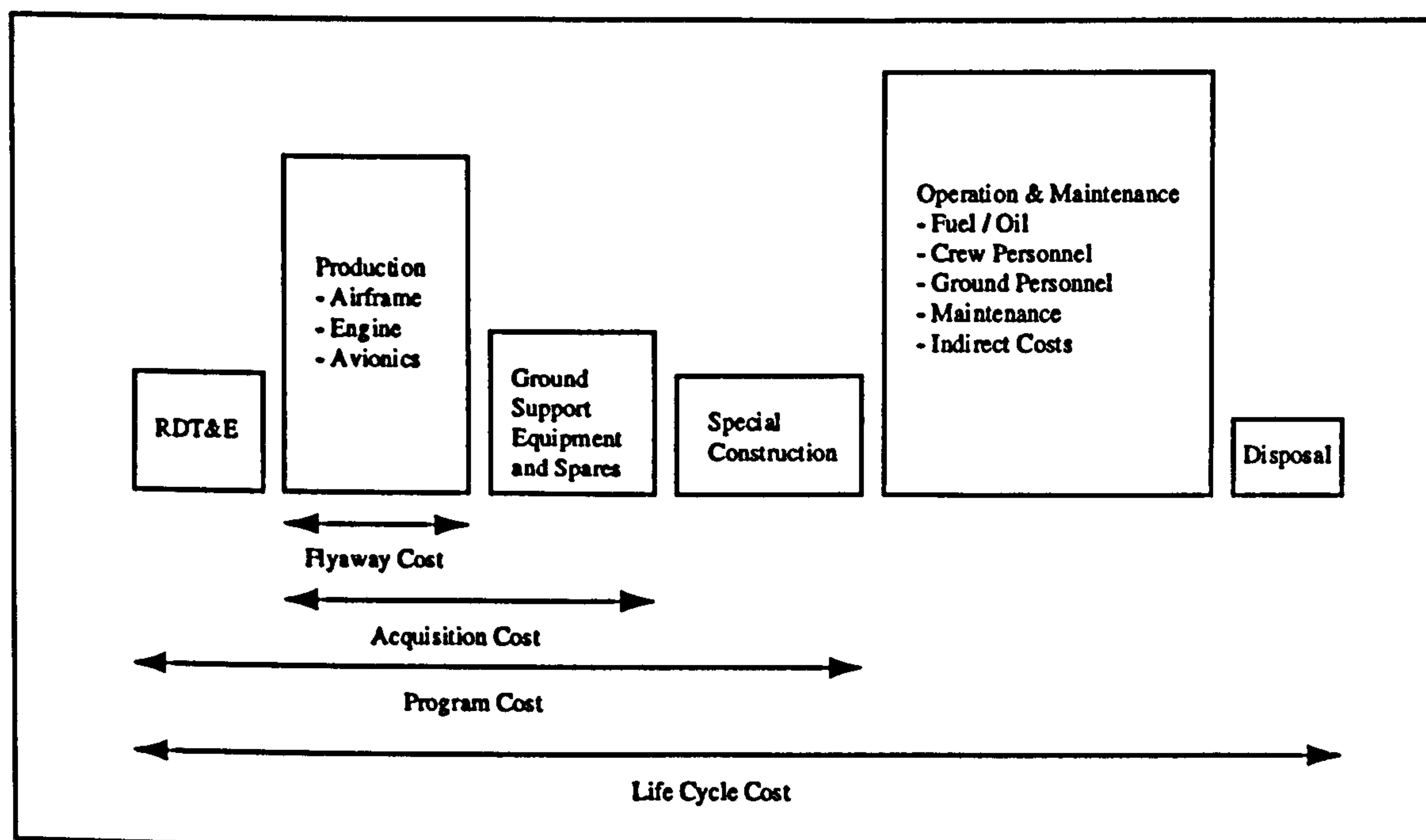


Fig. 2.5 Elements of aircraft life cycle cost.

2.6 Case Study

For the purpose of demonstrating the capabilities of CONCEPT, a case study is performed. This will show how CONCEPT is used to carry out the different conceptual design modules. The test case should be of a current combat aircraft of which sufficient information is available about the design characteristics. The F-16 resembles a good example of such aircraft, reflected by its reputation and production numbers.

2.6.1 Design Requirements for the F-16

The design requirements of the F-16, (Refs. 20, 21 and 22), are:

- Single-engine one pilot.
- The basic payload consists of internal gun and two wing-tip mounted heat seeking missiles.
- Conventional tail, moderate aspect ratio wing.
- Mission profile as shown in Fig. 2.6
- 1000 ft takeoff and landing distance.
- 130 knots approach speed.
- Mach 2 dash speed at 30,000 ft.
- 20 degrees/second instantaneous rate of turn at 350 knots at 20,000 ft.

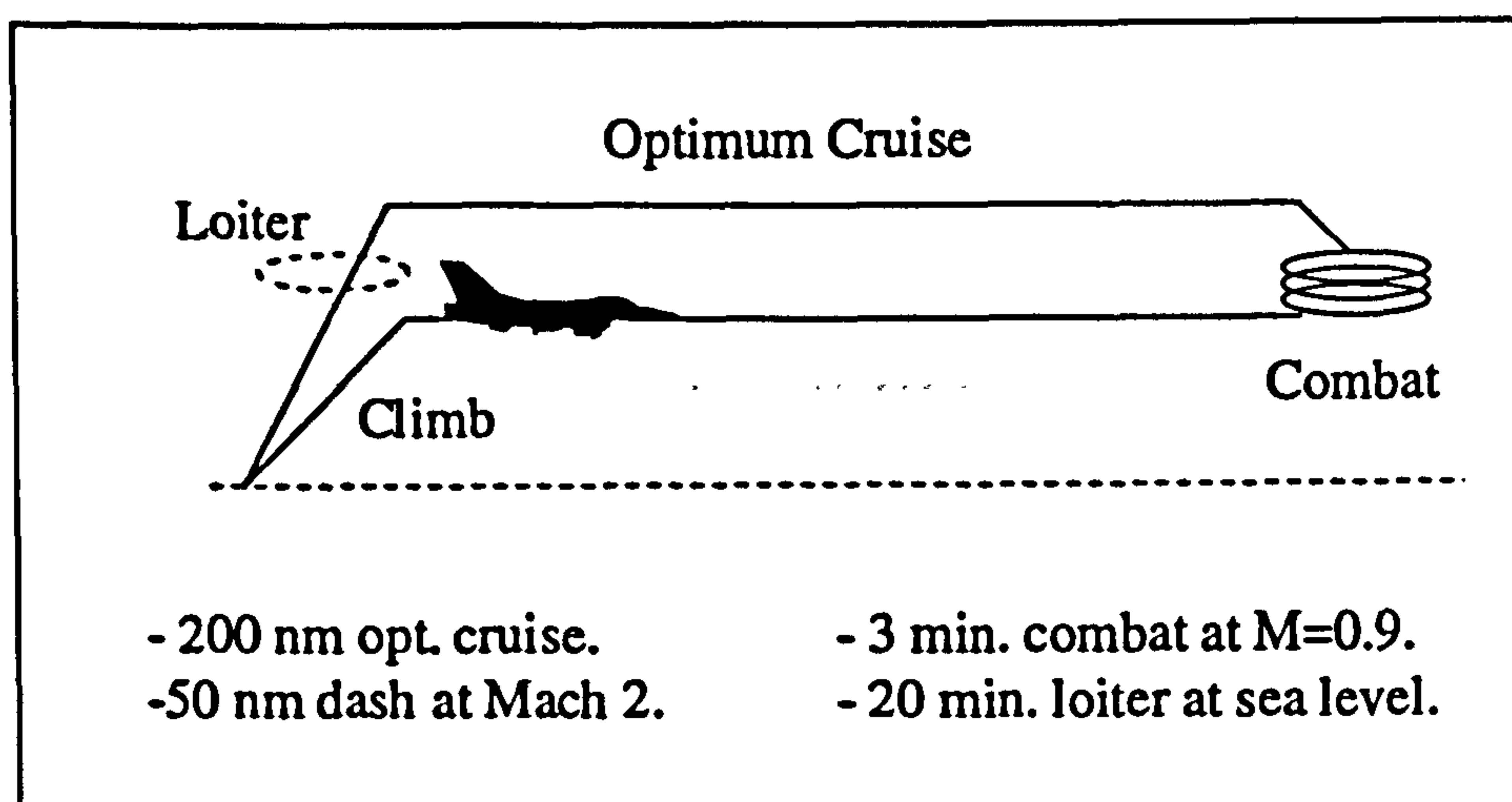


Fig. 2.6 Test case mission profile

2.6.2 Design Input Data

The data required by CONCEPT to perform the initial sizing and conceptual design for this test case is provided as a default value in the program. These data can be changed by editing the source code.

2.6.3 Test Case Results

Table 2.1 shows a comparison of some major design parameters of the test case and those given by CONCEPT. Fig 2.7 shows a graphical comparison of the two. The sizes of the main components and the takeoff weight is compared with the F-16 ones. The figure gives non-dimensional comparisons of each item. It is seen that the biggest design difference is in the order of 20% and that is the cost, which depends on other design factors, such as the number of aircraft to be produced. 2,000 F-16 aircraft have been built until now. The cost module gave good cost estimations when applied to new aircraft projects such as the Gripen JAS-39 which has an acquisition cost of 35 million dollar if sold on large batches. Fig. 2.8 shows the cost trend of Gripen as obtained by CONCEPT.

Parameter	F16	CONCEPT
Takeoff Weight	9790	8319.557
Wing Area	27.87	30.3
Fuselage Length	14	13.85
Fin Area	5.09	4.4
Horizontal Tail Area	5.92	6.18
Cost	20	24

Table 2.1 Test case major results

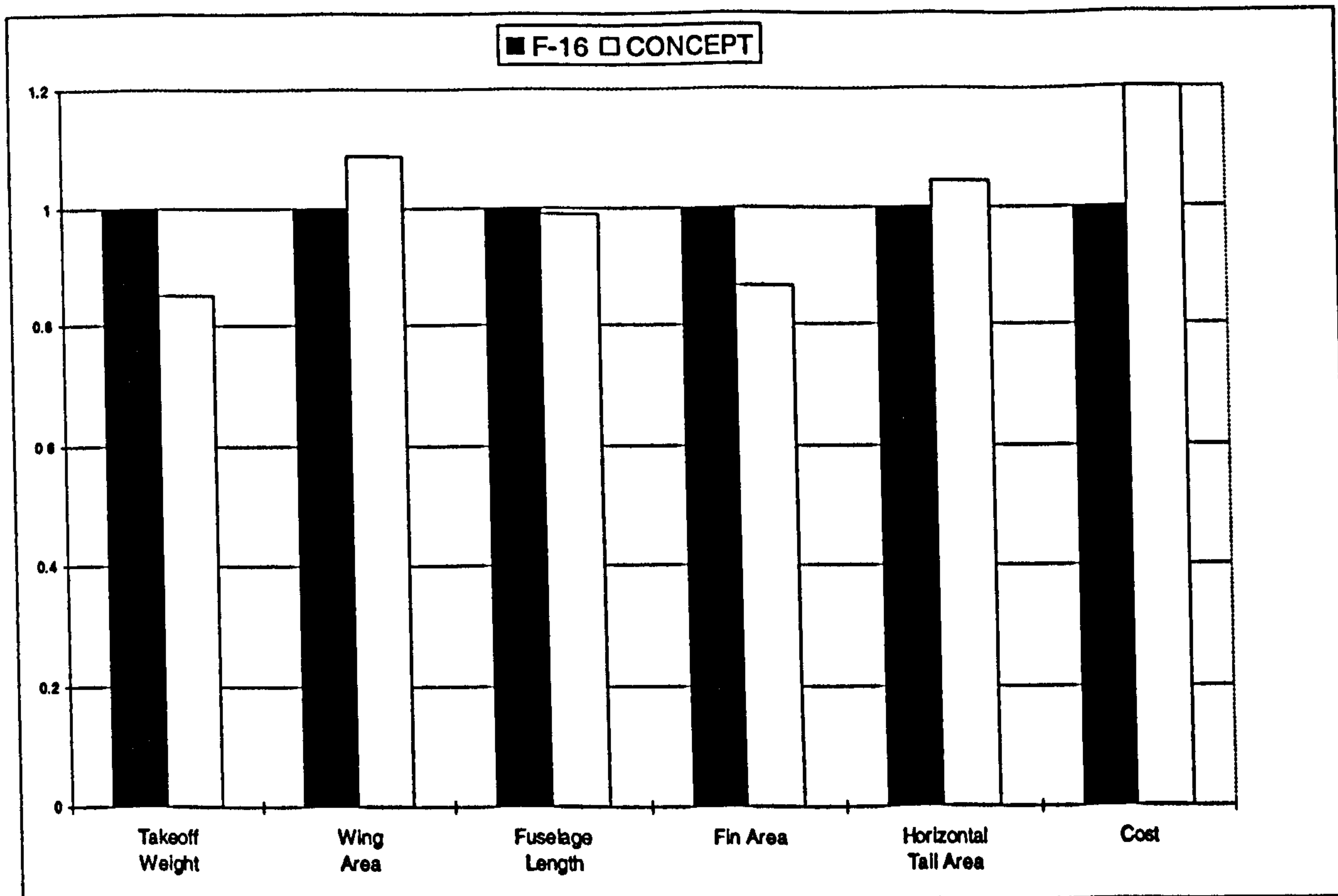


Fig. 2.7 Test case results

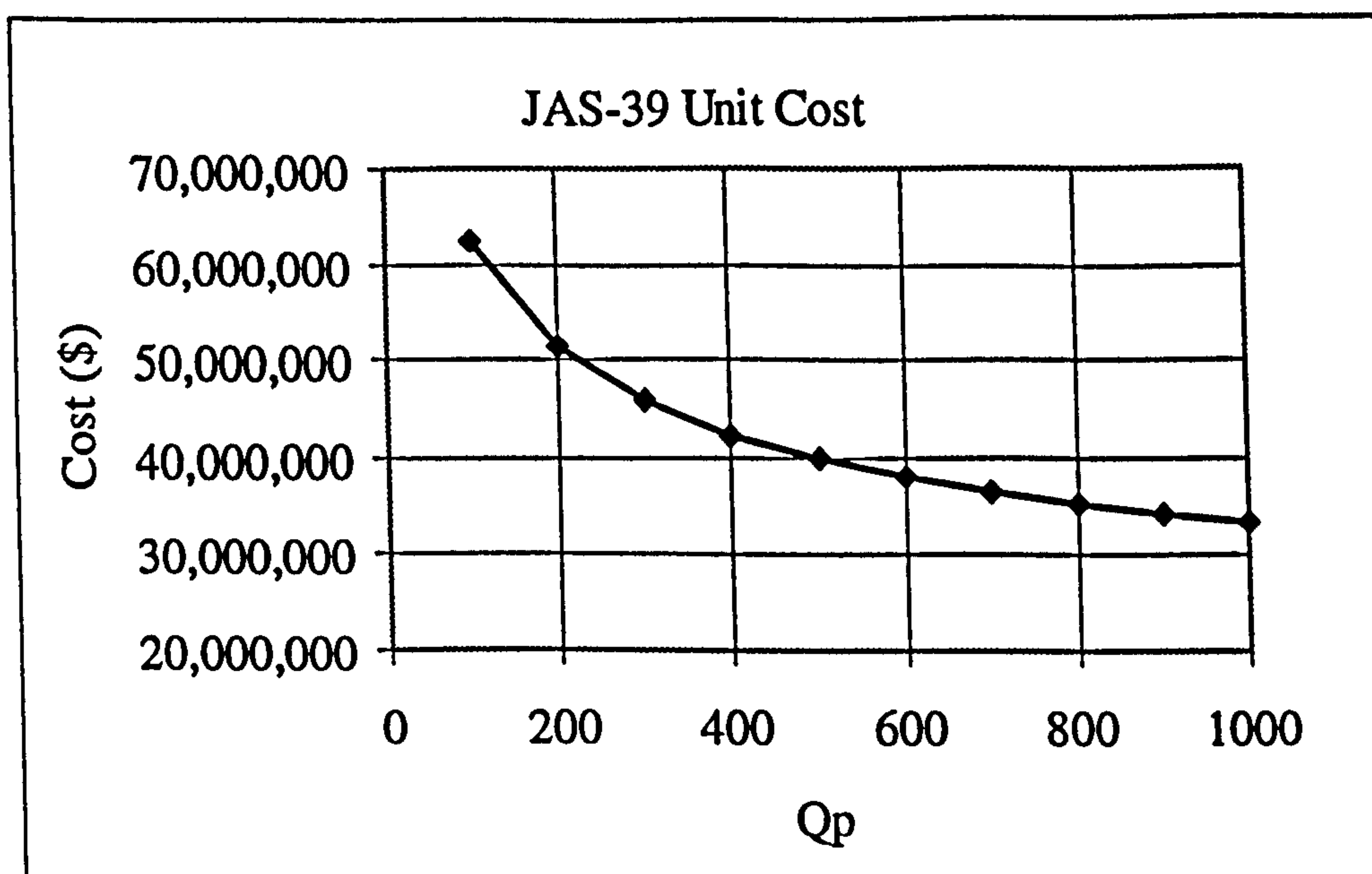


Fig. 2.8 Acquisition unit cost of the Gripen JAS-39

Chapter Three

Reliability and Maintainability Estimation

3.1 Introduction to R&M

Aircraft Reliability and Maintainability (R&M) strongly affects the aircraft effectiveness. In the past years R&M was not a major issue in the conceptual design process. But for the latest generation of combat aircraft, such as the European Eurofighter 2000 and the American ATF (Advanced Tactical Fighter) F-22, R&M is considered one of the major characteristics of the design and has been incorporated at first design phase (Refs. 23 and 24). Predicting realistic R&M figures of a combat aircraft during the conceptual/preliminary design phases is a continuing problem for both the designers and the operators. This is primarily due to the paucity of hardware detail which is available for analysis and evaluation during the early design stage. In this chapter, a statistical approach is presented to estimate the aircraft R&M in a way to be used to quantify the design effectiveness.

3.2 Data Collection and Compilation

This section describes the effort to collect the R&M data of modern and operational combat aircraft. These data have been compiled in a way to give similar units for each aircraft.

3.2.1 R&M Data Collection Effort

The tool most essential to the accomplishment of a link between the conceptual design parameters and the expected R&M figures of the new design is a comprehensive R&M data collection system. Information gathered by this system must be of sufficient detail for this task. The primary considerations in the selection of these data are:

1. The selection should cover a wide range of performance/design aspects of combat aircraft.
2. The data should belong to mature aircraft with good operational history.
3. The operators of these aircraft should have a reliable and accurate R&M data collection and registration.

It was felt from the start of this research that there would be difficulties in getting such data. This is because data of this nature are very limited, or not available, in the academic literature. A further problem is that these data may be restricted for reasons of National Security. To overcome this problem, the author made the request of the data as an official request from the Saudi Cultural Office in London to the Royal Saudi Air Force (RSAF) HQ in Saudi Arabia. Because the requested data formats - Failure Rate and Mean Time To Repair (MTTR) for system level - , are not readily available in the RSAF AUTOLOG system, the author had to travel several times to extract the data in the required format. This caused alterations to the research time plan, by working in other research subjects and compiling and analysing the data as they arrived. The main sources for the data were:

1. Cranfield University, Department of Aerospace Technology (DAeT). The DAeT has considerable material on aircraft design in general. R&M data have been provided to the DAeT from the RAF Maintenance Centre at Swanton Morley. These data relate to recent British-made combat aircraft.
2. RSAF HQ, Maintenance and Engineering Department.
3. RSAF HQ, Research and Analysis Department. This channel provided useful data for the aircraft which are not in service with the Saudi Air Force. The Lear Siegler Company of USA is the main consultant to this department and they provided the data through their official contact with the American aircraft manufacturers.

3.2.2 Data Compilation

The data to be analysed are consistent with the detail of aircraft main systems R&M records. All US data, for each aircraft system, are tabulated according to the Work Unit Code (WUC) classification system. The US Air Force specifications require

standardisation of WUC only at the system level. Table 3.1 shows the WUC codes and the system description corresponding to each code. The RAF classification system is slightly different as shown in second part of Table 3.1. It was therefore essential to establish compatibility of the data before using them in parallel in the analysis. Combat aircraft maintenance is categorised into three levels, organisation (on aircraft), intermediate (off aircraft, base shop), and depot (to manufacturer or a special base equipped for this maintenance). Maintenance data are recorded according to the maintenance actions which occur in each level. The maintenance actions which comprise organisational level are:

1. Remove and Replace,
2. Repair,
3. Check;

for intermediate level they are;

1. Bench check
2. Repair
3. NRTS (not repairable this station, sent to depot)
4. Condemned.

The data collected belongs to the unscheduled type failures and corresponding maintenance actions.

3.3 The Approach Used in Data Analysis; Pareto Principle

The general process of reliability quantification involves three phases:

1. Apportionment (or budgeting): i.e., the process of allocating reliability objectives among various elements which collectively make up a high-level product.
2. Prediction: i.e., use of previous performance data plus probability and statistic theory to calculate the expected failure rates for various components.
3. Analysis: i.e., identification of the strong and weak portions of the design to serve as a basis for improvements, trade-offs, and similar actions.

It was felt from the beginning, that finding a realistic relationship between the R&M and the conceptual/preliminary design variables could be difficult for each system. Even at the system level, each aircraft consists of more than 30 different systems. Many of these system's R&M figures are not directly related to the way the aircraft is designed. So it was felt from the beginning that it was important to find an approach which estimates the whole aircraft R&M, while eliminating systems whose R&M are not heavily dependant on the design itself.

3.3.1 Pareto Principle

Vilfredo Pareto was an 18th century Italian economist, who observed that about 80% of the wealth of the country was owned by about 20% of the population. Pareto's analysis is one of the main tools of quality control studies. It is used when selecting the most important things on which to focus, thus differentiating between the 'vital few' and the 'trivial many' (Refs. 25 and 26).

3.3.2 Reliability Data Trends

The reliability data of each aircraft are sorted in a descending order. The data are then plotted to visualise the failure rate trends. Figs. 3.1 to 3.4 shows the trends for each aircraft. Fig. 3.5 shows a comparison between the oldest aircraft in the data base F-4 and the most recent one, aircraft (E). This curve shows that the Pareto distribution is maintained regardless of the aircraft age. The next investigation was to apply Pareto analysis for each aircraft. Fig. 3.6 shows the Pareto distribution of aircraft (H). The data in the third column are the cumulative addition of the percentage of each system based on the total failure rate. As shown in the Figure, systems that contribute to 80% (the few systems) of the total failure rate are investigated. Appendix B contains Pareto graphs and data for all aircraft. It was found that the few systems varied from one aircraft to another. This variation also exists in the rank of certain repeated systems in the Pareto distribution. It was found that some systems appear in the few systems such as airframe, fuel and propulsion system. For these systems, reliability prediction equations are derived separately as described in Appendix B.

3.3.3 Pareto's Curve Parameters

Pareto's distribution of the few systems of each aircraft is analysed to find its mathematical equation. The general Pareto distribution are given by (Ref. 27):

$$F(x) = 1 - (b/x)^a, \quad x > b$$

A statistical package was used to find the best-fit equation for each distribution (Ref. 28). The results are shown in Figs. 3.7 to 3.11. It was found that the trend of the few systems follows another form of Pareto's distribution given by;

$$y = ax^b, \quad b < 1 \tag{3.1}$$

In order to approximate the failure rate distribution of aircraft main systems, it was required to define the following parameters which are necessary to define the Pareto's curve as shown by Fig. 3.12

1. The highest failure-rate figure, FR(1).
2. The lowest failure-rate figure, FR(8).
3. Number of systems per aircraft, NoS

The failure rate distribution of the aircraft systems are then given by the 80% of the few systems and a fixed value for the rest of the systems. The methodology of finding a mathematical link between the above parameters and the conceptual preliminary design parameters consisted of two elements:

1. Selecting general design parameters that are not specifically related to a certain system. This is because the few systems differ from one aircraft to another, plus the difference in their rank in the list.
2. Introducing a new design parameter which reflects the technology improvements over the years, and its effect on the component reliability. This is called the Year Factor (YF). The YF is an integer number found by subtracting the current year and the production year of the oldest aircraft in the data base, in this study the F-4 aircraft.

Highest Reliability Figure

It is essential to estimate the first reliability figure since it defines the shape of the Pareto equation. Table 3.2 shows the failure rate of the worst system of each aircraft. Because of the unknown nature of the first system, which has the highest failure rate figure, a simple equation of general form and reflecting design parameters is to be found. The first attempt was to eliminate the effect of the year factor and to consider only the four modern aircraft data. It was found that a good correlation exists between the aircraft empty weight and the number of engines, with the failure rate of the first system. Fig. 3.13 shows the good match between the selected parameters and the failure rate. The failure rate of the first system $FR(1)$ is found to be given by the following equation:

$$FR(1) = 0.00815W_e N_e - 23.6345N_e \quad (3.2)$$

The second approach was to take into account the effect of the year factor (YF) in estimating the first reliability figure. The approach was to find the best correlation by using the superposition approach. Firstly to study the effect of the year factor alone on aircraft of similar design parameters. And secondly to use all the data and their corresponding design parameters. It was found that the highest failure-rate figure $FR(1)$ is best approximated by the equation:

$$FR(1) = \frac{M \cdot N_e \cdot W_e}{111} YF^{-0.4356} \quad (3.3)$$

Fig. 3.14 shows the results of the above equation.

The Last Reliability Figure

The Last reliability figure $FR(8)$ is the failure rate of the last system of the few systems. Again the $FR(8)$ was to be found as an equation of the year factor and some design parameters. It was found that this figure correlates well with the maximum Mach number and Number of engines in the aircraft. The $FR(8)$ is given by:

$$FR(8) = 22N_e \cdot M \cdot YF^{-0.5144} \quad (3.4)$$

Fig. 3.15 shows the good match between the actual FR(8) values and those found by the above equation.

Number of Systems

The number of systems in an aircraft reflects its complexity. It was found that there was a good linear correlation between the number of systems and the aircraft empty weight.

Table 3.3 contains the empty weight and the number of aircraft systems.

The number of systems (NoS) in an aircraft could be approximated by the integer of:

$$NoS = 0.0025W_e + 6.6084 \quad (3.5)$$

Fig. 3.13 shows the actual number of aircraft system and that given by the above linear equation. Once the number of systems has been estimated, the reliability figures, of those systems which contribute to 80% of the total failure rate, is computed using the proper fit equation. The reliability figures of the rest of the systems is assumed to be constant and equal to that of FR(8).

3.4 Aircraft Maintainability Estimation

The same approach was used to estimate the maintainability of the aircraft systems. Systems maintainability are required to be defined as Mean Time To Repair (MTTR). This is because this unit is more suitable to use in the Mission Simulation Model discussed in the next chapter. Again the Pareto's analysis was applied to the MTTR data of the aircraft systems. It was found that the data did not closely follow the Pareto's distribution. Appendix B contains the MTTR data as well their Pareto's distributions. For the methodology validation, real maintenance data are used of aircraft of similar size. Future work should be done, when suitable data become available

American		British	
WUC	SYSTEM	MDC	SYSTEM
11	AIRFRAME	BB	AIRFRAME
12	FUSELAGE COMPARTMENT	BC	FUSELAGE COMPARTMENT
13	LANDING GEAR SYS.	BD	LANDING GEAR SYSTEM
14	FLIGHT CONTROLS	BE	FLYING CONTROL SYSTEM
17	ESCAPE	CD	ENGINES
24	AUXILIARY POWER	CE	SECONDARY POWER SYSTEM
27	ENGINES	CK	POWER PLANT INSTALLATION
29	POWER PLANT INST.	EB	ENVIRONMENTAL SYSTEM
41	ENVIRONMENTAL SYS.	EC	ELECTRICAL POWER GENERATION
42	ELECTRICAL SYS.	EE	LIGHTING SYSTEM
44	LIGHTING SYS.	EF	HYDRAULIC POWER GENERATION
45	HYDRAULIC SYS.	EG	FUEL SYSTEM
46	FUEL SYS.	EH	OXYGEN SYSTEM
47	OXYGEN SYS.	EK	MISCELLANEOUS UTILITIES
49	MISC. UTILITIES	FB	INSTRUMENTS
51	INSTRUMENTS	FC	GUIDANCE & FLIGHT CONTROL SYSTEM
56	FLIGHT REFERENCE	FF	ALL WEATHER LANDING SYSTEM
57	INT GUIDE/FLIGHT C	FG	FLIGHT REFERENCE
58	IN-FLT TEST EQ	GB	HF COMMUNICATION
62	VHF COMM.	GD	UHF/VHF COMMUNICATION
63	UHF COMM.	GE	INTERCOMMUNICATION SYSTEM
64	INTERPHONE	GF	IFF SYSTEM
65	IFF	GG	EMERGENCY COMMUNICATIONS
66	EMERG. RADIO	GK	MISCELLANEOUS COMMUNICATIONS
67	COM/NAV/IFF INT	HB	RADIO NAVIGATION
71	RADIO NAV	HD	GENERAL NAVIGATION
72	RADAR NAV	HE	WEAPON AIMING SYSTEM
73	BOMBING NAV	HF	COMPUTING SYSTEM
74	WEAPON CONTROL	HG	ELECTRONIC COUNTER MEASURES
75	WEAPON DELIVERY	HH	PHOTOGRAPHIC/RECONNAISSANCE
76	COUNTERMEASURES	HJ	DISPLAYS
77	PHOTO/RECONN	HK	MISCELLANEOUS AVIONICS
91	EMERG. EQUIP	JB	GUN SYSTEM
96	PERSONNEL EQUIP	JD	WEAPON DELIVERY SYSTEM
97	EXPLOSIVE DEVIC	KB	ARRESTOR HOOK SYSTEM
		KC	PERSONNEL EQUIPMENT
		KE	EJECTION SEAT EQUIPMENT
		KH	EXPLOSIVE DEVICES
		SW	SOFTWARE

Table 3.1 American and British system definitions.

A/C	We	Ne	FR(1)
F	8273	1	42.12
H	10810	2	133.33
T	13890	2	178.91
E	14515	2	186.27

Table 3.2 The highest FR.

Aircraft	We	No. of Systems
F	8273	27
H	10810	35
T	13890	39
E	14515	45

Table 3.3 Number of systems.

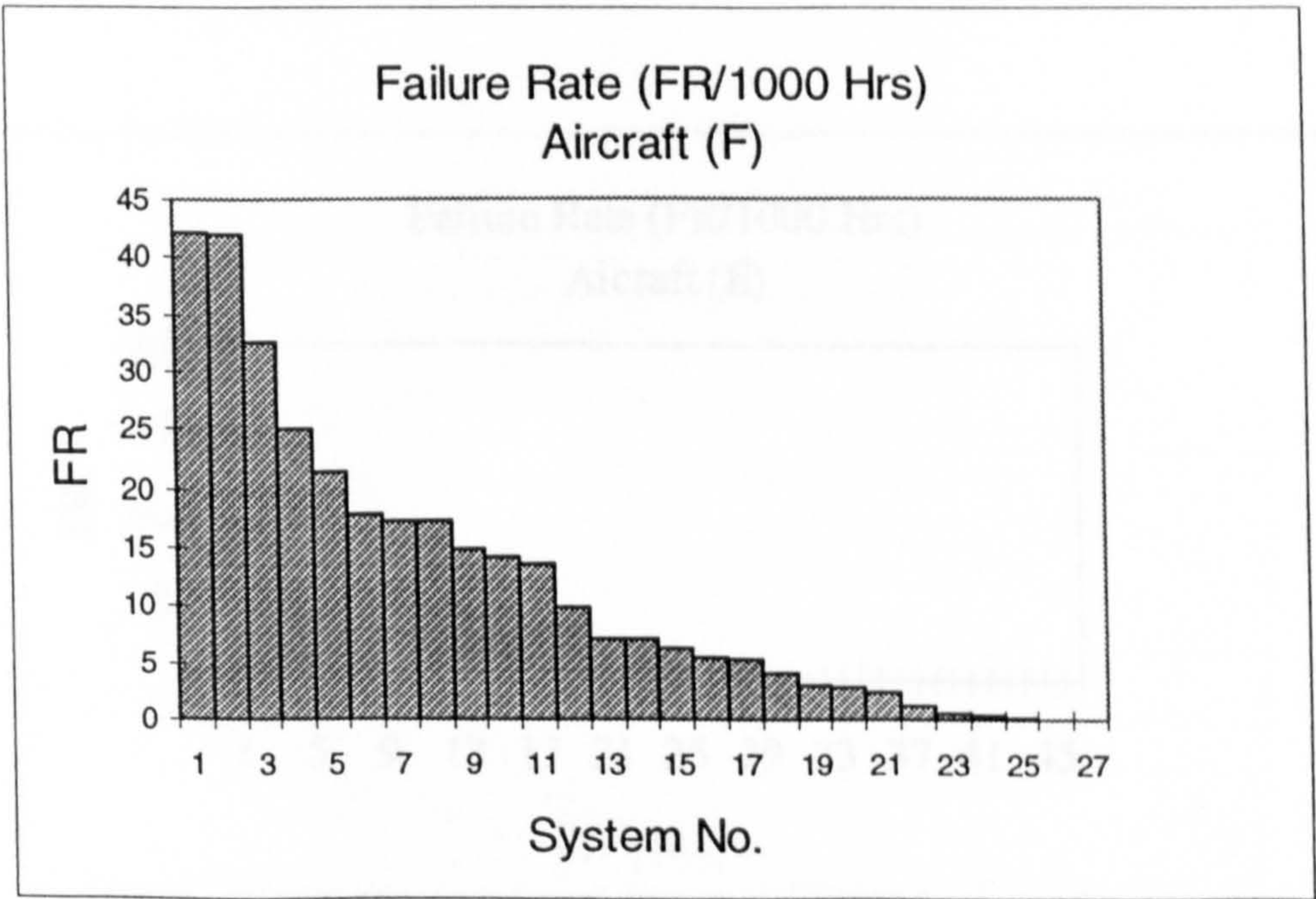


Fig. 3.1 Reliability data trend for aircraft F

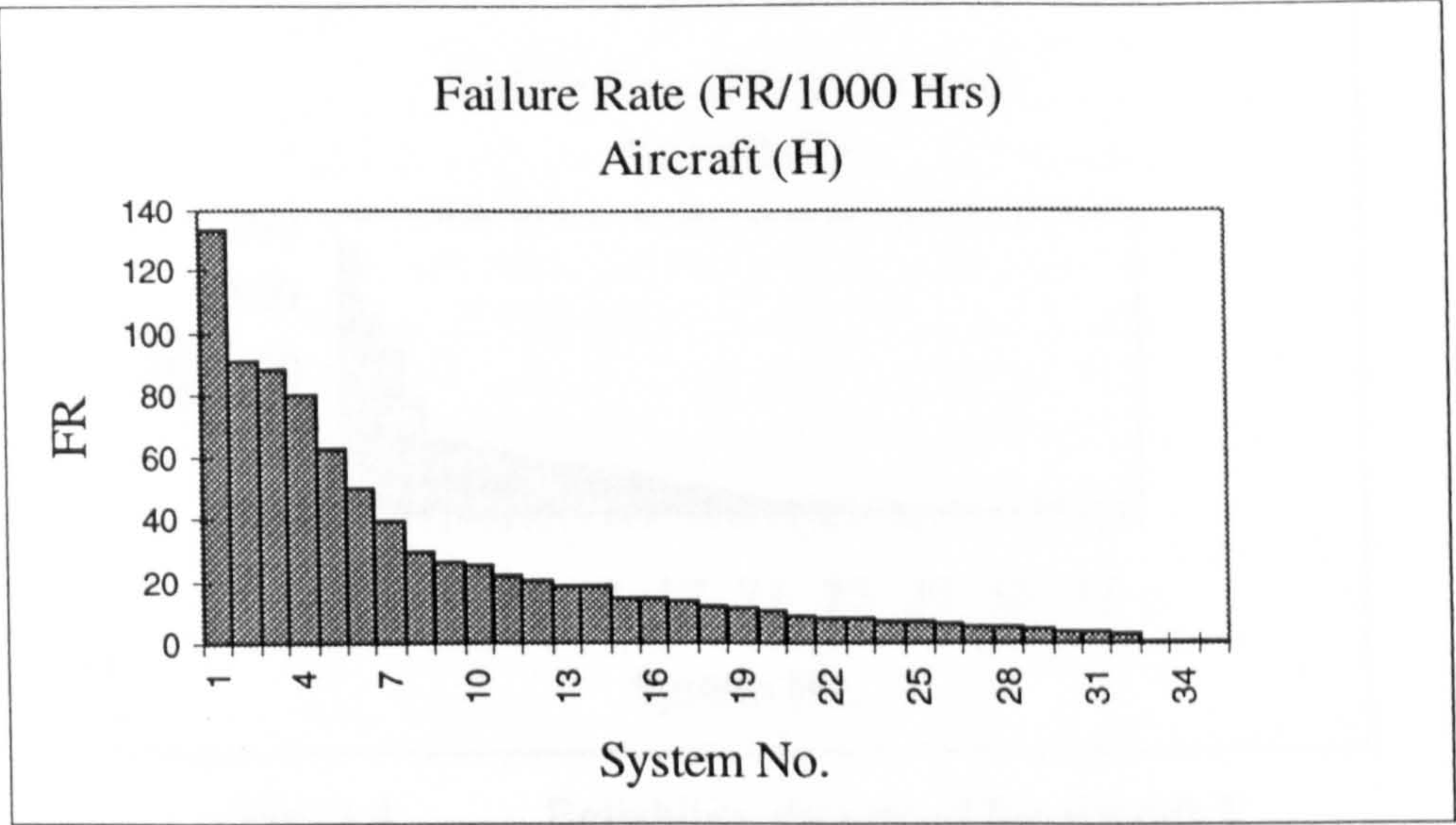


Fig. 3.2 Reliability data trend for aircraft H

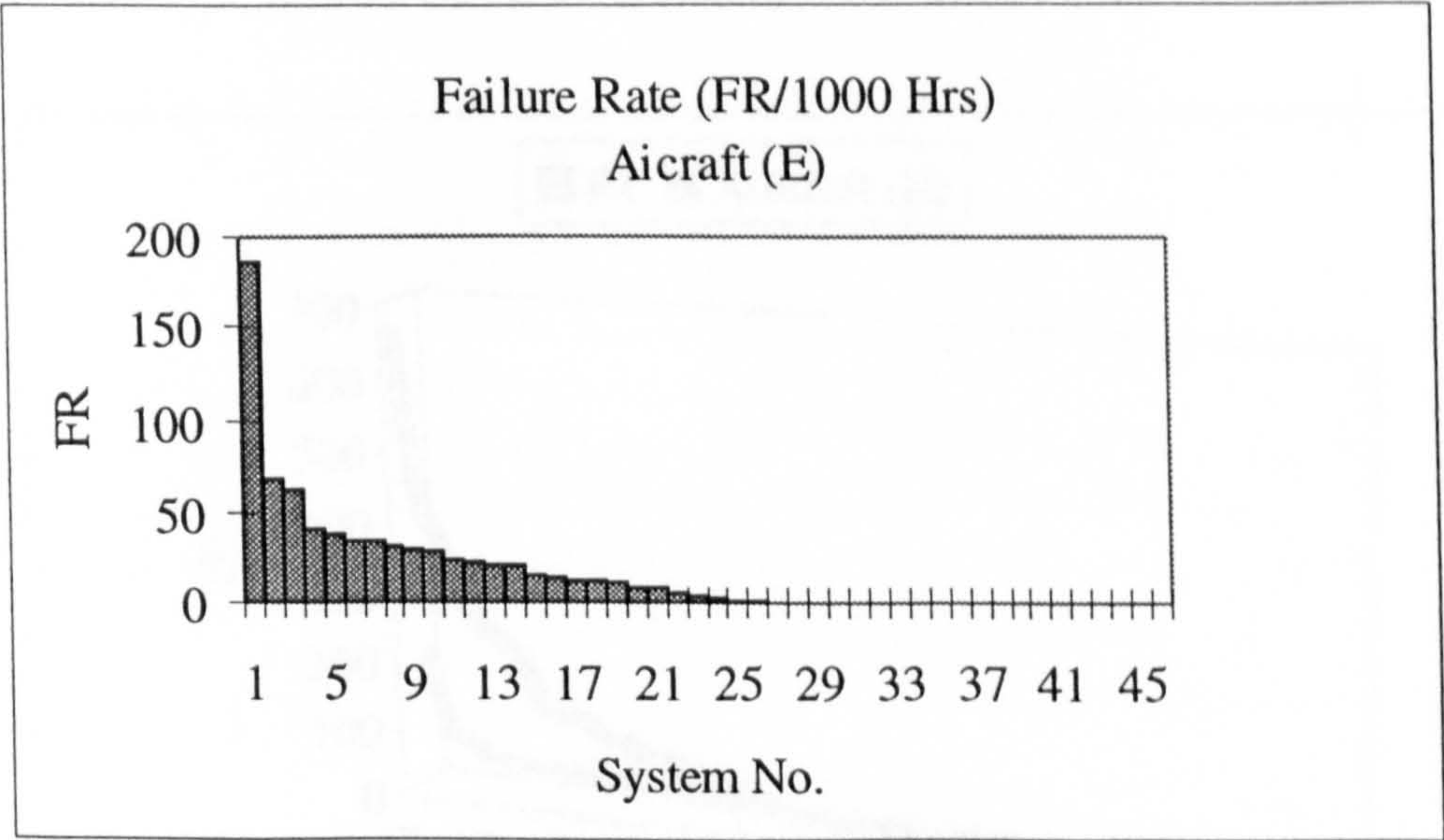


Fig. 3.3 Reliability data trend for aircraft E

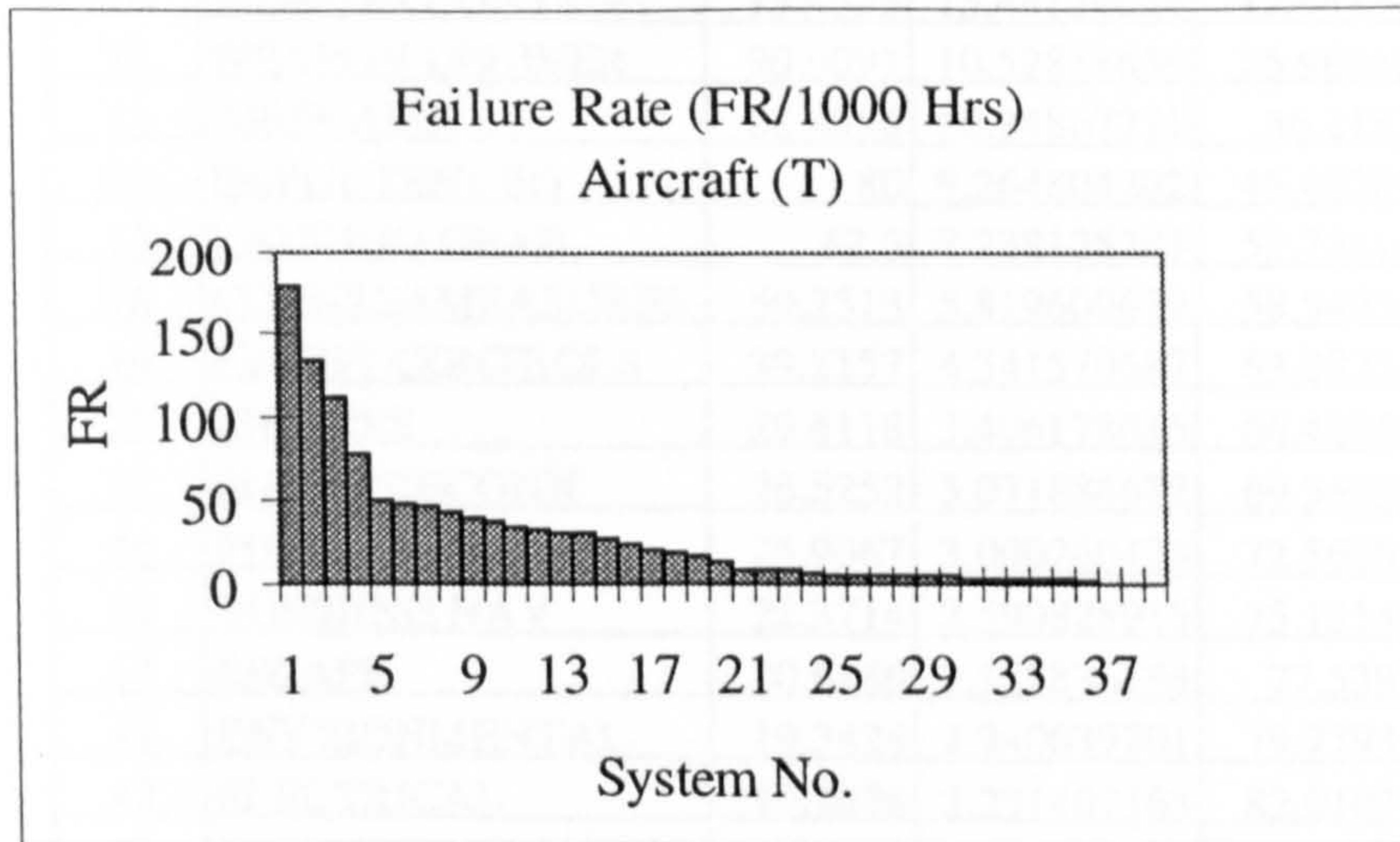


Fig. 3.4 Reliability data trend for aircraft T

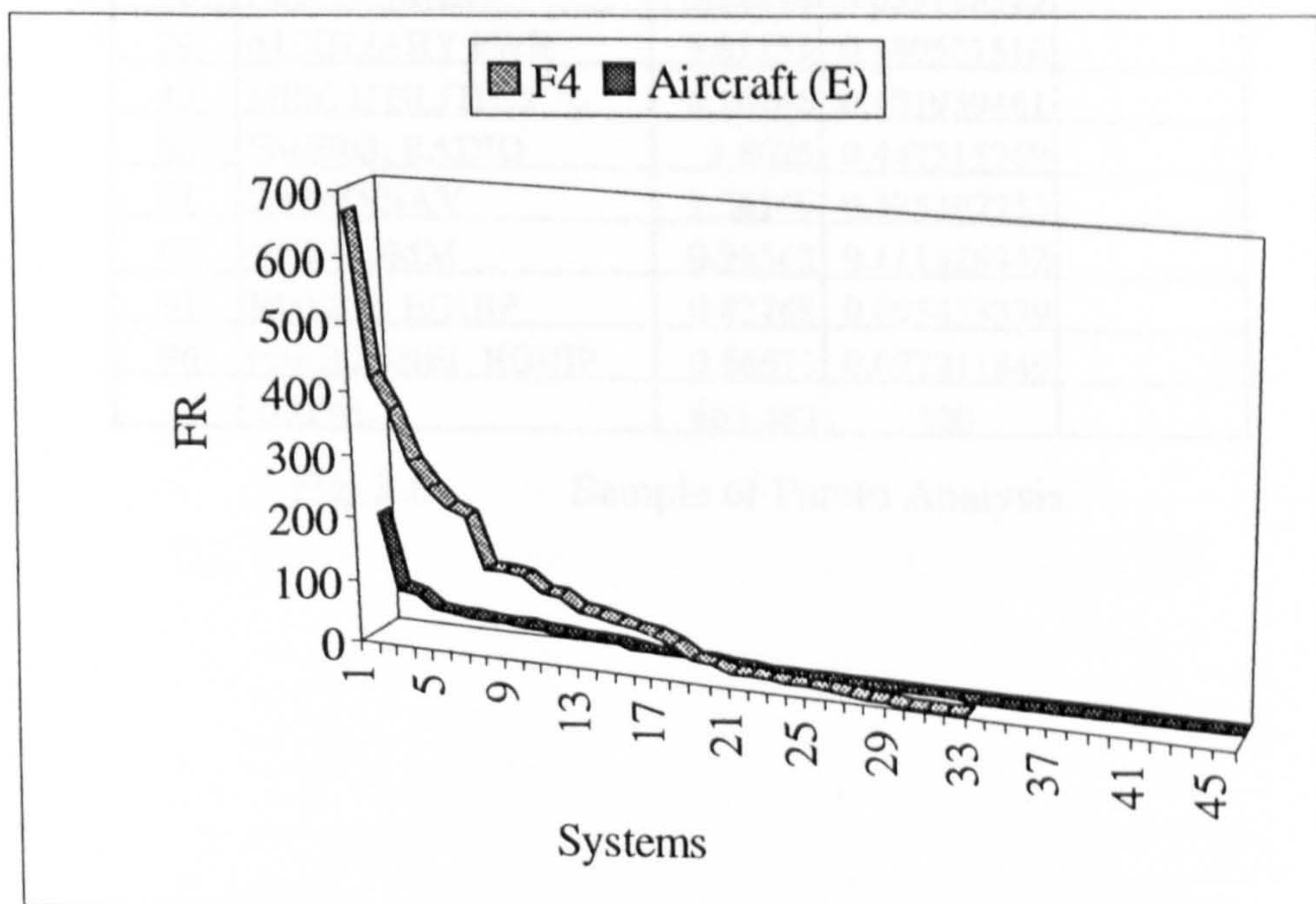


Fig. 3.5 Pareto distribution of old and new aircraft.

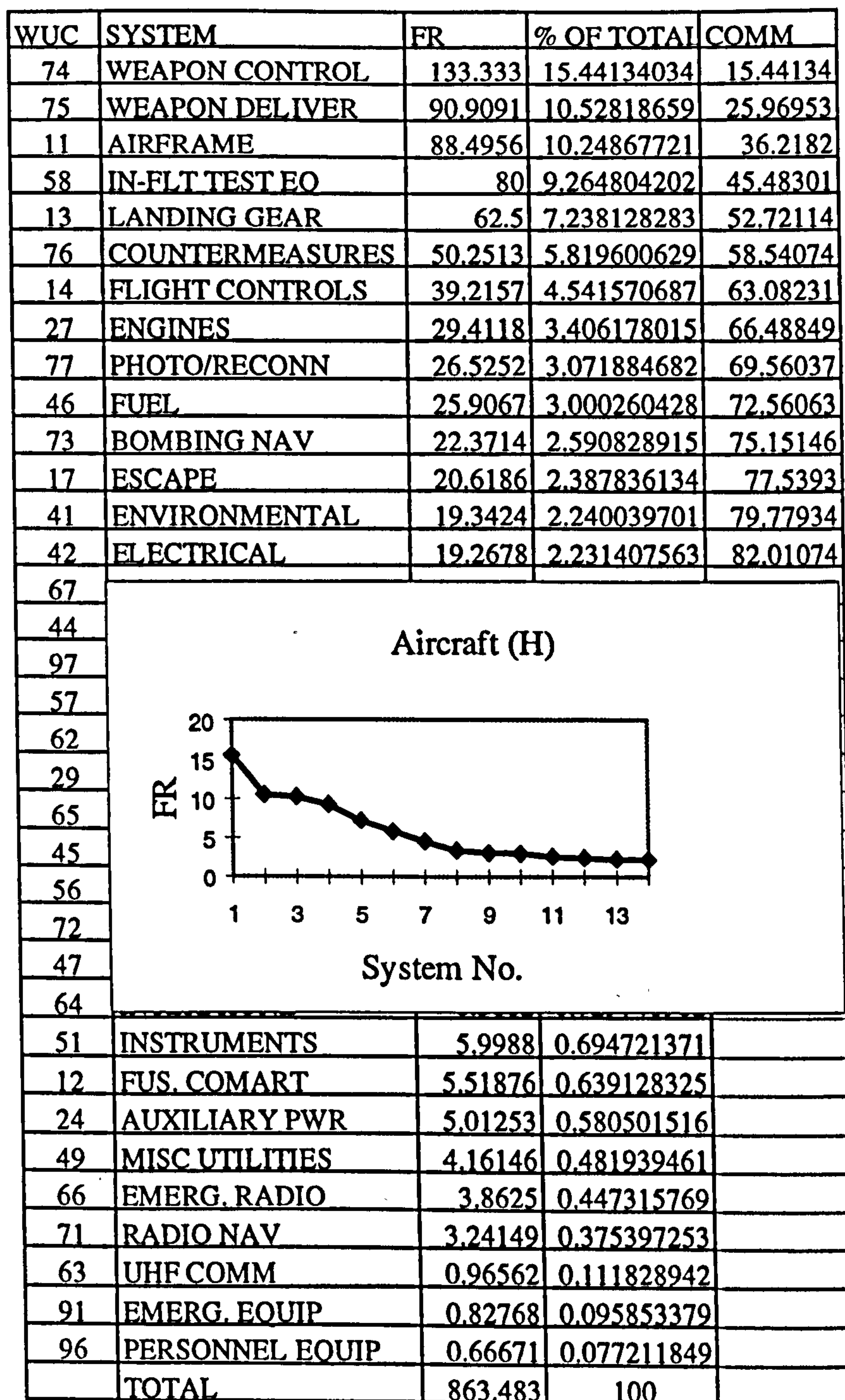


Fig. 3.6 Sample of Pareto Analysis.

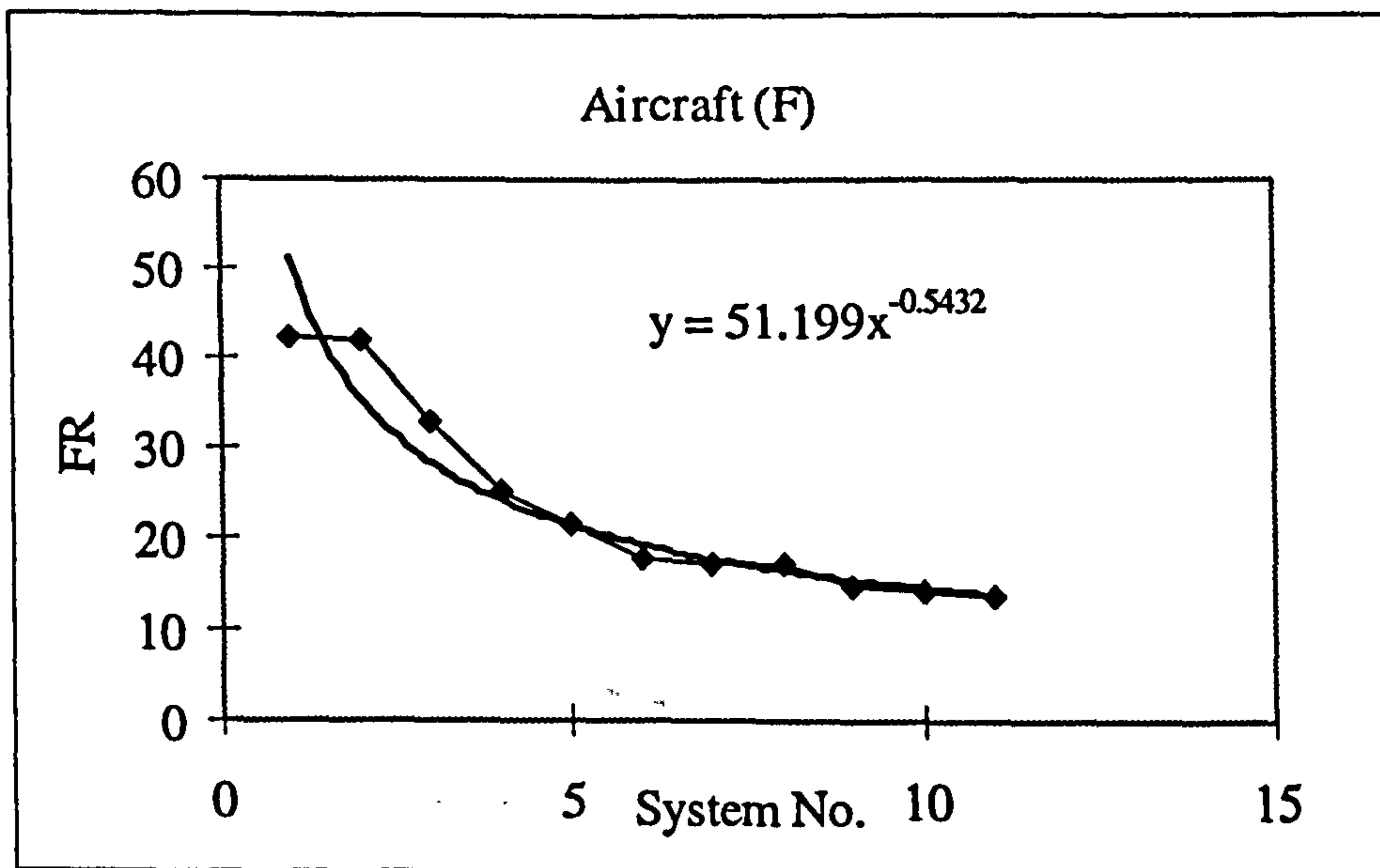


Fig. 3.7 Pareto chart and equation of aircraft (F)

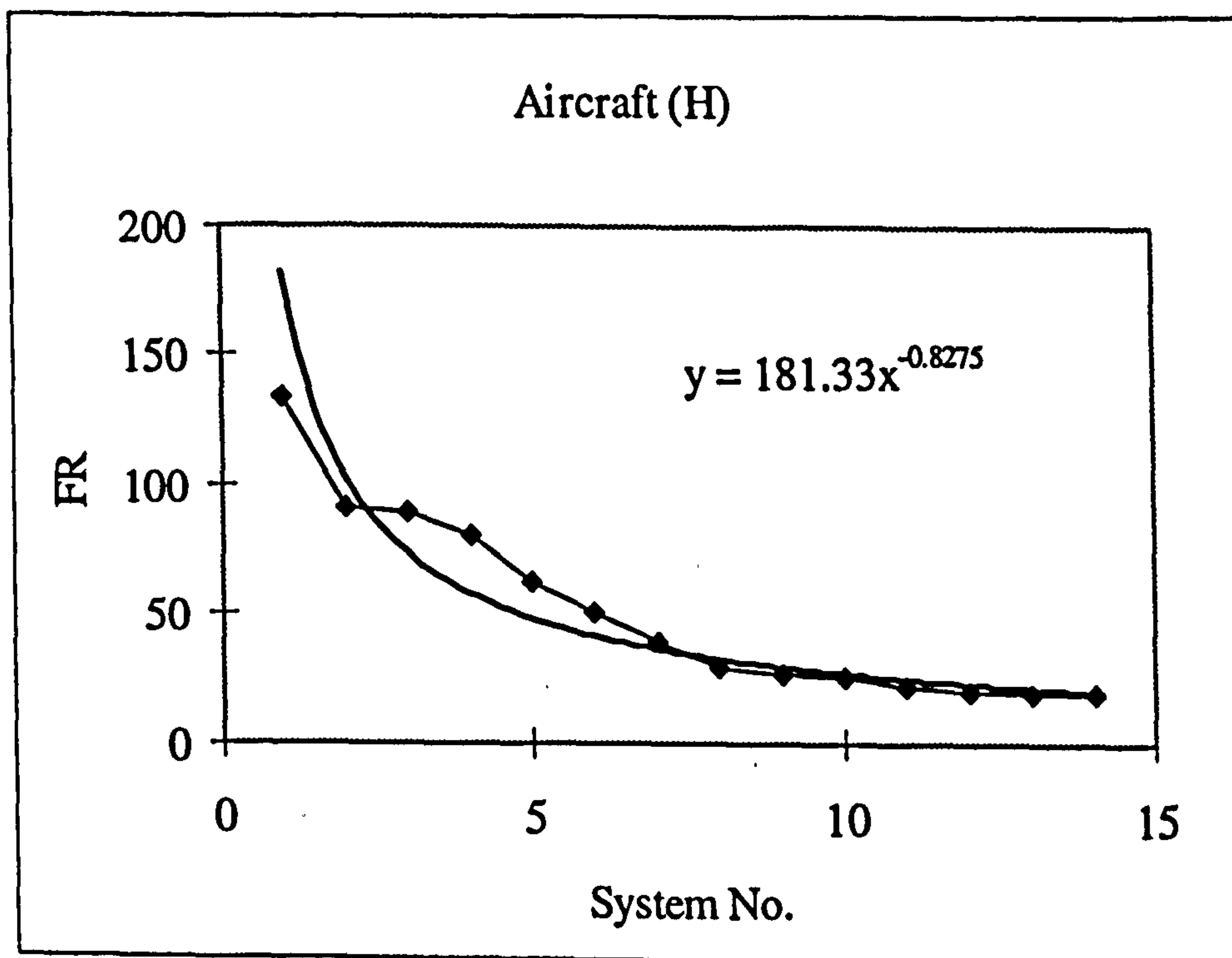


Fig. 3.8 Pareto chart and equation of aircraft (H)

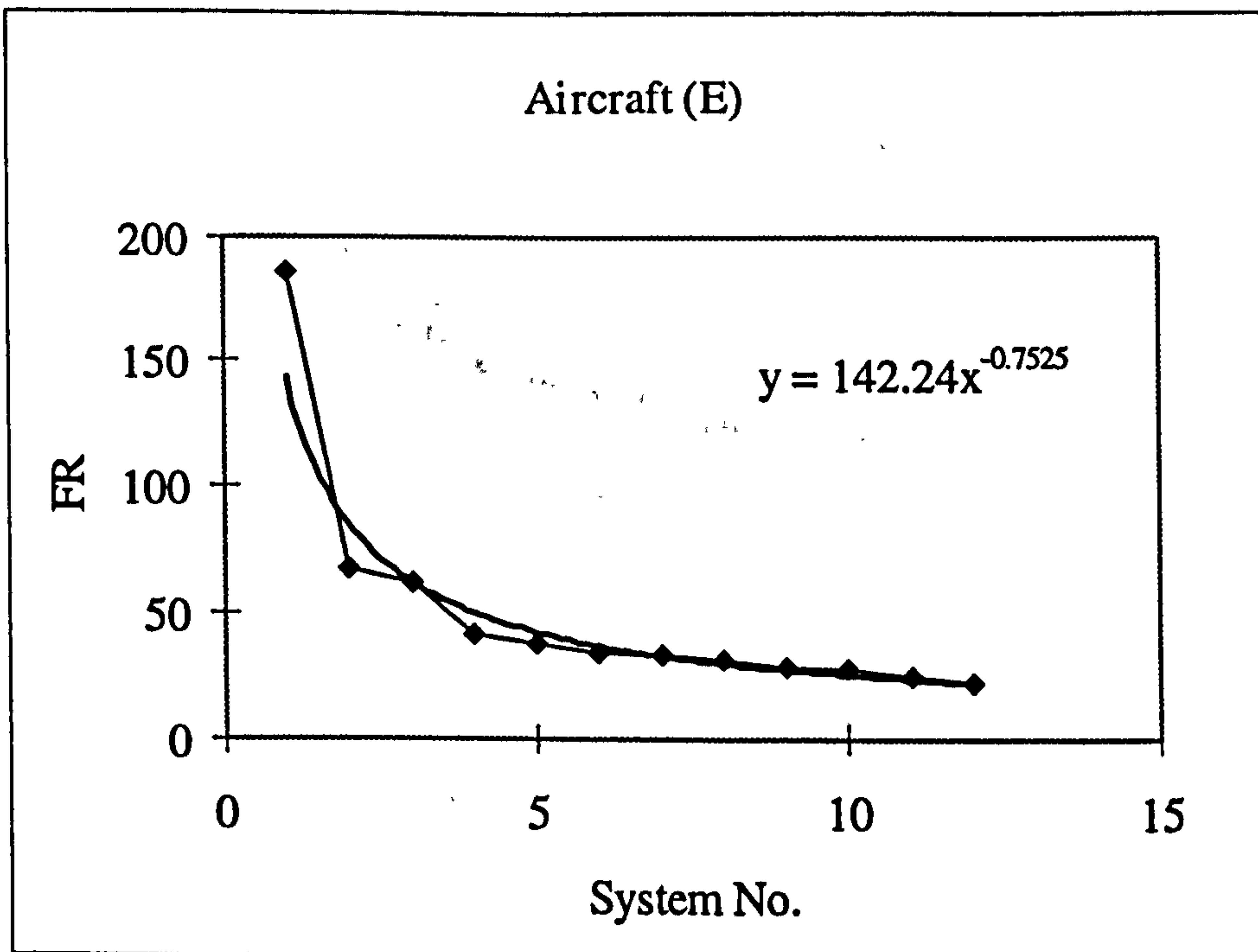


Fig. 3.9 Pareto chart and equation of aircraft (E)

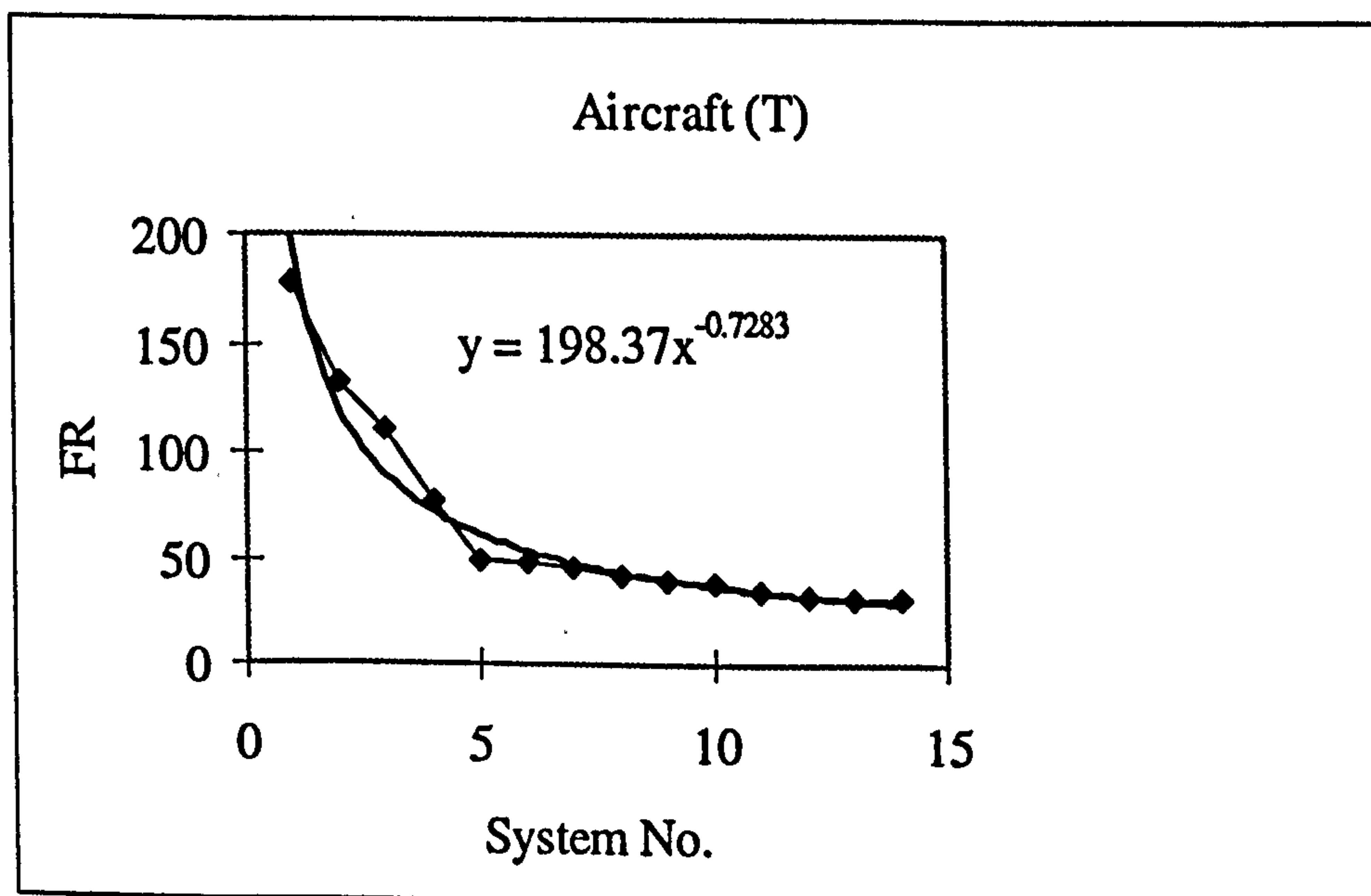


Fig. 3.10 Pareto chart and equation of aircraft (T)

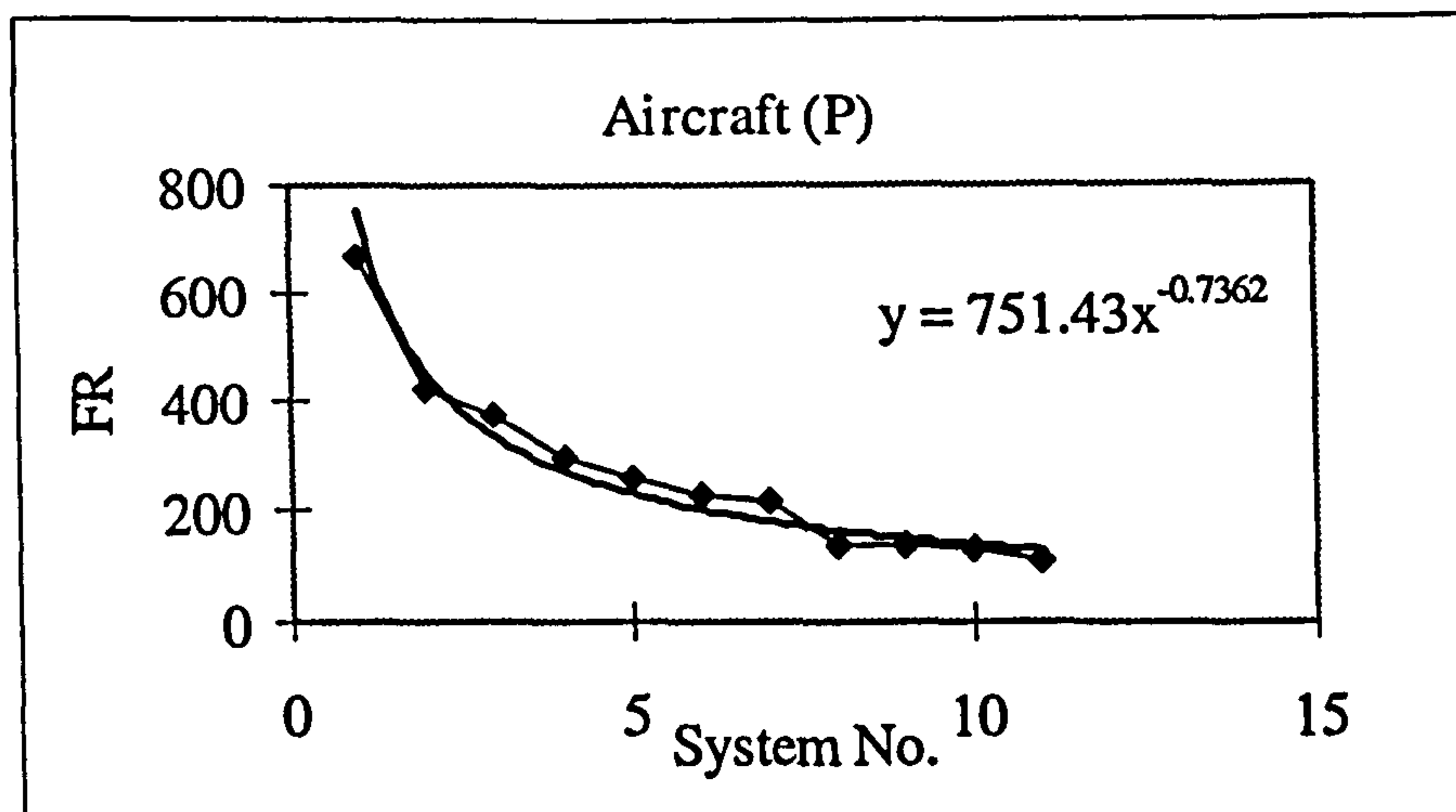


Fig. 3.11 Pareto chart and equation of aircraft (P)

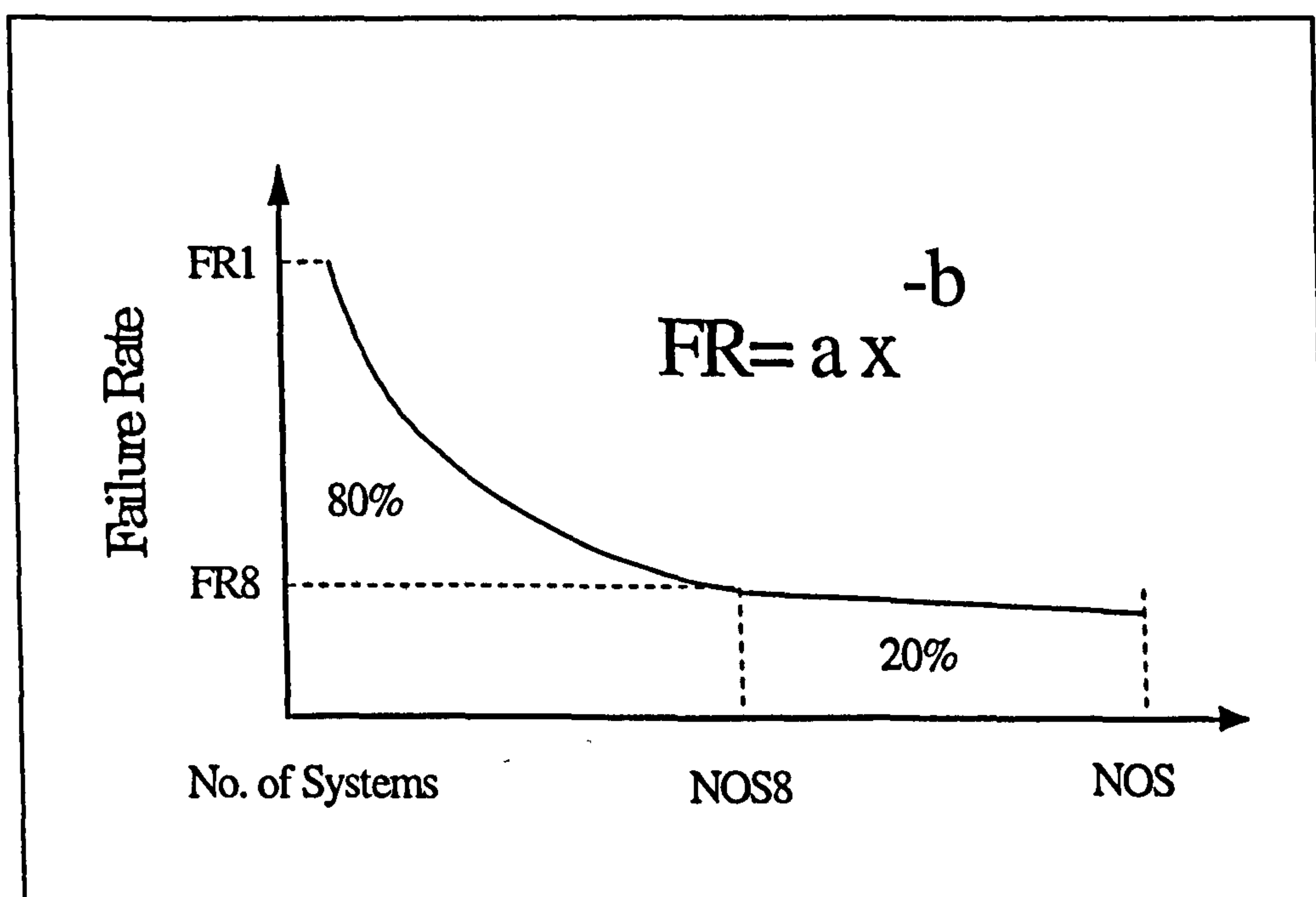


Fig. 3.12 Parameters that defines Pareto distribution curve.

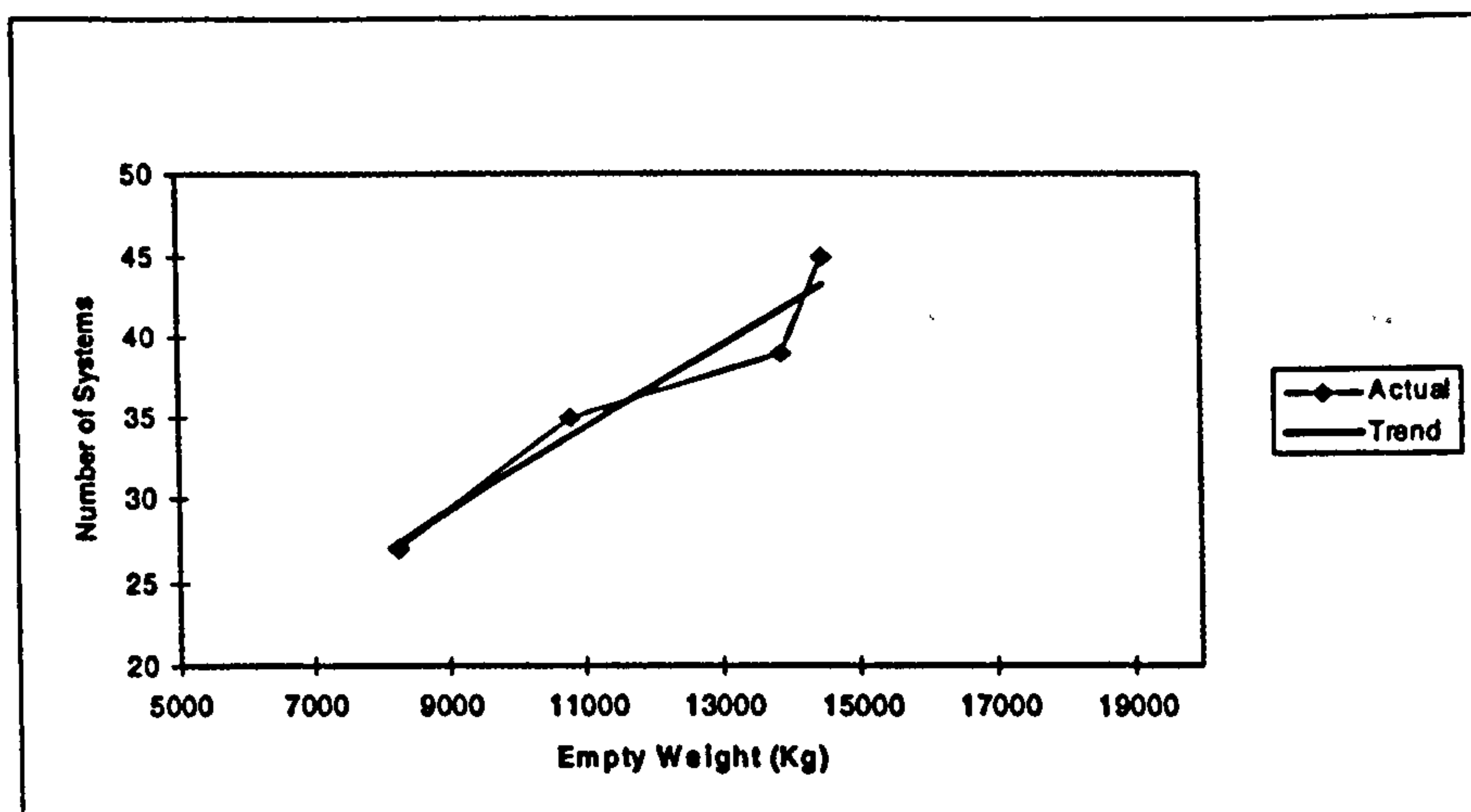


Fig. 3.13 Number of systems

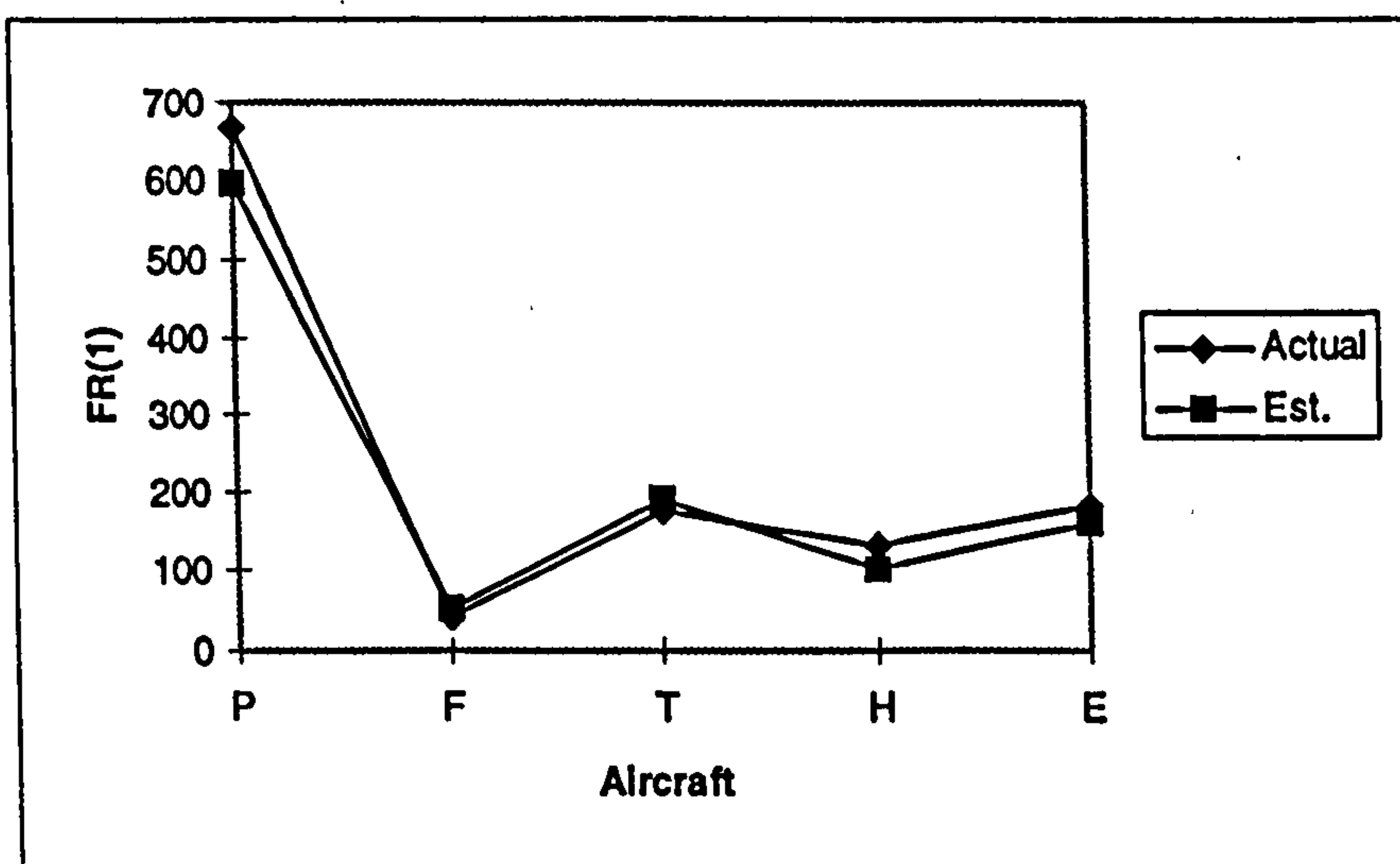


Fig. 3.14 Actual and estimated values of FR(1)

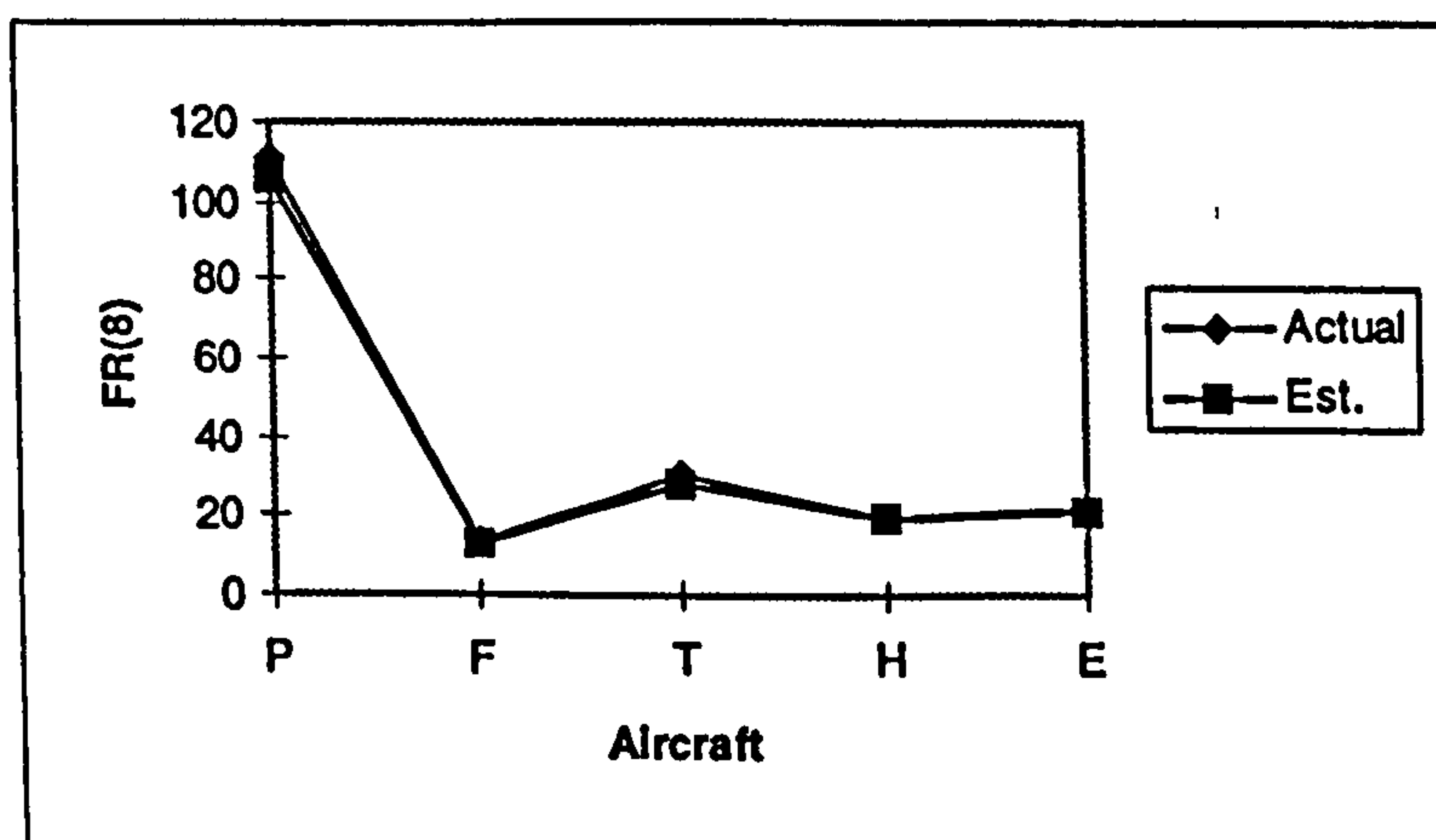


Fig. 3.15 Actual and estimated values of FR(8)

Chapter Four

Interactive Survivability/Vulnerability Assessment

4.1 Introduction to Aircraft Survivability

Today, combat aircraft survivability is near the top of the priority list of design disciplines for combat aircraft. Designing survivable combat aircraft requires design tools and knowledge of the fundamentals of the survivability discipline. The fundamentals are founded on two major principles of survivability enhancement: try not to get hit (susceptibility reduction), but if you do get hit, don't die (vulnerability reduction). To evaluate the effectiveness of survivability design features, the designer must have tools to quantify this discipline. Aircraft combat survivability is defined (Ref. 13) as "the capability of an aircraft to avoid and/or withstand a man-made hostile environment". The inability of an aircraft to avoid the radars, guns and guided missiles is referred to as the susceptibility of the aircraft. An aircraft's susceptibility can be measured by the probability the aircraft is hit while on its mission, P_H . The inability of an aircraft to withstand any hits by the hostile environment is referred to as the vulnerability of the aircraft. An aircraft's vulnerability can be measured by the conditional probability the aircraft is killed given a hit, $P_{K/H}$. The survivability of an aircraft can be measured by the probability of survival, P_S , which depends upon the aircraft susceptibility and vulnerability according to the equation:

$$P_S = 1 - P_H P_{K/H}$$

Thus, survivability is enhanced when susceptibility and vulnerability are reduced. Estimating the aircraft's (P_d) susceptibility from the conceptual design requires complex codes which are highly classified. The susceptibility has been incorporated in the MSM as a user-defined value. This chapter contains a brief description of the fundamentals of the aircraft vulnerability discipline. It also presents an interactive vulnerability assessment methodology to be incorporated at the early design stage.

4.2 Aircraft Vulnerability

In this section, a brief description of aircraft vulnerability will be presented. More details of this design discipline can be found in the MIL-STD-2069 which describes the standard survivability requirements for an aircraft program, (Ref. 14). Also a text book has been published which presents this discipline as a teaching subject in the Aeronautical Engineering education programs, (Ref. 13). An aircraft consists of many components, each of these individual components has a level of vulnerability. Consequently, each component's vulnerability contributes in some measure to the overall vulnerability of the aircraft. The critical components on aircraft are those which, if either damaged or destroyed, would lead to an aircraft kill. The quantification of the vulnerability of the individual components and the total aircraft vulnerability is known as vulnerability assessment. A vulnerability assessment is a required survivability program task and should be conducted early in the life of any aircraft development program. Once the vulnerability of each components has been quantified, design modification should be done to reduce the aircraft's vulnerability. This design task is called vulnerability reduction.

4.3 Identification of the Critical Components and their Damage-Caused Failure Modes

The general procedure for determining the critical components and the consequent effect of their damage to the aircraft is:

1. Selection of the aircraft kill levels to be considered.
2. Assembly of the technical and functional description of the aircraft.
3. Determination of the critical components of the aircraft and their damage-caused failure modes for the selected kill level.

4.3.1 Aircraft Kill Levels

The categories normally used in vulnerability assessments are the attrition kill and the mission abort kill. The attrition kill is a measure of the degree of aircraft damage that renders it incapable of being repaired or not economical to repair, so that it is lost from

the inventory. Because the elapsed time between the onset of damage and the eventual loss of the aircraft is an important parameter of vulnerability, four different attrition kill levels have been defined:

- (1) **KK kill:** Damage that will cause an aircraft to disintegrate immediately upon being hit. this is sometimes referred to as a catastrophic kill.
- (2) **K kill:** Damage that will cause an aircraft to fall out of manned control within 30 s after being hit.
- (3) **A kill:** Damage that causes an aircraft to fall out of manned control within 5 min after being hit.
- (4) **B kill:** Damage that causes an aircraft to fall out of manned control within 30 min after being hit.

The mission abort kill is the measure of the degree of aircraft damage that prevents the aircraft from completing its designated mission.

4.3.2 Critical Component Analysis

Critical component analysis consists of the following steps:

1. Identify the flight and mission-essential functions that the aircraft must perform in order to continue to fly and to accomplish its mission. Flight essential functions are those system and subsystem functions required to enable an aircraft to sustain controlled flight. Mission essential functions are those system and subsystem functions required to enable an aircraft to perform its designated mission.
2. Identify the major systems and subsystems that perform these essential functions.
3. Identify the system-essential functions relationship. Failure Mode and Effect Analysis (FMEA) could be used to identify the relationship between each possible type of individual component or subsystem failure mode and the performance of these essential functions.
4. Relate component or subsystem failure modes to combat-caused damage. The Fault Tree Analysis (FTA) is used to perform this step.

5. Develop a visual presentation of the list of critical components, known as the kill tree. The kill tree identifies the redundant and non-redundant critical components for the selection kill level.

4.3.3 Aircraft Damage-Caused Kill Modes

There are unlimited kinds of kill modes that an aircraft system or subsystem can experience. Some of the most important ones are listed in Table 4.1 (Refs. 13 and 14).

Fuel System	Fuel supply depletion - In-tank fire/explosion Void space fire/explosion - Sustained exterior fire - Hydraulic ram
Electrical System	Loss of electric power
Flight Control System	Loss of control power -Damage to control actuators - Damage to control surfaces - Damage to control rods
Propulsion System	Fuel ingestion - Inlet flow distortion - Component damage
Structural System	Structural removal - Penetration
Crew	Injury - Incapacitation - Death

Table 4.1 Some damage-caused kill modes.

4.4 Vulnerability Assessment

Vulnerability assessment is the process of determining numerical values for the measures of vulnerability. Vulnerability assessment is usually conducted at the detail design phase to evaluate a design project. This section presents the vulnerability assessment procedures as depicted from (Refs. 13 and 14).

4.4.1 Vulnerability Measures

Because of the wide nature and degree of lethality of air-defence systems, the vulnerability of an aircraft varies with the type of the threat encountered. If a hit on the aircraft must occur in order for a threat to be effective, such as a small arms projectile and a contact-fused High Explosive (HE) warhead, one measure of vulnerability is the conditional probability that the aircraft is killed, given a random hit on the aircraft ($P_{K/H}$). Another measure of vulnerability to impacting damage mechanisms is the aircraft vulnerable area (A_v). This is a theoretical threat-presented area that, if hit by a damage mechanism, would result in an aircraft kill. The vulnerable area of the i th component is defined as the product of the presented area of the component in the plane normal to the approach direction of the threat (A_{pi}) and the probability of kill of the component given a hit on the component ($P_{k/hi}$). Thus,

$$A_{vi} = A_{pi} P_{k/hi} \quad (4.1)$$

The kill probability of the i th component given a random hit on the aircraft ($P_{k/Hi}$) is the product of the probability the component is hit - given the hit on the aircraft - ($P_{h/Hi}$) and the probability the component is killed given a hit on the component ($P_{k/hi}$). Thus,

$$P_{k/Hi} = P_{h/Hi} P_{k/hi} \quad (4.2)$$

From Eq. (4.1) we have,

$$P_{k/hi} = A_{vi} / A_{pi} \quad (4.3)$$

When the hit on the aircraft is randomly located,

$$P_{h/Hi} = A_{pi} / A_p \quad (4.4)$$

and, hence combining Eq.(4.2) with (4.3) and (4.4)

$$P_{k/Hi} = A_{vi} / A_p \quad (4.5)$$

4.4.2 Nonredundant Components Without Overlap

Assume that the aircraft consists of (N) critical components whose functions are not duplicated by any other component. The components are arranged in such a manner that no one component overlaps any other component when viewed from a given aspect. Any hit on the aircraft takes place along a shotline that passes completely through the aircraft. Thus, no more than one component can be hit on any one shotline. As an example of such model, consider the aircraft shown in Fig. 4.1. This aircraft consists of three critical components, a pilot (C1), one fuel tank (C2), and one engine (C3). And none of these components overlap from this aspect. The probability of killing this aircraft, given a random hit on the presented area shown can be derived using the kill expression:

$$Kill = (C1) \text{ OR } (C2) \text{ OR } (C3) \dots\dots \text{OR } (C_N) \quad (4.6)$$

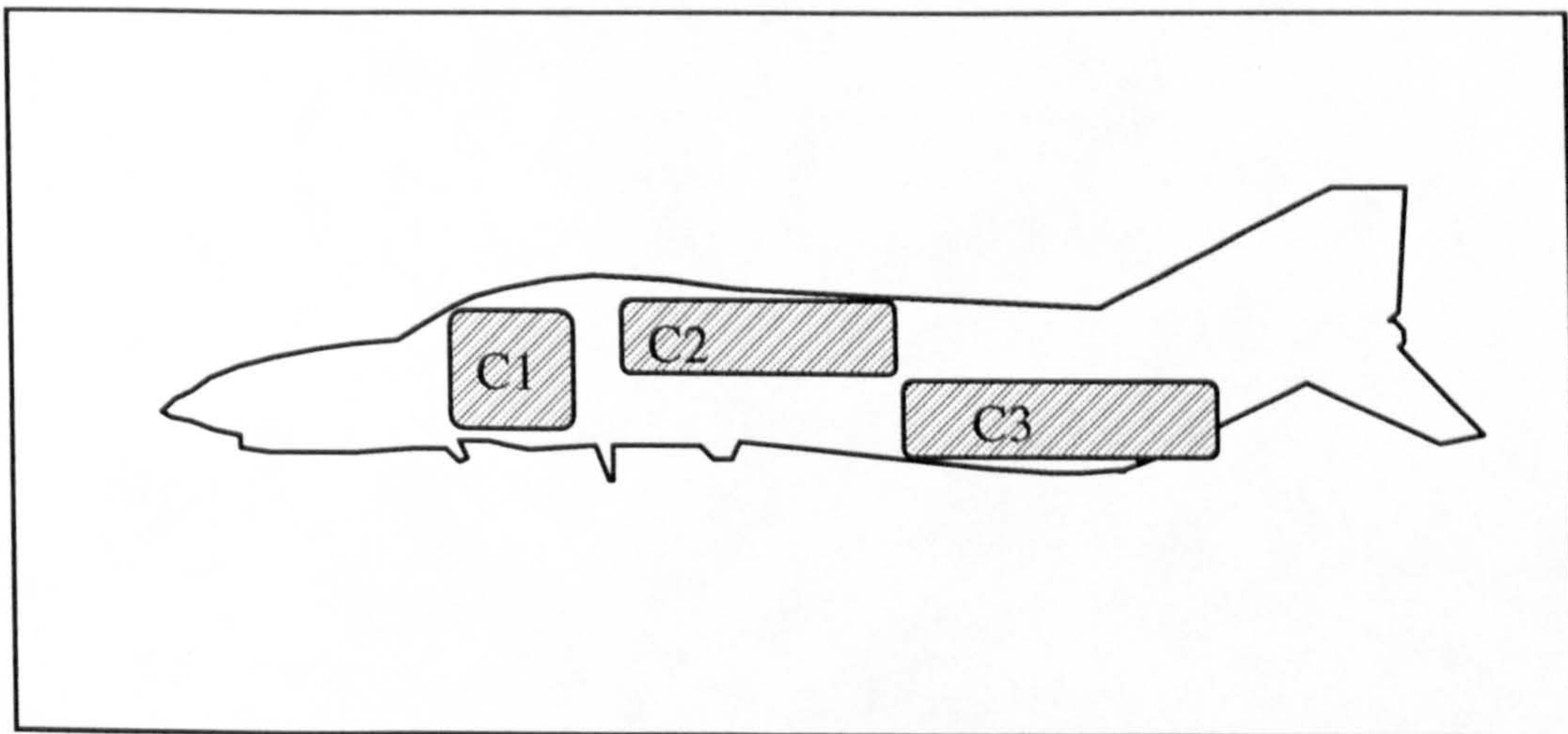


Fig. 4.1 Nonredundant components without overlap

Thus the probability of killing the aircraft given a hit on the aircraft is just the sum of the individual probabilities of killing each of the critical components given a random hit on the aircraft. Thus, for an aircraft kill given a hit,

$$P_{K/H} = P_{k/H1} + P_{k/H2} + \dots + P_{k/HN} = \sum_{i=1}^N P_{k/Hi} \quad (4.7)$$

in terms of the vulnerable area,

$$P_{K/H} = \sum_{i=1}^N \frac{A_{vi}}{A_p} = \frac{1}{A_p} \sum_{i=1}^N A_{vi} \quad (4.8)$$

4.4.3 Nonredundant Components With Overlap

In the real world and for certain threat aspects, components overlap others. Fig. 4.2 illustrates an overlap for the example aircraft. The dimension of the overlap area is determined by the overlap geometry. There can be any number of critical components along a shotline within the overlap region. Any kill to one of these critical components leads to an aircraft kill. So the overlap area (A_{po}) is now considered as a separate component and is given by:

$$A_{vo} = A_{po} P_{k/ho} \quad (4.9)$$

The vulnerable area of the overlap area contributes to the aircraft vulnerability in the same manner as the vulnerable areas computed in the nonredundant, no overlap case. However, overlapping also requires that the overlap area be subtracted from the total presented area of each overlapping component contributing to the overlap. The net effect of the component overlap can be a desirable reduction in the aircraft vulnerable area, provided the damage inflicted by the hit in the overlap area does not cause other problems.

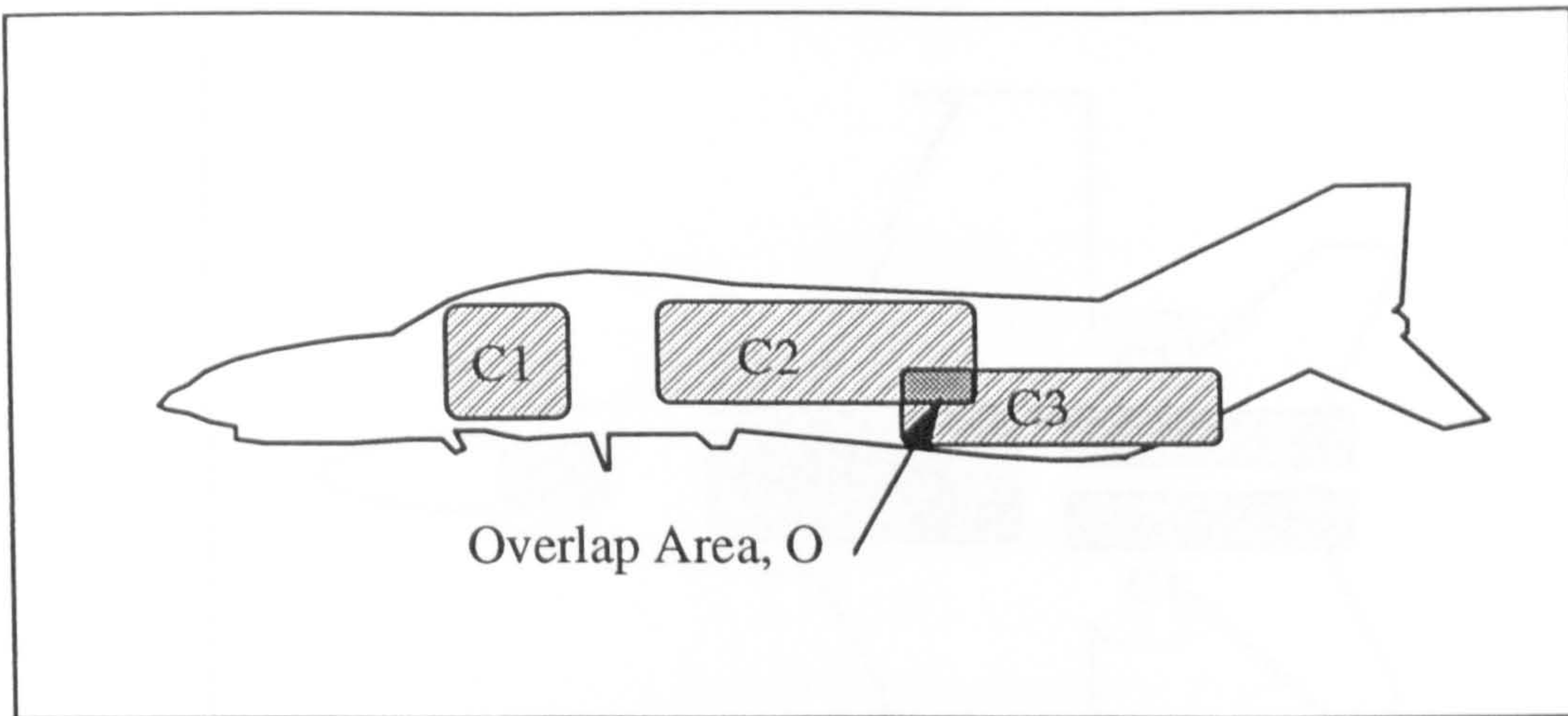


Fig. 4.2 Nonredundant components with overlap

4.4.4 Some Redundant Components Without Overlap

This case is shown by Fig. 4.3. The kill expression for the redundant aircraft model becomes:

$$Kill = (C1) \text{ OR } (C2) \text{ OR } ((C3) \text{ AND } (C4)) \quad (4.10)$$

The kill probability of the aircraft in this case is:

$$P_{K/H} = 1 - (1 - P_{k/H1})(1 - P_{k/H2})(1 - P_{k/H3}P_{k/H4}) \quad (4.11)$$

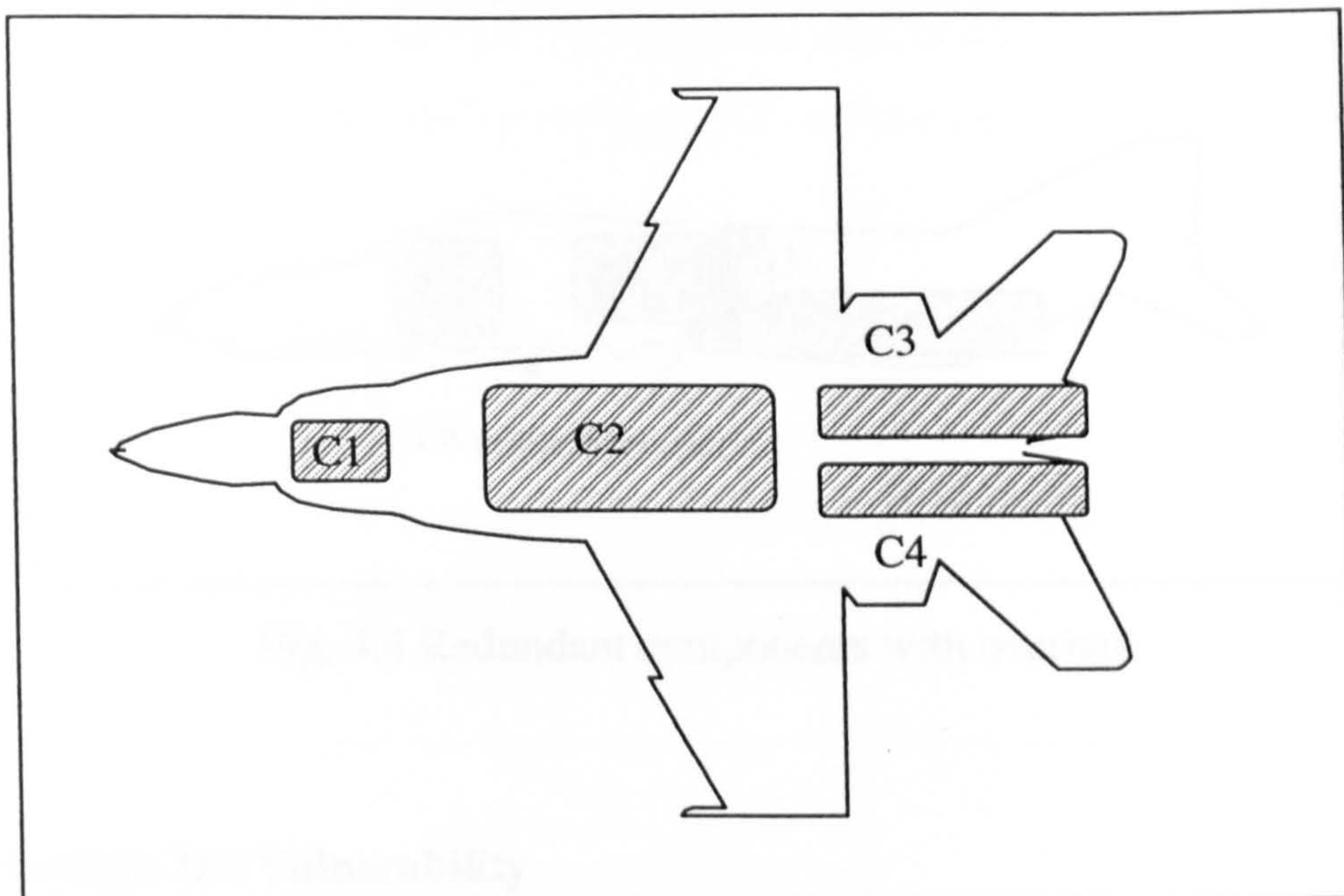


Fig. 4.3 Some redundant components without overlap

4.4.5 Redundant Components With Overlap

In this case a single hit penetrating the overlap area will have a probability of killing both redundant components, and hence the aircraft, Fig. 4.4. Thus, it will be necessary to add the vulnerable area of the overlap region to that of the nonredundant critical components. In essence, the overlap region becomes another critical component, as in the nonredundant model with overlap. For example, if there are two components among the components along the shotline, such as component (C2 & C3), the probability that both are killed, which is assumed to cause an aircraft kill, is equal to the product of their individual probabilities of kill.

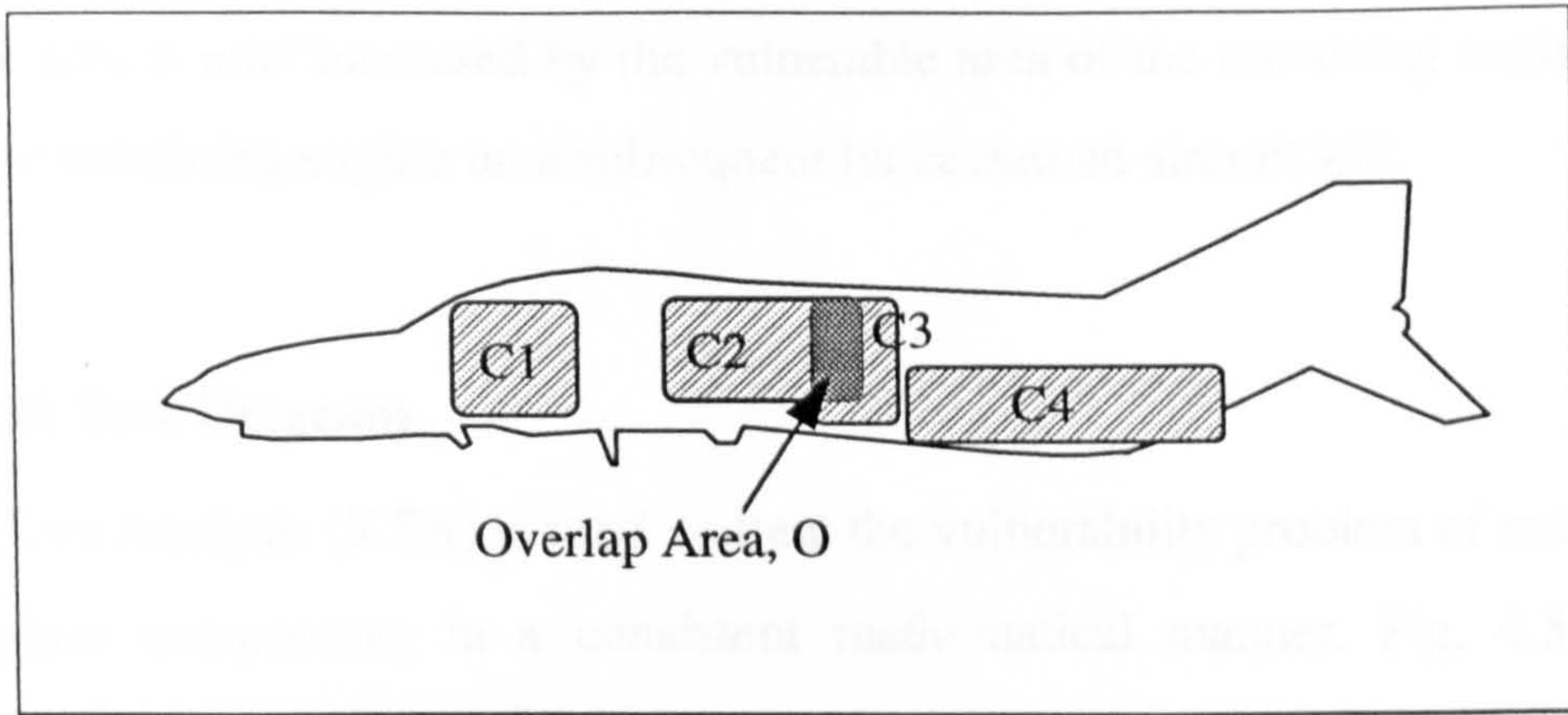


Fig. 4.4 Redundant components with overlap

4.4.6 Multiple Hit Vulnerability

The general vulnerability analysis case is to consider that the aircraft, if hit, will receive more than one hit. The probability that the i th component still survives after n random hits on the aircraft, denoted by $(\bar{P}_{s/Hi}^{(n)})$, is equal to the product of the component survival probabilities for each of the n hits on the aircraft. Thus,

$$\bar{P}_{s/Hi}^{(n)} = \bar{P}_{s/Hi}^{(1)} \bar{P}_{s/Hi}^{(2)} \cdots \bar{P}_{s/Hi}^{(n)} = \prod_{j=1}^n P_{s/Hi}^{(j)} \quad (4.12)$$

where $(P_{s/Hi}^{(j)})$ is the probability the i th component survives the j th hit on the aircraft. The probability the aircraft is killed after n hits is :

$$\bar{P}_{K/H}^{(n)} = 1 - \bar{P}_{S/H}^{(n)} = 1 - \prod_{j=1}^n (1 - P_{K/H}^{(j)}) \quad (4.13)$$

In the multiple hit assessment, the redundant aircraft model has to be viewed differently. If the redundant aircraft takes the first hit in the vulnerable area of a redundant component, the aircraft is not killed, but the aircraft vulnerable area will be increased for the second hit. For example, if one of two engines is killed in the first hit, the aircraft

vulnerable area is now increased by the vulnerable area of the remaining engine, because a kill of the remaining engine on a subsequent hit causes an aircraft kill.

4.4.7 Kill Tree Diagram

The Kill Tree Analysis (KTA) is used to treat the vulnerability problem of redundant and nonredundant components in a consistent mathematical manner. Fig. 4.5 shows an aircraft with three critical components.

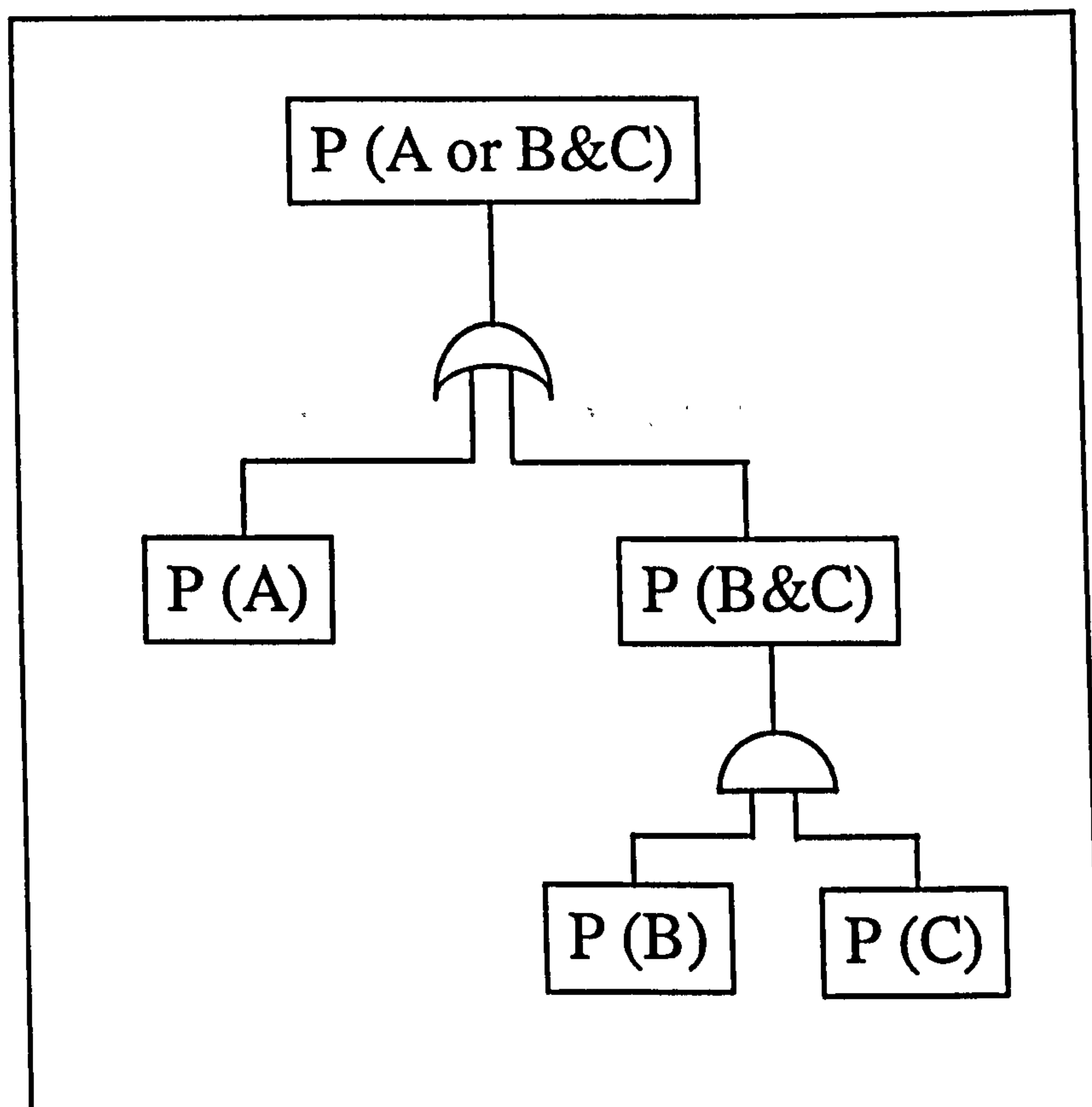


Fig. 4.5 Critical components tree.

Component (A) is nonredundant, while components (B) and (C) are redundant. The probability of killing component (B) and (C) constitutes two independent events, that is, each component has its certain projectile mass and velocity combination for a kill. So the probability that both will be killed is :

$$P_{k(bc)} = P_{kb} P_{kc} \quad (4.14)$$

When a given aspect/view does not possess a homogenous area containing portions of components B and C, then for a single shot, (P_{kb}) and (P_{kc}) are mutually exclusive events, hence,

$$P_{k(bc)} = P_{kb} P_{kc} = 0 \quad (4.15)$$

The aircraft kill probability is then given by:

$$P_{k(aircraft)} = P_{ka} + P_{k(bc)} - P_{k(abc)} \quad (4.16)$$

4.5 Vulnerability Results Presentation

There are two standard aircraft aspects/views scenarios for vulnerability assessment and analysis. For a minimum level, the six major aspects shown in Fig. 4.6 are usually considered for each kill level. The 26-views shown in Fig. 4.7 are usually considered when a more detailed or a computerised analysis is performed. Each view represents the direction resulting from a 45-degrees increment along all the three principle directions.

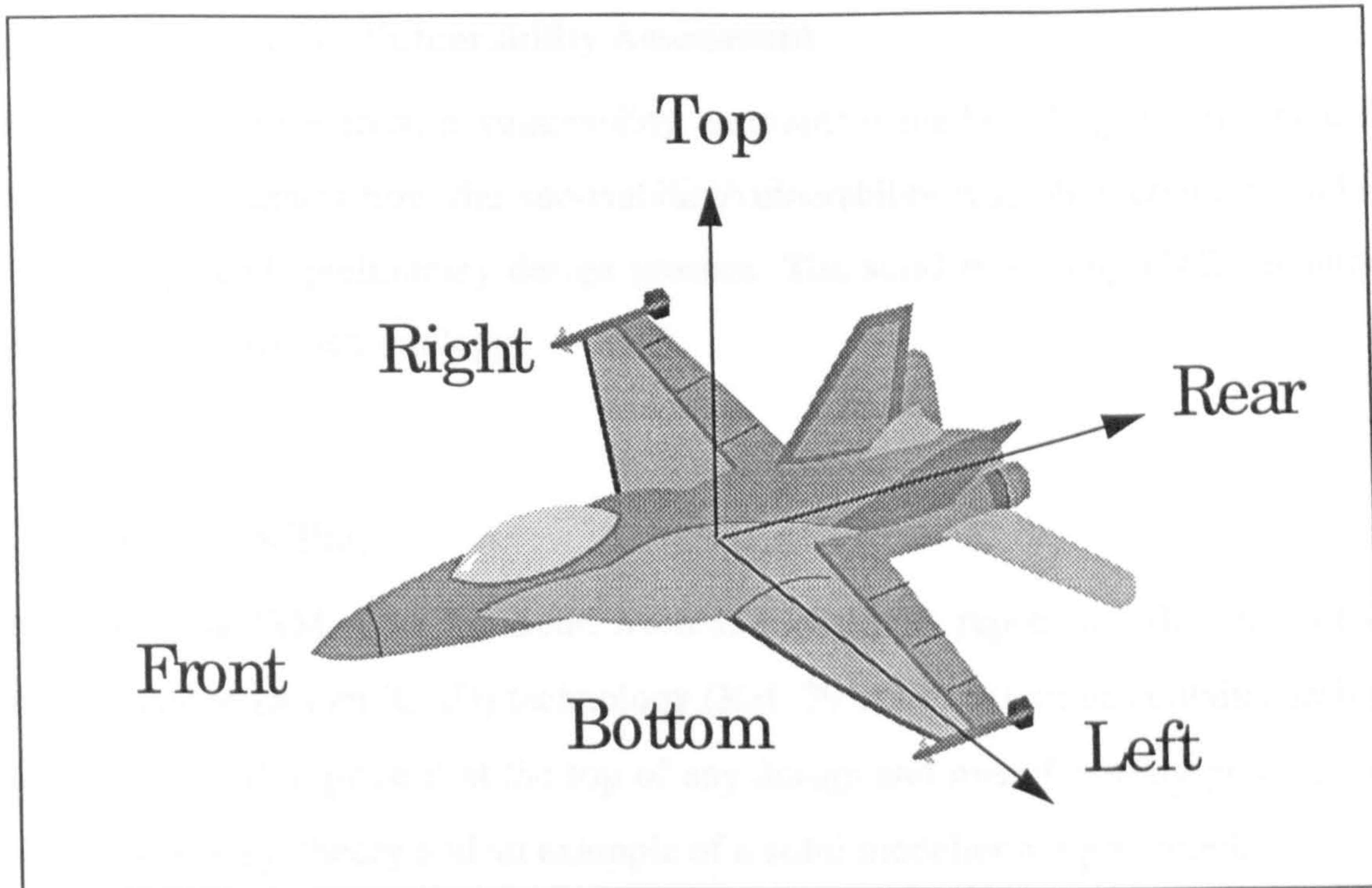


Fig. 4.6 The six aircraft aspects

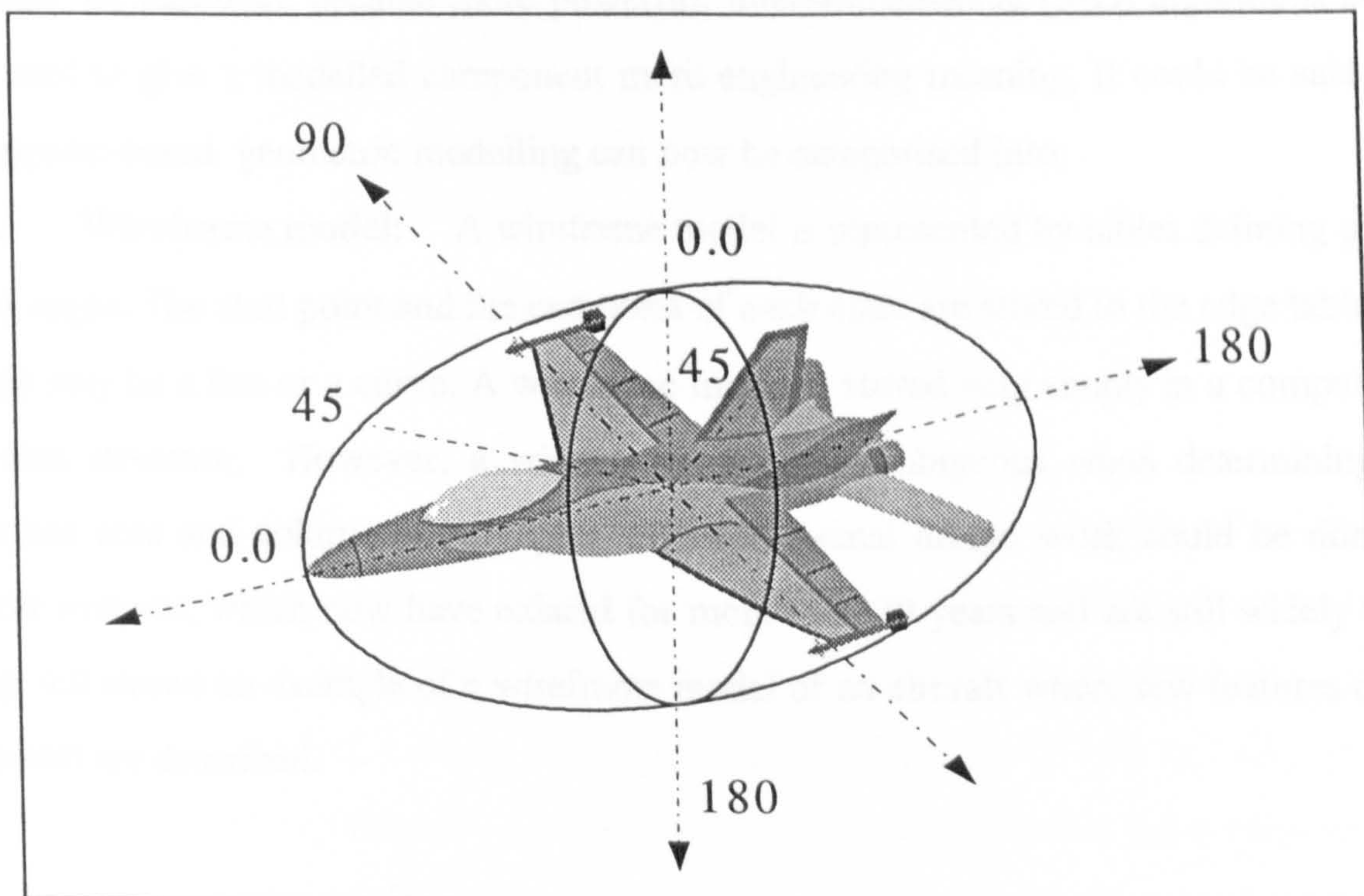


Fig. 4.7 The 26 aircraft aspects

4.6 The Interactive Vulnerability Assessment

In these following sections, a vulnerability assessment methodology is presented. This methodology illustrates how the survivability/vulnerability discipline could be linked to the conceptual and preliminary design process. The solid modelling CAD technique is used to provide this methodology.

4.7 Solid Modelling

Solid Modelling (SM, also for Solid Model) techniques represents the state-of-art in Computer Aided Design (CAD) technology (Ref. 29). SM technique contains design and analysis features that place it at the top of any design and manufacturing process. In this section, the history, theory and an example of a solid modeller are presented.

4.7.1 The Evolution of Solid Modelling

CAD technology has undergone enormous changes in the past two decades. CAD systems began as a two-dimensional (2-D) automated drafting, not computer aided design. As hardware became more powerful, three-dimensional (3-D) algorithms could be used to give a modelled component more engineering meaning. It could be said that computer-based geometric modelling can now be categorised into:

A. Wireframe model: A wireframe model is represented by tables defining points and edges. The start point and the end point of each edge are stored in the edge table. An edge may be a line or a curve. A wireframe model is stored very simply in a computer as a data structure. However, a wireframe model is ambiguous when determining the surface area and volume of an object, Fig. 4.8. Actual design work could be done on these systems, which now have existed for more than 20 years and are still widely used. Fig. 4.9 shows an example of a wireframe model of an aircraft where few features of the aircraft are described.

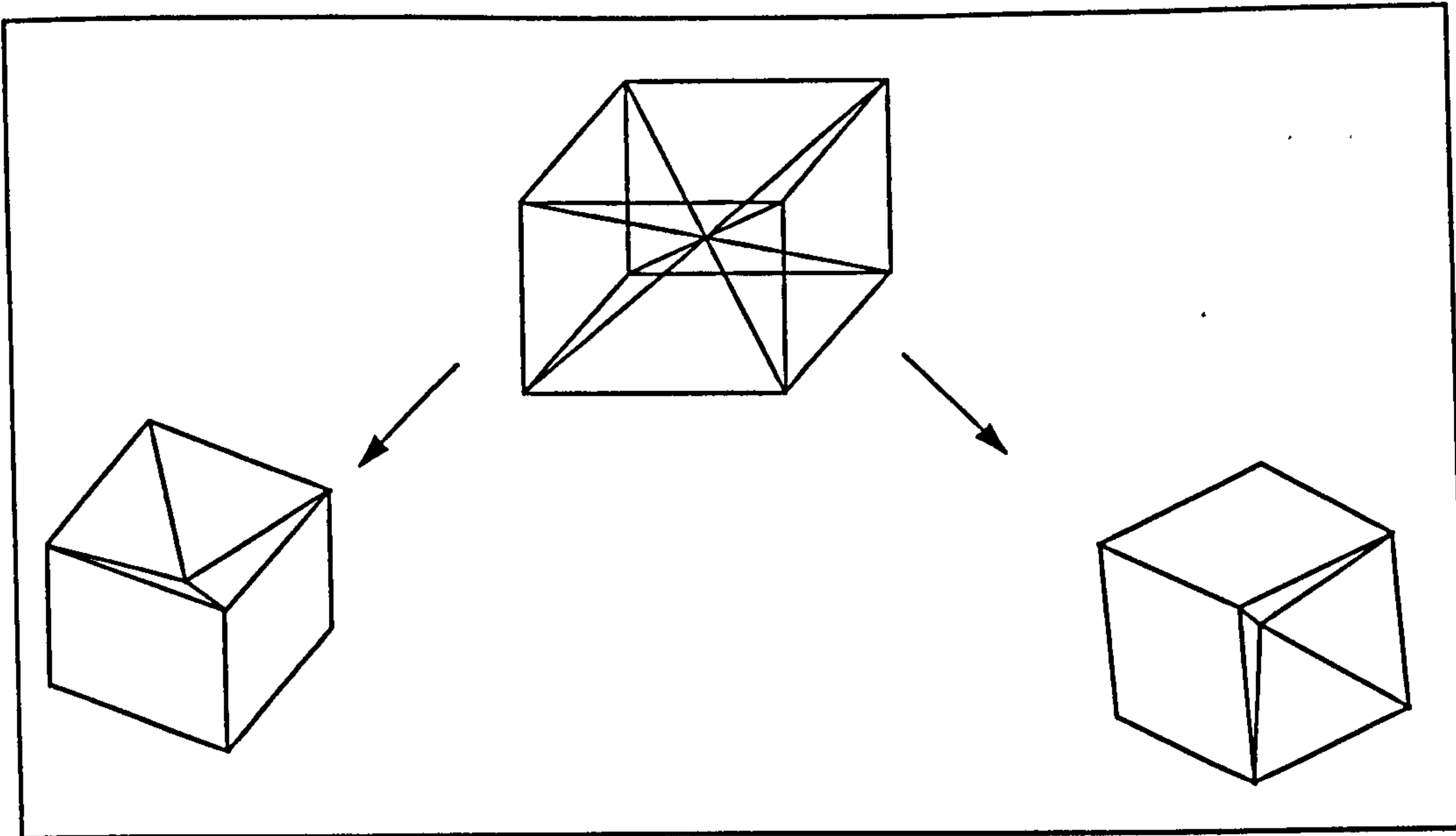


Fig. 4.8 Wireframe ambiguity

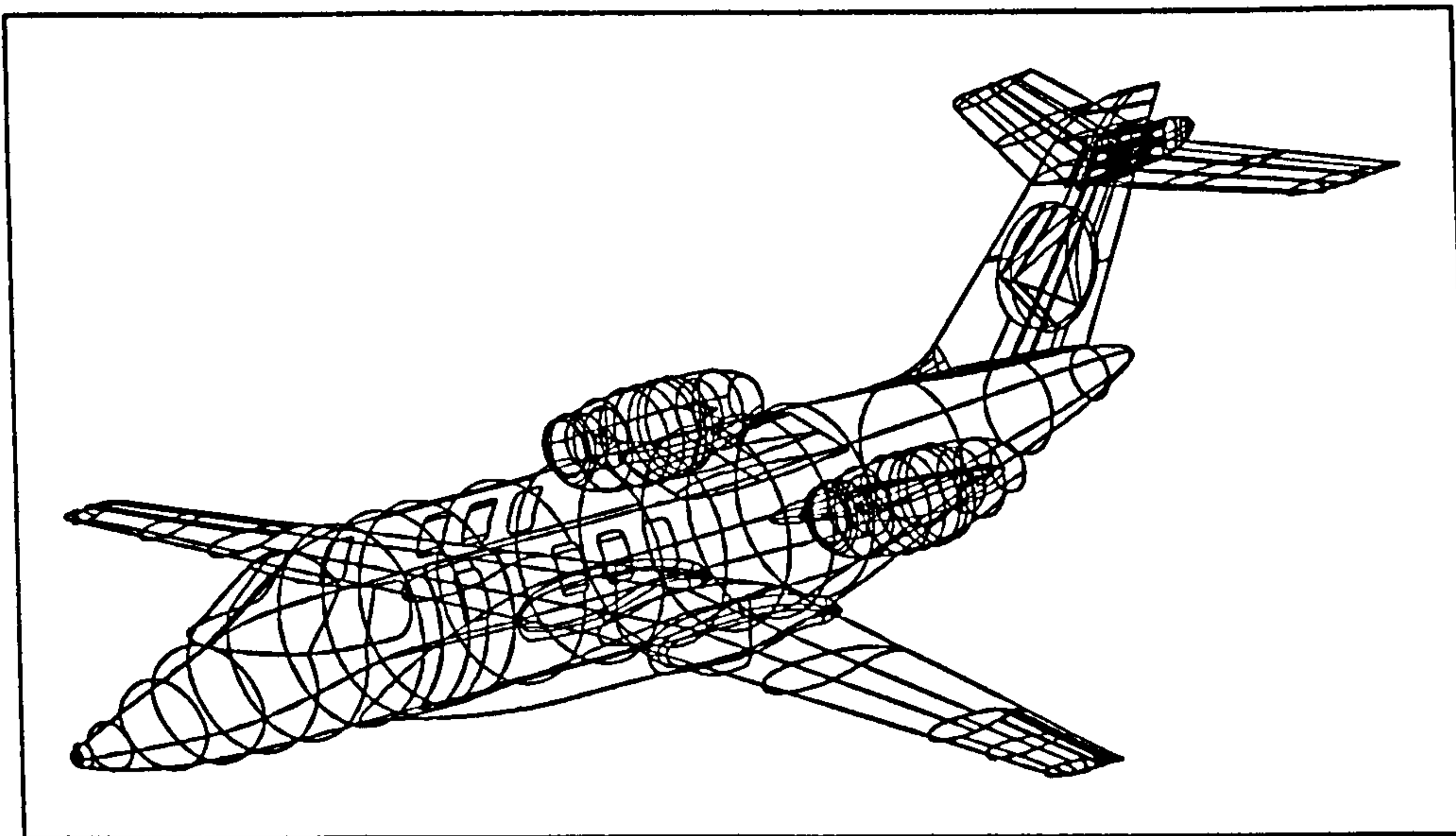


Fig. 4.9 A wireframe aircraft model

B. Surface model: A surface model is represented by tables of edges and points, as is a wireframe model, plus a table of faces. The face table stores information on which edges are attached to each face. Fig. 4.10 shows an example of a surface model. In the face table, a record of face (F1) stores edges (E1,E2,E3 and E4). In most conventional CAD systems for free-form surfaces, surface models have been used as internal representations. However, a surface model is a set of faces, and as such is ambiguous when determining the volume of an object. With surfaces being defined to the computer, it could figure out that one “thing” was behind another “thing”. Surface

modelling systems greatly reduced the ambiguity of 3-D wireframe technology. They were also a major aid to the designers, who could now use the systems more for design than for drafting. The pictures could serve as the basis for discussions and design reviews with other functions. Figure 4.11 shows a surface model of the same aircraft as Fig. 4.9.

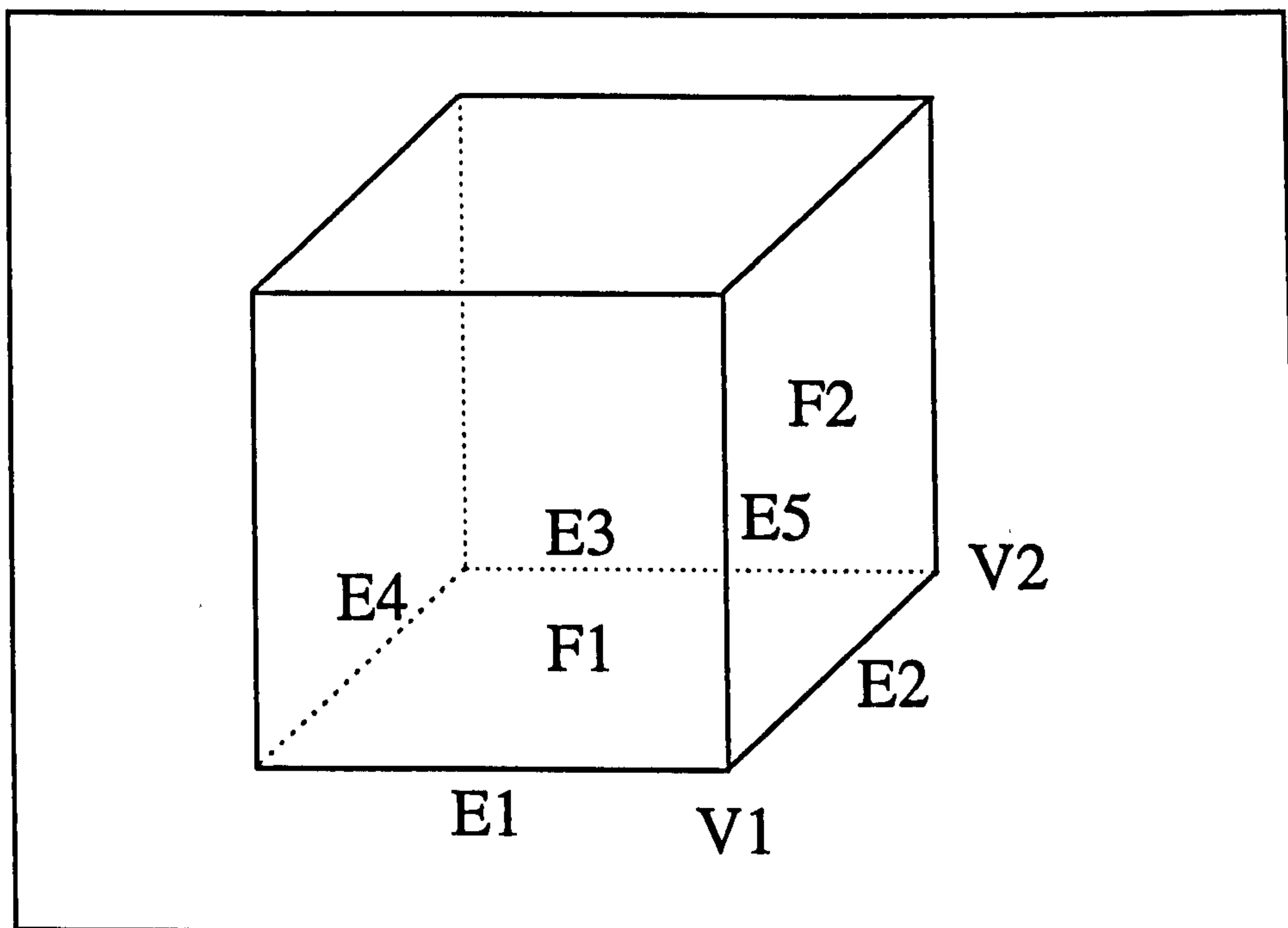


Fig. 4.10 Surface model topological relationships.

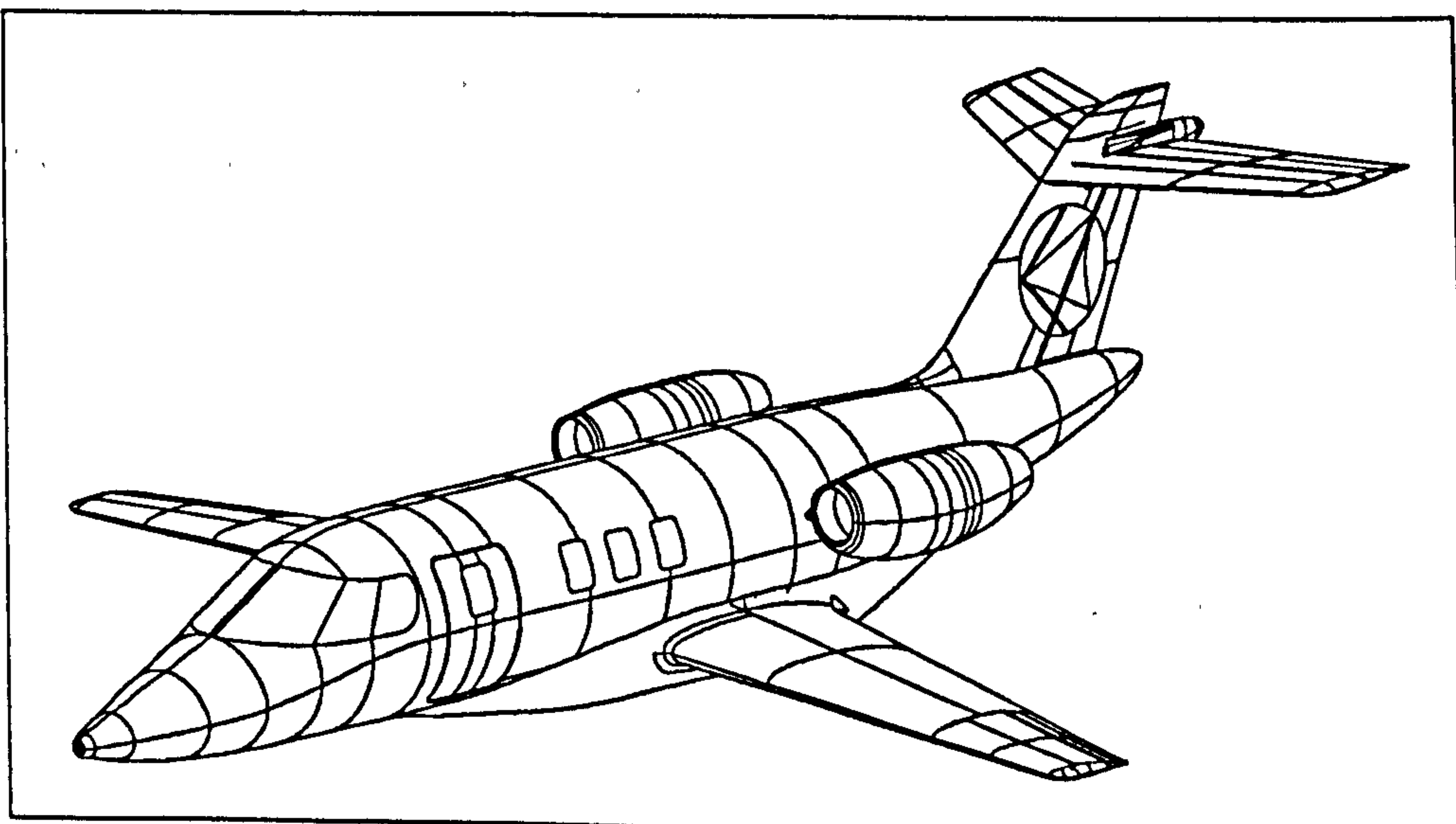


Fig. 4.11 Surface model of an aircraft.

C. Boundary representation model: A boundary representation, (B-rep) of a model is a surface model of more geometrical details. It has information on the *faces*, *edges* and *vertices* in a surface model, plus topological information which defines the relationships between the faces, edges and vertices. As an example of topological information, edge (E2) of Fig. 4.10 runs between vertices (V1) and (V2), and meets faces (F1) and (F2). Vertex (V1) is connected to edges (E1, E2, and E5). Because boundary representations include such topological information, a solid is represented as a closed space in 3-D space.

D. Solid model: A solid model is a computer description of closed, solid, 3-D shapes represented by an analytical framework within which the 3-D material can be completely and unambiguously defined (Ref. 30). With these added features, the computer could automatically calculate the volume enclosed by those surfaces. Given a density of the material enclosed by the surfaces, it could automatically provide all mass properties, including inertia and weight.

4.7.2 Solid Modelling Techniques

In any solid modeller system, standard solid modelling techniques are used to model a component, depending on its complexity. These techniques are:

1. Simple Primitive Shapes

These shapes are analytically well defined shapes. Among the ones used are:

Ellipsoid:

Referring to Fig. 4.12, an ellipsoid can be defined by specifying a vector (\vec{V}) from the origin to the centre of the ellipsoid, and by specifying three vectors ($\vec{A}, \vec{B}, \vec{C}$) which are mutually perpendicular, and whose magnitudes define the eccentricity of the ellipse. Thus,

$$|\vec{A}| = |\vec{B}| = |\vec{C}| \text{ defines a sphere.}$$

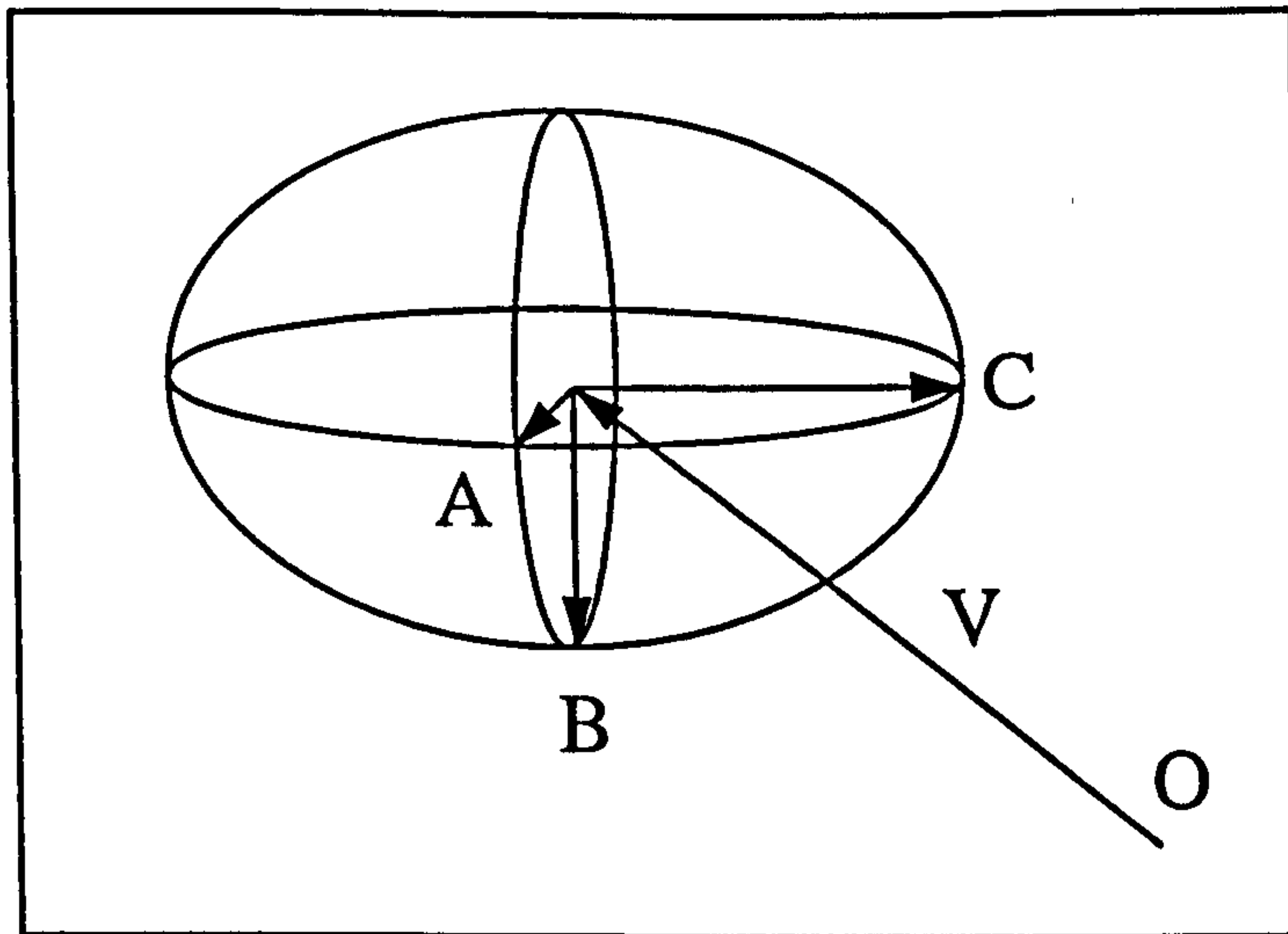


Fig. 4.12 Geometrical definition of an ellipsoid

Truncated General Cone:

Referring to Fig. 4.13, a truncated general cone can be defined by specifying a vector

(\vec{V}) from the origin to the centre of the base ellipse, two perpendicular vectors (\vec{A}) and (\vec{B}) which define the orientation and eccentricity of the lower ellipse, a vector (\vec{H}) which defines the height and slant of the cone, and two more perpendicular vectors (\vec{C}) and (\vec{D}) which define the orientation and eccentricity of the upper ellipse.

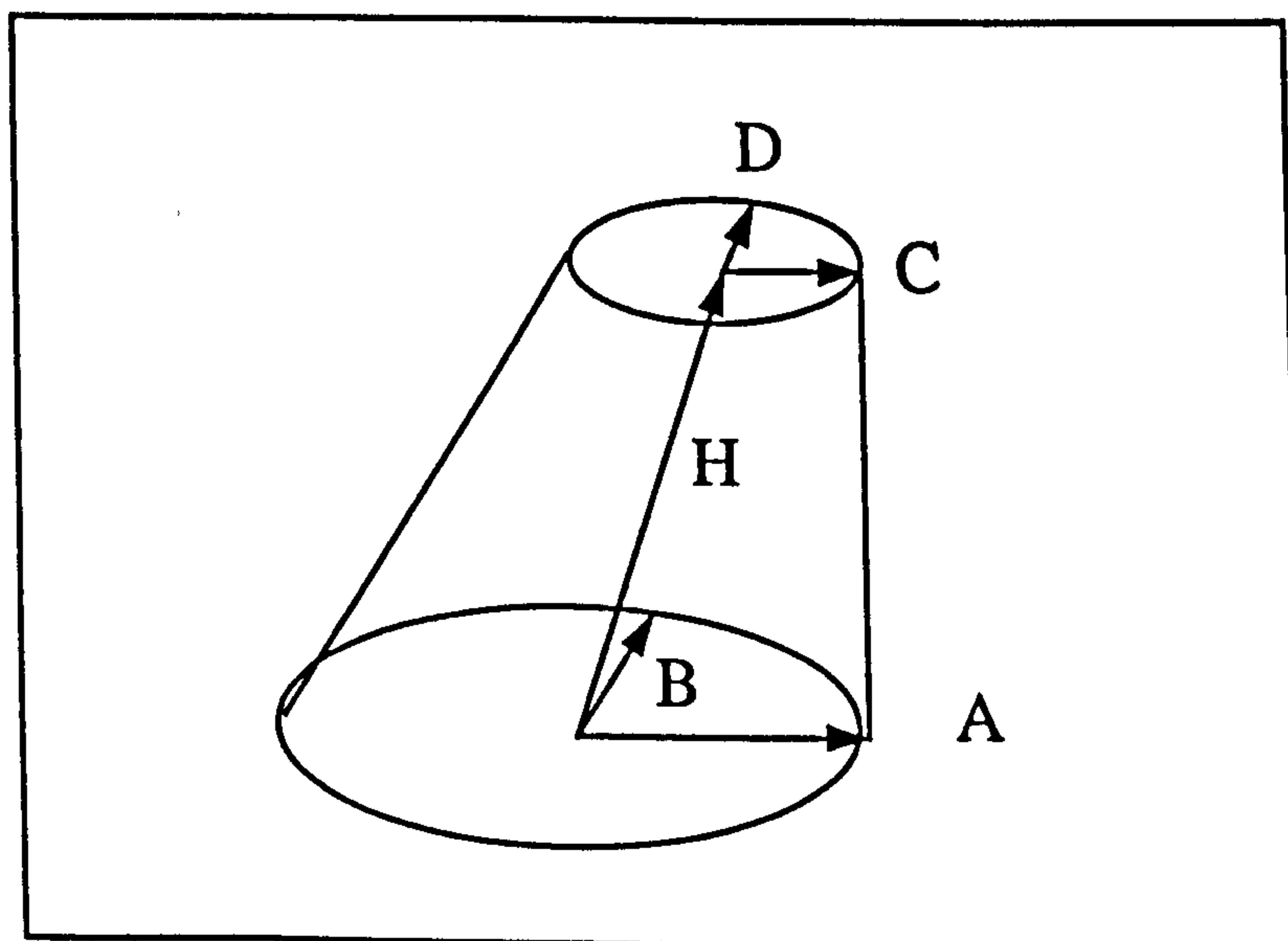


Fig. 4.13 Geometrical definition of a cone

Torus:

As shown in Fig. 4.14, a torus can be created by sweeping a circle of radius ($R2$) about an axis. The centre of the (swept) circle traces a circular path of radius ($R1$). The location and orientation of the torus is specified by its origin (O) and a directional vector(\vec{V}).

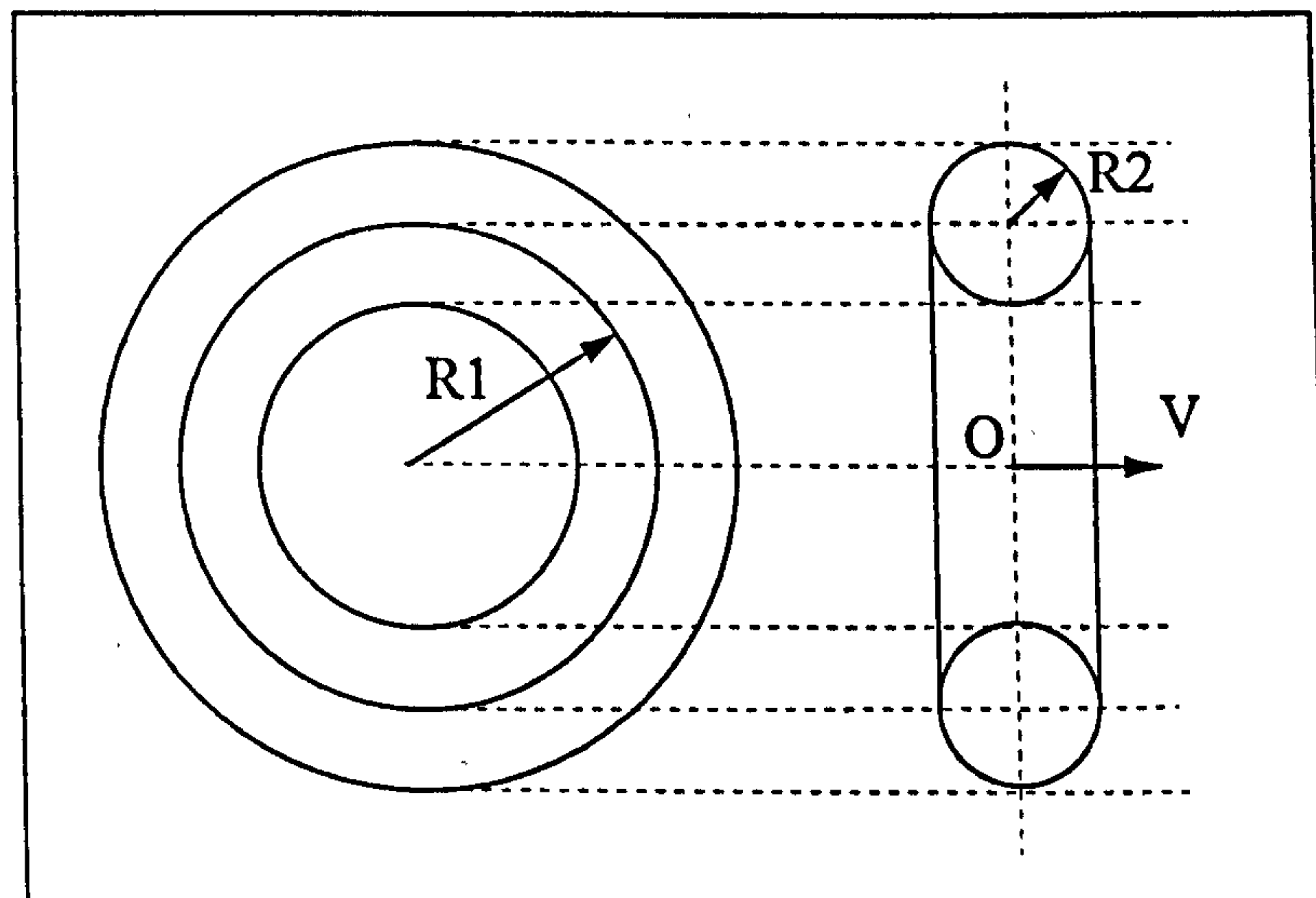


Fig. 4.14 Geometrical definition of a torus.

Box:

A solid box is created by specifying the origin of the box (O), an orientation vector (\vec{V}) and three variables which define the size of the box (i.e. width, length and height) as shown in Fig. 4.15.

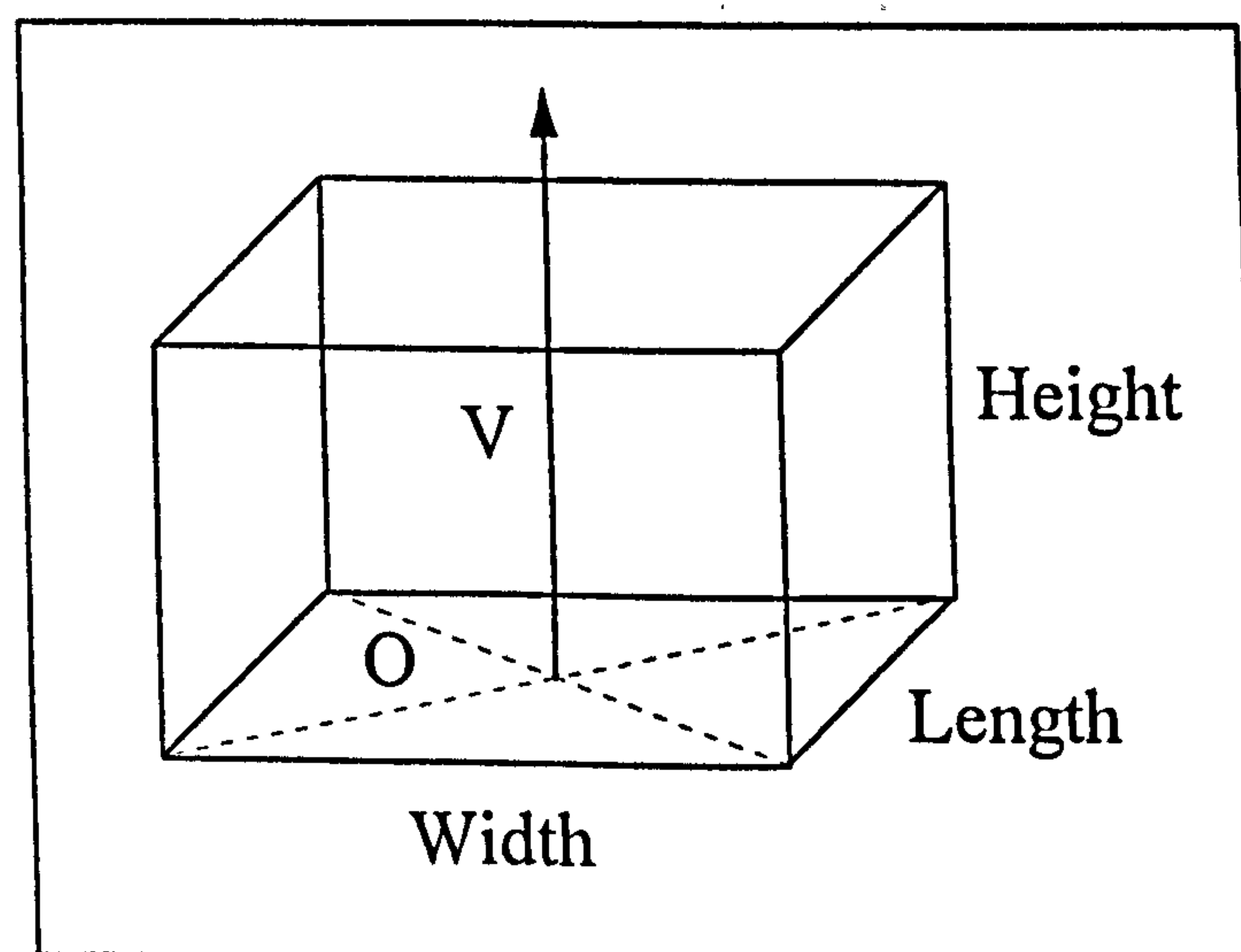


Fig. 4.15 Geometrical definition of a box.

2. Constructive Solid Geometry (CSG)

One of the most useful tools for making a complete solid is Boolean Operation. Boolean set operations are a natural way to combine shapes. Using a Boolean operation, a new solid is made from two or more intersecting solids. The Boolean operations are:

Subtraction

The result of subtracting two solids is all the volume of the first solid, less any common volume with the second solid. The Operator (-), signifies subtraction and is useful in hollowing a body, removing an odd shaped piece of a solid or accounting for edge intersections of walls, plates, piping or other connected solids.

Intersection

The intersection operation, (+), combines two solids saving only their common volume. Unusual shapes can be attained using this operator and it is commonly used to “save” a piece of a shell as in, perhaps, a radar dish, or to use only a portion of a simple primitive in a component’s definition. Intersection between two solids having no common points would, of course, be the Null set which is a region having no evaluation potential.

Union

The concept of union is the antithesis of intersection. The union operator (U) joins solids so any volume in at least one is part of the resulting volume. The union operation allows several related parts of a single component, that overlap or trail one after another, to be defined in one region. The union operation is useful in creating fuel and hydraulic lines. Fig. 4.16 illustrates the Boolean operations on solid bodies.

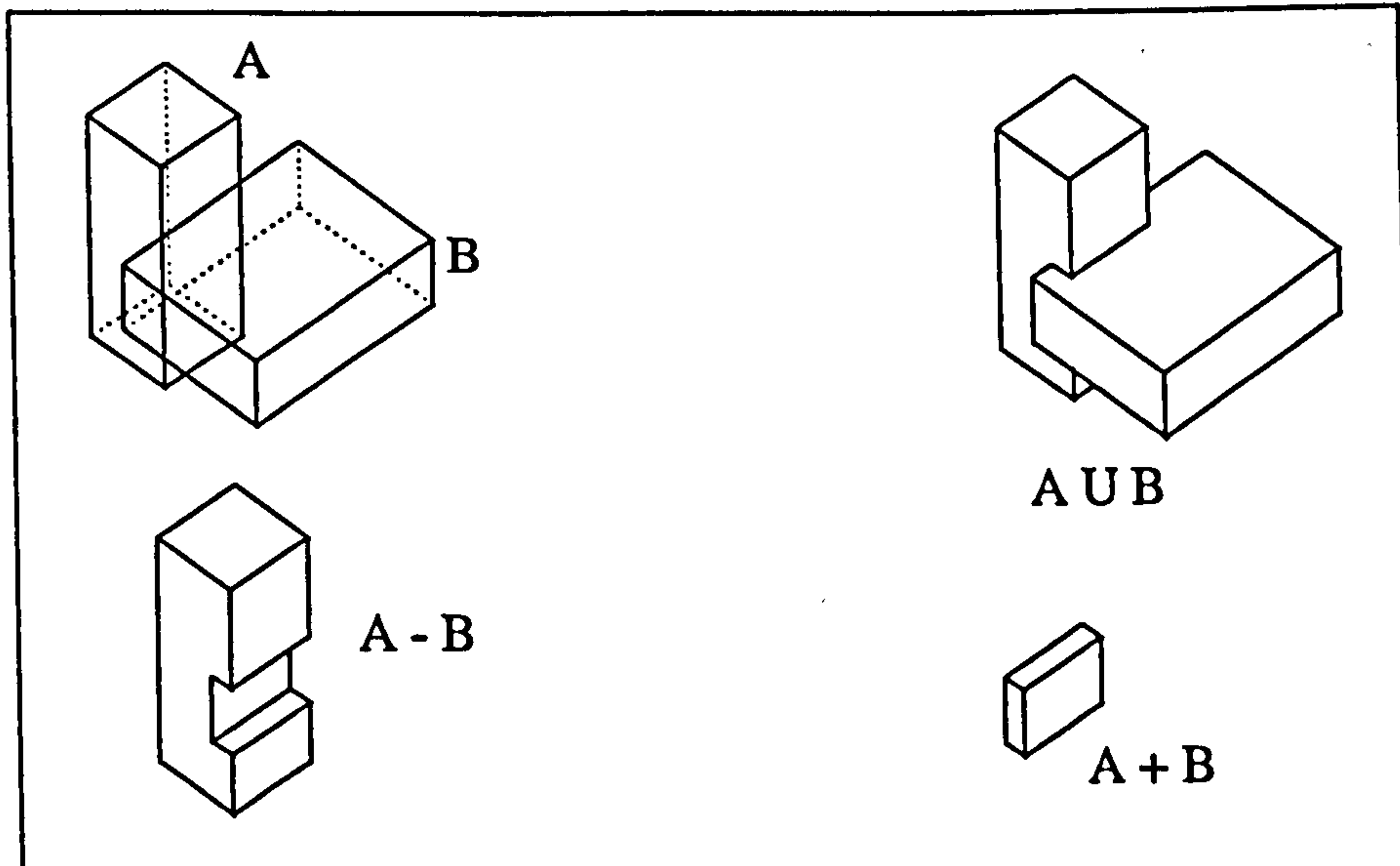


Fig. 4.16 Boolean operations on solid bodies

3. Converting a wireframe to solid

The techniques used to generate a wireframe body can be used to convert the resulting model to a solid model. There are many general wireframe techniques to create a 3D shapes that can be converted to solid models, among them:

1. **Swinging:** Fig. 4.17 shows a wireframe 3D geometry resulting from swinging (rotating) curve (A) around 360° around an axis of rotation.
2. **Sweeping:** A 3D wireframe cylinder of height (H) and a diameter (D) can be created by sweeping a circle of diameter (D) a distance (H), Fig. 4.17.

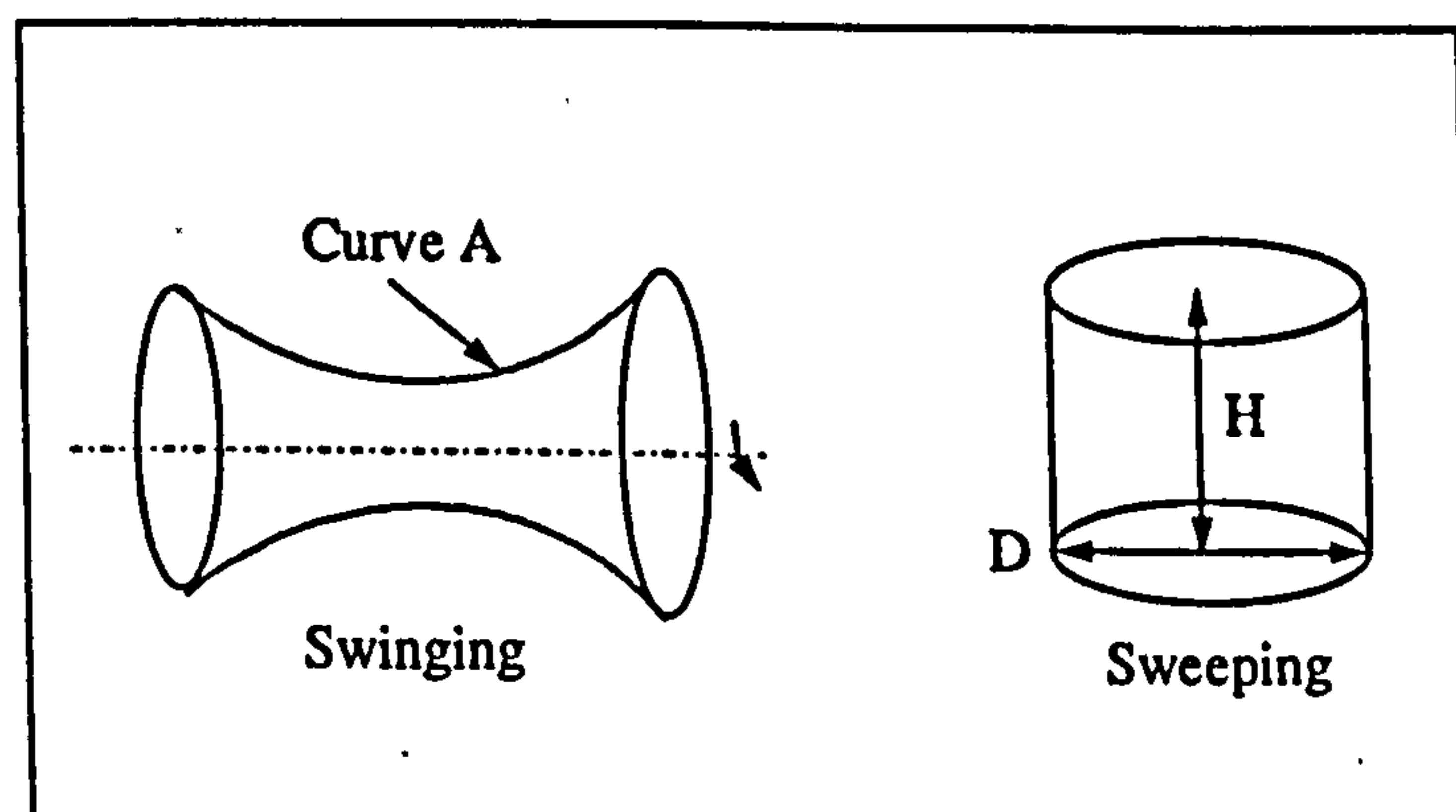


Fig. 4.17 Swinging and sweeping.

3. **Lofting:** A lofted wireframe body is created by interpolating (linking) a set of curve segments as shown by Fig. 4.18

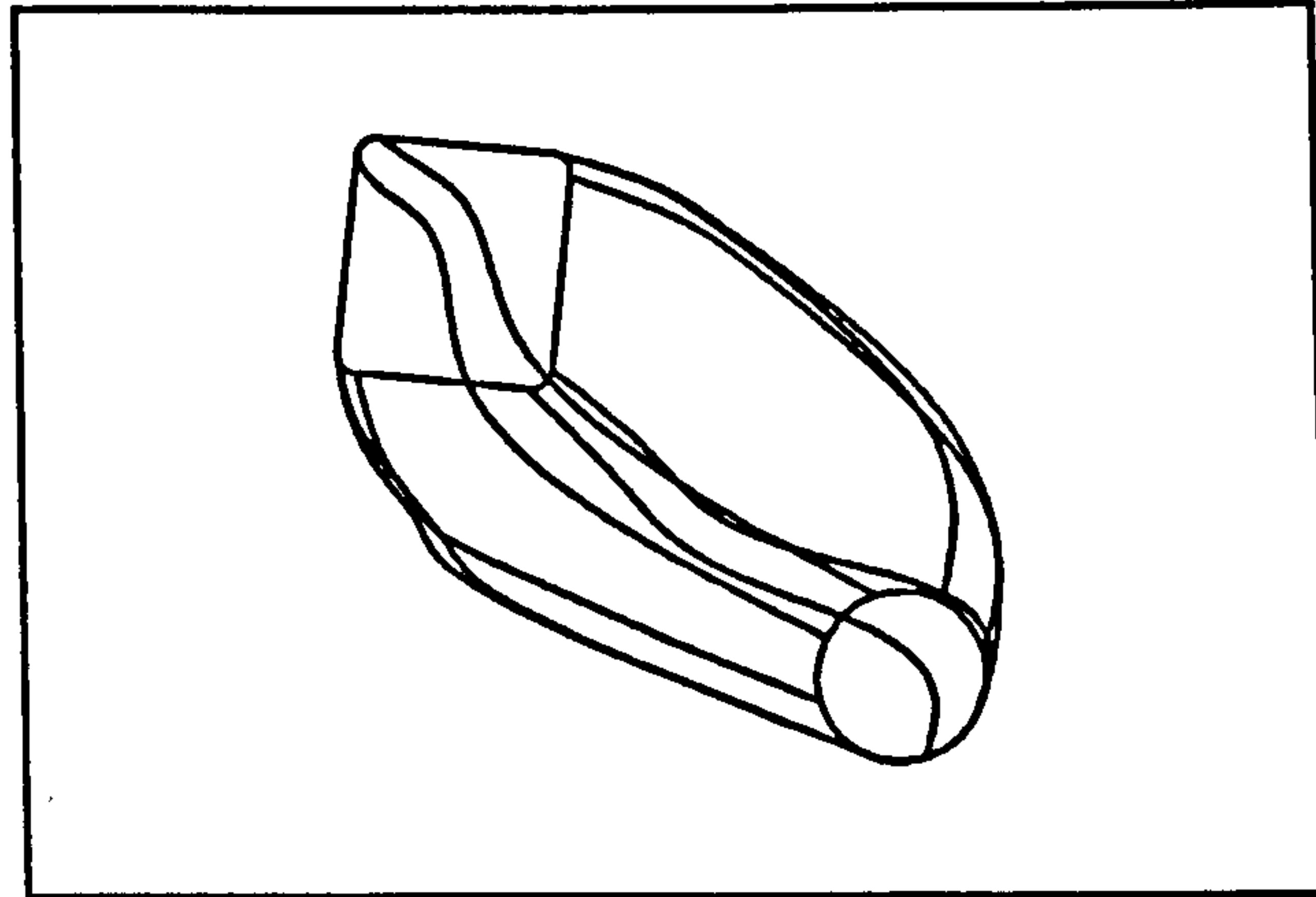


Fig. 4.18 Lofting of curve segments

4.8 Parasolid Solid Modeller

Since the aim was to find a methodology by which the vulnerability design discipline could be linked interactively with the conceptual design synthesis, it was felt from the beginning that a Programmable CAD system had to be used. Although most of the available CAD systems have a solid modelling capabilities, the following problems were realised after some investigation:

1. Creating an aircraft and its components using existing CAD systems will not serve the target of including the vulnerability discipline in the design process. This is because the geometry modelling in existing CAD systems is done mainly through the computer keyboard.
2. A standard vulnerability assessment technique does not exist, and has to be modelled as an external driver to the CAD system.

The next step was to investigate the current programmable graphical packages available in the University through the Computer Centre. It was found that there was a good collection of graphical packages, most of them belonging to the wireframe and surface modelling families. At that time, a solid modeller called Parasolid had been purchased by the College of Aeronautics to be used for a research contract. At the beginning, the

author found significant difficulties in handling the package. This was because this package has been made to develop special CAD systems, and not to use it as a CAD system itself. Also the package has been designed mainly to be run with the C language. The author spent more than four months in an effort to make the program work under a standard FORTRAN language, and to solve installation-related problems.

4.8.1 About Parasolid

Parasolid is a programmable solid modeller which has the following capabilities, (Ref. 41):

- Build and manipulate solid objects.
- Combine solid objects into assemblies.
- calculate mass and moments of inertia.
- Perform clash detection analysis.
- Produce graphical output files in various ways.
- Store and retrieve objects and assemblies.

Parasolid is a B-rep geometric modeller. This means that it represents solids by their boundaries. Also Parasolid has the capabilities of building analytically defined shapes as well performing Boolean operations.

4.8.2 Interfaces to Parasolid

Fig. 4.19 shows how the Parasolid interfaces work. The Calling Program (C or FORTRAN) is the means by which the user uses the Package to manipulate objects and control the information of the modeller. This is called the Kernel Interface (KI).

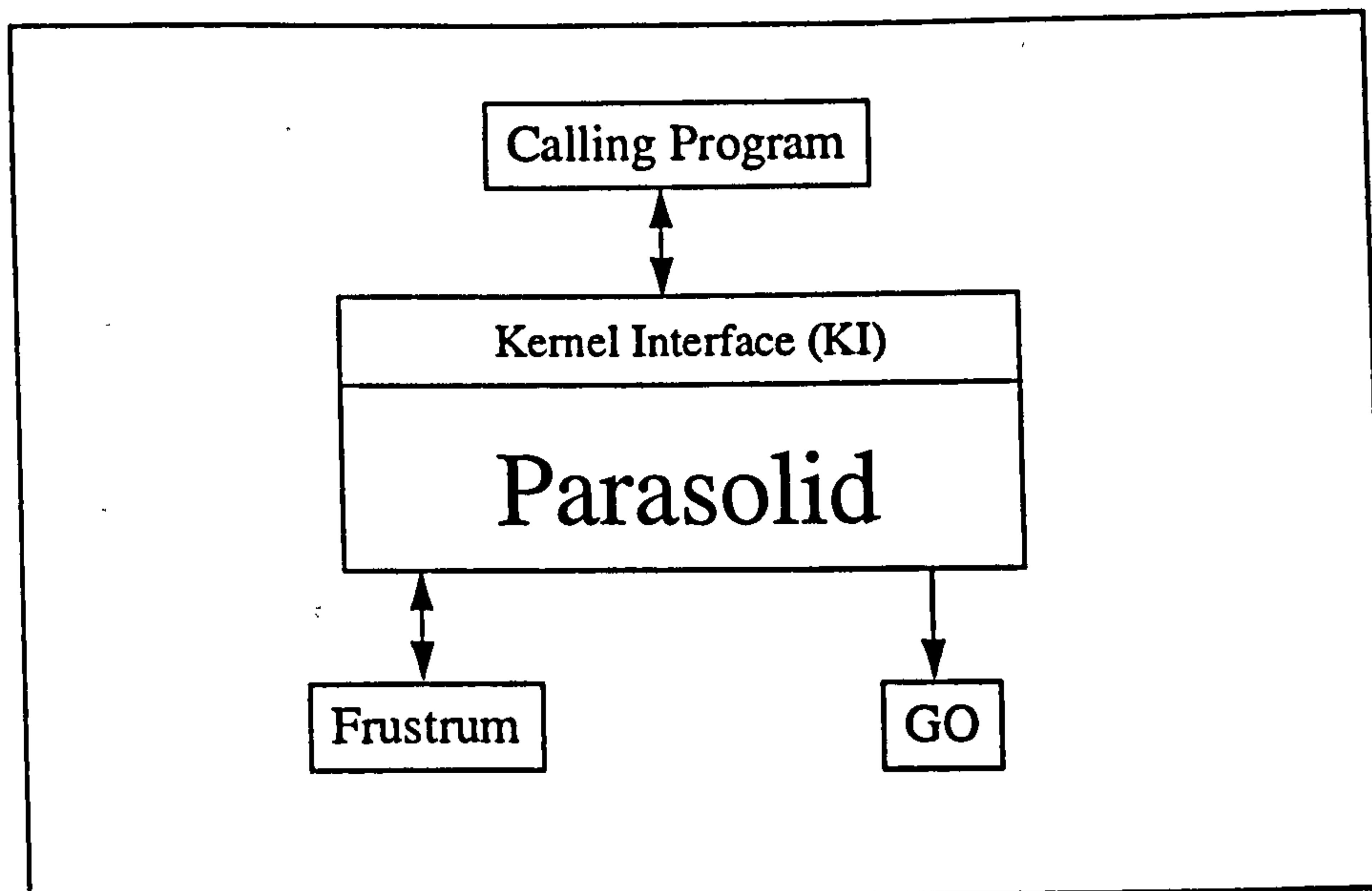


Fig. 4.19 Parasolid Interface

The KI is a library of routines which provides access to Parasolid. These routines are used for building, changing and combining parts. Also it includes routines for controlling the way in which the modeller performs certain operations, and for asking it to produce pictures of the parts. The Frustrum is a set of user-written routines which provide access to Parasolid. They are called by the KI when data needs to be saved or retrieved. The Frustrum is used to manage the storage of data which the KI outputs through the Frustrum. The Graphical Output (GO) routines must also be written by the system builder. Unlike the Frustrum, the output from these routines is not data files, but rather instructions to the user graphics system for drawing pictures requested from the KI.

4.8.3 Parasolid Programming Concepts

Parasolid is written in the "C" language and is designed to be called using the same language. The package also can be called from a suitable implementation of FORTRAN. To facilitate this compatibility with FORTRAN, the KI follows the following conventions:

- KI routine names consist of six characters.
- KI routines do not return a function value.

- KI routines require only integer, double precision and character data types as arguments and the only data structure used is the array.
- All arguments are passed by reference.

Each routine function header consists of :

- Routine name.
- Brief description.
- List of received arguments.
- List of specific errors.
- detailed description.

The received arguments pass information from the application program to the KI. The application program must declare a variable of the appropriate type for each argument, and set this to the required value. The address of the variable is then passed to the KI function for each argument. The returned arguments pass information from the KI to the application program. Again, the application program must declare variables to correspond to each of the returned arguments in a KI routine. The following KI function illustrates the programming concept of Parasolid:

CALL CRBXSO(vec_pos,vec_axis,width,length,height,box,ifail)

The above function *CRBXSO* is a KI function to create a solid box. It receives:

<i>vec_pos</i>	an array containing the (x,y,z) of centre of base of box.
<i>vec_axis</i>	an array containing the (x,y,z) direction of box axis.
<i>width</i>	a double-precision for the box width.
<i>length</i>	a double-precision for the box length.
<i>height</i>	a double-precision for the box height.

And returns:

<i>box</i>	an integer which holds the 'tag' of the box created.
<i>ifail</i>	an integer which indicates the failure, if any, of the call function.

4.8.4 Building Assemblies

Grouping solids into representative models is a special combination task. Assemblies let the user represent collections of bodies as part of a single model. They can contain other assemblies as well as solids, generating a tree-like structure, Fig. 4.20.

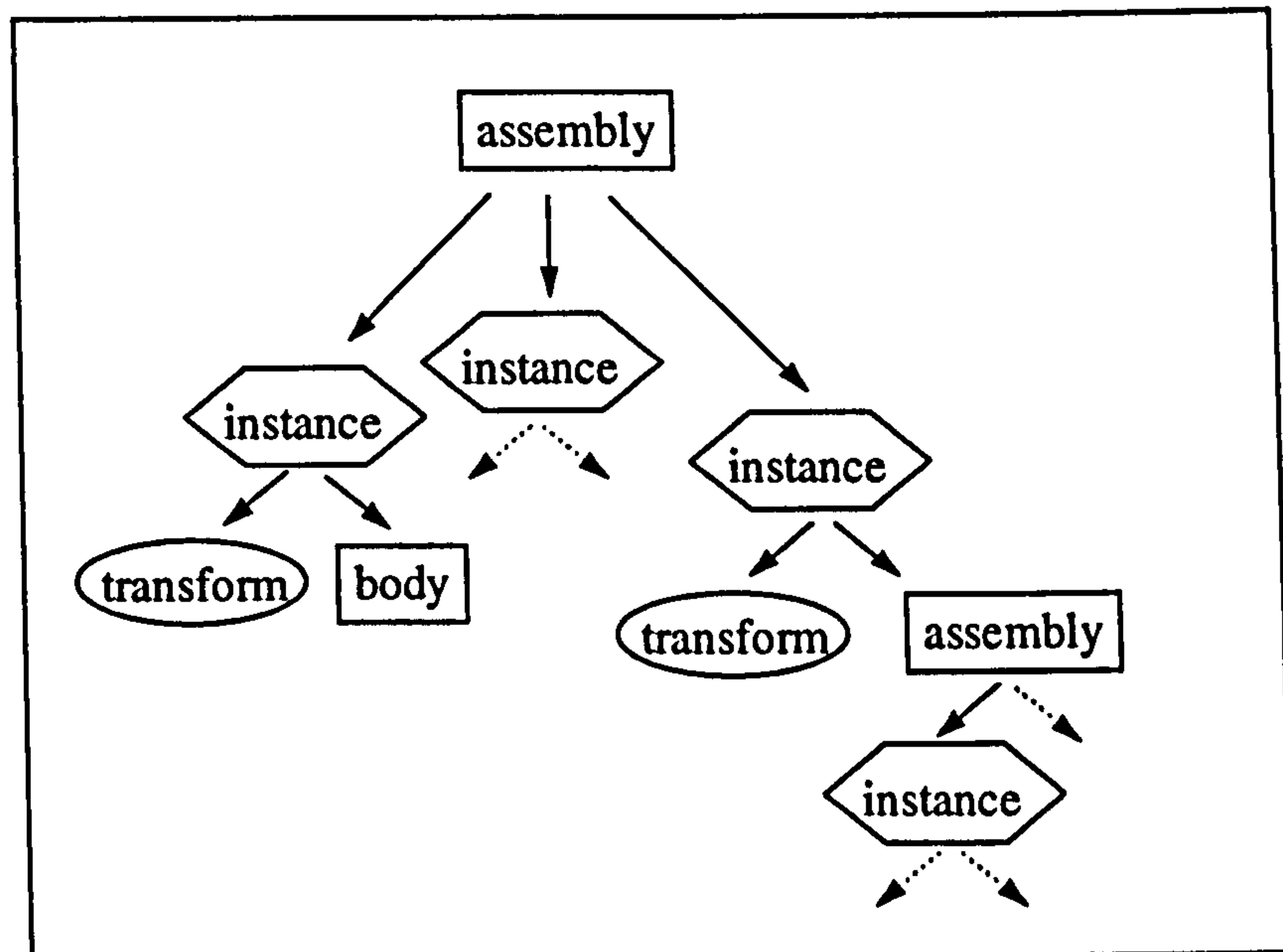


Fig. 4.20 General assembly structure

The user starts by creating an empty assembly, and then adds '*instances*' to it. An instance is a pointer identifying a part, together with a definition of its location in the assembly (a '*transformation*'). It is possible to instance the same body (or assembly) several times in an assembly, and because each new instance only points to the part rather than copying it, a lot of internal disk space is saved.

4.9 Model Building

Moving towards creating the vulnerability assessment methodology, an aircraft geometrical model has to be implemented. This consists of selecting a reference point and a reference vector which acts as a location guidance for the aircraft components as given by the conceptual design synthesis. Also an assembly philosophy has to be defined which makes modelling a general combat aircraft possible.

4.9.1 Assembly Reference Point and Reference Vector

In order to establish a systematic and easy modelling and assembly process, a reference point and a reference vector are to be defined based on the aircraft geometry. The aircraft nose is selected to be the reference point since it is the first station ($X = 0$) in any aircraft design synthesis. The reference vector is chosen to be the vector starting from the reference point and ending, say at the centre point of aircraft engine at the engine face, Fig. 4.21.

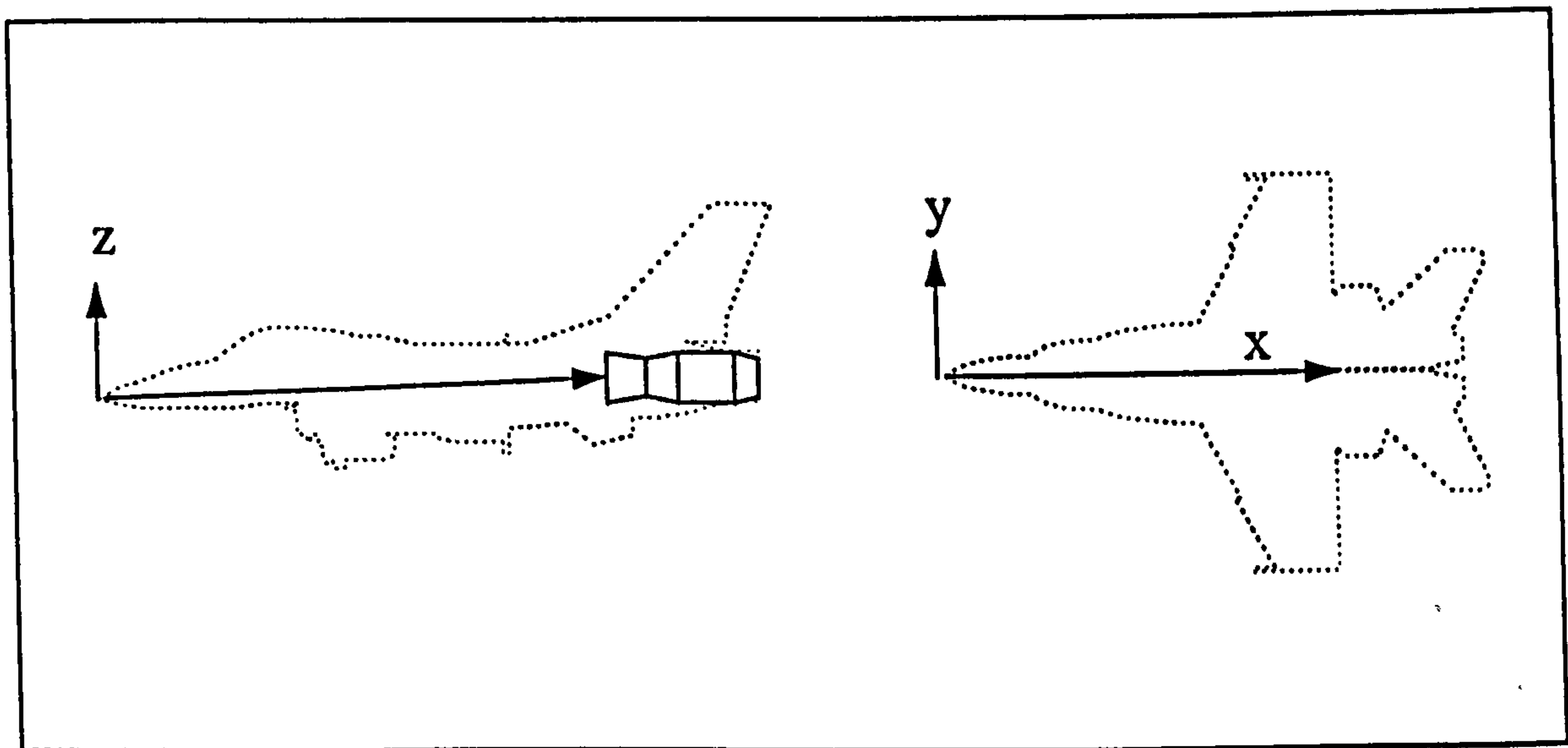


Fig. 4.21 Modelling reference point and reference vector

If the aircraft has two engines, then the reference vector is the line passing through the reference point and a point halfway between the two engines at engines centres. The reference point and reference vector serve as a location address of components to be modelled as defined by the design synthesis.

4.9.2 Model-Building Methodology

To perform a vulnerability assessment of a new aircraft, considerable detail of the critical components is required. This is not usually feasible at the conceptual/preliminary design phase where usually only part of the external geometry is defined (aircraft main components). It was, therefore, required to find a way to find the modelling requirements of critical systems. These modelling requirements are:

1. Component position and orientation relative to the reference point and vector.
2. Component geometry layout (shape)
3. Component size (volume).

The key to building a systematic modelling philosophy was then to:

1. Make the modelling process to follow from outside to inside. This top-down approach starts by the aircraft external body (skin), i.e. main components, then modelling what components are covered by the outer skin.
2. Finding a modelling relationships between the well-defined main components and the inside ones. This relationship uses the three modelling requirements listed above, in relation to the aircraft external shape.
3. The main component serves as a “parent” to the inside subcomponent “child”. The “child” subcomponent is assembled relative to the reference point and reference vector of the “parent” component. For example, the wing is defined by a set of design parameters such as its location (reference point and vector), thickness ratio, taper ratio, span, etc. (shape and size). A parent-child relationship can be defined between the wing and the fuel tank inside the wing. This automatically enables the “child” to move along with the parent when the parent location is changed.

4.10 Aircraft's Components Modelling

Fig. 4.22 shows the vulnerability assessment methodology as linked to CONCEPT design synthesis. The solid-based aircraft description is mainly defined by CONCEPT. Unlike transport aircraft, combat aircraft take many shapes and configurations. In order to establish a general modelling methodology capable of modelling a wide range of combat aircraft, the aircraft is divided into its main components. Each component is a parametric feature which depends on CONCEPT. When combining these main components into an assembly, they form the model representing the aircraft. Appendix C contains detail modelling techniques of the aircraft components.

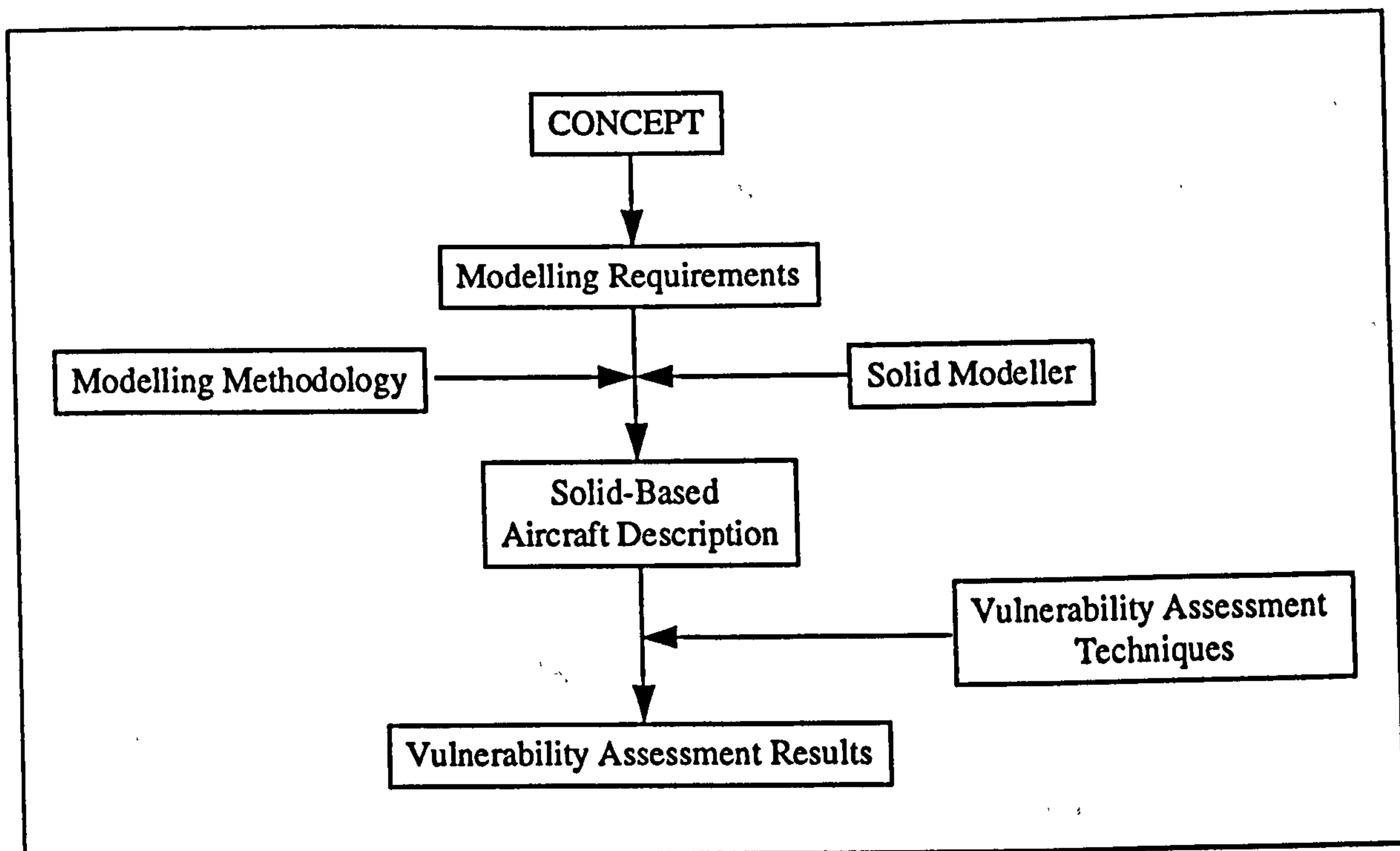


Fig. 4.22 Vulnerability assessment methodology

The aircraft is assumed to be composed of the following main components.

1. Radome.
2. Cockpit.
3. Fuselage
4. Wing
5. Horizontal Stabiliser.
6. Vertical Stabiliser.
4. Engine(s)
8. Intake Ducts.

Following a brief description of how these main components are modelled. Appendix C contains the modelling techniques used to approximate the aircraft component and how they are linked with CONCEPT.

4.10.1 Aircraft Radome

Most combat aircraft radomes are of conical shape. The radome is constructed by a Boolean subtraction of two cones, so that the hollowed cone represent the radome structure. The radome reference point lies on the aircraft reference point. “Child” components are located inside the radome. These are radar dish, radar avionics box and forward electronics bay.

4.10.2 Cockpit

The cockpit structure is created by conducting Boolean operations on a solid cylinder. The cockpit structure acts as a shield to the pilot body which is a critical component. The pilot body is created by a Union Boolean operation of Simple Primitive Shapes.

4.10.3 Fuselage

The fuselage is created by a developed solid-lofting procedures. The aircraft fuselage from the radome station to the engine exit plane is divided into a number of longitudinal sections, each station is segmented into eight 2D curve segments then lofted with its counterpart in other sections. Again CONCEPT design parameters specify the size of the resulting solid body with some direct user input. The landing gear is modelled by a Boolean union of simple primitive shapes.

4.10.4 Wings

The wing is modelled as a trapezoidal planform. A subroutine in the solid modeller creates trapezoidal platforms which can be used for the flying surfaces and wing fuel tanks. “children” to the wing are :

1. Wing spars, which are modelled as solid boxes. The spars are automatically placed inside the wing and take its shape.
2. Fuel tanks, which are modelled as trapezoidal shapes.
3. Flying control surfaces, such as ailerons and flaps are modelled as trapezoidal shapes and automatically located at the designated place.

4. Fuel & hydraulic lines, are modelled as solid pipes (cylinders) running behind the front spar and in front of the rear spar.

4.10.5 Empennage

The tailplane is modelled the same way as the wing except that a layout CONCEPT design variable controls the modelling process of the tailplane. This is to enable the modeller to create different tailplane layouts. The fin is also modelled the same way with its rudder(s).

4.10.6 Engines

An engine is created by a series of Boolean operations on a solid cylinder. The nozzle part is approximated by Boolean operations on a cone solid shape.

4.10.7 Intake Ducts

The engine intakes, of rectangular shape, are modelled using a series of Boolean operations on a solid box. Those of semi-circular shape are modelled from a solid cylinder. A CONCEPT design variable controls the shape and location of the intakes. The engine ducts are modelled using the lofting modelling process. The duct is lofted from the exit of the intake to the face of the engine.

4.11 Shotlines Assessment Technique

One of the standard vulnerability assessment techniques is the shotline assessment. This is done by superimposing a planar grid over the aircraft model and then passing parallel shotlines or rays from the threat direction towards the grid nodes as shown by Fig. 4.23. A list of the penetrated components is generated. These components are then used to quantify the aircraft kill probability based on the threat intensity and direction. Based on solid modelling techniques an interactive shotline assessment technique has been developed using Ray Tracing on the solid modelling.

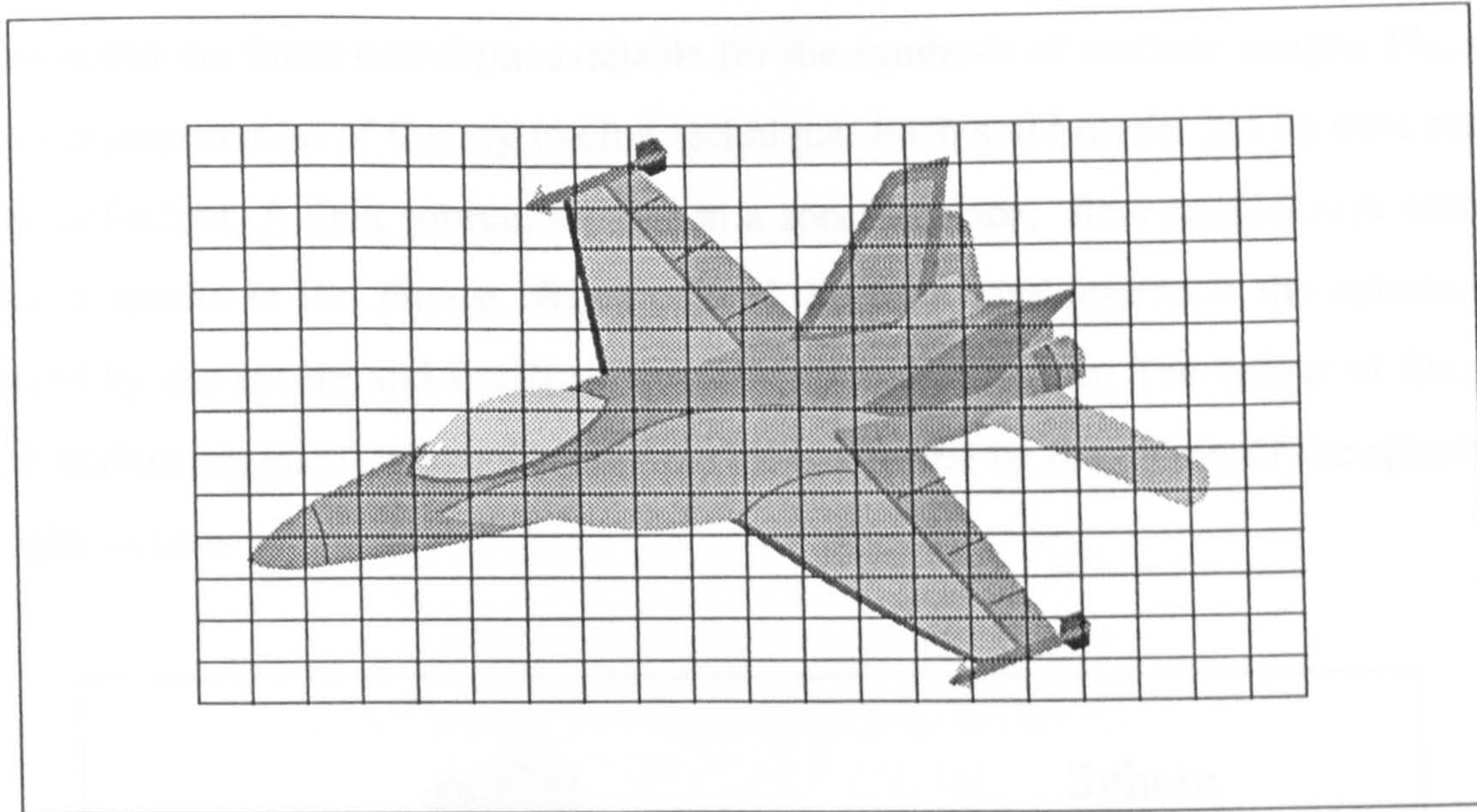


Fig. 4.23 Shotline grid over an aircraft model

4.11.1 Shotline Assessment

This assessment is used to generate a shotline description of the aircraft undergoing vulnerability assessment. This is done by modelling, geometrically, the external surface of the aircraft and its individual critical internal components. Shotline descriptions are obtained by superimposing a planar grid over the target model, then passing parallel shotlines from the attack direction (normal to the grid), through the individual grid cells. Shotlines are randomly located along the grids and allowed to penetrate the aircraft body, penetrating first the outer structure, then the inside components, until leaving the aircraft body. Each component hit by a shotline is used to build a list of component descriptions, which is used for further vulnerability assessment. The shotlines are fired from the standard vulnerability assessment directions discussed earlier.

4.11.2 Ray Tracing

Ray tracing is a CAD solid modelling technique by which photo-realistic images can be created. This technique simulates the interaction between objects and light. Ray tracing theory is mainly based on mathematically modelling light and solid objects. Ray tracing

is considered the finest technique available for the synthesis of realistic images. Fig. 4.24 gives a representation of the ray tracing technique. Each solid model has its own surface colour definition. A light source, located in a specific place, fires parallel rays onto the object, a sphere in the Figure. When one of the light rays intersects the sphere, it is reflected by the sphere and finally crosses the computer screen. The colour of the pixel (small surface segment) where the light ray hit is affected by the colour of the sphere and the light source.

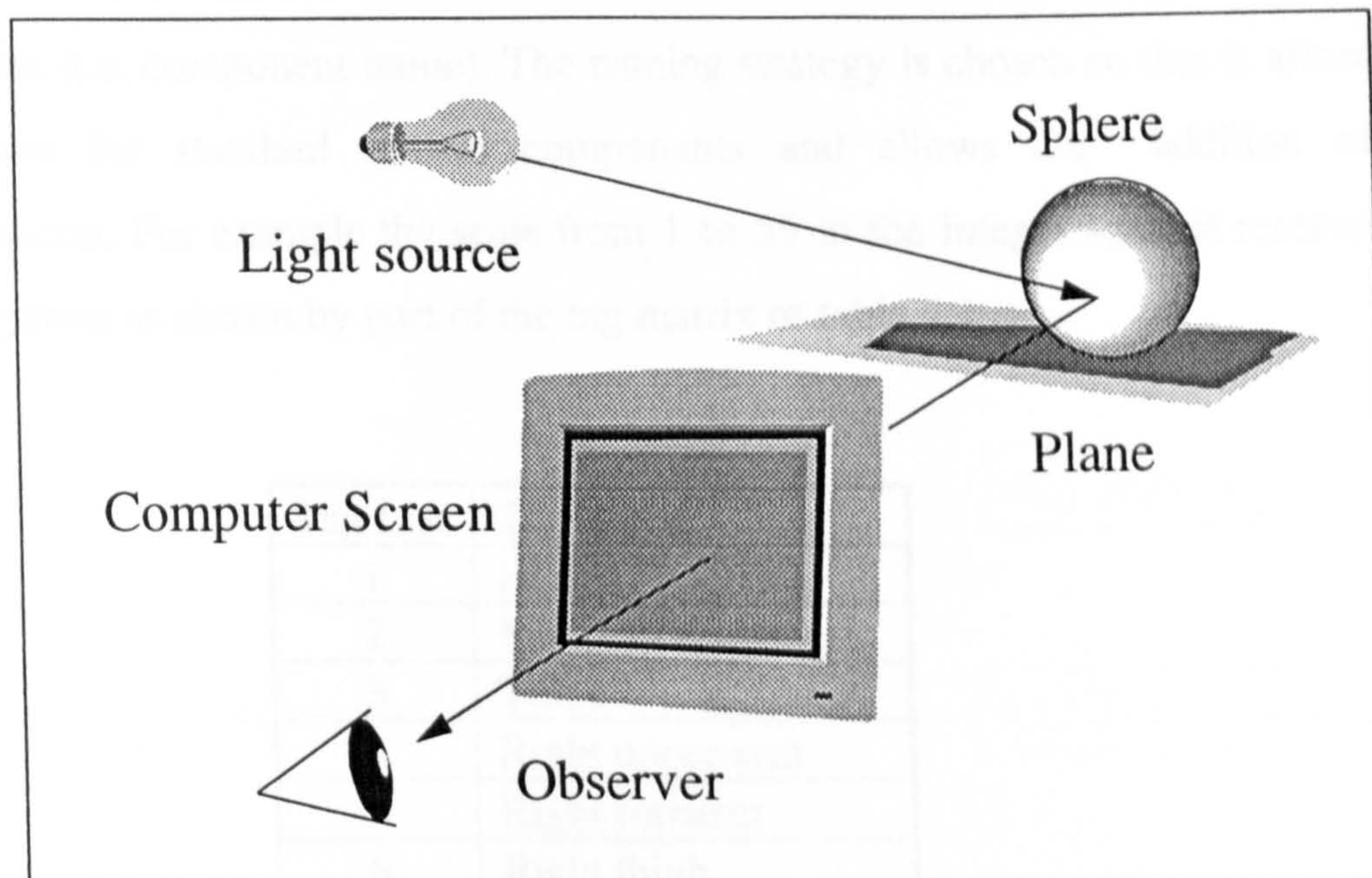


Fig. 4.24 Ray tracing concept.

For the vulnerability assessment, the ray tracing technique has been modified to be used to create a shotline routine. This modification was mainly to enable the ray-tracing to act as a shotline and generate a list of components penetrated (hit) by each ray (shotline). A solid modelled component is composed of finite surface segments. Each segment has its geometric definition in space and a topological relationships with the solid model. The theory behind the ray tracing is based on a vector intersecting a defined surface segment in the space.

4.11.3 Component's Name Definition

Each component modelled using the solid modeller has its unique definition in the assembly. An internal integer number, returned by a modelling function or modelling operation, in the form of a tag-name parameter, defines each component modelled. This is done in order to build the aircraft assembly, which is composed of a variable number of critical systems. It is also to find a way to model the relationships between the components functions, and so a new and different naming strategy is implemented. A tag matrix of two columns is created, which is used to store the component tag number and tag name (i.e. component name). The naming strategy is chosen so that it allocates fixed addresses for standard critical components and allows the addition of more components. For example the scale from 1 to 39 in the integer scale is reserved for the crew system as shown by part of the tag matrix of table 4.1

Tag List	Tag Name
1	Head
2	Neck
3	Torso
4	Right upper arm
5	Right forearm
6	Right thigh
7	Right lower leg
8	Left upper arm
9	Left forearm
10	Left thigh
11	Left upper arm

Table 4.1 Sample of the tag matrix

4.11.4 Component's Probability of Kill

A different array contains the Probability of Kill (Pk) value of each component built as a separate module. Creating a separate Pk database file enables the performing of vulnerability assessments of different threat types and intensities. Pk data is another set of classified data, which the user has to collect. The determination of a component Pk is a very difficult task and requires a combination of component analysis and engineering

judgement. Although limited gunfire testing provides some insight into the effects of projectile and fragment damage potential, there is no universal methodology for arriving at a numerical value for P_k (Ref. 13)

4.11.5 Internal Kill Tree Analysis

Kill tree analysis (KTA) is used to compute the final aircraft kill probability based on the number of hits and the component relationship. The KTA analysis has the advantages of taking the effect of redundant components on the aircraft vulnerability. Fig. 4.25 shows the flow diagram of the shotline assessment modules.

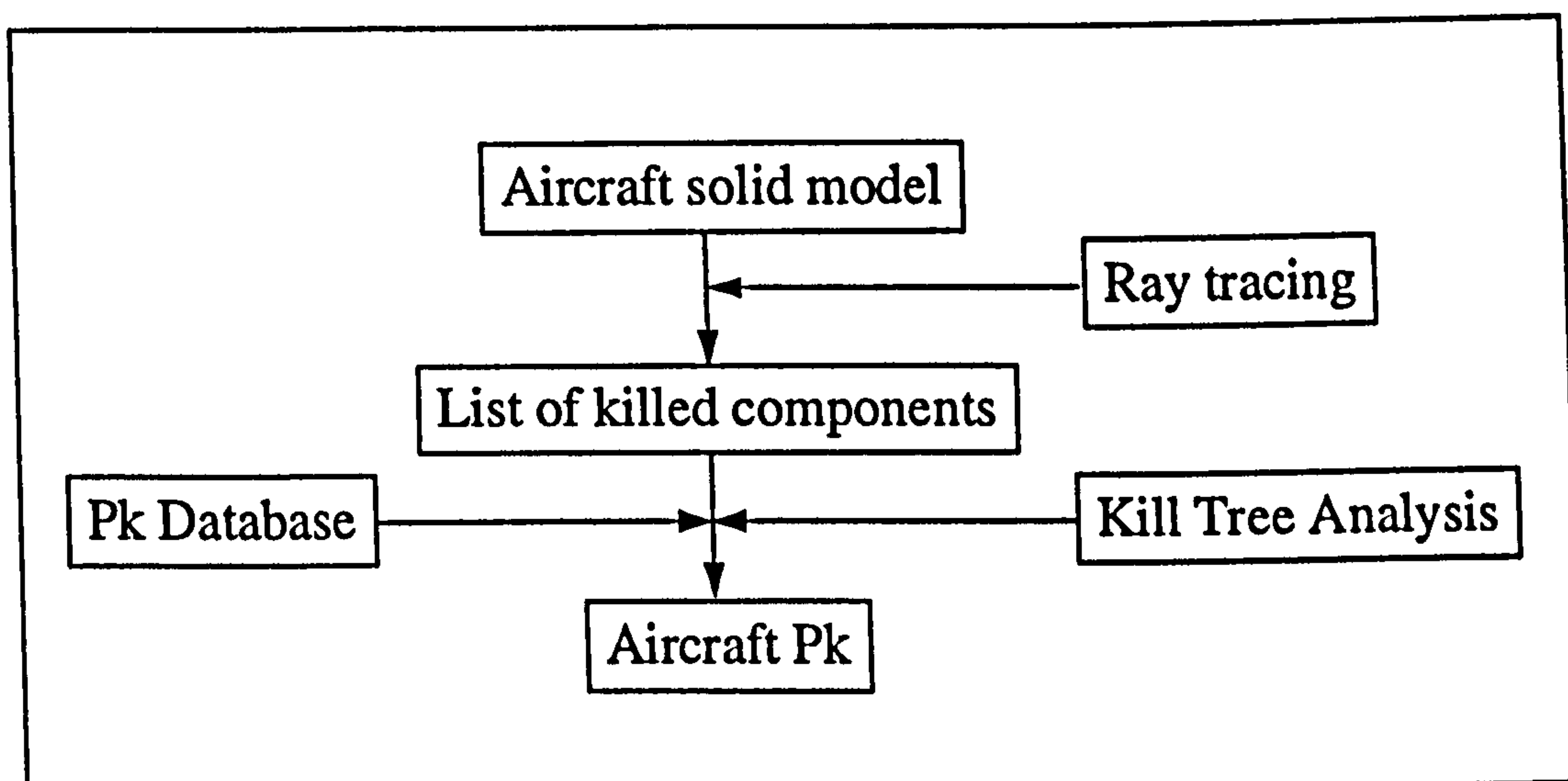


Fig. 4.25 Shotline assessment modules.

4.12 Vulnerable Area Assessment

The vulnerability of an aircraft component depends on the width of the component that is exposed to the threat direction. And also depends on the location of this component inside the aircraft body. Shielding a critical component by non critical components is a good vulnerability design practice. To complete the solid modelling interactive vulnerability assessment methodology, a numerical method has been developed to calculate the presented area of a component. The calculated area can be fed to the shotline assessment tool, discussed above, to conduct a vulnerable area analysis of the design. The approach used to compute the presented area of a component is also based

on the ray tracing technique. The presented area of a component is actually the shaded area of an object when the light source, the component, and the shade are on-line. A carpet-grid of fine mesh is placed at a distance from the object and in a plane perpendicular to the required direction. Each grid node acts as a light source, which is counted when it hits the object. The presented area is calculated by adding the small square areas of grids that all rays fired from their nodes hit the object, Fig. 4.26. Appendix C contains the numerical approach and the algorithm. The vulnerable area is not included in the shotline assessment, and consequently the aircraft's kill probability. This is because the probability of killing a component is simulated by the random rays penetrating the aircraft body.

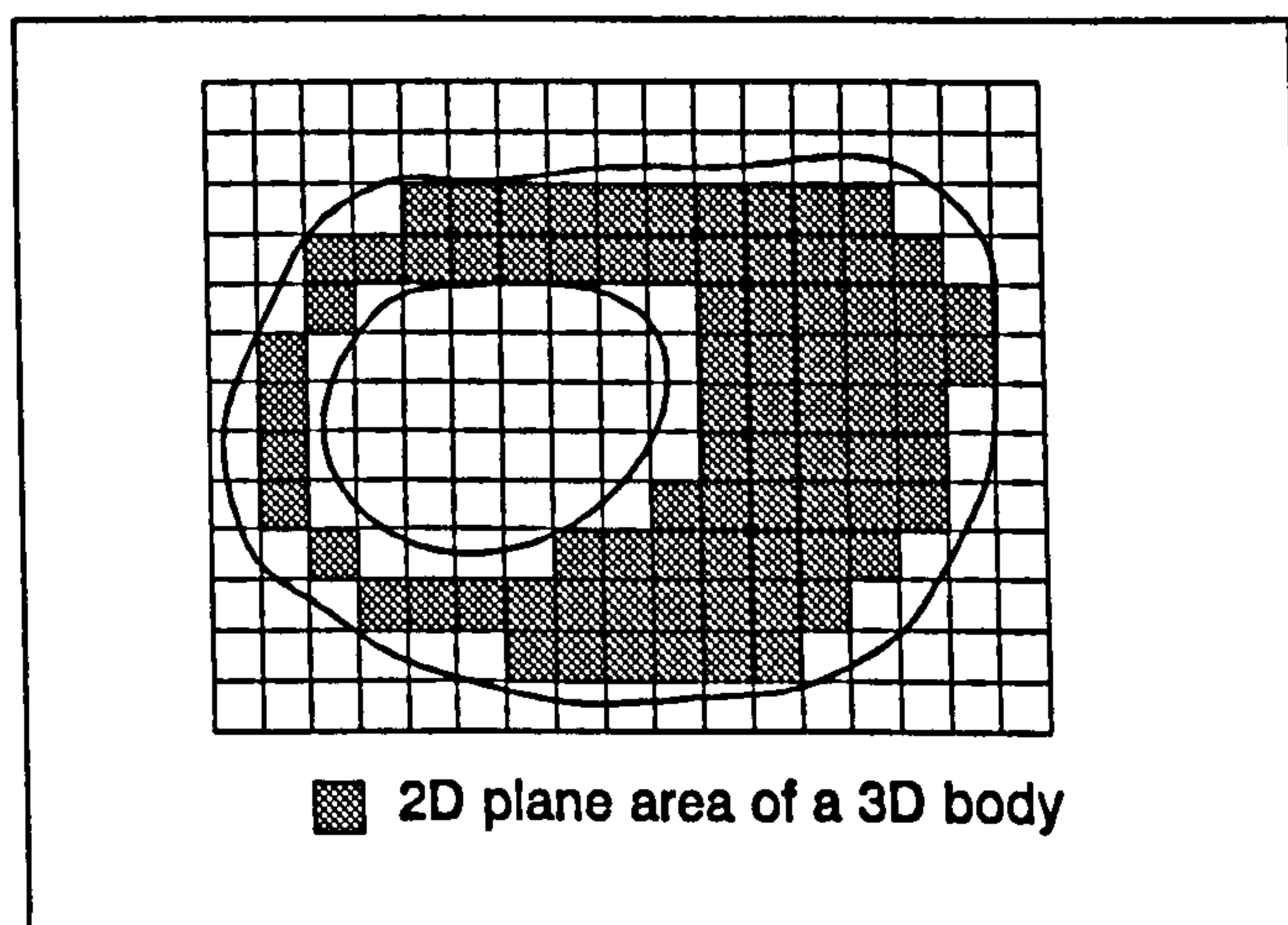


Fig. 4.26 Vulnerable area computation

Chapter Five

The Mission Simulation Model

5.1 Introduction

This chapter illustrates the simulation model used to study the effect of aircraft availability (R&M) and survivability on a squadron Sortie Generation Rate (SGR). The Mission Simulation Model (MSM) simulates the major operational activities of a squadron of aircraft in a wartime environment. Other sizes of operational unit could be used, say a flight wing or fleet.

5.2 Simulations, Techniques and Languages

Simulations, and especially computer simulations, are widely-used terms to describe a large class of mathematical modelling techniques. The main parameter linking these techniques are that they model time-dependent systems (Ref. 32). The concept of system simulation became a reality in the early 1950s when a shift in emphasis occurred from looking at parts of a problem, to examining the simultaneous interactions of all parts. This shift was partially due to the fact that system simulation experiments had become feasible on electronic computers, which themselves were undergoing order-of-magnitude advances in speed. Simulation techniques depend mainly on the physical behaviour of the problem to be studied. The essence of a simulation is that the state-changes of the system are modelled through time. Hence it is important to consider how time-flow might be handled within the simulation. There are two techniques for time handling in simulation modelling:

1. **Time Slicing:** This is done by moving the time interval forward based on equal time intervals. This approach involves updating and examining the model at regular intervals. Thus, for a time slice of length (dt), the model is updated at time $(t+dt)$ for changes occurring in the interval $[t \text{ to } (t+dt)]$.

2. **Next-event technique:** Here, a variable time increment is used to avoid slack periods of varying length. This approach uses an event-log, which is only examined and updated when it is known that a state change is due. These state changes are usually called events and, because time is moved from event to event, the approach is called the next-event technique. The simulation of a squadron operation is an example of Discrete Events Simulation (DES). This technique of simulation, DES, is widely used in manufacturing systems planning. DES concerns the modelling of a system in which state changes can be represented by a collection of discrete events. Logical relationships comprise the other set of structures that are used to describe a system. In a logical relationship the model checks to see whether a condition holds. If it does, a certain action takes place. If it does not hold, an alternative action takes place (Ref. 33). Because of the increasing use of simulation modelling, special computer languages/packages have been developed specially for simulation studies. Most of these languages/packages, such as SLAM, are either modified/written using a high-level programming language such as FORTRAN. Reference (34) contains more detailed material on recent simulation techniques. FORTRAN has been chosen to be compatible with the other modules

5.3 The MSM

The MSM is a UNIX-based, discrete event model using the FORTRAN structural language. The source code, input/output sample files, and code algorithms can be found in Appendix D. The MSM describes the major aspects of the operational environment of a mature squadron of combat aircraft at an Air Base in an air campaign.

5.3.1 Purpose of the Model

The model was needed to evaluate an aircraft Sortie Generation Rate (SGR) based on the effectiveness disciplines discussed in Chapter One. The MSM is intended to provide the capability to evaluate how a squadron of aircraft would perform in the operational environment. The SGR is dependent on the inherent R&M of the aircraft, and also the manner and operational environment in which it is operated and maintained. For instance, availability is determined by how the aircraft is operated, the frequency of use, how often

it fails, the time required to repair the aircraft, and the maintenance resources available at the time of each failure. Since the interrelationships of these factors can be quite complex, simulation is a valuable tool in examining the relationships and predicts system performance in different operational environments.

5.3.2 The Scenario to Simulate

The scenario chosen to model and simulate is a 24-hour air campaign lasting for a defined number of days. At the beginning of each day, a defined number of sorties are scheduled for launch. The sortie launch times are randomly selected during the day, but different from the days followed. The selection of an aircraft to perform a flying mission is random from aircraft in the front line. The aircraft failures are based on the reliability characteristics of its individual systems. The aircraft maintenance time is based on the maintainability of its individual system maintainability characteristics. The aircraft maintenance is carried-out throughout the day. During the sorties, an aircraft is withdrawn (i.e. killed) from the inventory based on the aircraft survivability characteristics.

5.3.3 Aircraft States

Each aircraft in the squadron transits between three locations, front line, maintenance, and mission area. Also, the state of an aircraft during the simulation changes according to its location. Logic flags are used to model the location and state of each aircraft. The logic flags make the simulation model efficient through fast tracking of the changes happening to each aircraft minute by minute. An aircraft selected to fly a sortie transits from front line location to the mission area location. Having completed the sortie, the aircraft returns to the front line location. After landing, if the aircraft is found to have a failure, it will transit from the front line to the maintenance location. When repaired, the aircraft returns to the front line ready to be called for a mission. If an aircraft is killed in a mission a 'Kill' logic flag is changed, which tells the program to stop all simulated activities and events on this aircraft. Fig. 5.1 shows the MSM Location and State Logic Flags. Transit between Maintenance and Front Line is based on failures/repairs occurring on aircraft systems along the simulation. These failures/repairs depend on R&M characteristics of each system and the accumulated flying time on each system. There are

two time clocks for each aircraft, Fig. 5.2 . The first one stores the cumulative flying time of each aircraft during the simulated days. The second time clock is for each system on an aircraft. This clock stores the cumulative operation time per system. When a system undergoes repair the system time clock is reset.

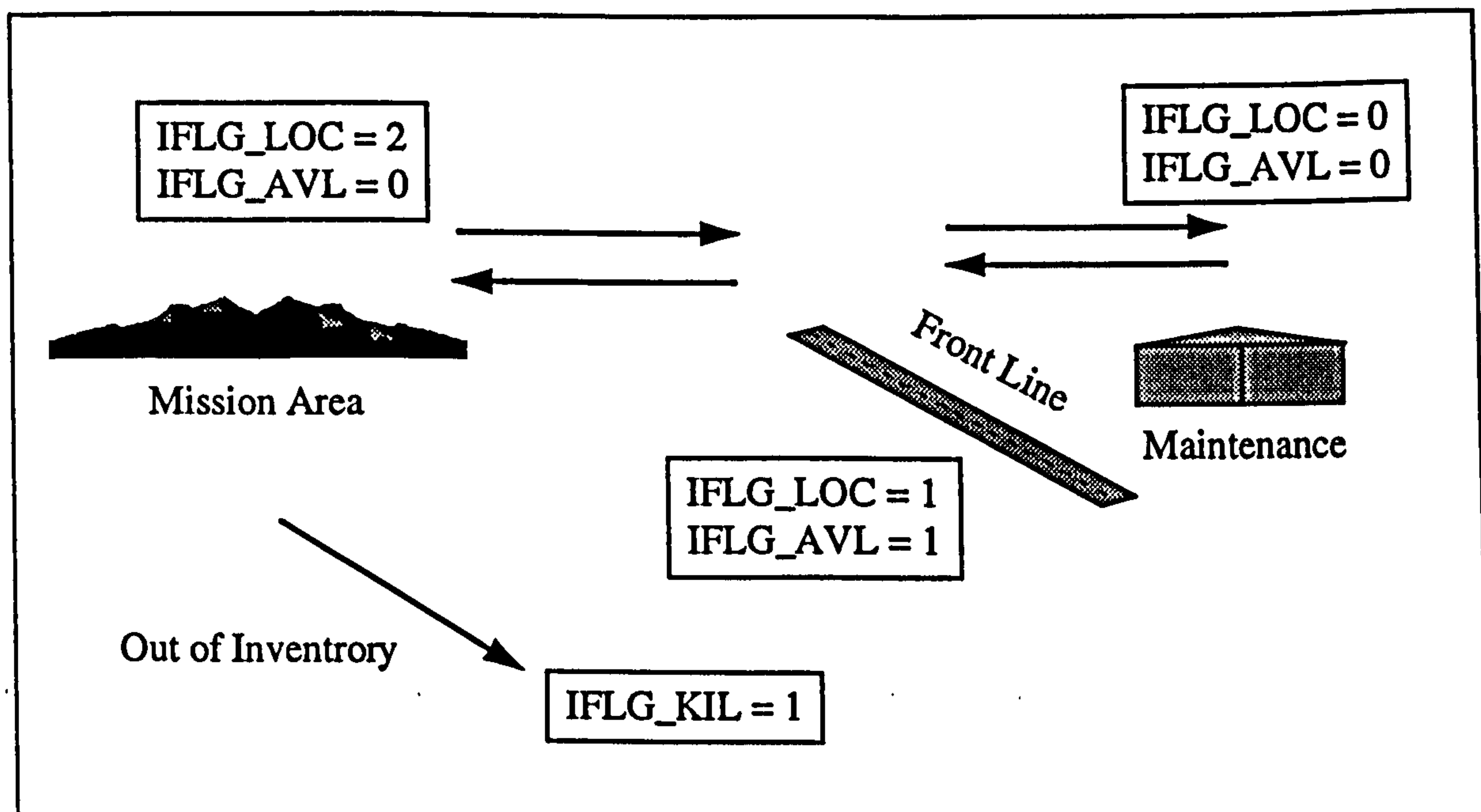


Fig. 5.1 Aircraft State and Logic Flags.

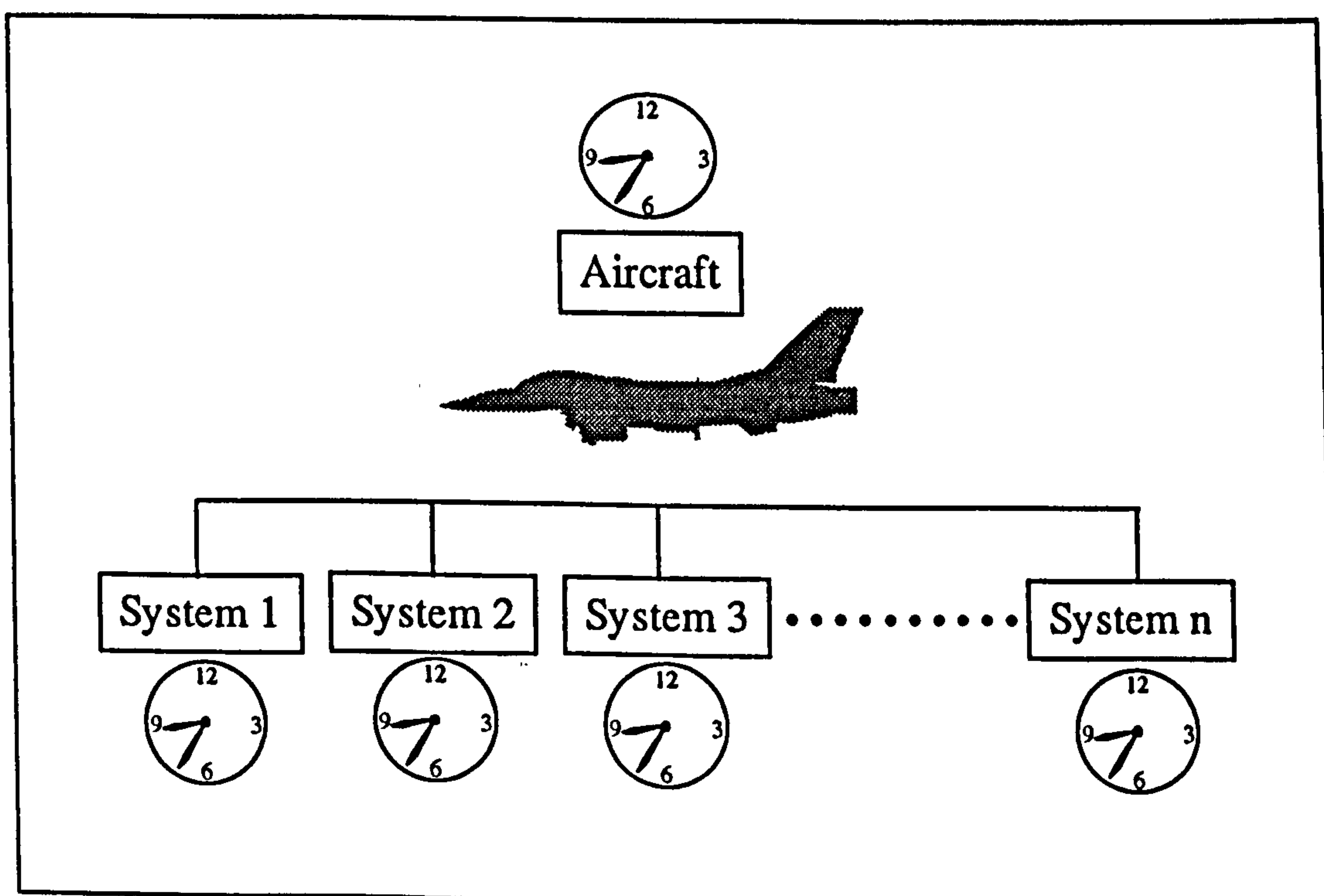


Fig. 5.2 Time clocks for each aircraft.

5.4 Events Sequence

Based on the time slicing simulation technique described above, an integer, *IMIN*, representing ONE minute is used as the main time driver of the simulation process and its parallel events activities. All simulated events are time-defined by two time variables, the *TIM_CUR* and the *IDAY*. *TIM_CUR* is a four-digit real number representing a 24 hour-per-day time. The *TIM_CUR* is found by converting the cumulative *IMIN* counter into 24 hour-per-day time. The *IMIN* counter starts from zero, and runs to 1440 (number of minutes per day). The *IDAY* variable represents the simulated day. *IDAY* is increased by one when the *IMIN*=1440.

- **Sorties Launch Times**

At the beginning of each day, the sorties to be launched that day are scheduled along the day. Due to the nature of the MSM, which simulates a squadron of combat aircraft in a wartime scenario, the launch times of the sorties are randomly selected. The sortie launch times are then sorted in ascending order and stored in the matrix :

TIM_SOR_CAL(NO_SOR_DAY)

- **Parallel Events Attributes**

After scheduling the random sorties launch times of the day, the *IMIN* counter starts advancing the simulation time minute by minute which is reflected in the 24 hour-per-day time *TIM_CUR*. At each minute the following group of parallel events takes place, Fig. 5.3,:

1. **Send Aircraft to a Mission**

This event takes place when the current time is equal to a sortie call time, i.e.

TIM_CUR = *TIM_SOR_CAL(I)*

Based on this event, an aircraft is selected randomly from the *Front Line* using the aircraft tail number. The Availability and Location Logic Flags of the aircraft selected are set to the following:

IFLG_LOC(I) = 2

IFLG_AVL(I) = 0

2. Return an Aircraft From a Mission

This event takes place when the simulated day and time equal to the day and time of a launched aircraft. When an aircraft is launched, the expected time and day of return is computed and stored in an array. This is equivalent to the Estimated Time of Arrival (ETA) in flight scheduling. The return time and day of an aircraft sent to a mission is found by adding the sortie's launch time and the sortie time, i.e.

$$TIM_CUR + TIM_SOR = IDAY_RET_MIS(I), TIM_RET_MIS(I)$$

The Availability and Location Logic Flags of the aircraft undergoing this event are set to the following:

$$IFLG_LOC(I) = 1$$

$$IFLG_AVL(I) = 1$$

3. Send Aircraft to Maintenance

This event takes place when one or more of the Work Unit Code (WUC) systems are failed. When an aircraft is launched for a mission, the clock time of the aircraft and its systems are incremented by its flying time in that sortie. After each sortie, the failure clocks for each WUC system are checked to see if a failure did occur; an aircraft is sent to maintenance when:

$$TIM_AC_SYS(I,J) = TIM_SYS_FAIL(I,J) \quad I \text{ Aircraft \& } J \text{ System}$$

In practice, aircraft systems/components will not fail after the same operating time but will fail at different times in the future. Consequently, these times-to-failure obey a probability distribution which may, or may not, be known and which describes the probability that a given system/component fails within a certain specified time. The exponential distribution is the most widely known and used distribution in reliability evaluation of systems. The time-to-failure (T) is computed for each system at the beginning of simulation based on the failure rate (λ) of the system and a uniform random number (U), (Ref. 34)

$$T = -\frac{1}{\lambda} \ln(1-U) \quad (5.1)$$

The Availability and Location Logic Flags of the aircraft undergoing this event are set to the following:

$$IFLG_LOC(I) = 0$$

$$IFLG_AVL(I) = 0$$

4. Return an Aircraft From Maintenance

This event takes place when the current simulated time and day is equal to the time and day that has been estimated to repair the aircraft. So this event takes place when:

$$IDAY = IDAY_RET_MNT(I)$$

$$TIM_CUR = TIM_RET_MNT(I)$$

The Availability and Location Logic Flags of the aircraft undergoing this event are set to the following:

$$IFLG_LOC(I) = 1$$

$$IFLG_AVL(I) = 1$$

5. Withdraw Aircraft From Inventory

In the MSM, an aircraft is allowed to be lost (killed) by eliminating the aircraft undergoing this event from inventory. The aircraft survivability is transformed into a probability of attrition figure. The attrition rate as defined by the Air Force analysts is a percentage of aircraft killed per 1,000 sorties, (Ref. 42). Again using the cumulative sorties counter and uniform random number, an aircraft in a mission is said to be killed when the random attrition rate is less than the input probability of kill figure which is a function of the aircraft or the environment. The Kill Flag, *IFLG_KIL*, of an aircraft undergoing this event is set to one. That is :

$$IFLG_KIL(I) = 1$$

Based on this setting the model will skip all the simulation events and adopts the attributes of an aircraft which has its Kill flag set to zero. Fig. 5.4 shows the flow diagram of the MSM program.

5.5 MSM Output

The MSM main output is the daily cumulative sorties that have been launched successfully. The MSM treats the operational events of each aircraft individually. Therefore, aircraft's time-events details, such as maintenance down times and front-line ready-times could be obtained.

5.6 MSM Limitations

The MSM was programmed in a modular way which enables further expansions to the main module. Since the MSM was intended to measure the effect of effectiveness disciplines on the aircraft SGR in a wartime environment, some assumptions have been included in the model. The MSM does not consider the following parameters which could be the subject(s) of future studies.

1. Aircraft scheduled maintenance activities. (normally ignored in wartime)
2. Effect of spare parts availability.
3. Maintenance personnel availability and skills.
4. Non flying times due to weather.

In order to include these factors in the MSM, separate algorithms are required for each parameter.

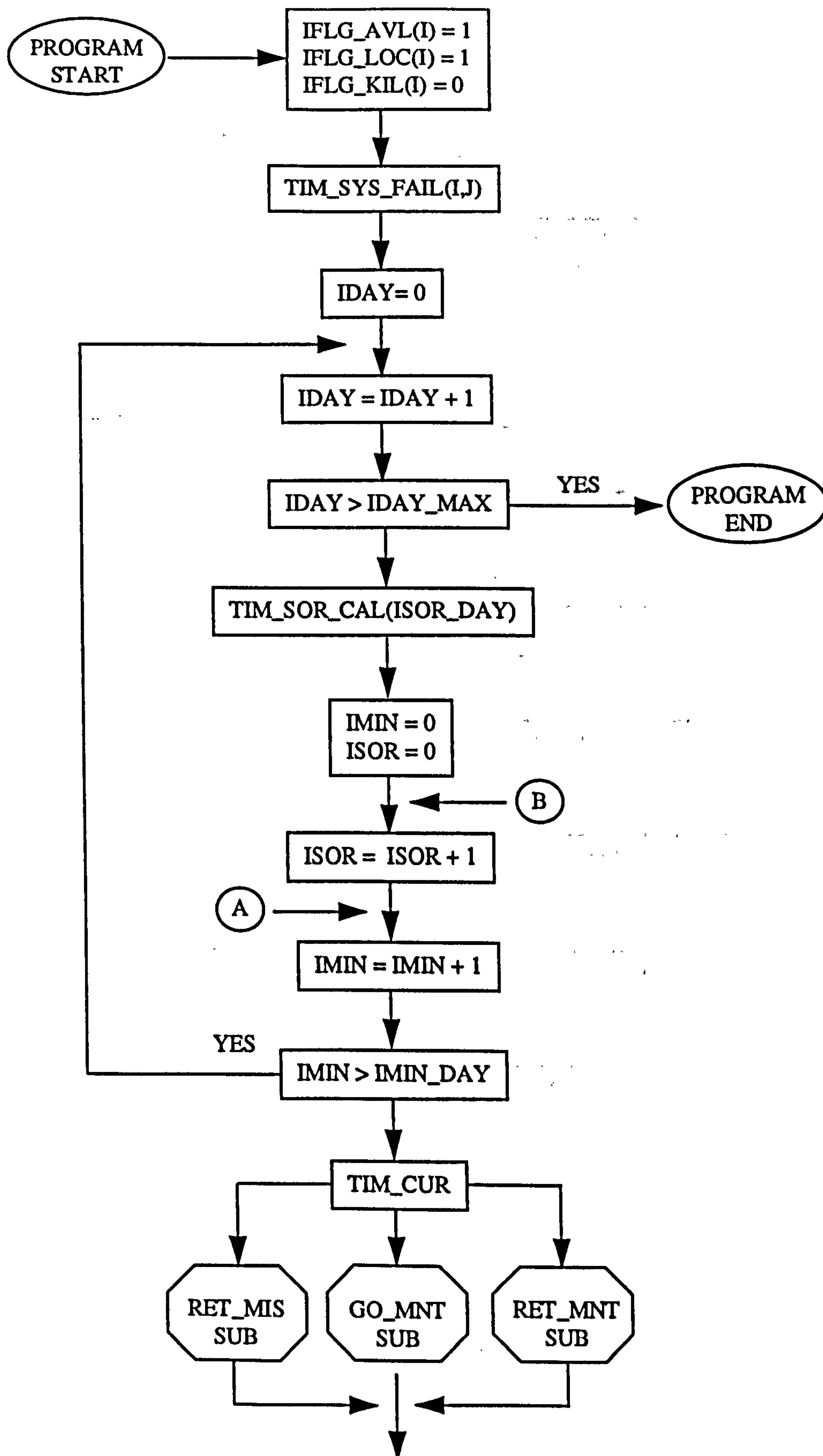


Fig. 5.4 MSM Program Flow Chart.

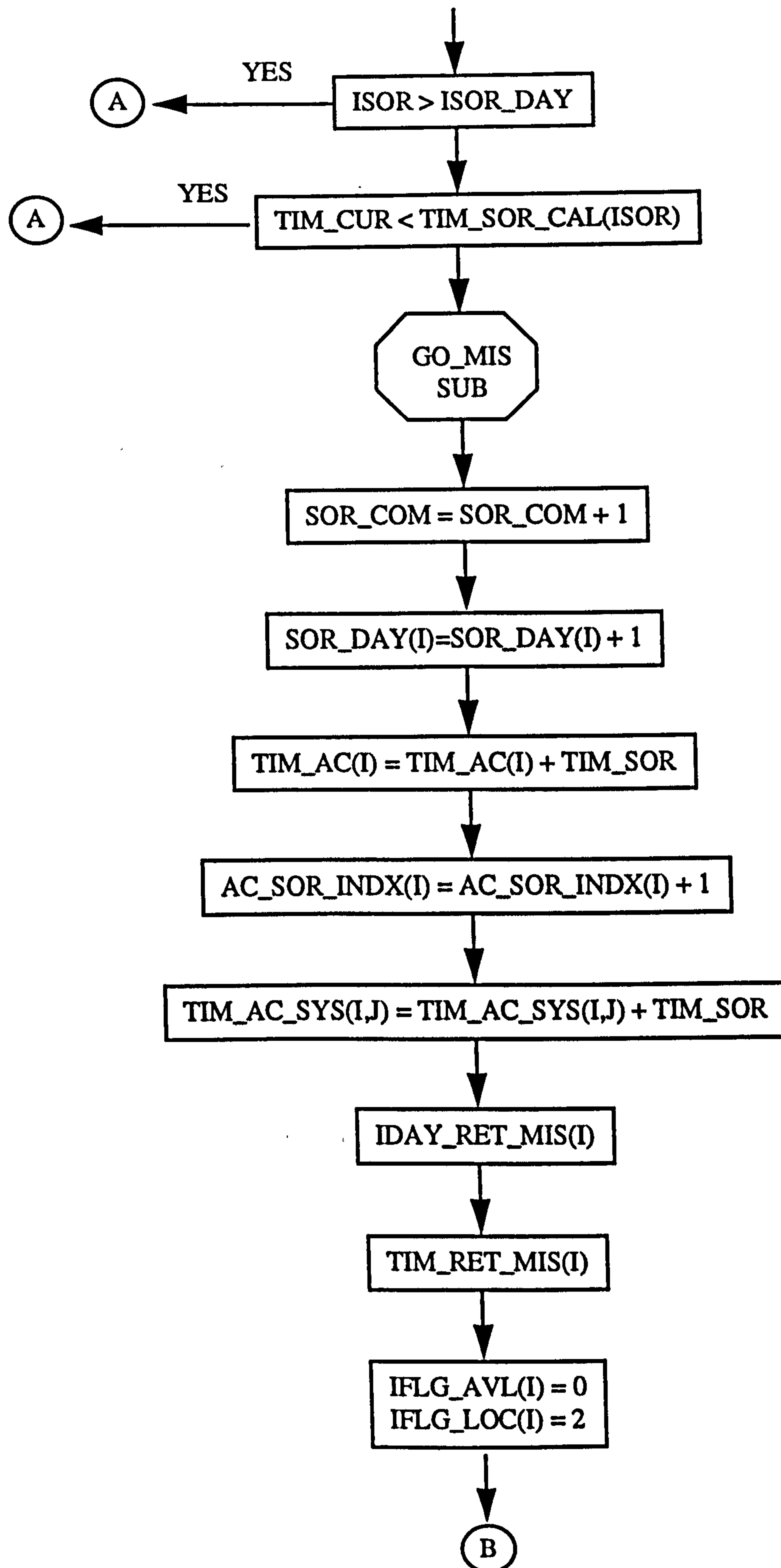


Fig. 5.4

Cont.

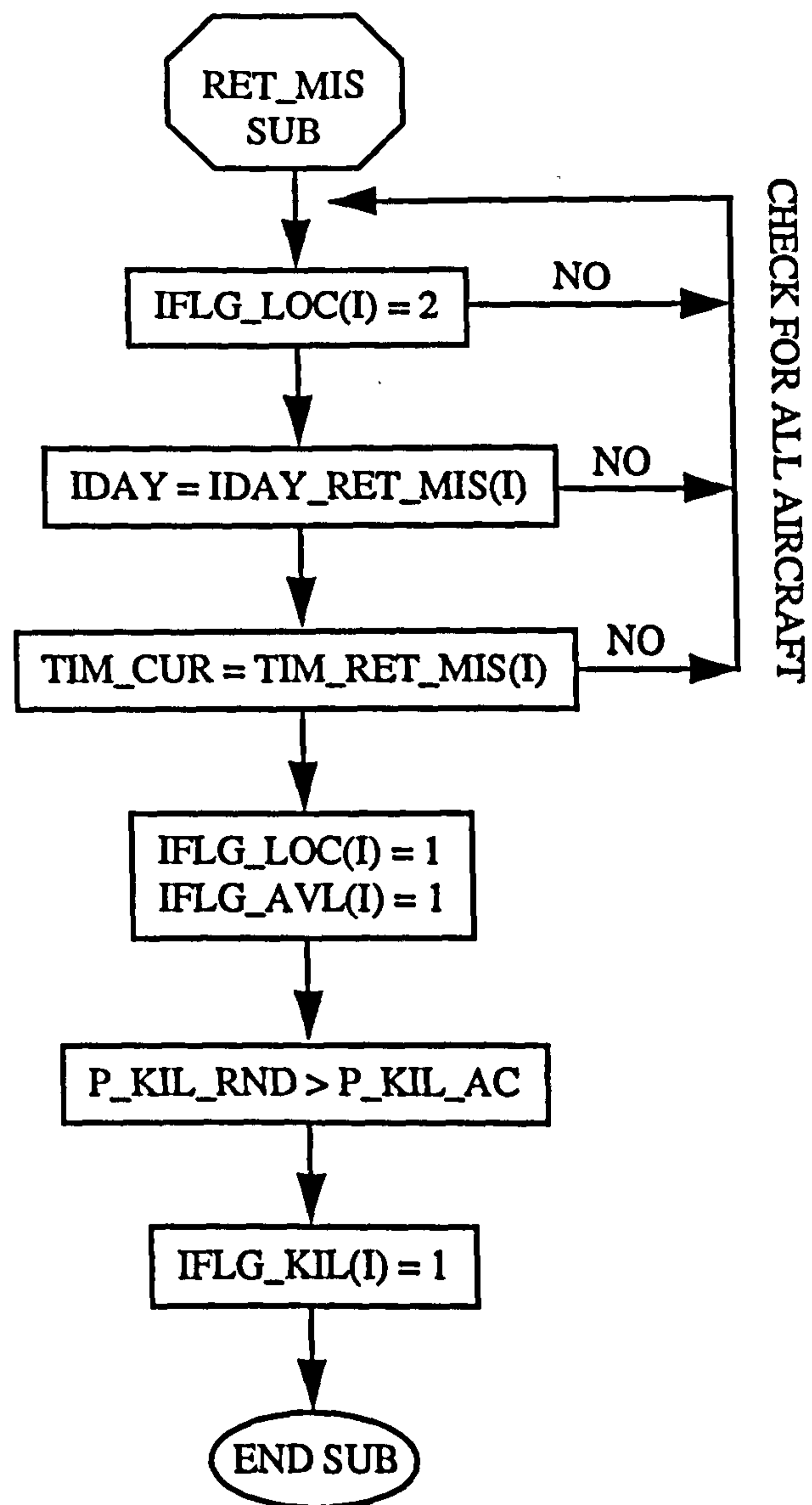


Fig. 5.4

Cont.

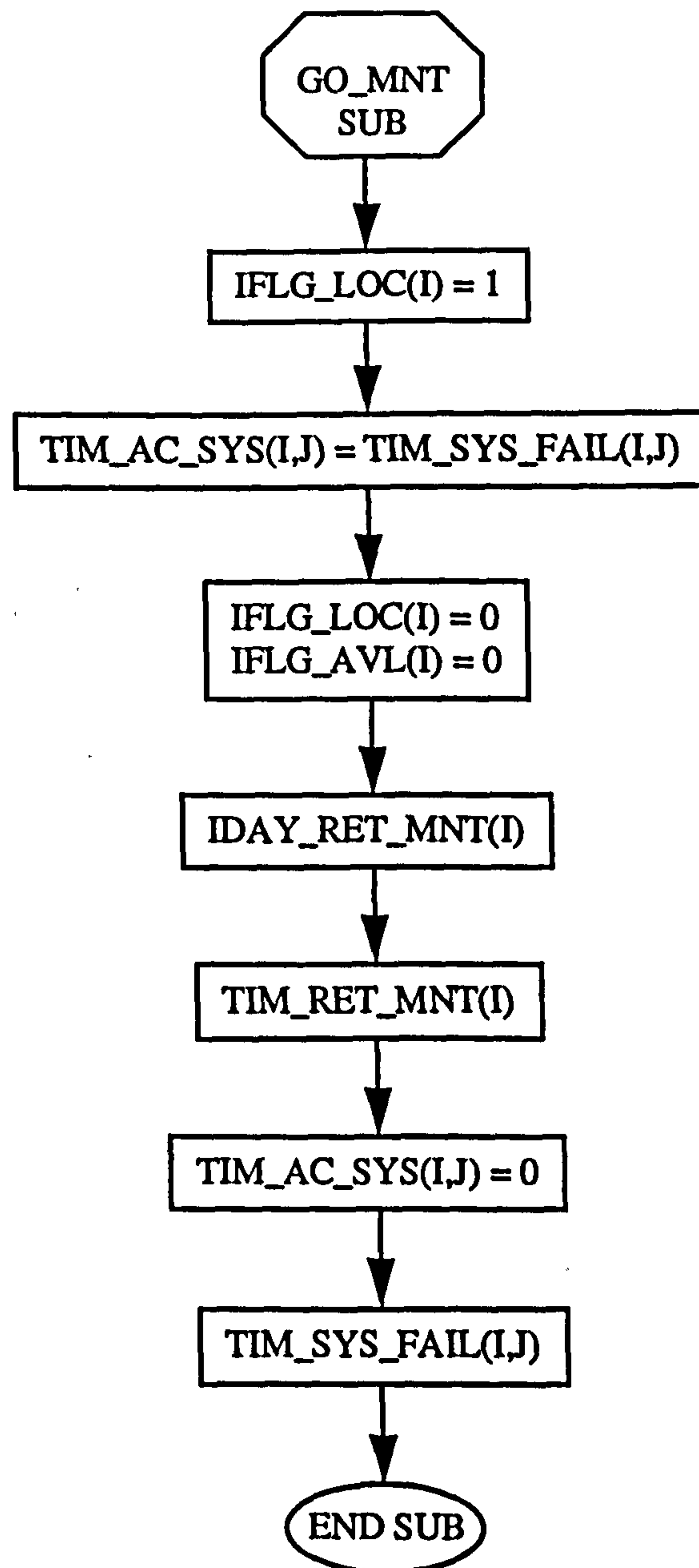


Fig. 5.4 Cont.

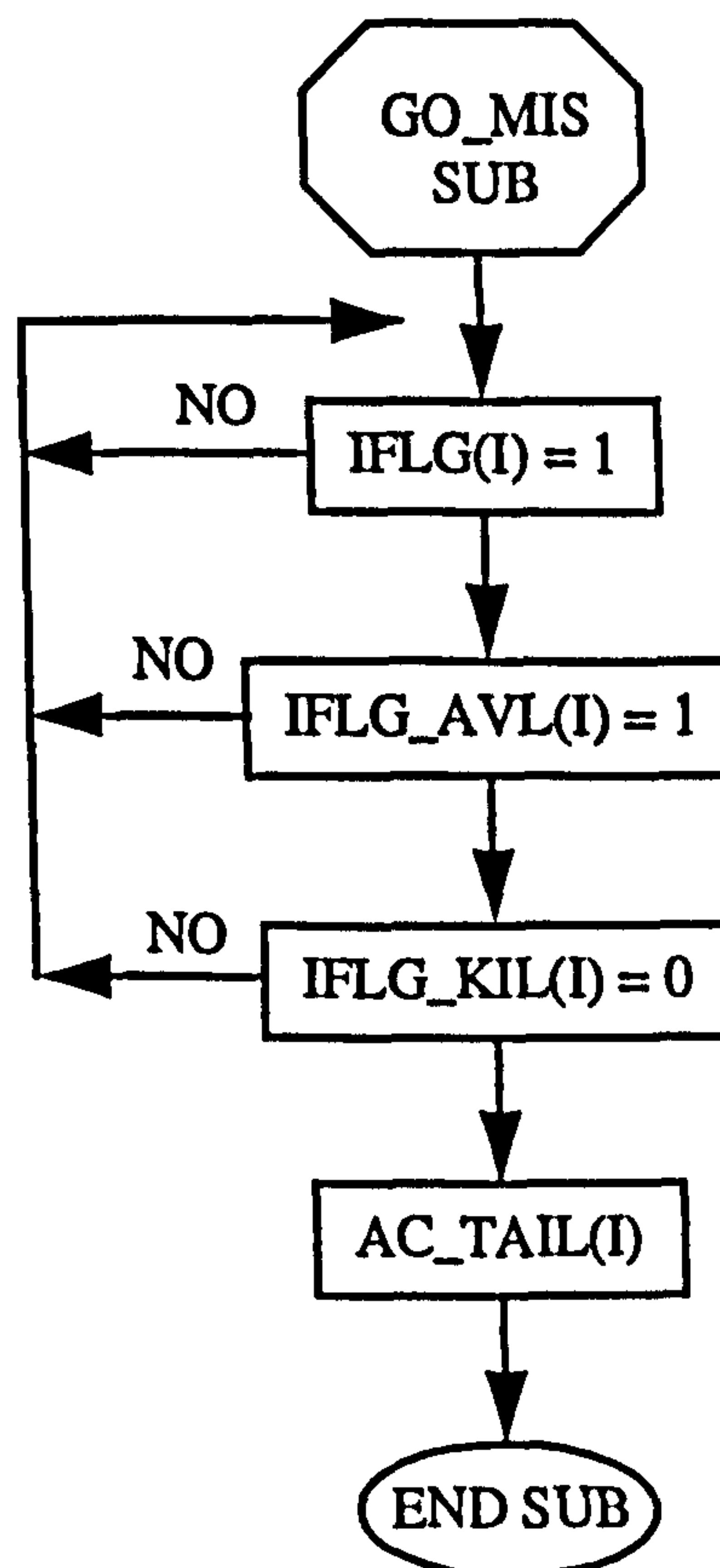
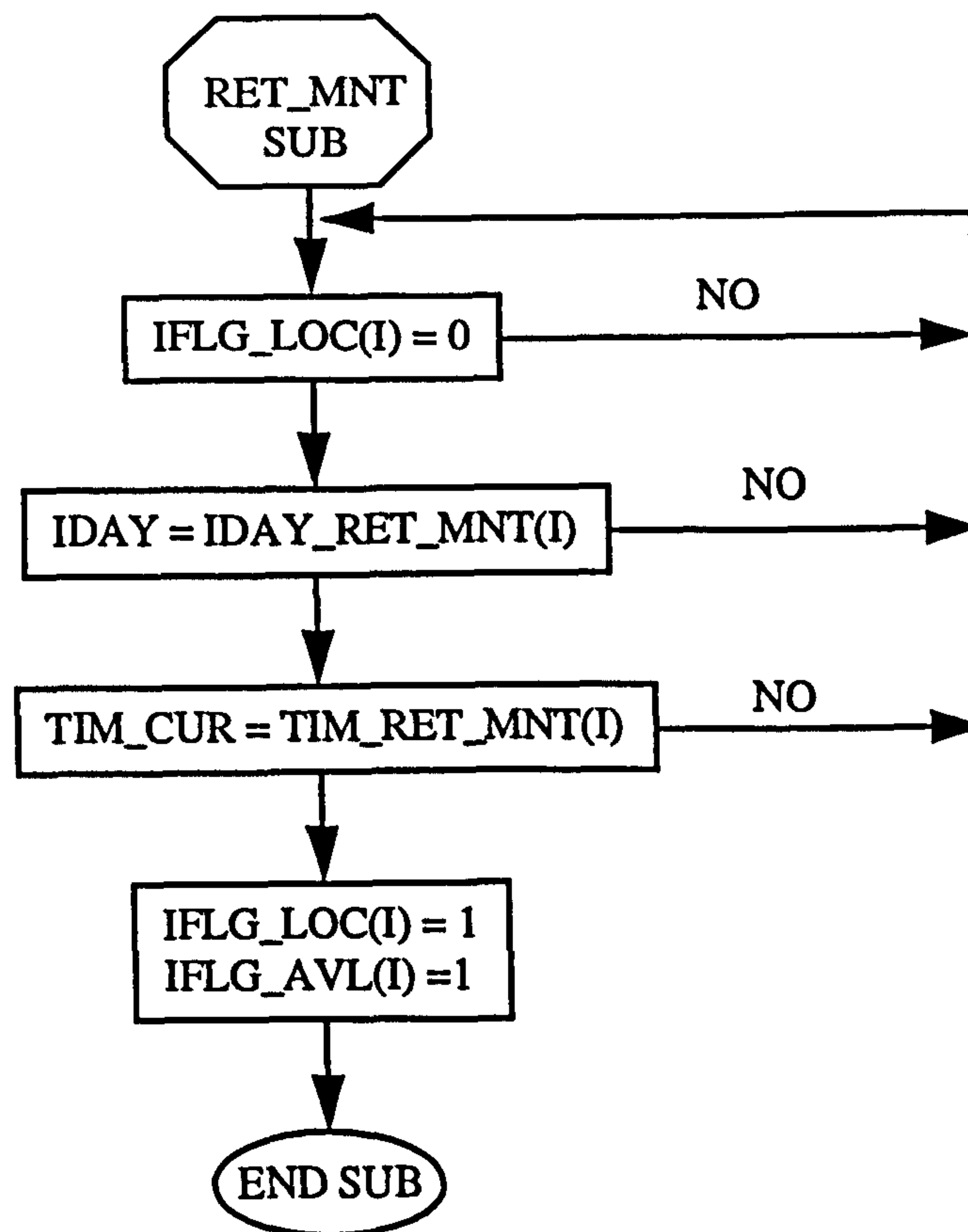


Fig. 5.4

Cont.

Chapter Six

Methodology Applications and Validations

6.1 Application Introduction

This chapter illustrates the use of the methodology and how it can be integrated with the conceptual/preliminary design phase. Also some test cases show that some modules of the methodology could be used as stand-alone tools for the purpose of evaluating combat aircraft in operation. The validation work can be divided into two parts, the first one compares the effectiveness methodology with available figures from recent conflicts such as the Desert Storm operation. The second part is to show an example of the use of the methodology to investigate the impact of aircraft characteristics on combat effectiveness.

6.2 Module's Data Flow

The main modules of the methodology communicate with each other through the file transfer process. Fig. 6.1 shows the four main modules and the files that transfer between them. Each file name is composed of two parts, the first reflects the name of module that generated it, and the second part reflects the name of the module incorporating it. These files are as follows:

<i>des_con.in</i>	Contains CONCEPT related data such as the design requirements.
<i>con_srv.in</i>	Contains CONCEPT data that are required to create the solid aircraft model.
<i>con_rm.in</i>	Contains data that are required to perform R&M estimation.
<i>con_msm.in</i>	Contains performance data for the MSM module.
<i>des_srv.in</i>	Contains data similar to the file <i>con_srv.in</i> to do an existing aircraft modelling.
<i>srv_msm.in</i>	Contains the kill probability figures required by the MSM.
<i>des_msm.in</i>	Contains external input data to perform the MSM alone.
<i>des_rm.in</i>	Contains external input data similar to <i>con_rm.in</i> .

rm_msm.in Contains the R&M data required by the MSM.

msm.out Contains the SGR and other output figures of the MSM.

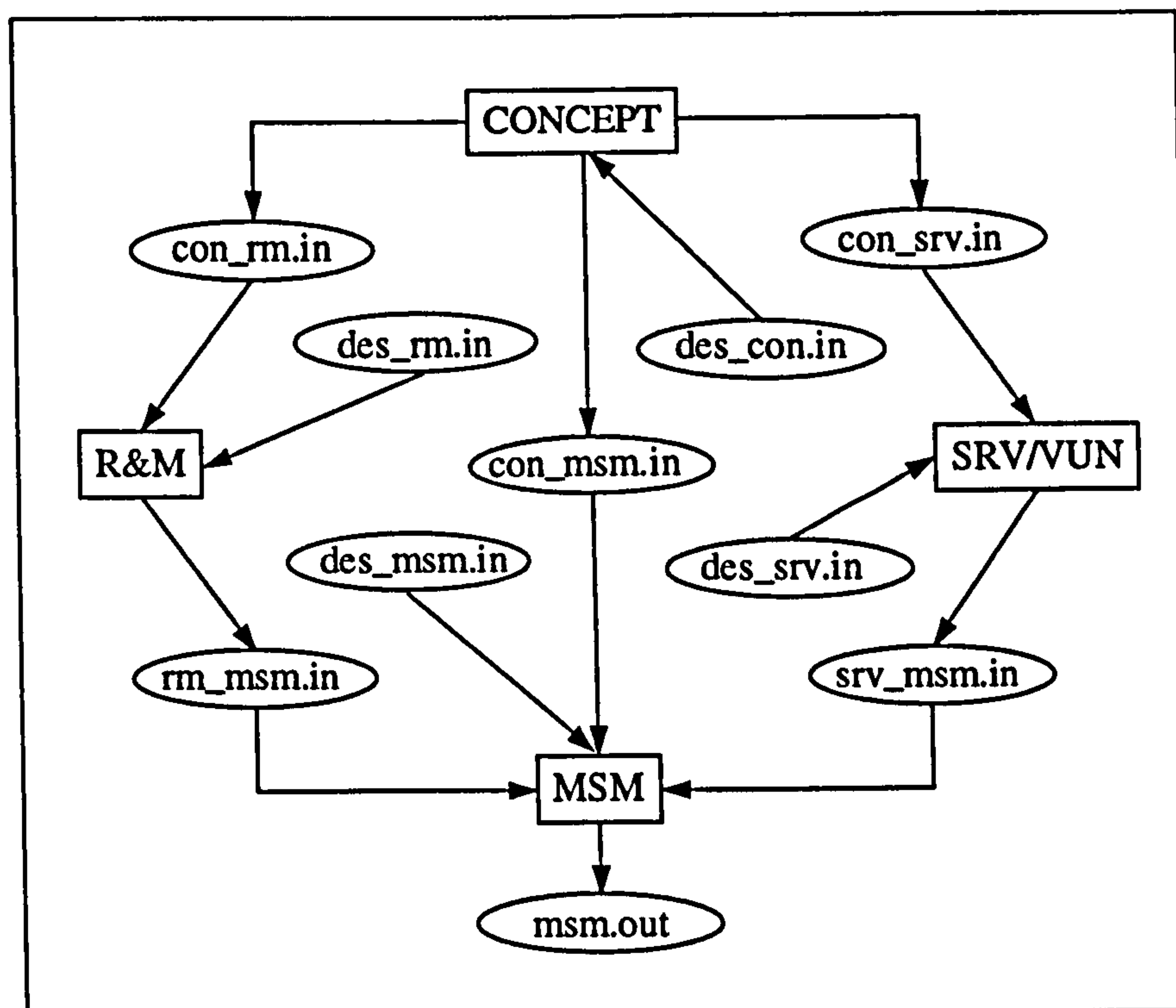


Fig. 6.1 Main modules and files

6.3 Desert Storm Operation

The Desert Storm Operation was a good example of air-power effectiveness. The operation lasted 39 days only, in which more than 100,000 sorties were flown. Two aircraft were selected for the validation. The F-15E Strike Eagle and the F-16 Falcon.

6.3.1 F-15E Operation

Two F-15E's squadrons (total of 24 aircraft) were deployed in the Desert Storm Operation. These aircraft were operated from Al-Kharj base 80 km south of Riyadh City. The F-15Es flew more than 2100 sorties averaging 3.27 hours per sortie and 54 sorties per day, (Refs. 35, 36 and 37). More than 11.2 million Pounds of ordnance were delivered. There were two combat losses, the cause is unknown, but most likely were

due to ground fire. The above data with the R&M data of the F-15E were input to the MSM model. Fig. 6.2 shows the sortie generation rate as given by the MSM. All sorties scheduled for launch were flown ($39 \times 54 = 2106$ sorties). The Mission Capable Rate (MCR) is the percent of time the aircraft is mission capable. Fig. 6.3 shows the MCR of each of the F-15Es as given by the MSM. The MCR figures of the F-15Es agree with the figures from Ref. (10) and shown in Fig. 6.4. The flying loads in terms of number of sorties flown by each aircraft is shown by Fig. 6.5. The Figure shows similar loads on each aircraft in the squadron.

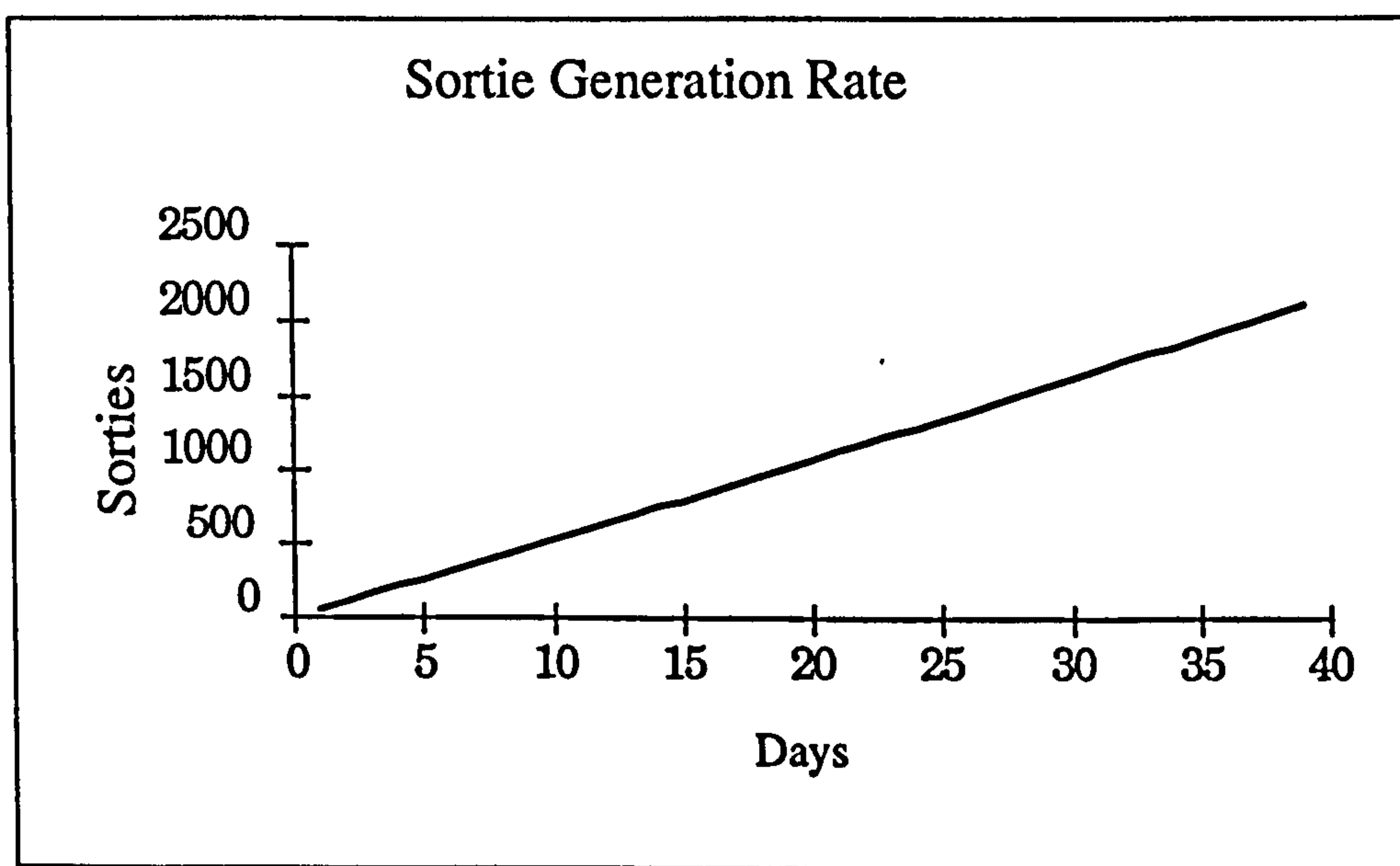


Fig. 6.2 F-15E's SGR

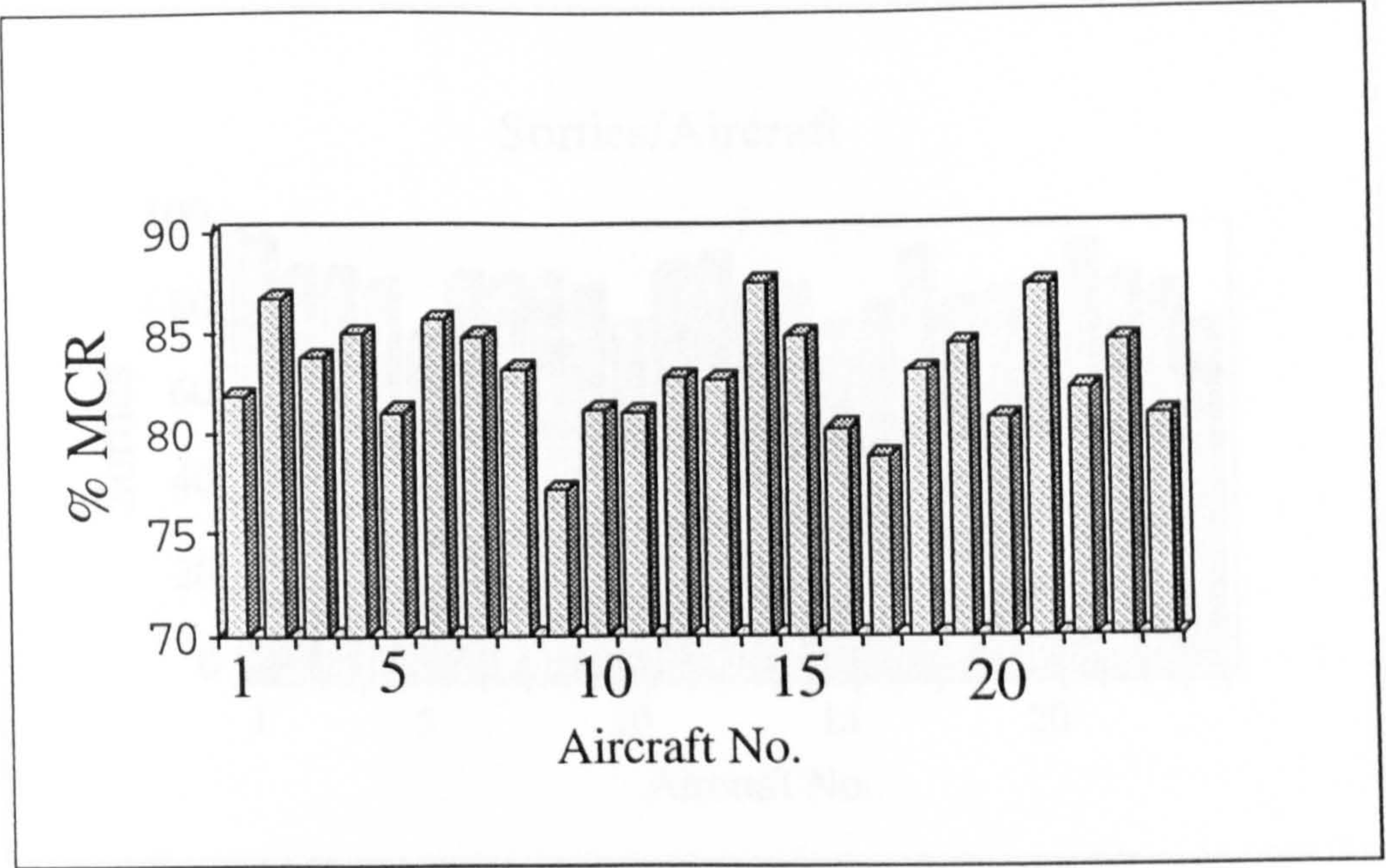


Fig. 6.3 F15E Mission Capable Rate

6.2.3 Data Operations

24 F15E aircraft deployed in the Gulf War. These aircraft flew 12,483 sorties and were

operational for 8,444 hours. The F15E aircraft were deployed in the Gulf War for 12,483 sorties and were

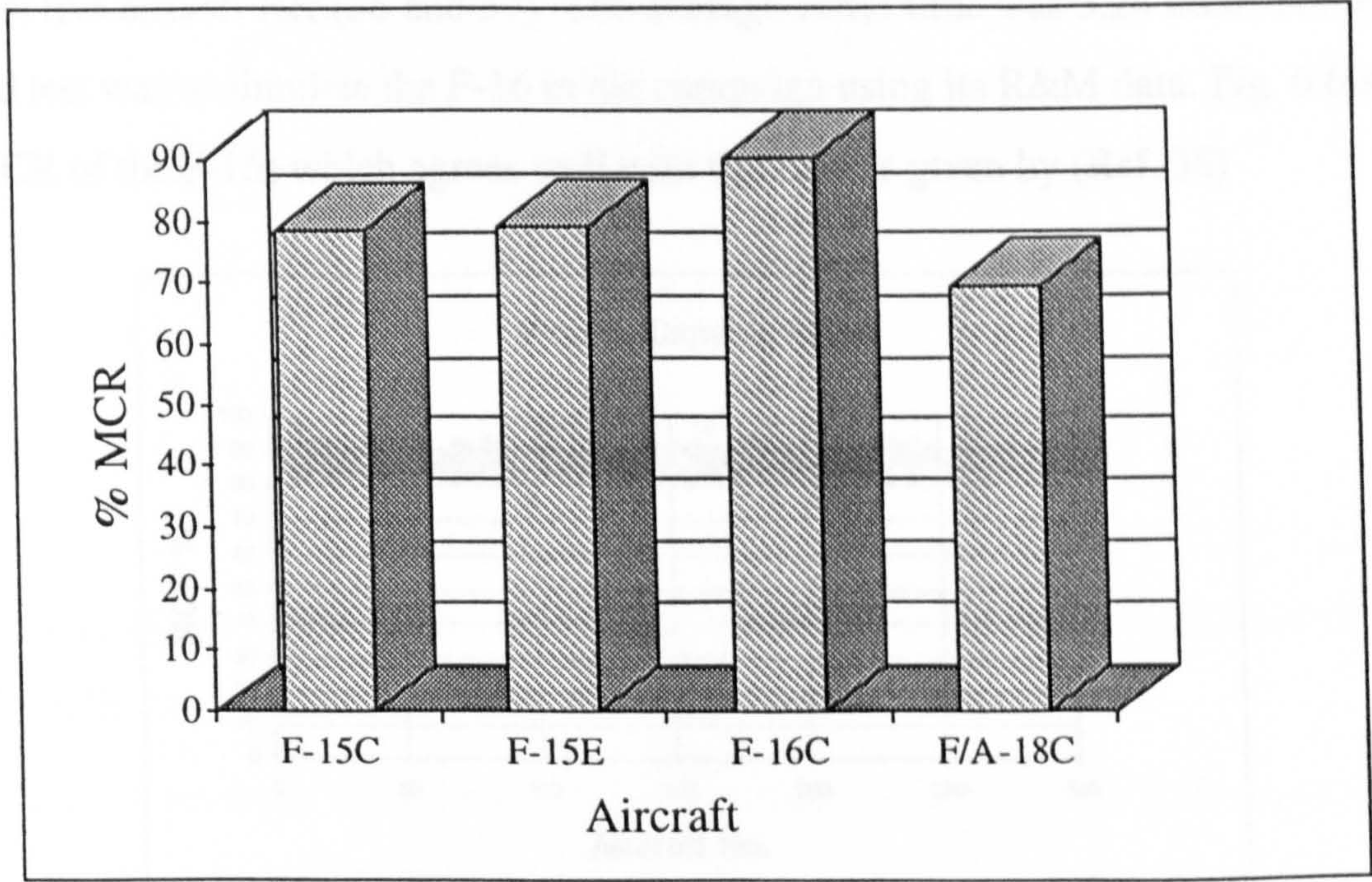


Fig. 6.4 Mission capable rates at Desert Storm.

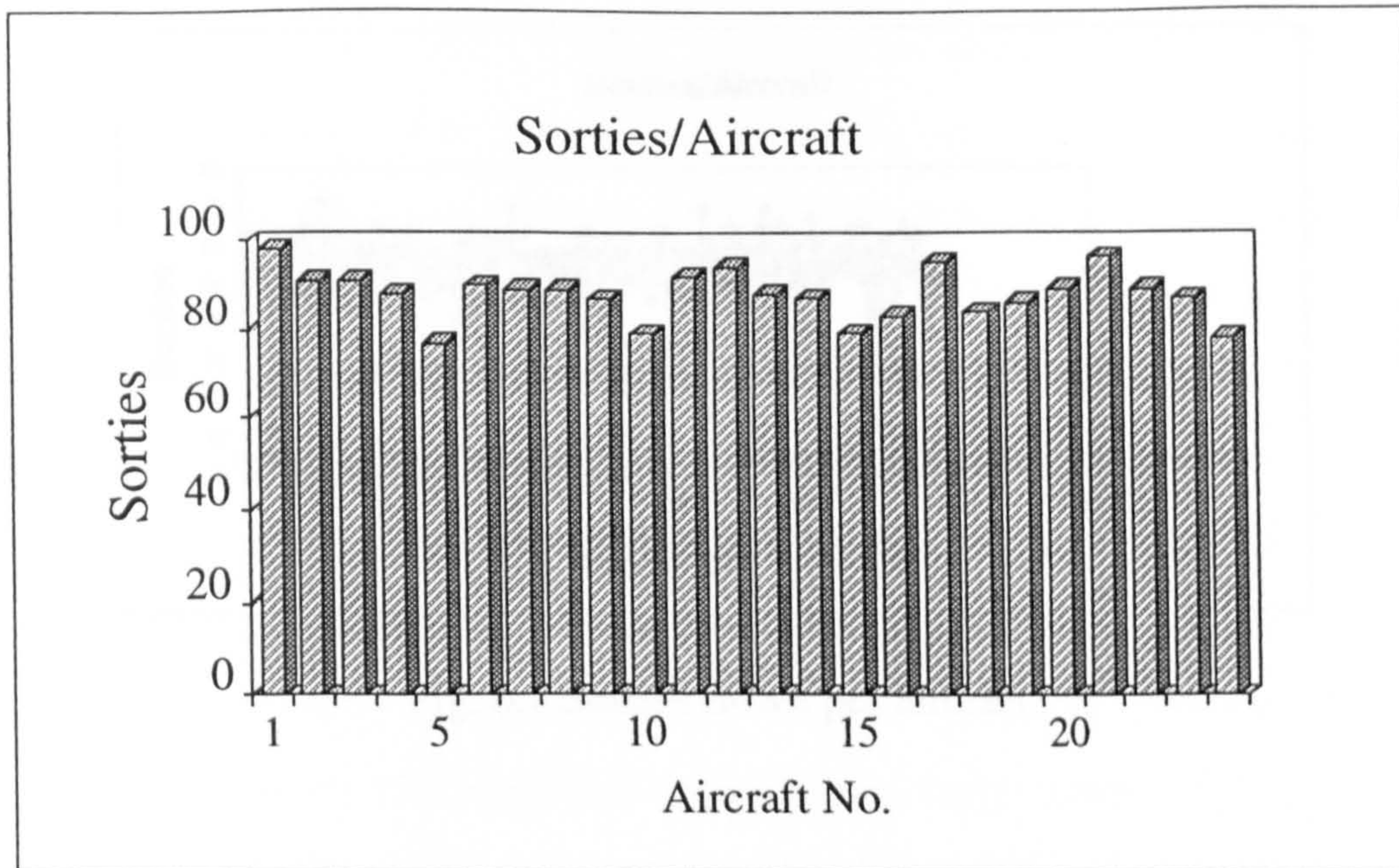


Fig. 6.5 F15E's sorties per aircraft.

6.3.2 F-16 Operation

251 F-16's were deployed in the Gulf War. Those aircraft flew 13,480 combat sorties and lost five aircraft Ref.(36 and 37). The average sortie time was 3.24 hours/sortie. The second test was to simulate the F-16 in the campaign using its R&M data. Fig. 6.6 shows the MCR of the F-16s which agrees well with the figures given by (Ref. 38)

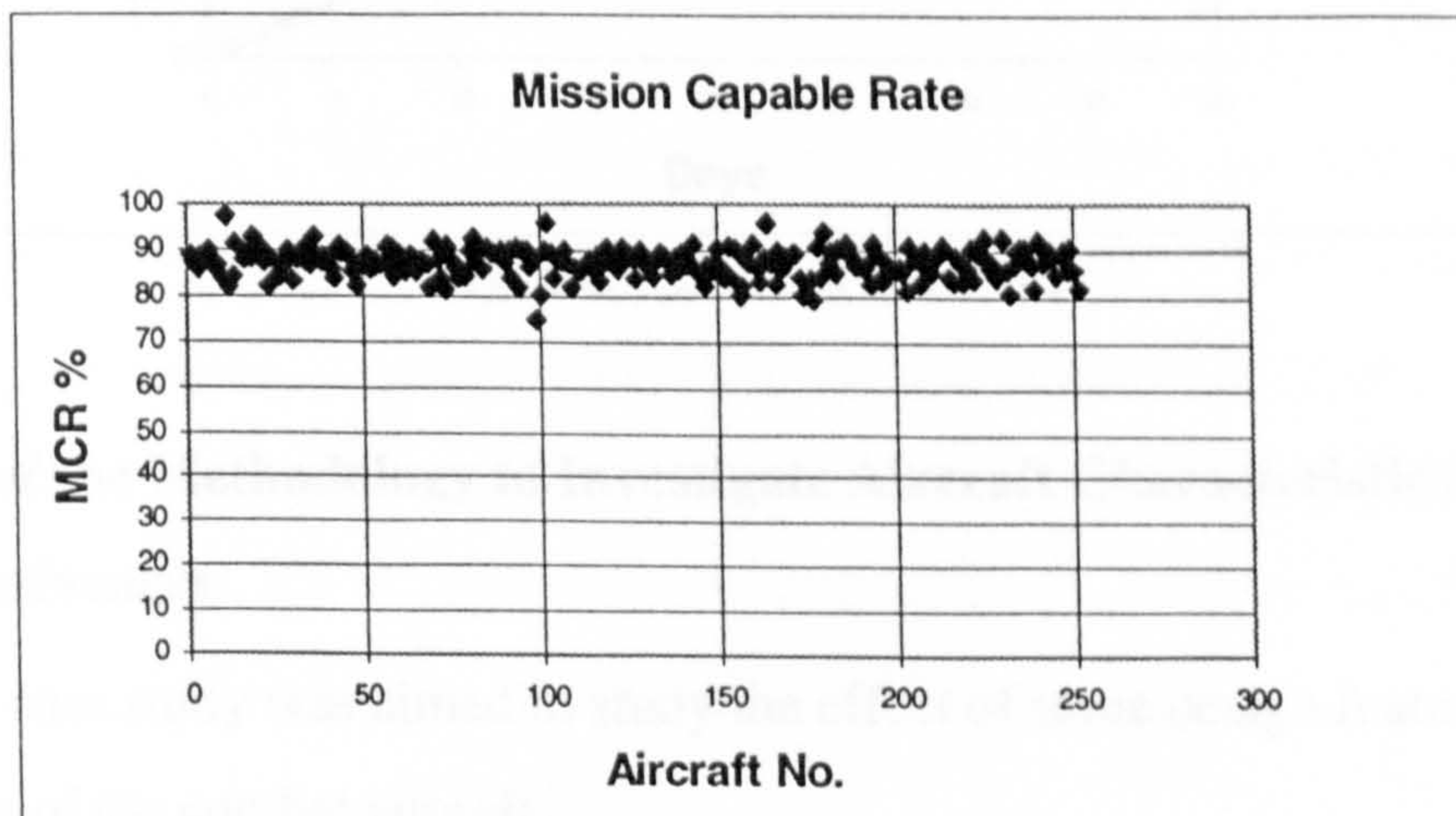


Fig. 6.6 F-16 Mission Capable Rate

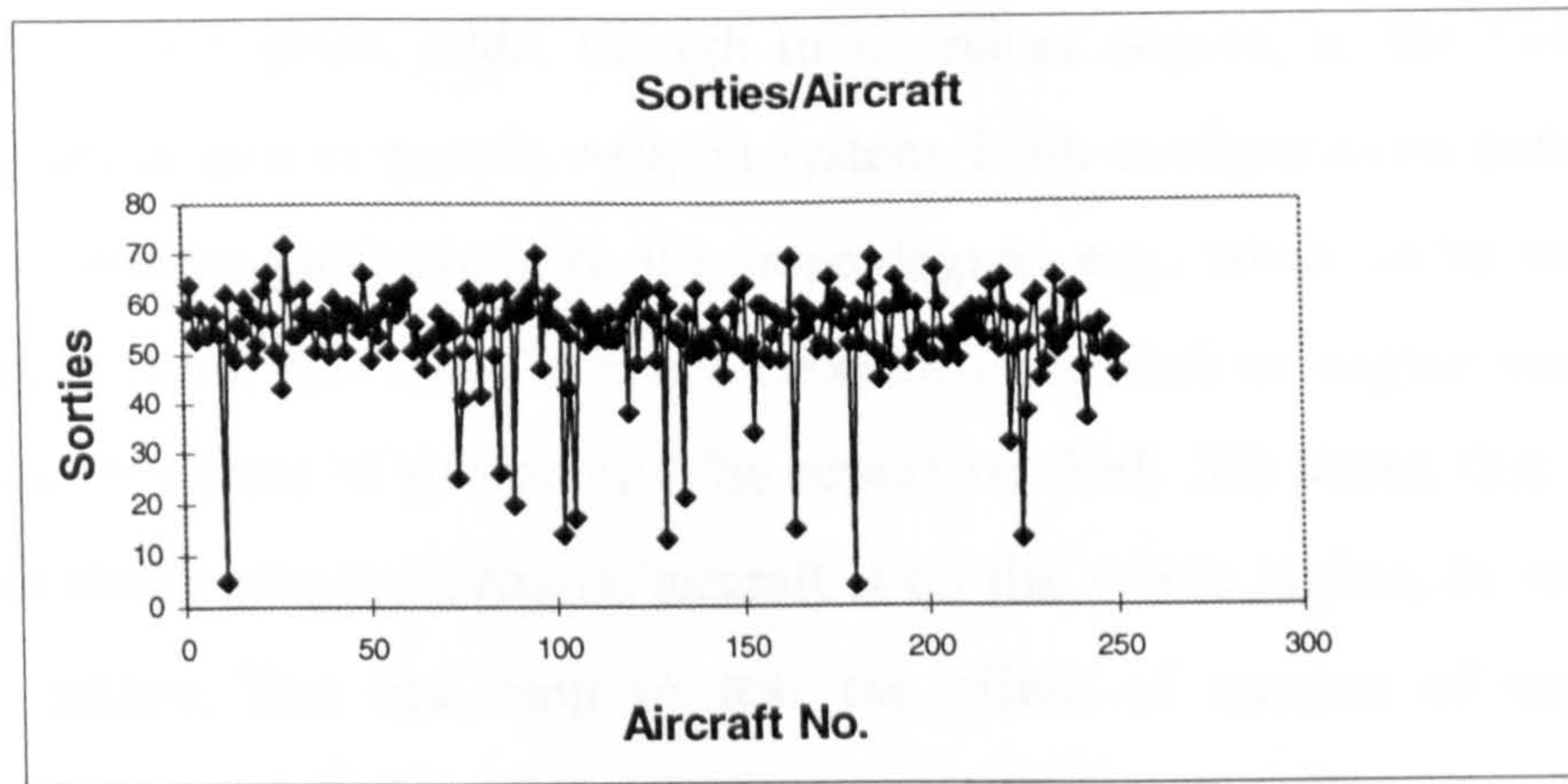


Fig. 6.7 Sorties flown per aircraft

The sortie generation rate of the F-16s, Fig. 6.8, shows that all the sorties required are launched and none was lost due to aircraft unavailability. The SGR of the two aircraft agrees with their operational performance during the Desert Storm data.

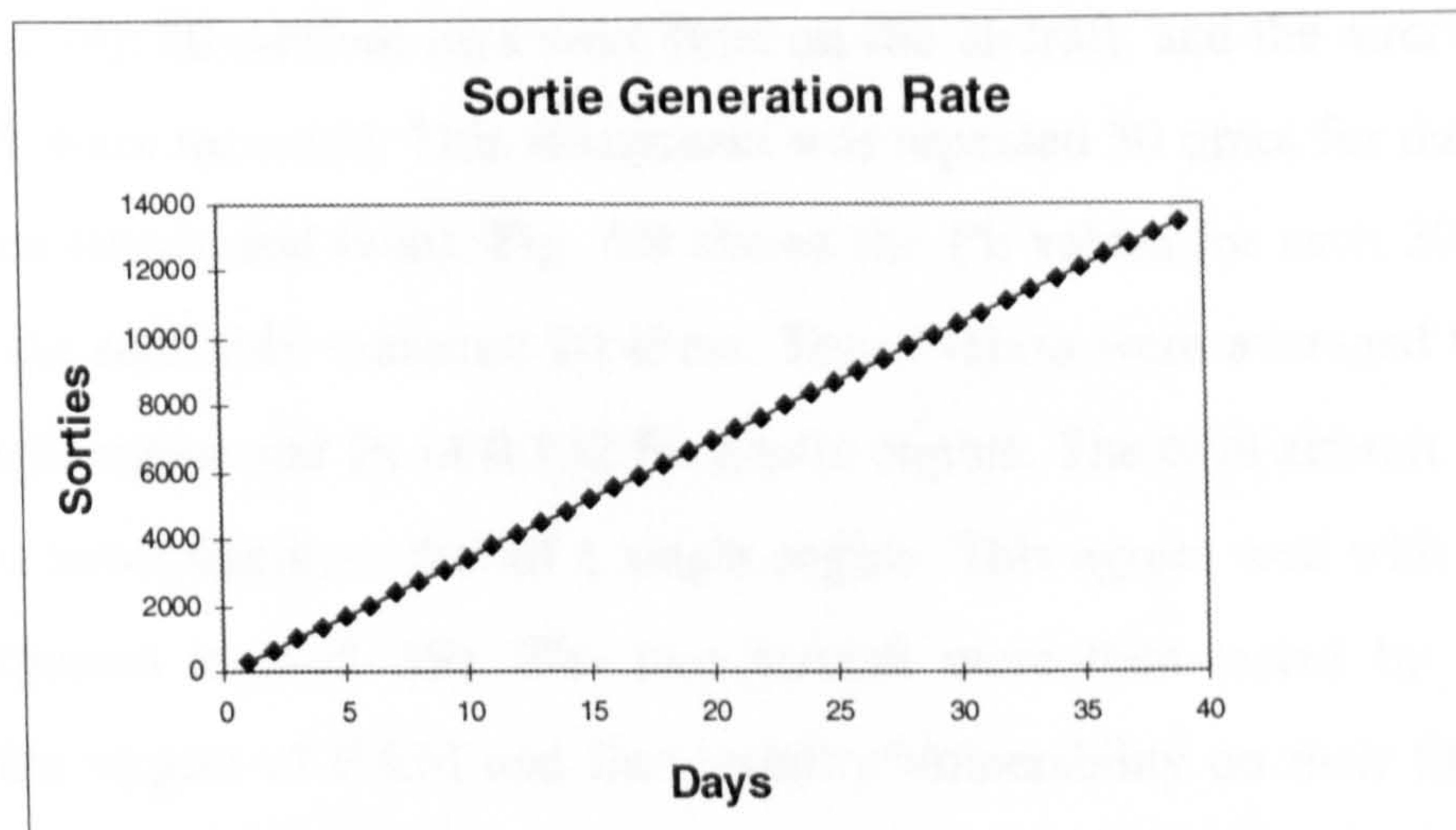


Fig. 6.8 SGR of the F-16

6.4 Use of the Methodology to Investigate Aircraft Characteristics and their Effectiveness

This type of case study was aimed to study the effect of some design features on the effectiveness of the combat aircraft.

6.4.1 Number of Engines

The long-running debate about single-engine versus twin-engine fighter aircraft is still alive. Doubling the number of engines and, consequently, increasing the volume and the

surface of the power plant, adds, though to a smaller degree, to the likelihood of an aircraft being hit by gun or missile weapon system. Both configurations (single and twin-engine) are vulnerable particularly to the same degree, e.g., when hit by guided missiles with IR homing head; however, it is not necessarily so that an engine being hit would cause damage or failure of the other. The report of (Ref. 39) states that the historical combat survivability of a twin-engine aircraft is on the whole higher, by some estimates 15 to 25% higher. The first step to test the effect of number of engines on the effectiveness of a combat aircraft is to select a baseline design. The aircraft selected for sizing is required to deliver a payload of 2000 pound of ordnance (4 Mk-82 Bombs) and have a combat radius of 300 NM. The aircraft has a conventional tail, maximum Mach number of 1.8. Both aircraft are identical except for the number of engines. The first case to investigate is to choose the worst direction from which the weapon has the most effectiveness on the aircraft. The engine kill figures due to this threat were taken from (Refs. 13 and 14). 20 random rays were fired on the aircraft, and the aircraft Pk due to the engine Pk were recorded. This assessment was repeated 30 times for the two aircraft configurations (single and twin). Fig. 6.9 shows the Pk values for each 30 independent runs due to the randomly scattered 20 shots. These values were averaged to give Pk of 0.2 for a single engine and Pk of 0.152 for a twin engine. The twin aircraft configuration is 24% more survivable than that of a single engine. This agrees well with the historical estimates reported in (Ref. 39). The two aircraft were then tested by the MSM to investigate the impact of R&M and Survivability/Vulnerability on their SGR. An input probability of kill equal to 0.005 are selected first. For each aircraft 3 sorties/day were required for 30 days of simulation. Each squadron was assumed to consist of 24 aircraft. The average sortie time is set to 3 hours. Fig. 6.10 shows the effect of R&M on SGR of the two configuration. The single-engined aircraft flew 2051 sorties and the twin engine flew 1929 sorties (maximum figure = $3 \times 24 \times 30 = 2160$ sorties).

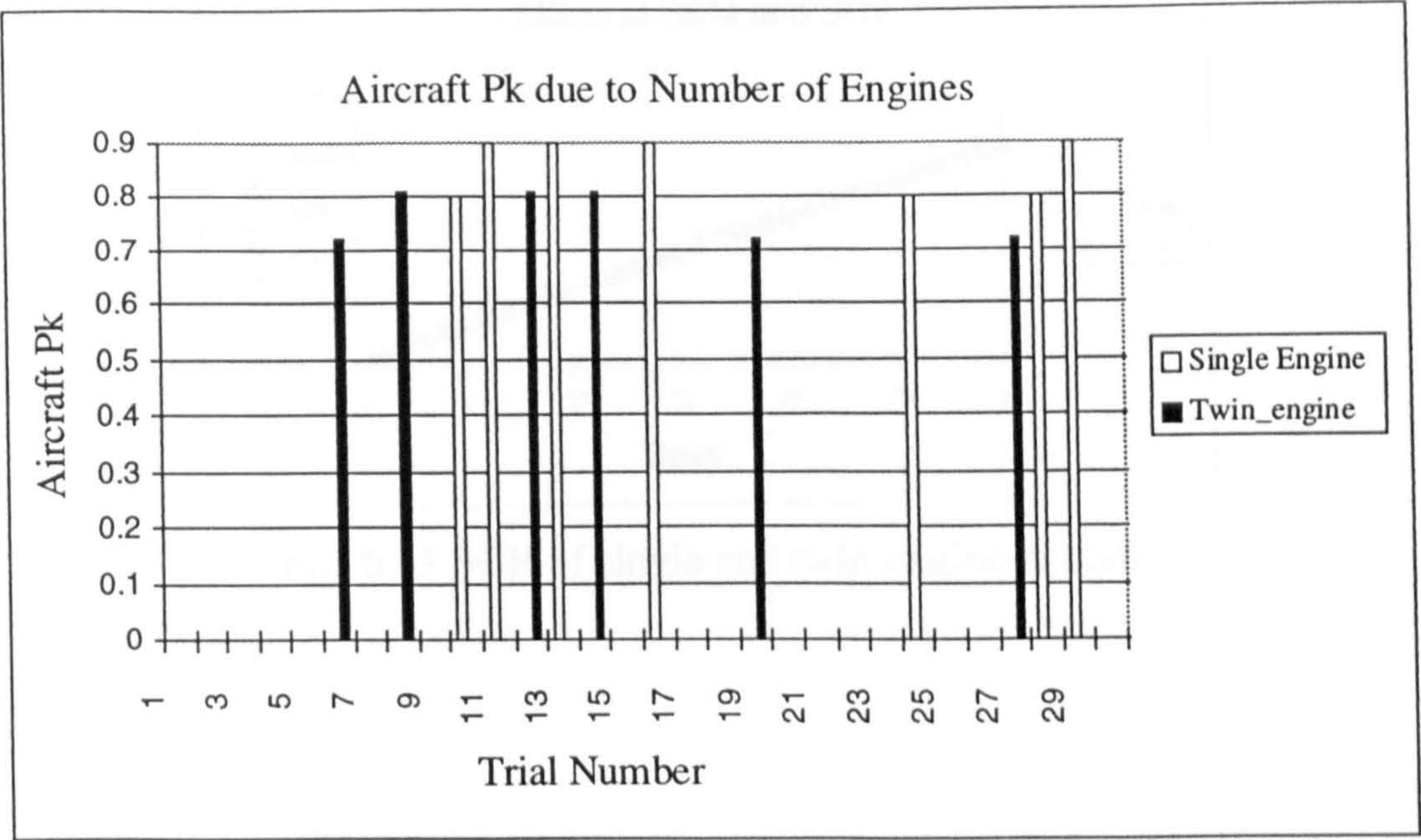


Fig. 6.9 Aircraft Pk at different hits

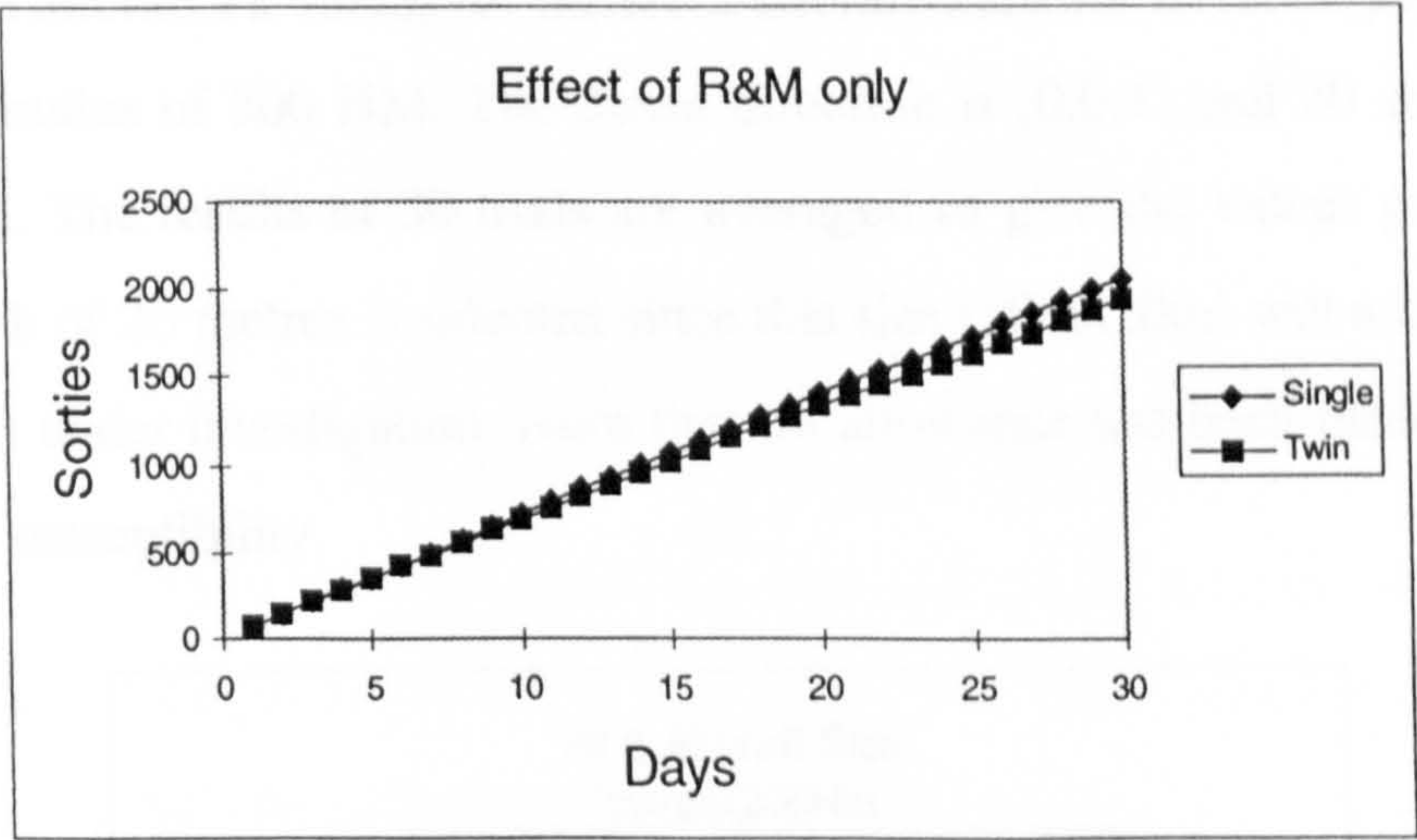


Fig. 6.10 SGR of a single and twin-engine aircraft

The second run was using the same R&M figures but taking the reduced vulnerability of the twin-engined configuration. The Pk was set to be 24% less than that of the single engined. For these parameters the effectiveness of the two aircraft are almost identical as shown by Fig. 6.11. The single engine aircraft flew 2051 sorties and the twin flew 2021 sorties.

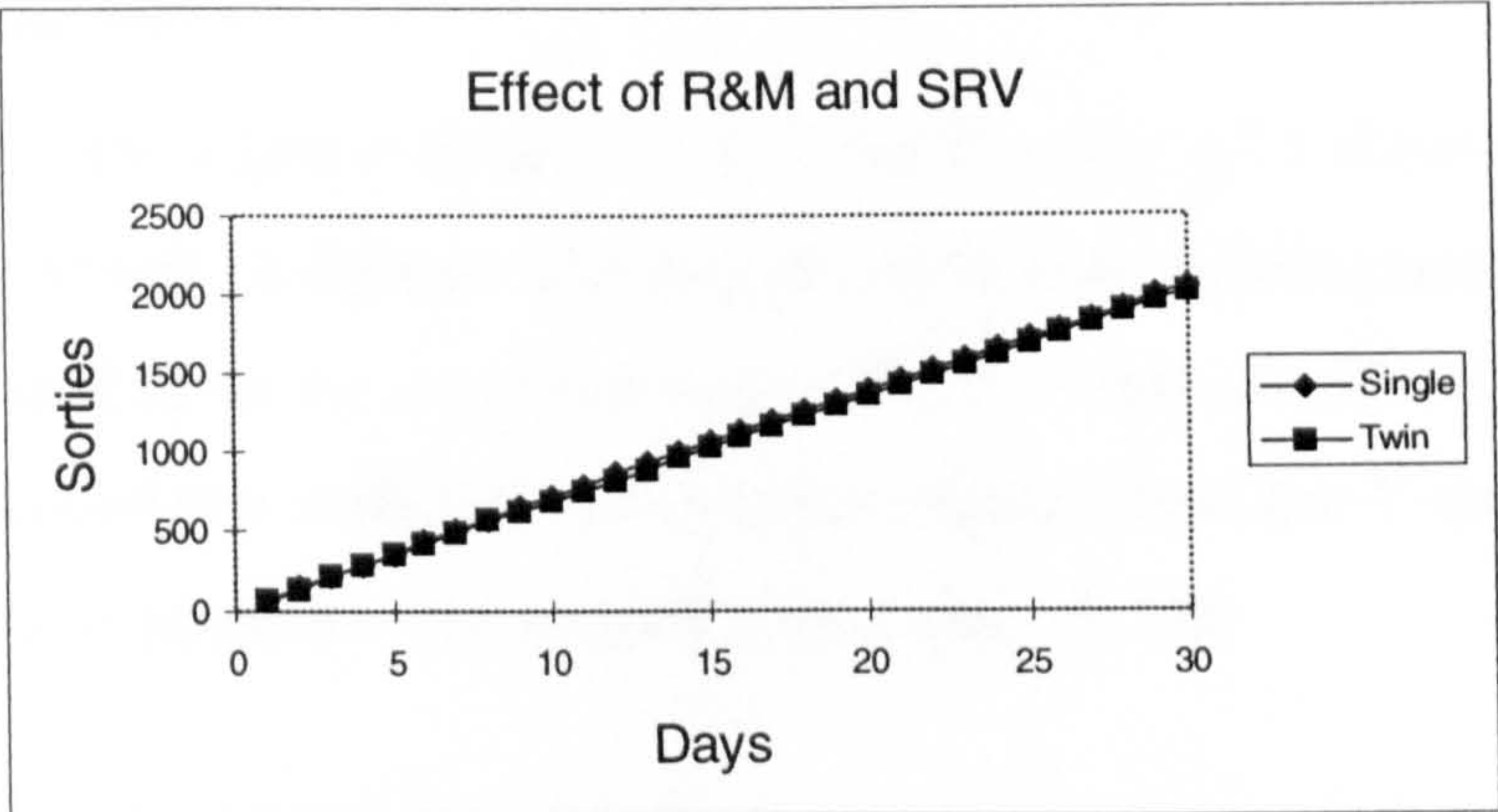


Fig. 6.11 SGR of single and twin-engine aircraft

6.4.2 Payload and Range

Aircraft payload and range affect the empty weight of the aircraft and hence its size. Fig. 6.12 shows the aircraft Pk values for different aircraft sized for different payloads and the same combat radius of 300 NM. The threat direction is (0,0,1) and 20 shots were fired on the aircraft. The results of 30 trials are averaged to give the values presented in the Figure. A mesh of 20 metres is selected since this size (20mx20m) will accommodate the size of aircraft under investigation. Note that no allowance has been made for the effect of the size on susceptibility.

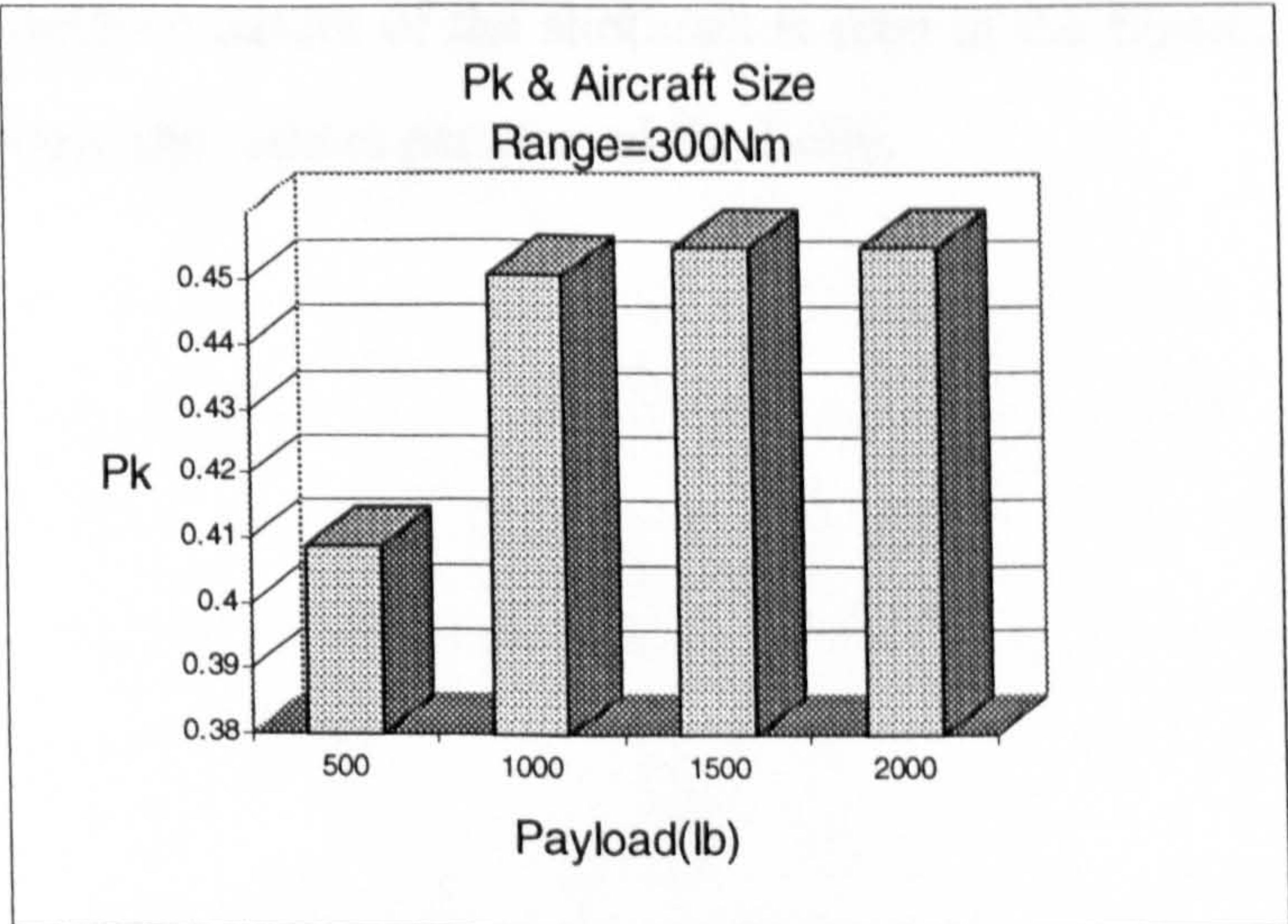


Fig. 6.12 Aircraft size effect on its Pk.

6.4.3 Threat Direction

Threat direction is a key factor on aircraft vulnerability. Fig. 6.13 shows the effect threat direction on the aircraft Pk figures. The first direction to be investigated is the worst one which is corresponding to the direction-vector $(0,0,1)$ - bottom-side of the aircraft, see Fig. 4.21. The second one is $(0,1,1)$ which is 45 degrees from the Y-axis. The third one corresponds to shots parallel to the aircraft lateral axis, $(0,1,0)$

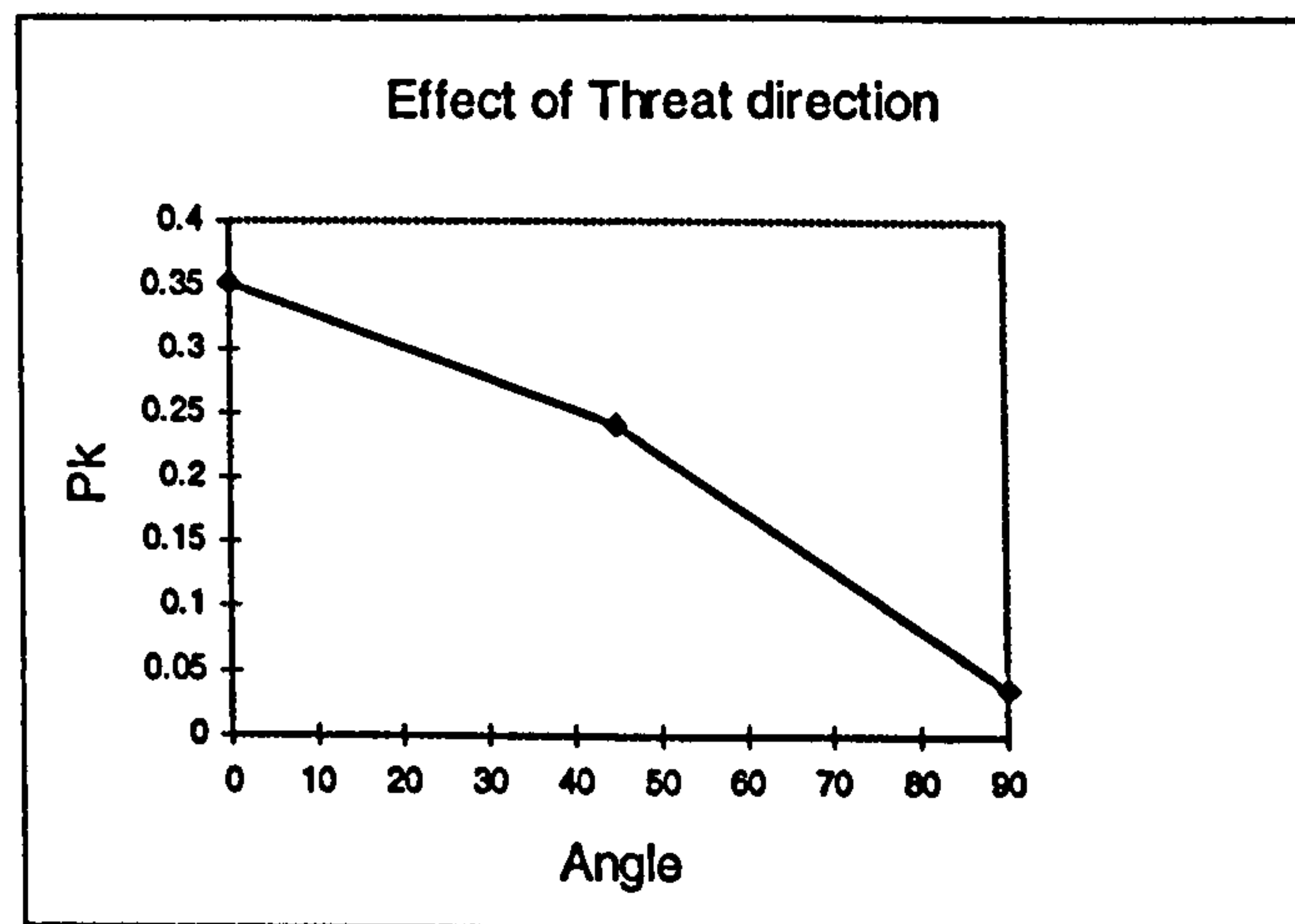


Fig. 6.13 Pk from different directions

The aircraft for this test is a twin-engine aircraft sized to carry a payload of 2000 lb and has a combat radius of 300 NM. Fig. 6.14 shows the solid model of the aircraft as well as the shots which penetrated the aircraft. For this case 50 shots were fired and repeated for 50 times. The random-nature of the shotlines is seen in the figure, where some shots have passed the target and others penetrated the body.

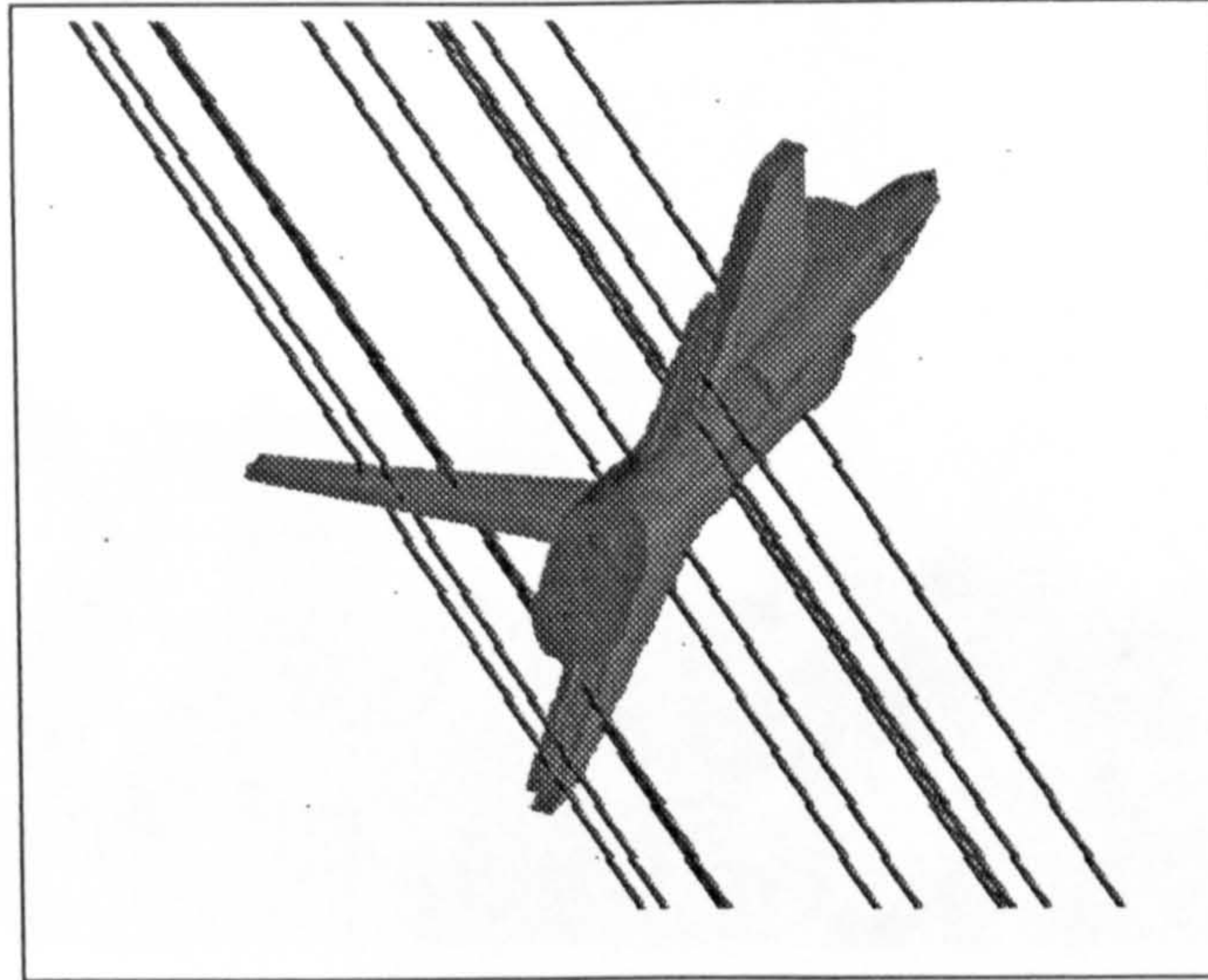


Fig. 6.14 Target and threat interaction

6.5 Use of the Methodology for Aircraft Evaluation

The combat effectiveness of two fighters were evaluated. The two aircraft are of similar category but one incorporates low radar cross section or stealth. The F-22 is a replacement for the F-15 air-superiority multi-role aircraft. Their combat effectiveness is investigated, taking into account the following:

- The enhancement of the F-22 R&M figures.
- The reduced susceptibility of the F-22.
- The supersonic cruise capacity of the F-22

2. Aircraft Modelling

The two aircraft were modelled using the technical dimensions and the 3-views drawings obtained from (Ref. 40). As expected the solid modeller approximates the F-15, shown in Fig. 6.15, better than the F-22, Fig. 6.16. This is because the F-22 fuselage cross section is blended with the wing, whereas that of the F-15 is of the simple rectangular shape with rounded corners. The solid modeller is capable of modelling the diamond shape of the F-22 flying surfaces.



Fig. 6.15 The F-15E .

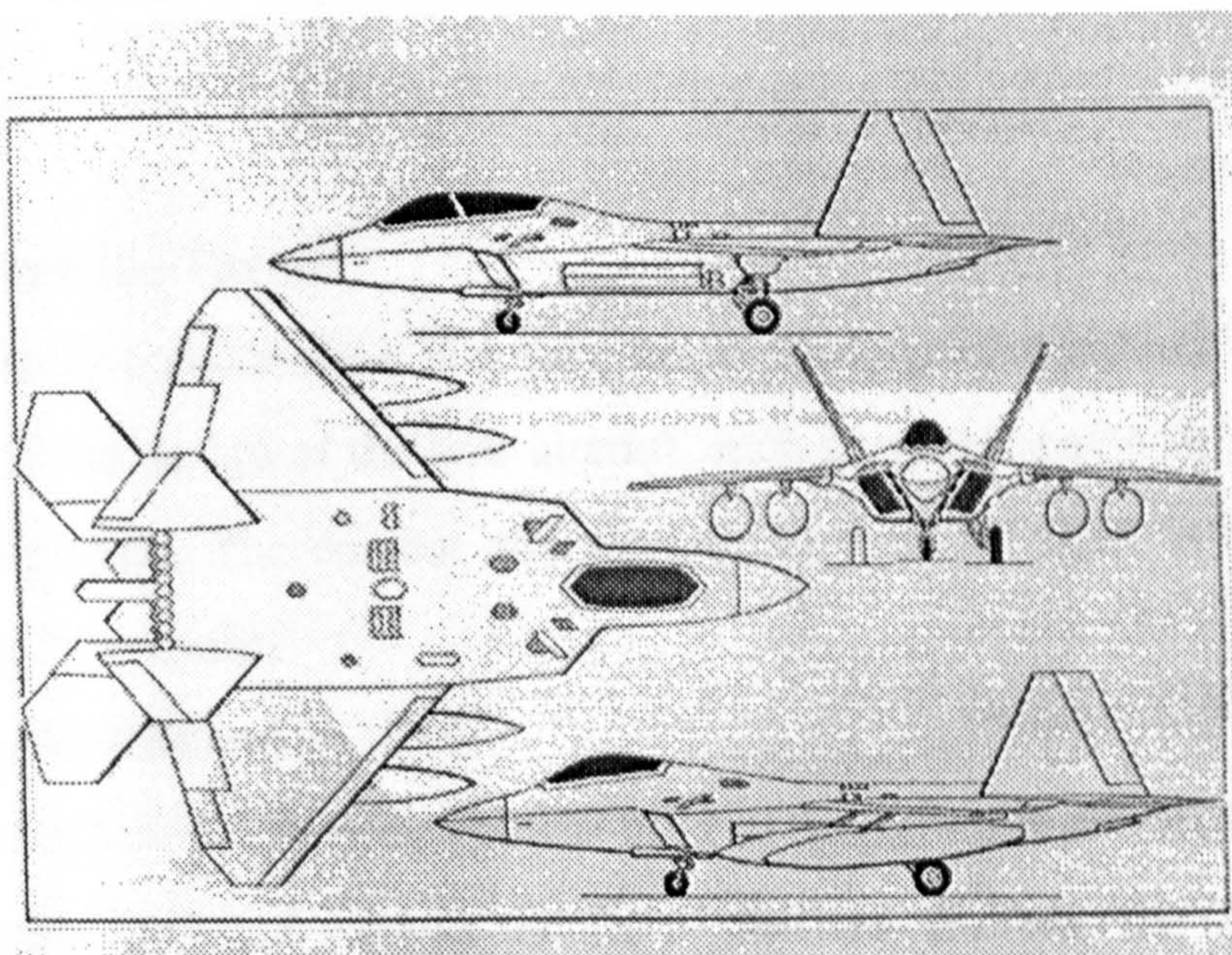


Fig. 6.16 The F-22

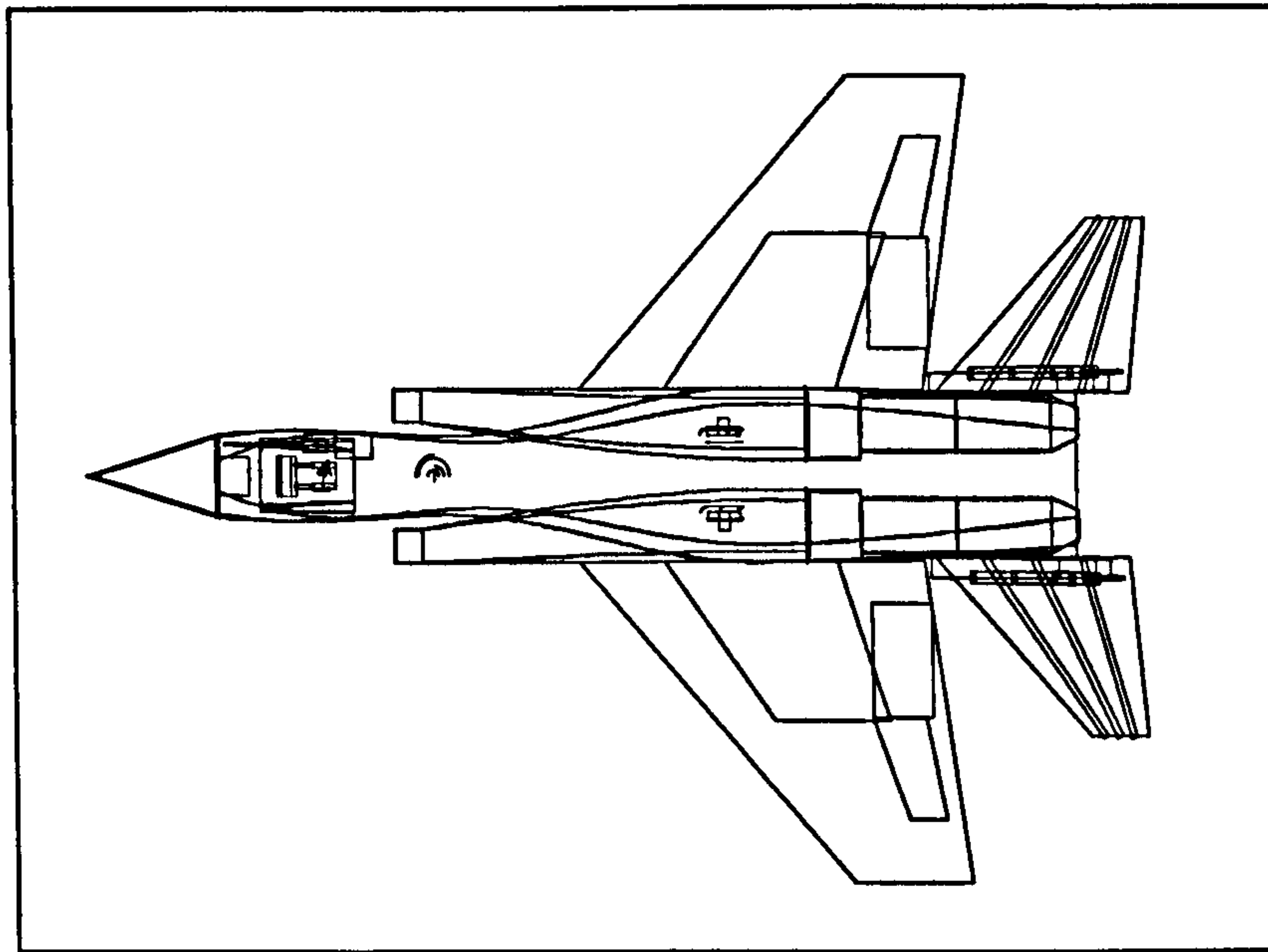


Fig. 6.17. Top view of the F-15 from the solid modeller.

The Mission and the Threat

The mission under consideration is a long range air-to-ground strike . The operational requirements of the design of the two aircraft, such as speed, payload, survivability and R&M are considered. The combat effectiveness in terms of SGR is the effectiveness measure of the two aircraft.

Vulnerability Assessment

The vulnerability assessment program was used to quantify the aircraft Pk from different threat directions. Fig. 6.18 shows the Pk of the two aircraft. The X-axis shows the threat direction. zero angle represents firing on the aircraft from bottom and 90 degrees represent firing on the aircraft from the side views. The figure shows that their is a slight reduction in vulnerability of the F-15.

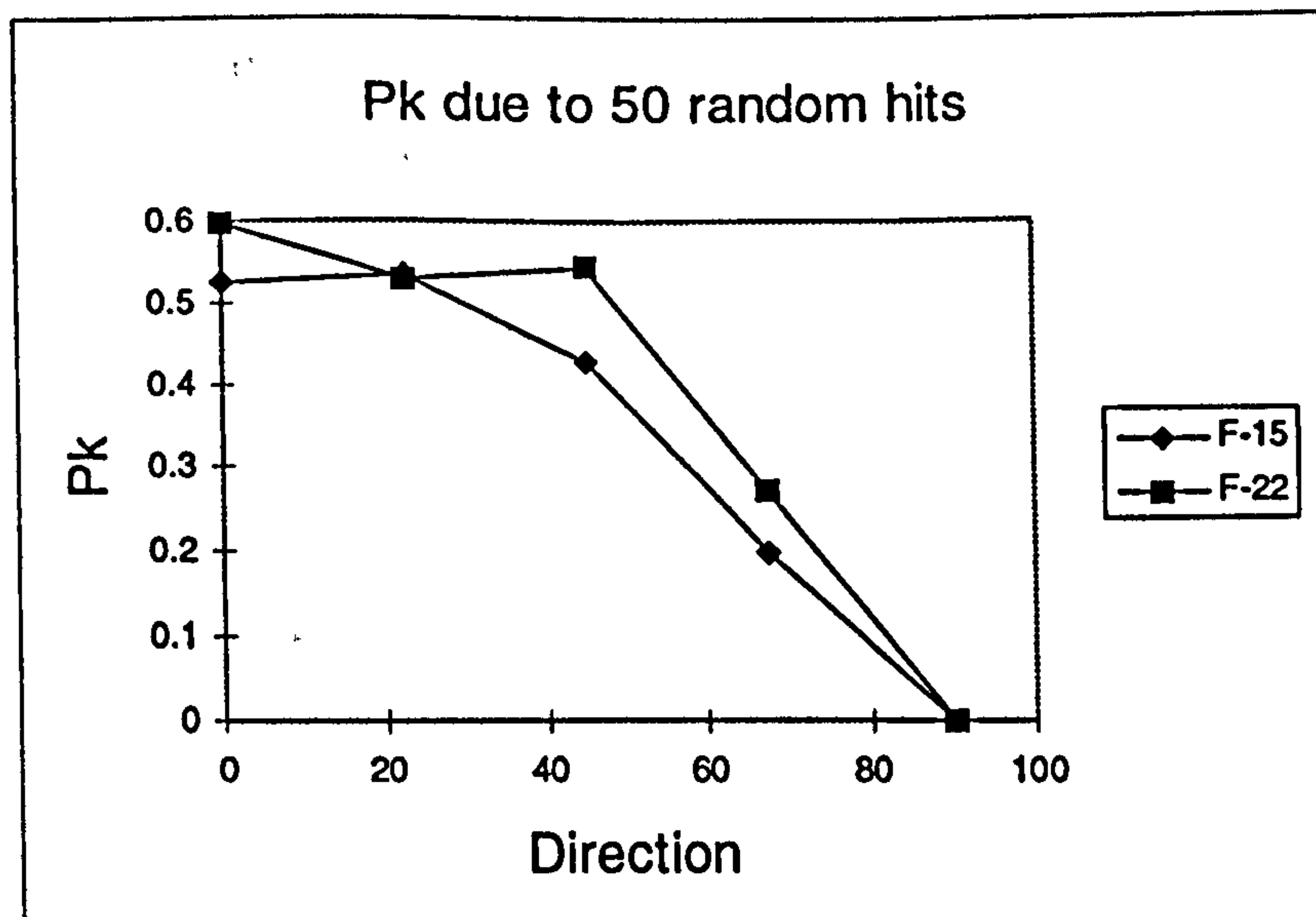


Fig. 6.18 Pk due to 50 random shots in the 20m rectangle

The second test was to investigate the effect of bottom-to-front direction variation in the two aircraft vulnerability. Again zero angle represents firing into the aircraft from bottom and 90 degrees corresponds to the front side of the aircraft. Figure 6.19 shows that the two aircraft are almost similar in vulnerability, this is because of the similar size and the same values of critical components kill probabilities.

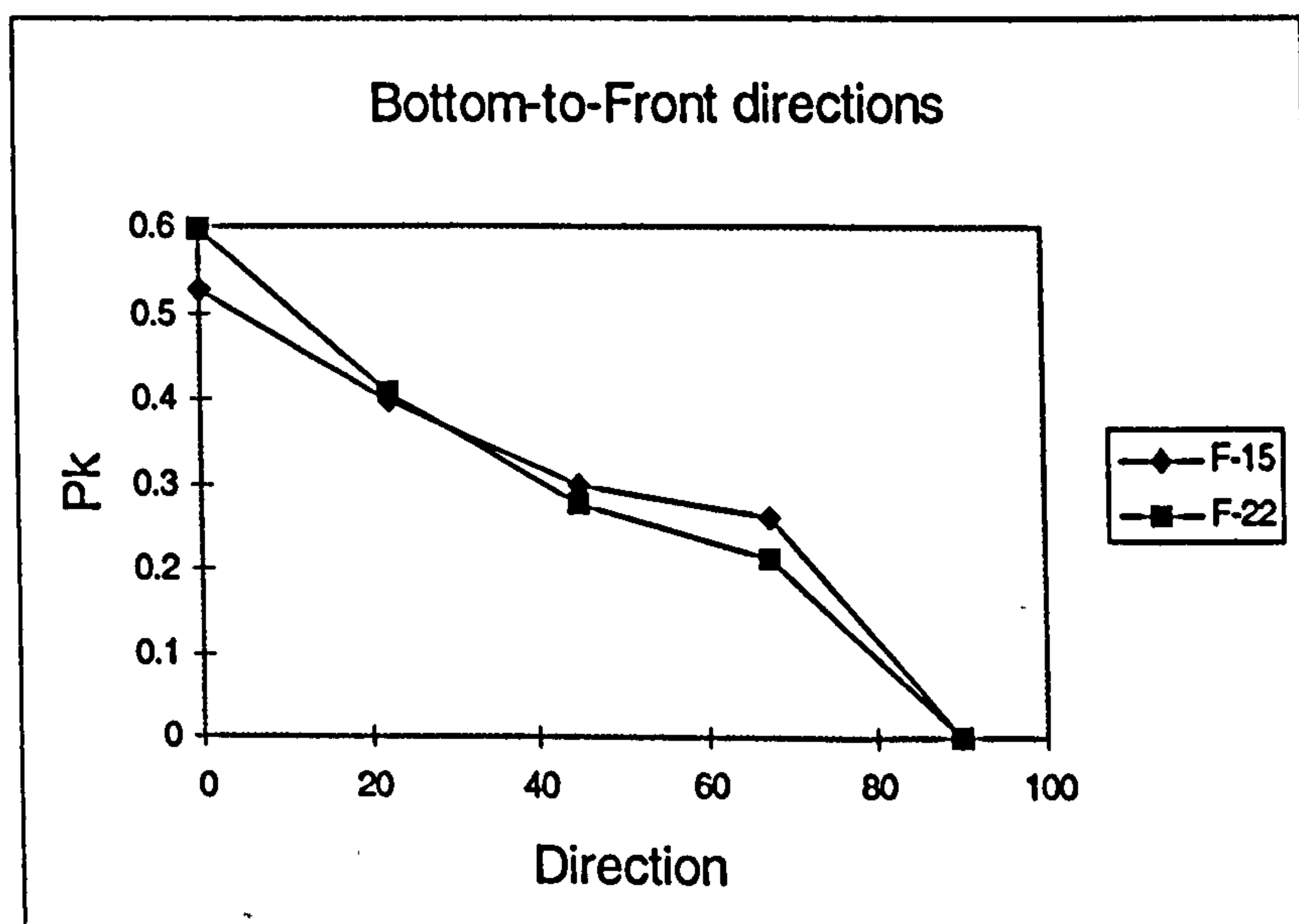


Fig. 6.19 Pk of the two aircraft.

Effectiveness Assessment

The MSM program was used to study the combat effectiveness of the two aircraft. The MSM program was slightly modified to incorporate the effect of low susceptibility of the F-22 aircraft or other stealth aircraft. The aircraft kill probability is generally the multiple result of the probability of detection, probability of hit having been detected and the probability of kill having been fired upon. The last two terms are already incorporated in the interactive survivability/vulnerability module. The probability of detection is a function of the degree of stealth features in the design and/or the Electronic Counter Measures (ECM) installed in the aircraft.

Effect of R&M

The F-22 is reported to be better than the F-15E by the factor of two in terms of its R&M values. The actual R&M of the F-22 is approximated from that of the F-15E. The MSM was used to investigate the impact of the R&M on the effectiveness of the two aircraft. The probability of detection was equal for both aircraft ($P_d=1.0$) and the attrition was set to be that experienced in the Gulf War (0.005). Fig. 6.20 shows the commutative sorties along the conflict days of the two aircraft. It is clear that the F-22 generated more sorties than the F-15. (893 sorties to 662 sorties respectively). Doubling the R&M figures improved the combat effectiveness by 35%.

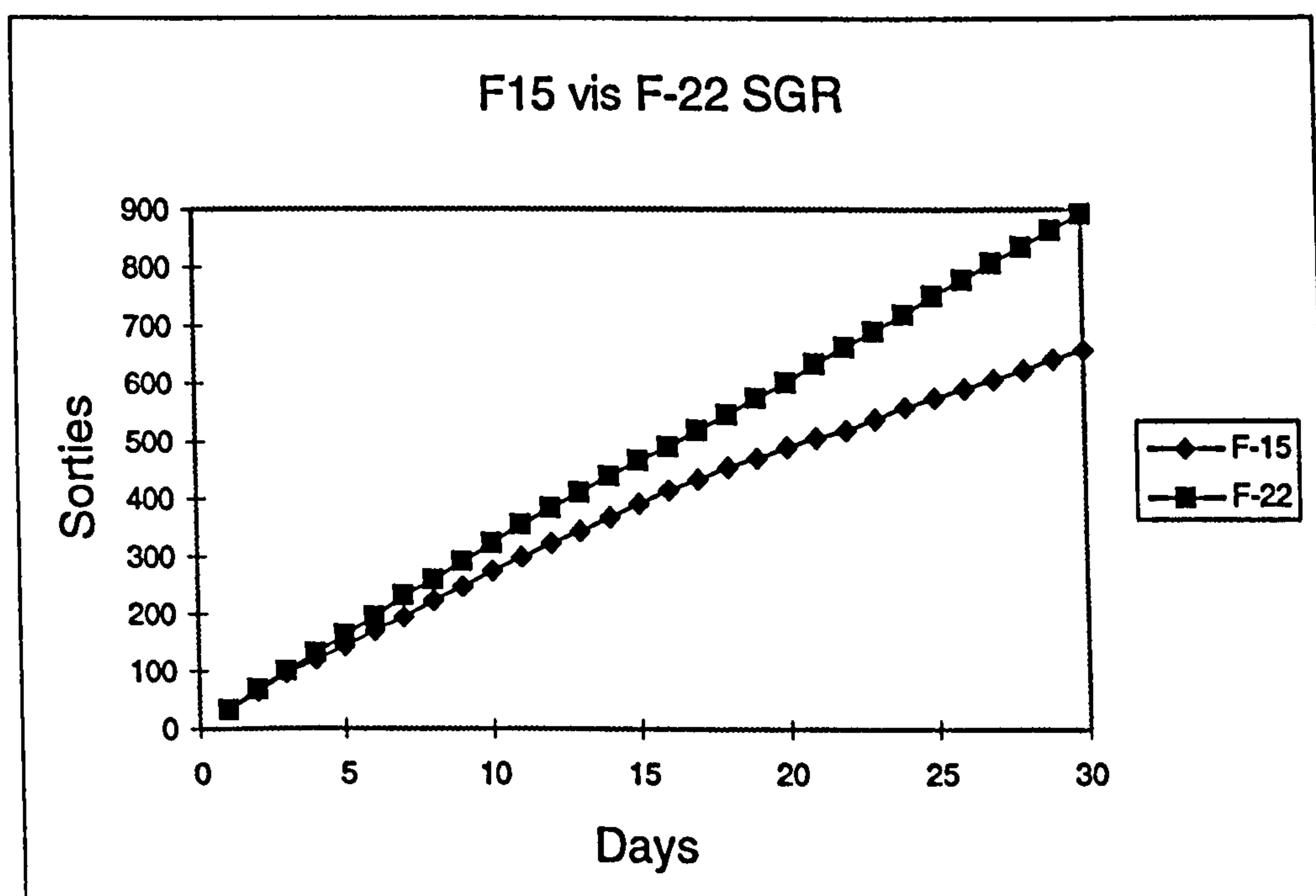


Fig. 6.20 Effect of R&M

Effect of RCS

The second test case was to investigate the effect of susceptibility (probability of detection). Fig. 6.21 represents the F-22 case, 48 sorties per day, and the $P_k=0.05$. The figure shows a large effect of the susceptibility on the SGR. There is a more than 50% increase in effectiveness when the P_d is improved by 10%. However the F-22 RCS could give an even lower figure than this.

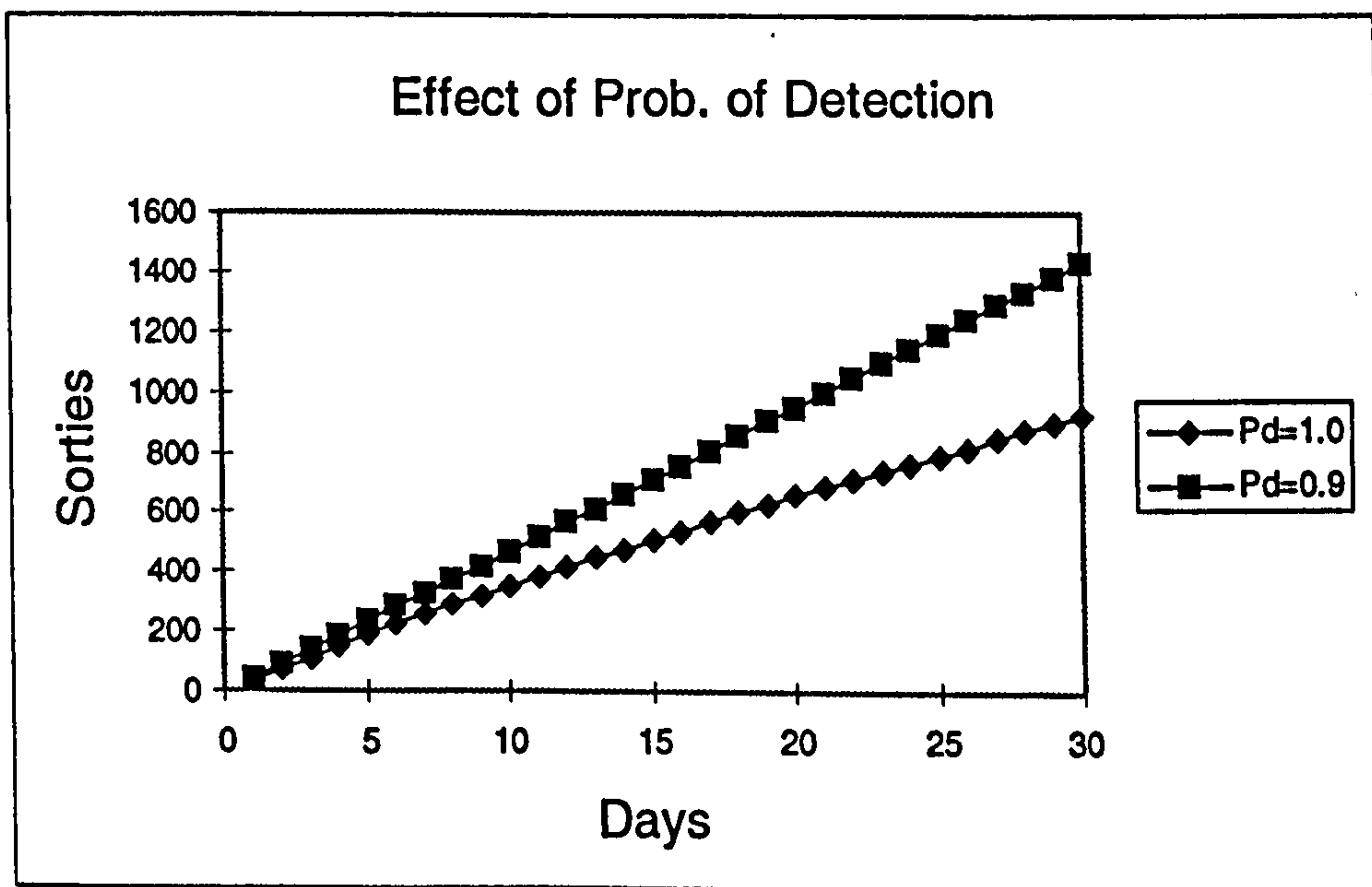


Fig. 6.21 Effect of RCS.

Chapter Seven

Discussion

7.1 Introduction

The aim of this research work was to integrate new design disciplines into the conceptual/preliminary design phase of a combat aircraft. These disciplines have different scientific backgrounds which made finding an integration methodology the driver of this research. The discipline-related researches conducted were:

- Developing a simple design synthesis to cover a wide range of combat aircraft.
- Simulating the operational environment of a group of aircraft in a wartime scenario.
- Investigating the R&M trends of modern combat aircraft.
- Developing a design automated vulnerability assessment tool.
- Integrating the disciplines under consideration such as to give a single measure of merit of the design.

7.2 Research Development and Evolution

This research started in June 1993 and focused on combat aircraft effectiveness in general. It was thought at the beginning that the research would be of the operational analysis type. In-depth literature research and conversation with contacts within industry reflected the importance of integrating new disciplines into the conceptual design phase of a combat aircraft. Most of the research on some of the effectiveness disciplines, like the MSM and the graphical automated vulnerability assessment, were not thought of during the early stages of this research. The need for an integration mechanism of these different types of combat effectiveness disciplines resulted in a research effort to build quantification methodologies for these disciplines. Most of the research time was spent on developing quantification methodologies for these disciplines and integrating the methodology into the conceptual design phase. The discussion of the current research can be divided according to the main effectiveness disciplines.

7.3 The Design Synthesis

The design synthesis research was aimed at establishing a general design synthesis for conventional combat aircraft. The design synthesis (CONCEPT) is mainly the result of integrating the initial sizing method of Ref.(5) and the geometry design modules and algorithms developed by Lovell (Ref. 1). Some modifications have been implemented to obtain the dimensions and geometric characteristics of the main aircraft components to be used in the automated graphical solid modelling. In summary, the design synthesis was to provide an easy and fast method of evaluating the impact of the design requirements on the size and weight of the aircraft.

Considerable amount of assumed data are required to start the iterative computational process to calculate the takeoff and fuel weight to satisfy the design and performance requirements. This is obvious at this early stage of the conceptual stage, since it reflects the importance of the experienced designer and the data he creates from the few rough sketches in front of him.

The landing-gear sizing of Lovell gave unrealistic results for gear leg length and wheel size compared with the sizes of current combat aircraft. In reality, the landing-gear length is not only derived by the loads on them. The ground clearance and the ground-rotation body clearance also affect the length of the landing-gear legs. The method of determining the landing-gear wheel diameter and width of Ref. (5) gives more realistic outputs. The length of the gear legs was taken as an input design value, which reflects the sizes of current fighters.

The fuselage sizing at the conceptual/preliminary design phase is not very well defined. The initial fuselage length estimation methods found in the literature are of empirical nature and relate the fuselage length to the takeoff weight and the maximum Mach number. Lovell's method is based on minimising a given length found by adding the

length of major components to be packaged inside the fuselage body with the following constraints:

- Intake diffuser aft of cockpit.
- Rear spar of wing box aft of engine-intake plane.
- Wing positions on body side aft of intake plane.

The above constraints that drive the fuselage length are valid for the specified base-line configuration defined in Lovell's synthesis. The fuselage length in the geometry-based synthesis was derived by adding the lengths of the main items. This method showed reasonable accuracy as depicted in the test case.

Tail sizing was performed using the iterative method illustrated in Lovell, which uses the empirical fin and tailplane volume ratios. The method assumes that the trailing-edge of the surfaces at the body-root coincide with the engine exit-plane. This method has been modified to allow for varying the position of the fin and the tailplane. The iterative sizing method of the tail surfaces gave good results for the case tested and converged with few iterations.

The unit acquisition cost estimation was linked to the design synthesis. Many of the cost driving factors are related to manufacturing and economic issues, but some are related to the aircraft design characteristics. The cost estimation methodology seems to give good approximation of an aircraft acquisition cost. The test case, which resembles an F-16, gave reasonable results. The small error is due to the assumption that 2000 aircraft are to be built and the actual F-16 orders exceed 2500 aircraft now.

7.4 Estimation of R&M

Estimating the R&M figures of a new design is a continuing research challenge. Most new aircraft R&M values are estimated by comparing the current design with similar existing one from field R&M data. The R&M study showed that recent R&M data of modern aircraft are the key for future more accurate R&M estimation methods. Much

effort and time was spent collecting the data through extensive contacts and visits to industry. The analysis of the data using Pareto's principle proved critical for realistic future reliability estimation. The trend evolved from the reliability data analysis has the same characteristics. However, the variation of the ranking of the few systems led to difficulties in finding accurate reliability estimation equations. The maintainability data trend did not reasonably match Pareto's trend. Estimating aircraft maintainability may require exploring more than the design parameters, such as the skill of maintenance personnel and the availability of the required repair tools in the maintenance hanger.

7.5 The MSM

The MSM represents the simulation of time-dependent operational activities happening in a squadron of combat aircraft in a wartime scenario. Although FORTRAN is not the language commonly used for simulation modelling, FORTRAN COMMON blocks are used heavily to model parallel activities occurring along the simulated time. Using the FORTRAN language paved the way for integrating such disciplines with conceptual/preliminary design syntheses which are mainly written in FORTRAN. The algorithms of the MSM were programmed in modular form for efficient programming and to allow for future expansion. Simulating the operation of a squadron of 24 aircraft in a 30 days war scenario took only 20 seconds using the DEC-Alpha RISC work station. The same problem took around 20 minutes using a 486-DX PC machine. The MSM model is based on some assumptions which are valid during wartime operations such as only unscheduled maintenance is undertaken. Also, it assumes the availability of all maintenance related matters. Testing the MSM using aircraft performance in the Gulf War showed the reasonable accuracy of this model. The MSM gives more data than the SGR of the simulated squadron along the operation days. Data such as the mission capable rate, sorties per aircraft and the maintenance actual call times can be analysed.

7.6 Solid Modelling Vulnerability Assessment

The solid modelling CAD technique is the most accurate graphical modelling of an engineering product. In recent aircraft projects, such as the Boeing 777, extensive solid

modelling has been done to investigate many design-related problem such as efficient component location, ducting, piping, and automatic component interference checking. The ACSYNT design synthesis (Ref. 7) uses a surface modelling CAD technique to give the user a fast 3D visual image of the design aircraft. Also, some area computation is used for aerodynamic and performance calculations. Integrating solid modelling into the conceptual/preliminary design synthesis reflects the most benefit from interactive CAD. The automated vulnerability assessment tool demonstrated the feasibility of integrating solid modelling representation whilst in the conceptual/preliminary design loop. Again, using FORTRAN as the calling language of the graphical solid library, and its different modelling techniques made this integration more efficient. Simple primitive shapes were shown to be useful for modelling some aircraft components with good geometrical accuracy, such as the pilot's body and the landing gear. Furthermore, actual aircraft critical components, can be represented by simple primitive shapes. Fuel lines, hydraulic lines and control surfaces actuators are some examples. Modelling skill techniques and 3D imagination are required to arrive at an efficient Boolean modelling operation of some components such as the radome and flying surfaces. The strength of the solid modelling graphical programming is reflected by the ability to create complex aircraft parts such as the fuselage and the engine ducts. Lofting 2D curve segments together, then knitting them to form a closed shape can be easily implemented to model future aircraft fuselage shapes of smooth-blend or flat-edges. Ray tracing techniques, which were originally intended for shading 3D images, are used for body-intersection checking by modifying the ray into a solid long cylinder. Doing this opened the door to modelling two vulnerability standard assessment practices: shotlines generation and vulnerable area computation. The shotline generation using the interactive solid modeller allowed the assessment from any threat direction compared with the standard six and 26 standard directions. Defining the aircraft as an assembly of critical systems allows adding more components to the assembly by simply inserting the program part with the corresponding model. It also allows studying the effect of a single component or a group of components on the aircraft vulnerability. The effect of size or orientation of a component can be also investigated. In general, the automated solid modelling and graphical representation of

the synthesised aircraft gave the vulnerability assessment process a fast, and efficient form.

7.7 Effectiveness Studies

Effectiveness of a combat aircraft is the most meaningful measure of merit to their users, the Air Forces. The Gulf War showed that combat aircraft are the most effective weapon systems. The effectiveness methodology gave figures that, in the past, were known from historical observations. For example, selecting the number of engines for a new fighter project is driven by many factors. Many design engineers in favour of multi-engine configurations claim that it will be twice as survivable as the single-engine version. The effectiveness methodology was used to investigate the vulnerability of single and twin engine configurations and showed a figure in the range of the observed value.

Aircraft payload and range is reflected in the increasing size of the aircraft, and hence in its increasing kill probability. The effect of threat direction on aircraft kill probability is significant, since some critical systems are more exposed from certain directions. Approaching and leaving the target area manoeuvres should benefit from this fact.

The F-22 is intended to replace the F-15 air-superiority aircraft. The growing cost of the F-22 project and its unit acquisition cost have put the aircraft in the effectiveness evaluation against the F-15. The F-22 is more survivable (less susceptible), more reliable and maintainable and more manoeuvrable than the F-15 but the question is how much is it more effective?. The effect of R&M enhancement on the aircraft effectiveness was realised and quantified. Doubling the R&M figures improved the combat effectiveness by 35%. The F-22 is less susceptible than the F-15 due to its low RCS design. This will decrease the probability of detection P_d and hence increase the aircraft survivability and its effectiveness. It was shown that a 50% increase in effectiveness resulted from lowering the P_d by 10%. This effect made selecting a low RCS conceptual configuration for new aircraft projects one of the first requirements. However, the high effectiveness of

the F-22 compared to the F-15E should be also weighed against the fact that the F-22 is almost three times the cost of the F-15E.

Chapter Eight

Conclusions and Recommendations

8.1 Conclusions

An effort has been made to produce a combat aircraft effectiveness design methodology. Aircraft R&M and vulnerability/survivability disciplines have been integrated into the conceptual/preliminary design process.

Creating an accurate design synthesis which can handle a wide range of design requirements requires starting with the initial sizing iterative methods to estimate an initial takeoff weight and fuel weight. The takeoff and fuel weight calculated are the drivers of the second stage, the geometry based synthesis.

The only way to approach a reliable R&M estimation methodology for combat aircraft is to have R&M data of recent fighters. A statistical analysis approach relating R&M trends with aircraft design parameters gives meaningful trends that can be used for a design R&M estimation. Aircraft maintainability estimation should include factors that are away from the aircraft itself but affect its maintenance down time.

Programmable solid modelling techniques can be incorporated into a conceptual/preliminary design synthesis to provide the synthesis with accurate and fast geometry or size related calculations. Solid modelling the aircraft critical components, and integrating them into one assembly, plus the using of ray-tracing CAD techniques gave an automated and flexible vulnerability assessment tool.

Simulating the operational environment of a combat aircraft gives measures of merit of the effectiveness of the design, such as the sortie generation rate (SGR). The effectiveness methodology can provide the designer with insights into the impact of different disciplines on combat effectiveness.

8.2 Recommendations

The Following summarises a few areas which can be the subject of future work:

- Creating Knowledge-Based design rules for a general design synthesis of combat aircraft. This will enhance the design by accurately providing crucial design data for a wide range of aircraft configurations.
- Integrating the programmable solid modeller with the conceptual/preliminary design phase such that it provides accurate and fast estimates of area, mass, volume and centre of gravity to the design synthesis
- Performing the survey-type research to investigate and model the factors that affect aircraft maintainability characteristics.
- Extending the MSM activities to take into account peace-time operational activities such as the scheduled maintenance tasks and spare parts availability.
- Link the effectiveness methodology with an optimiser, to improve the efficiencies of trade-studies.

References

1. Lovell, D. A. The Application of Multivariate Optimisation to Combat Aircraft Design. RAE 88003, January 1988.
2. Serghides, V. C Design Synthesis for Canard-Delta Combat Aircraft. PhD Thesis, Cranfield Institute of Technology, 1987.
3. Kehayas, N. ASTOVL Combat Aircraft Design Synthesis and Optimisation. PhD Thesis, Cranfield Institute of Technology, 1992.
4. Siegers, F. Design Synthesis for Swept-Wing Combat Aircraft Incorporating Stealth Technology. CoA Report No. 9402, Cranfield University, October 1994.
5. Raymer, D. P. Aircraft Design: A Conceptual Approach, AIAA Education Series, 1989.
6. Raymer, D. P. RDS : a PC-based aircraft design, sizing and performance system, AIAA-92/4226.
7. Jayaram, S., Myklebust A. and Gelhausen P. ACSYNT : a standards-based system for parametric computer aided conceptual design of aircraft. AIAA- 92/1268.
8. The Mission Trade-Off Model (MTOM) Part I, Model Description, JTCG/AS-76-001, US Department of Defence, Dec. 1977.
9. Burleigh, C.D. Mission Readiness of Combat Aircraft. M.Sc. Thesis, Cranfield Institute of Technology 1980.

10. Capt Letitia, M. Pohl. Evaluation of F-15E Availability During Operational Test. IEEE 1991 Winter Simulation Conference Proceedings, Phoenix, AZ, USA, December 1991.
11. Harmon, D. F. et al. Maintainability Estimation Relationships, Proceedings of the AIAA Annual Reliability and Maintainability Symposium, Washington, D.C., January 28-30, 1975.
12. Serghides, V. C. Development of a Reliability and Maintainability Prediction Methodology for Aircraft Conceptual Design Process, M.Sc. Research Thesis, Cranfield University 1985.
13. Ball, R. Fundamentals of Aircraft Survivability, AIAA Educational Series, 1988. American Institute of Aeronautics and Astronautics., Inc., Washington, DC, 1989.
14. MIL-STD-2069. Requirements for Aircraft Nonnuclear Survivability Program. Department of Defence, Washington 20301, August 1981.
15. Levy, R. L. and Dixon-Hiester. Interactive Vulnerability Assessment Model. AIAA-91/3163.
16. Kitowski, J. V. Combat Effectiveness Methodology as a Tool for Conceptual Design. AIAA-92/1197.
17. Wheelock, R. B. The Role of Mission Effectiveness Analysis During Preliminary Design. AIAA-92/1260.
18. Nicolai, L. M. Fundamentals of Aircraft Design. distributed by School of Engineering, University of Dayton 1975.

19. Burns, J. W. Aircraft Cost Estimation Methodology and Value of a Pound Derivation for Preliminary Design Development Applications., 53rd Annual Conference of Society of Allied Weight Engineers Inc., Long Beach, CA 23-25 May 1994.
20. Buckner J. K. Aerodynamic Design Evolution of the F-16. AIAA-74-935.
21. Jane's, All the world's aircraft, 1973/74.
22. F-16 Fighting Falcon Program Overview, Lockheed Aerospace, ASD 90-1779, 1990.
23. Jane's, Future Combat Aircraft Conference Proceedings. London 1987
24. Mullin, S. N. The Evolution of the F-22 Advanced Tactical Fighter. AIAA-92/4188
25. Wadsworth et al. Modern Methods for Quality Control Improvement. John Wiley & Sons, 1985.
26. David Straker. A Toolbook for Quality Improvement and Problem solving. Prentice Hall International (UK) Limited 1995.
27. Nancy R. Man. Methods for Statistical Analysis of Reliability and Life Data. John Wiley & Sons, Inc., 1974.
28. Microsoft Excel, Ver. 6.0a, Microsoft Corporation, 1995.
29. Thomas A. Ludwinski. CAD/CAM/CAE Reshapes Engineering Processes. Aerospace America. June 1993, pp 16-18.

30. Chiyokura, Hiroaki. Solid modelling with Designbase : theory and implementation. Addison-Wesley, 1988.
31. Glassner, A. S. An Introduction to Ray Tracing. Academic Press, 1989.
32. Michael Pidd. Computer Simulation in Management Science. 3rd Edition, John Wiley & Sons, Inc., 1992.
33. George S. Fishman. Concept and Methods in Discrete Event Digital Simulation. John Wiley & Sons, 1973.
34. Roy Billinton and Ronald N. Allan. Reliability Evaluation of Engineering Systems. 2nd ed., Plenum Press, 1992.
35. Dick Pawloski. Changes in Threat Air Combat Doctrine and Force Structure. 30th Edition, Lockheed Fort Worth Company, March 1995.
36. Armed Forces Journal, March & June and July 1994.
37. Stan Morse. Gulf Air War Debrief. Aerospace Publishing Limited, London.
38. F-16 Support System Presentation For The Royal Saudi Air Force. Technical Document, Lockheed Fort Worth Company, February 1994.
39. Viktor Pavlenko. Tactical aircraft: One Engine or Two?. Military Technology, Aug. 1994, pp 73-77.
40. Jane's All The World Aircraft 1994/1995
41. Parasolid Programming Reference Manual, Electronic Data Systems, Cambridge, UK, December 1992.

42. Walker, J.R. Air-To-Ground Operations, Brassey's Air Power: Aircraft, Weapons Systems and Technology Series, Brassey's Defence Publishers Ltd, 1987.
43. Fuhs, Allen E, The No-See-Um book : Radar Cross Section Lectures. Published by American Institute of Aeronautics and Astronautics.

APPENDIX A

Design Synthesis Description and Algorithms

A.1 INTRODUCTION

This appendix is a simple guide for the CONCEPT program. It provides the mathematical formulation for the design synthesis and the reasoning and the methodology that leads to the development of the code. In general, the design synthesis can be considered as a combination of the initial sizing methodology of (Ref. 5 and 18) and the detail synthesis of (Ref. 1). Changes have been made to enable linking the synthesis with the graphical solid modeller. The aircraft main components are geometrically defined by means of size, location and orientation.

A.2 INITIAL SIZING AND CONCEPTUAL DESIGN

This part presents the method and algorithms used to estimate the initial size of the aircraft. The main target of the initial sizing design process is to estimate the takeoff weight, empty weight and the fuel weight required to fly the mission.

A.2.1 TAKEOFF-WEIGHT BUILD-UP

Takeoff gross weight can be broken into crew weight, payload weight, fuel weight, and the remaining empty weight,

$$W_0 = W_c + W_p + W_f + W_e \quad (A1)$$

The crew and payload weights are both known since they are given in the design requirements. The only unknowns are the fuel weight and the empty weight. However, they are both dependent on the total aircraft weight. To formalise the iterative equation, both fuel and empty weights can be expressed as a fraction of the total takeoff weight, i.e. (W_f / W_0) and (W_e / W_0) . Thus

$$W_0 = W_c + W_p + \left(\frac{W_f}{W_0} \right) W_0 + \left(\frac{W_e}{W_0} \right) W_0 \quad (\text{A2})$$

This can be solved as follows:

$$W_0 = \frac{W_c + W_p}{1 - (W_f / W_0) - (W_e / W_0)} \quad (\text{A3})$$

A.2.2 MISSION SEGMENT WEIGHT FRACTION

The mission segment weight fractions (W_i / W_{i+1}) are calculated for each mission segment along the mission profile. If the mission includes a weight drop, it is necessary to actually calculate the weight of the fuel burned during every mission leg, and sum for the total mission fuel. For each mission segment, the fuel burned is then equal to:

$$W_{fi} = \left(1 - \frac{W_i}{W_{i-1}} \right) W_{i-1} \quad (\text{A4})$$

The total mission fuel, W_{fm} , then is equal to:

$$W_{fm} = \sum_1^x W_{fi} \quad (\text{A5})$$

For engine start, taxi and takeoff, the weight fraction is estimated historically for fighters. A reasonable estimate is:

$$\frac{W_1}{W_0} = 0.97 - 0.99 \quad (\text{A6})$$

The climb and acceleration to cruise altitude and Mach number M (starting at Mach 0.1) is approximated as follows:

$$\text{Subsonic: } \frac{W_{i+1}}{W_i} = 1.0065 - 0.0325 M \quad (\text{A7})$$

$$\text{Supersonic: } \frac{W_{i+1}}{W_i} = 0.991 - 0.007 M - 0.01 M^2 \quad (\text{A8})$$

For cruise the Breguet range equation is used for aircraft with jet-engine(s)

$$\frac{W_i}{W_{i+1}} = \exp \frac{-RC}{V(L/D)} \quad (\text{A9})$$

For loiter, the weight fractions are found from the endurance equation as

$$\frac{W_{i+1}}{W_i} = \exp \frac{-EC}{L/D} \quad (\text{A10})$$

For combat, the mission requirements usually specify one of the following:

1. Specified number of minutes at maximum power and a particular Mach number and altitude, and/or
2. Specified number of turns at maximum power and a particular load factor, Mach number and altitude.

The weight of the fuel burned is equal to the product of thrust, specific fuel consumption, and duration of the combat (d), so the mission segment weight fraction is:

$$\frac{W_{i+1}}{W_i} = 1 - C(T/W)(d) \quad (\text{A11})$$

where T/W is the thrust-to-weight ratio at combat phase.

For the descent and landing phase a historical approximation is used. A reasonable estimate is:

$$\frac{W_{i+1}}{W_i} = 0.99 - 0.995 \quad (\text{A12})$$

Again, a historical approximation is used for landing and taxi back,

$$\frac{W_{i+1}}{W_i} = 0.992 - 0.997 \quad (\text{A13})$$

A.3 SIZING OF BASIC ITEMS

The basic items are those which are not affected by the sizing process. Aircraft radome part, cockpit and the inside electronic and hydraulic bays are considered to be somewhat fixed for the range of aircraft under investigation.

A.3.1 RADOME

The nose diameter is defined from a specified radar dish diameter, DAR , and an increment, $EDAR$, to allow for clearance. A linear variation of cross-sectional area with axial distance, gradient $GOFI$ is assumed.

The cross-sectional area of the fuselage at radar dish position, OFI , is:

$$OFI = \frac{\pi}{4} (DAR + EDAR)^2 \quad (\text{A14})$$

The radius is:

$$RAR = 0.5(DAR + 2EDAR) \quad (A15)$$

and the radome length is:

$$XFR = \frac{OFI}{GOFI} \quad (A16)$$

Behind the radar dish a fuselage length, LAR, is allowed for related avionics.

Following these there is a second bay of length LAX1 containing further avionics. The front bulkhead of the cockpit is situated at the rear of this bay. Its distance from the aircraft nose XA is:

$$XA = XFR + LAR + LAX1 \quad (A17)$$

A.3.2 COCKPIT

The arrangement of the cockpit is shown in Fig. A.1 and is based on military specifications. The dimensions HC1, HC2, HC3, HC4, HCSEAT, LCFOOT, QCSEAT, QCEYE and EHC5 are specified input design data . From these the following are derived:

$$QCFOOT = \sin^{-1} \left[\frac{HC3 \cdot \sin(QCSEAT) + HCSEAT \cdot \cos(QCSEAT)}{HC2} \right] , \quad (A18)$$

$$HCEYE = HC1 \cdot \cos(QCSEAT) + HC3 \cdot \sin(QCSEAT) + HCSEAT \cdot \cos(QCSEAT) , \quad (A19)$$

$$LCEYE = HC1 \cdot \sin(QCSEAT) + HC2 \cdot \cos(QCFOOT) + LCFOOT , \quad (A20)$$

$$LCFL = HC2 \cdot \cos(QCFOOT) + LCFOOT + HC3 \cdot \cos(QCSEAT) - HCSEAT \cdot \sin(QCSEAT) + \frac{EHC5}{\cos(QCSEAT)} \quad , \quad (A21)$$

$$HC5 = HCEYE - LCEYE1 \cdot \tan(QCEYE1) \quad (A22)$$

A.4. GEOMETRY SIZING OF THE MAIN COMPONENTS

This part include the detail geometry definition of main aircraft components. Sizing the main components depends on the estimated initial design parameters and detail design algorithms.

A.4.1 ENGINE SIZING

The engine size is derived from a set of statistical equation based on historical data (Ref. 5). These equations give initial estimation of engine dimensions. (W_N is engine weight, L_N is length and D_N is engine diameter)

$$W_N = 0.063T^{1.1} M^{0.25} e^{(-0.81BPR)} \quad (A23)$$

$$L_N = 3.06T^{0.4} M^{0.2} \quad (A24)$$

$$D_N = 0.288T^{0.5} e^{(0.04BPR)} \quad (A25)$$

$$SFC_{\max T} = 2.1e^{(-0.12BPR)} \quad (A26)$$

A.4.2 LANDING GEAR SIZING

The landing gear is considered to be considered of the tire “wheel” and the structural leg. The tires are sized to carry the weight of the aircraft. Typically the main tires carry about 90% of the total aircraft weight. Nose tires carry only about 10%. The following equation are used (Ref. 5) for the estimation of the main tire size, (W_w weight-on-wheel)

$$DUMW = 1.59W_w^{0.302} \quad (A27)$$

$$BUMW = 0.098W_w^{0.467} \quad (A28)$$

A.4.3 FUSELAGE SIZING

The fuselage is sized such that it includes the major items inside it. The arrangement shown in Fig. A.2 is typical of the layouts adopted for some recent combat aircraft. Six fuselage sections (R, A, B, D, E, F) are chosen to ensure that within the limitations imposed by this layout there is adequate cross-sectional area in the fuselage to accommodate the items.

Section R, at the radar dish in the radome, is of circular shape. The diameter of the circle is given in the radome section.

Section A, at the front bulkhead of the cockpit, is a rectangular with circular corners of a fixed proportion (RFSA), Fig.A.3. The ratio of the sides is also fixed (RAHB). For this section we have:

$$HFA = BFA \cdot RAHB \quad (A29)$$

$$RADFA = RFSA \cdot BFA \quad (A30)$$

Once the area of the fuselage at this station, (OFA), is known the side length can be determined.

$$BFA = \sqrt{\frac{OFA}{RAHB - (4 - \pi) \cdot RFSA^2}} \quad (A31)$$

The depth of the underfloor, (HFA1), is:

$$HFA1 = HFA - HC5 \quad (A32)$$

Section B is located in the cockpit at the fore and aft position of the pilots eye point defined in Fig.A. 1 . From Fig. A.3;

$$HFB1 = HFA1 \quad (A33)$$

$$HFB = HFB1 + HCEYE + HC4 - RCCAN \quad (A34)$$

Section D is located at the front of the main landing gear bay. The pintle of the main landing gear leg is assumed to be at a fixed distance, (ELUP), forward of the rear of the main landing gear bay. The pintle is also positioned at a fixed fraction, (RLUPCW), of the wing mean aerodynamic chord, aft of the wing mean quarter chord point, (XWCQM). Hence,

$$XD = XWCQM + RLUPCW \cdot CWMA - ELUP \quad (A35)$$

Section D is defined in a different manner for single and twin engine installation, Fig. A.3.

For the single-engine installation the main wheels of the landing gear are assumed to be stored vertically and the intake diffuser duct is assumed to be circular.

The minimum height for this section is

$$HFDS = FDUMW \cdot DUMW \quad (A36)$$

The cross-sectional area of the intake duct at section D, (*OIDD*), is obtained using the assumption of a linear variation of cross-sectional area from the intake inlet to the engine front face:

$$OIDD = OII + \frac{XUMB - XII}{LIDG} (OIE - OII) \quad (A37)$$

The height of the diffuser duct at section D is then defined as the lesser of the main-wheel bay height and the diameter of the circle to produce the cross sectional area (*OIDD*),

$$OIDD = \min(FDUMW, DUMW) \quad (A38)$$

The diameter of the intake diffuser is then given by

$$BIDD = \frac{4 \cdot OIDD}{\pi \cdot HIDD} \quad (A39)$$

A minimum allowable value for the cross-sectional area at section D, (*OFDS*), is calculated using the shape factor (*FOFDK*) and the enclosing rectangle:

$$OFDS = FOFDK \cdot HFDS \cdot (2FBUMW \cdot BUMW + BIDD) \quad (A40)$$

The ratio of the actual cross-sectional area at section D, (*OFD*), to the minimum value is used to define a scaling factor

$$ROFDN = \frac{OFD}{OFDS} \quad (A41)$$

and hence to calculate the actual fuselage dimensions at section D

$$HFD = HFDS \sqrt{ROFDN} \quad (A42)$$

$$BFD = (2FBUMW \bullet BUMW + BIDD)\sqrt{ROFDN} \quad (A43)$$

Fig. A.3 shows the fuselage section for a twin engine aircraft. Sizing this section is the same for the single engine approach.

Sections E is at the engine face. The size of the cross sections depends on the engine size, engine separation and a fixed structural clearance, Fig. A.3. For a single engine aircraft

$$HFE = DP1 + 2EHP1 \quad (A44)$$

$$BFE = DP1 + 2EBP1 \quad (A45)$$

$$HFF = DP3 + 2EHP3 \quad (A46)$$

$$BFF = DP3 + 2EBP3 \quad (A47)$$

For Twin engine arrangements,

$$BFE = 2DP1 + 3EBP1 \quad (A48)$$

$$BFF = 2DP3 + 3EBP3 \quad (A49)$$

A.4.4 WING

The wing planform shown in Fig. A.4 is defined by input variables. Using the nomenclature of Fig. A.4 the following relations are obtained;

$$BW = (AW \bullet SW)^{0.5} \quad (A50)$$

where BW is the gross span, AW is the gross wing aspect ratio and SW is the gross wing surface area.

$$CWCC = \frac{2SW}{BW(1+UW)} \quad (A51)$$

where (CWCC) is the center-line chord of the gross wing and UW is the taper ratio of the gross wing

$$CWMG = \frac{1}{2} CWCC(1+UW) \quad (A52)$$

$$CWMA = \frac{2}{3} CWCC \left(UW + \frac{1}{(1+UW)} \right) \quad (A53)$$

$$CWCT = UW \bullet CWCC \quad (A54)$$

where CWMG is the geometric mean chord, CWMA is the aerodynamic mean chord and CWCT is the tip chord

$$QWL = \tan^{-1} \left(\tan(QW4) + \frac{CWCC}{2BW} (1-UW) \right) \quad (A55)$$

$$QW2 = \tan^{-1} \left(\tan(QW4) - \frac{CWCC}{2BW} (1-UW) \right) \quad (A56)$$

After estimating the fuselage width at the position of the centre section of the wing box, BFE, a further group of parameters relating to the nett-wing are obtained.

$$BWBB = BFC \quad (A57)$$

Span of the nett exposed wing

$$BWN = BW - BWBB \quad (A58)$$

Root chord of the nett wing (i.e. at the side of the body)

$$CWCB = CWCC \left(1 - \frac{BWBB}{BW} (1 - UW) \right) \quad (A59)$$

Taper ratio of the nett wing

$$UWCN = \frac{CWCT}{CWCB} \quad (A60)$$

Mean chord of the nett wing

$$CWMN = 0.5(CWCB + CWCT) \quad (A61)$$

Area of the nett wing

$$SWN = CWMN . BWN \quad (A62)$$

Aspect ratio of the nett wing

$$AWN = \frac{BWN}{CWMN} \quad (A63)$$

The structural box of the wing is defined by forward and rear spars at fixed fractions of the chord, outboard of the body side, and these wing halves are joined by an unswept box of constant sectional shape through the fuselage. Using the nomenclature of Fig. A.4 the following dependent variables are obtained; chord of the wing box at the body side

$$CWBB = CWCB.(FCWR - FCWD) \quad (A64)$$

The cross-sectional area of the centre section of the wing box (OWBB) is obtained by integrating the airfoil thickness distribution between the front and rear spar positions. Hence the volume of the centre section of the box is:

$$VWBB = BWBB.OWBB \quad (A65)$$

The fuel volume available for tankage is

$$VWBCF = UWBCF.VWBB \quad (A66)$$

where UWBCF is a utilisation factor to account for the structure etc. in the box.

The span of the fuel tank in the wing box external to the fuselage is

$$BWNF = FBWNF.BWN \quad (A67)$$

using the nomenclature of Fig. A.4, the taper ratio of the tank

$$UWCNF = 1 - \frac{BWNF}{BWN}(1 - UWCN) \quad (A68)$$

and hence the volume of the wing box available for the fuel tankage

$$VWBEF = UWBEF.OWBB.\frac{BWNF}{3}(1 + UWCNF + UWCNF^2) \quad (A69)$$

The total fuel volume contained in the wing is

$$VWF = VWBCF + VWBEF \quad (A70)$$

A.4.5 EMPENNAGE

The geometry of the tailplane and fin(s) is defined by a set of design data. The sizing of the empennage is performed using the tail volume coefficient method.

A.4.5.1 VERTICAL STABILISER

The initial sizing of the vertical tail is accomplished using the vertical tail volume coefficient, $REFFC$, but with different definition compared to (Ref. 1), in order to accommodate for the effect of offsetting the location of the vertical and the horizontal stabiliser along the longitudinal axis. The tail volume coefficient is defined as,

$$REFFC = \frac{SEFNV \cdot LEFCQM}{BWN \cdot SWN} \quad (A71)$$

$SEFNV$ is the projection of the fin area into the vertical plane containing the aircraft longitudinal axis. $LEFCQM$ is the fin moment arm and is measured from the mean quarter-chord point of the wing to the mean quarter-chord point of the nett fin. The distance of the of the latter from the trailing edge of the fin, measured at the root of the fin is:

$$LCFTE = \frac{\sqrt{SEFN} \sqrt{AEFN}}{3(1 + UEFN)} \left[\frac{(5 + 5UEFN - UEFN^2)}{AEFN(1 + UEFN)} - (1 + 2UEFN) \tan(QEFL) \right] \quad (A72)$$

The distance between the trailing-edge of the fin(s) and engine(s) exit plane, $XFLEN$, is defined by the external variable $RXFLEN$ which defines its magnitude as a fraction of fuselage length:

$$XFLEN = RXFLEN \cdot XFN \quad (A73)$$

The moment arm, Fig. A.5, is given by

$$LEFCQM = XFN - XWCQM - LCFTE - XFLEN \quad (A74)$$

Note that if XFLEN is negative then the fin is position aft the engine exit plane. Combining this equation with the definition of the fin volume ratio to eliminate LEFCQM, an expression is obtained in which the only unknown is the nett area of the fin, SEFNV. This may be solved iteratively to get the value of SEFNV.

The cant angle of the fins is QEF, measured from the vertical plane, and thus the fin area is found from

$$SEFN = \frac{SEFNV}{\cos(QEF)} \quad (A75)$$

and the following geometric parameters may then be calculated. The nett span of the fin:

$$BEFN = \sqrt{\frac{SEFN}{NFIN} \cdot AEFN} \quad (A76)$$

where NFIN is the number of fins. The chord of the fin at the body side:

$$CEFB = \frac{2 \cdot BEFN}{AEFN \cdot (1 + UEFN)} \quad (A77)$$

The mean aerodynamic chord of the fin is given by

$$CEFM = \frac{2}{3} \cdot CEFB \cdot \frac{1 + UEFN + UEFN^2}{1 + UEFN} \quad (A78)$$

Tail sizing is conducted using the tail volume coefficient method. Ref. 4, then used to determine the detailed shape of the empennage. This method assumes a conventional tail, a tailplane and a single fin. However this methods can be applied to twin-tail aircraft by letting the total fin areas equal to the area of the single fin.

A.4.5.2 HORIZONTAL STABILISER

The geometry of the tailplane and fin is defined by a set of input variables. The tailplane volume ratio is given by:

$$RETSW = \frac{SETN \cdot LETCQM}{SW \cdot CWMG} \quad (A79)$$

The tailplane moment arm LETCQM is measured between the mean quarter-chord point of the wing and the mean quarter-chord point of the tailplane. The variable, RXWCQM, defines the position of the quarter-chord point of the wing from the nose of the fuselage, as a fraction of the overall fuselage length XFN, i.e.

$$XWCQM = RXWCQM \cdot XFN \quad (A80)$$

The distance of the mean quarter-chord point of the tailplane from the trailing edge of the tailplane at the side of the fuselage:

$$LCTTE = \sqrt{SETN} \frac{\sqrt{AETN}}{3(1+UETN)} \left[\frac{(5 + 5UETN - UETN^2)}{AETN(1+UETN)} - (0.5 + UETN) \tan QETL \right] \quad (A81)$$

As the trailing edge of the tailplane is assumed to intersect the fuselage at the nozzle exit plane, the moment arm is therefore given by

$$LETCQM = XFN - XWCQM - LCTTE \quad (A82)$$

Combining this equation with the definition of the tail volume ratio to eliminate LETCQM, an expression is obtained in which the only unknown is the nett area of the tailplane, SETN. This may be solved iteratively and the following geometric parameters may then be calculated. The nett-span of the tailplane

$$BETN = \sqrt{SETN \cdot AETN} \quad (A83)$$

The chord of the tailplane at the body sides

$$CETB = \frac{2BETN}{AETN(1 + UETN)} \quad (A84)$$

A.5 AIRCRAFT ACQUISITION UNIT COST

The acquisition unit cost of the design aircraft is estimated using the method described by (Ref. 19). The method has been modified so that it could be implemented in CONCEPT as a subroutine. The variables appearing in the following equations has been classified as a design-related (such as aircraft speed, number of engines etc.) and non-design related variables such as labour rates. External data given by charts in the Ref. have been curve-fitted so that it could be modelled as equations in the program.

A.5.1 DEFINITIONS

Acquisition Unit Cost: Includes all costs incurred to place an aircraft on flight ramp, research, development, production tooling, assembly, military construction, spare parts and training.

Flyaway Unit Cost: The production cost for the basic aircraft, including airframe, propulsion system, avionics, and other purchased equipment.

Life Cycle Cost: The life cycle cost LCC of an aircraft program is given by:

$$LCC = C_{DDTE} + C_{ACQ} + C_{OPER} + C_{DISP} \quad (A85)$$

Where

C_{DDTE} Design, development, test and evaluation cost.

C_{ACQ} Acquisition cost.

C_{OPER} Operations & support cost.

C_{DISP} Disposal cost.

The life cycle cost (LCC) of an aircraft is influenced by both increased and decreased aircraft weight. Recurring and non-recurring cost is affected by weight, and the operational cost of the a/c is a function of aircraft weight throughout the aircraft life in the form of increase or decreased fuel cost. Design, development, test, evaluation, and production cost consists of the following cost categories:

- Airframe Engineering and Design.
- Development Support and Testing.
- Flight Test.
- Tooling.
- Manufacturing Labour.
- Quality Control
- Manufacturing Material
- Engine & Avionics

Acquisition Unit Cost

The acquisition unit cost C_{UA} is given by:

$$C_{UA} = \frac{C_{DDTE} + C_{PROD}}{Q_D + Q_P} \quad (A86)$$

Where:

C_{UA} Acquisition unit cost.

C_{DDTE}	Development Cost.
C_{PROD}	Total Production cost.
Q_D	Quantity of development aircraft.
Q_P	Quantity of production aircraft.

Development Cost

The total development cost can be determined by the following equation:

$$C_{DDTE} = C_{AED} + C_{DSC} + C_{FTAR} + C_{TD} + C_{MD} + C_{QD} + C_{MMD} + C_E + C_{AV} \quad (A87)$$

Where

C_{AED}	Development engineering cost.
C_{DSC}	Development support cost.
C_{FTAR}	Cost of flight test operations.
C_{TD}	Development tooling cost.
C_{MD}	Development manufacturing labour cost.
C_{QD}	Development quality control cost.
C_{MMD}	Development manufacturing materials cost.
C_E	Engine cost.
C_{AV}	Avionics cost.

Production Cost

The production cost can be estimated by the following equation:

$$C_{PROD} = C_{AEP} + C_{TP} + C_{MP} + C_{QP} + C_{MMP} + C_E + C_{AV} \quad (A88)$$

Where

C_{AEP}	Production engineering cost.
C_{TP}	Production tooling cost.
C_{MP}	Production manufacturing labour cost.

C_{QP}	Production quality control cost.
C_{MMP}	Production manufacturing materials cost.

Airframe Engineering (DT&E and Production)

The total airframe engineering hours for development (E_{HD}) and production (E_{HP}) can be estimated using the following equations:

$$E_{HD} = 0.066A^{0.796}S^{1.538}Q_D^{0.183}A_{TF}C_{AMC} \quad (A89)$$

$$E_{HP} = 0.066A^{0.796}S^{1.538}(Q_D + Q_P)^{0.183}A_{TF}C_{AMC} - E_{HD} \quad (A90)$$

Where:

A_{TF}	Judgement factor for advanced technology features. such as stealth, vectored thrust, and maximum speed. =1.0 for conventional aircraft =1.5 for unconventional aircraft (stealth and vectored thrust)
C_{AMC}	Judgement factor for advanced materials relative to conventional metal designs.

This factor is a function of the percentage of the advanced materials used in the aircraft. The equation inside Fig. A6 could be used to calculate the cost factor as a function of percentage of advanced materials.

S	Maximum speed (knots at best altitude)
Q	Quantity of aircraft to be produced (subscript D for development and P for production)
A	AMPR (airframe unit weight) in pounds.

Most aircraft costing methodology has been based on AMPR or airframe unit weight, and generally AMPR is estimated for a specific aircraft after weight empty is estimated. For conventional fighter/attack the following equation is used

$$AMPR = 0.422(W_{CFA})^{1.0492} \quad (A91)$$

For the next generation of fighter and attack aircraft that utilise advanced technology, AMPR can be approximated by:

$$AMPR = 0.52(W_{AT})^{1.0395} \quad (A92)$$

Where:

WE_{CFA} Weight empty of conventional fighter/attack aircraft.

WE_{AT} Weight empty of advanced fighter attack aircraft.

The engineering hourly labour rate varies with different airframe manufactures because of different rates. Fig. A7 can be used for an approximation of engineering labour rates. Engineering cost for the development phase can be estimated by:

$$C_{AED} = E_{HD} E_{RATE} C_S \quad (A93)$$

Where

E_{RATE} Engineering hourly rate.

C_S Judgement cost factor for program security requirements.

=1.05 to 1.1 for unclassified military programs.

=1.1 to 1.2 for classified programs

=1.2 to 1.4 for special access programs.

Engineering cost for the production phase can be estimated by:

$$C_{AEP} = E_{HP} E_{RATE} C_S \quad (A94)$$

Development Support (DT&E)

Development support is the non recurring manufacturing effort undertaken to support engineering during the DT&E phase of an aircraft program. It includes the cost of

manufacturing labor and materials required to support mock-up requirements, test, components, and other hardware needed for airframe design and development work.

The development support cost can be estimated by:

$$C_{DSC} = 0.0356 A^{0.903} S^{1.93} Q_D^{0.346} C_{PI} A_{TF} C_S \quad (A95)$$

Where

C_{DSC}	Development support in 1983 dollars.
A	AMPR weight.
S	Maximum speed (knots) at best altitude.
C_{PI}	Cost escalation factor (ratio of the consumer price index for "then year" and the C_{PI} for 1983)

Fig. A8 or the attached fitted equation can be used to find the consumer price index.

Flight Test Operation (DT&E)

Flight test cost includes all costs incurred by the aircraft manufacturer to complete flight test except the cost of the test aircraft. It includes flight test engineering planning, data reduction, manufacturing support, flight test instrumentation, spares, fuel and oil, pilot's salary, facilities rental, and insurance. The cost of flight test operations can be estimated by:

$$C_{FTAR} = 0.00558 A^{1.19} S^{1.401} Q_D^{1.281} C_{PI} A_{TT} C_S \quad (A96)$$

Where

C_{FTAR}	Cost of flight test operations.
A_{TT}	Judgement factor for advanced technology aircraft testing such as low observable (LO), very low observable (VLO), STOL, and VTOL aircraft. For conventional military aircraft $A_{TT} = 1.0$. For unconventional aircraft (including stealth features) $A_{TT} = 1.0$ to 2.0

Tooling (DT&E and Production)

Tooling includes hours required for tool design, N/C programming, tool planning, tool fabrication, production test equipment, maintenance of tooling, normal changes and production planning. The aircraft production rate is a variable that affects tooling cost. Higher production rates result in a higher tooling cost and will cause the unit flyaway cost to be slightly higher for a given production quantity. Tooling hours for development and production can be estimated by the following equations:

$$T_{HD} = 5.083A^{0.768}S^{0.899}Q_D^{0.18}R^{0.66}C_{AMC} \quad (A97)$$

$$T_{HP} = 5.083A^{0.768}S^{0.899}(Q_D + Q_P)^{0.18}R^{0.66}C_{AMC} - T_{HD} \quad (A98)$$

Where:

T_{HD}	Tooling hours for development.
T_{HP}	Tooling hours for production.
R	Production rate (aircraft per month).
C_{AMC}	Judgement factor for advanced materials tooling and manufacturing cost relative to % advanced composites and conventional metal aircraft designs. Fig. A6 is used to estimate its value.

Tooling cost for development C_{TD} and production C_{TP} can be estimated with the following equations:

$$C_{TD} = T_{HD}T_R C_S \quad (A99)$$

$$C_{TP} = T_{HP}T_R C_S \quad (A100)$$

Fig. A9 could be used to estimate the quality labor rate T_R

Manufacturing Labor (DT&E and Production)

Manufacturing labor hours include those hours necessary for machining, fabrication, and assembly of the major structure, installation of purchased parts, government furnished equipment, and subcontractor assemblies and components. Manufacturing labor hours for development M_{HD} and production M_{HP} can be estimated by:

$$M_{HD} = 43.61A^{0.76}S^{0.549}Q_D^{0.554}C_{AMC} \quad (A101)$$

$$M_{HP} = 43.61A^{0.76}S^{0.549}(Q_D + Q_P)^{0.554}C_{AMC} - M_{HD} \quad (A102)$$

Manufacturing labor cost for development C_{MD} and production C_{MP} can be estimated by the following equations:

$$C_{MD} = M_{HD}M_R C_S \quad (A103)$$

$$C_{MP} = M_{HP}M_R C_S \quad (A104)$$

Where M_R is the hourly rate used for manufacturing cost estimation. Fig. A10 or the attached equation could be used to estimate manufacturing labor rates.

Quality Control

Quality control includes the task of inspecting fabricated and purchased parts, sub-assemblies, and assembled components for standards specified by process standards, drawings, and specifications. The quality control man-hour requirement for development Q_{HD} and production Q_{HP} can be estimated by:

$$Q_{HD} = 0.13M_{HD} \quad (A105)$$

$$Q_{HP} = 0.13M_{HP} \quad (A106)$$

Quality control labor cost for development C_{QD} and production C_{QP} can be estimated by:

$$C_{QD} = Q_{HD}Q_R \quad (A107)$$

$$C_{QP} = Q_{HP}Q_R \quad (A108)$$

Where Q_R is the average hourly rate for quality control. Fig. A9 gives an approximation of the quality labor rate.

Manufacturing Material and Equipment (DT&E and Production)

Manufacturing material and equipment includes the raw material, hardware and purchased parts required for the fabrication and assembly of the airframe with the exception of engines and avionics. The cost of manufacturing materials for the development program C_{MMD} and the production C_{MMP} can be estimated by the following equations:

$$C_{MMD} = 96.677 A^{0.692} S^{0.639} Q_D^{0.803} C_{PI} C_{AMC} C_{LO} \quad (A109)$$

$$C_{MMP} = 96.677 A^{0.692} S^{0.639} (Q_D + Q_P)^{0.803} C_{PI} C_{AMC} C_{LO} - C_{MMD} \quad (A110)$$

Where:

C_{PI}	Cost escalation factor.
C_{AMC}	Advanced materials cost factor.
C_{LO}	Judgement cost factor of low observable materials, =1.1 to 1.2 for low observable. =1.2 to 1.3 for very low observable =1.0 for conventional aircraft.

C_{AMC} is a relationship of the amount of advanced materials used, expressed as a percentage of total structural materials. Fig. A6 is used to estimate its value.

Engine Cost

Engine cost for military aircraft with after-burners can be estimated by:

$$C_{ABE} = 320.65 T_{SL}^{0.9356} N_E C_{PI} \quad (A111)$$

Where

C_{ABE}	Cost of after-burning engines.
T_{SL}	Sea level maximum thrust.
N_E	Number of engines per aircraft.

Avionics Cost

The cost of avionics varies with the type and the quantity of aircraft and their mission requirements. It is important to use avionics uninstalled equipment weight for avionics cost estimates. The following equation gives an approximate cost of uninstalled avionics:

$$C_{AV} = W_{AV}(\$3950)C_{PI} \quad (A112)$$

Where:

C_{AV}	Avionics cost in then year dollars.
W_{AV}	Avionics Weight.
C_{PI}	Ratio of cost escalation factor for year of interest and 1983.

Design Based Variables

The following variables are found in both the design synthesis and the cost estimation equations:

A_{TF}	Technology judgement factor, 1.0 to 1.5 (F-15 to F-22)
S	Maximum speed (Knots)
A	Airframe unit weight (lb)

C _s	Program security judgement factor (1.05 to 1.4)
A _{TT}	Advanced technology testing judgement factor (1.0 to 2.0)
C _{AMC}	Advanced materials judgement factor.
C _{LO}	Low observable materials judgement factor (1.0 to 1.3)
T _{SL}	Sea level maximum thrust (lb)
N _E	Number of engines per aircraft.
W _{AV}	Avionics weight (lb)

A.6 TEST CASE RESULTS

The following is the CONCEPT output of the test case:-

TW_TO= 0.9187701
CL MAX = 1.797072
WS_STALL = 71.4392
WS_LANDING = 22.463
TKOF_PAR = 93.860
TKOF_PAR = 35.417
WS_TO = 48.3275
E= 1.024
WS_CRs = 64.996
WS_TO_CR= 68.583
G_ITR= 6.484715
WS_ITR= 47.79675
WS_TO_ITR= 56.23147
TW_STR= 0.57648
WS_STR= 43.5337
WS_TO_STR= 51.2161
-----INITIAL SISZING-----
W2_W1= 0.97725
WS_CRs= 53.8531570
LD_CRs= 10.660
W3_W2= 0.9666
W4_W3= 0.9840
-----DASH-----
WS_DSH= 52.4126
CD0_DSH= 0.0280
K_DSH= 0.2867
LD_DSH= 2.5741
W5_W4= 0.9748
TW_CO= 0.552
W6_W5= 0.9567

W8_W7= 0.984 W9_W8= 0.975 W10_W9= 0.967
WS_LO= 44.2878
Q0_LO= 121.720
LD_LO 12.994639
W12_W11= 0.977028
W14_W0= 0.760297
WF_W0= 0.254085

S I Z I N G I T E R A T I O N

W0_GSS	W0_CALC		
18288.46	16576.93		
18108.97	17929.48		
18101.13	18093.29		

RANGE_CRS	W_PAYLOAD	W0	WF
200.0000	1440.000	18100.55	4599.074

W_EMPT 11841.48
THRUST_TO_CALC= 16630.25
SF_ENGN= 0.5543416
LPG= 4.265500
ENGN_DIA= 0.9589563

FIRST SIZING ITERATION RESULTS

GROSS TAKEOFF WEIGHT (kg) = 8208.867
EMPTY WEIGHT (kg) = 5370.284
TOTAL FUEL WEIGHT (kg) = 2085.748
FUEL VOLUME REQUIRED (m3)= 2.677468
GROSS WING SURFACE AREA (m2) 29.90198

L A N D I N G G E A R

MAIN, D&W=	0.6128085	0.1668987	
NOSE, D&W=	0.4902468	0.1335190	

VOLUMES MAIN	NOSE	LEG_M	LEG_N
0.1034157	5.2948851E-02	1.7671458E-02	7.8539820E-03

E C S

ECS MASS (KG)= 48.92080
ECS VOL (M3)= 9.7841598E-02

E L E C T R I C A L S Y S

ELEC GEN. MASS (KG)= 136.0915
ELEC GEN.VOL (M3)= 0.2721829
XFR= 0.9939553

LAR= 0.6000000
TERM= 0.5921470
CWCB, LPG 0.0000000E+00 4.265500

Fuselage length

XFN= 13.59617

INTAKE DIFFUSER

XII,XIE 4.654011 9.330673
LIDG= 4.676662
OII OIE 0.5158929 0.7222500
LIDS= 5.753738
BII HII 1.015769 0.5078843

RADOME

DAR EDAR GOFI
0.6000000 5.9999999E-02 0.3442000
LAR MAR LAX1 MAX
0.6000000 150.0000 1.200000 300.0000
OFI XFR VFR WFR XA
0.3421194 0.9939553 0.1700257 1.424842 2.793955
VOL, AV. RADOME= 0.6000000

COCKPIT OUTPUT

HC1 HC2 HC3 HC4
0.7450000 0.6940000 0.3300000 0.2540000
QCSEAT HCSEAT QCEYE
0.4363322 0.2220000 0.2967059
QCFOOT HCEYE LCEYE
0.5130889 1.015864 1.046486
LCFL,HC5,XB
1.267909 0.6959209 3.840441

GROSS WING OUTPUT

BW CWCC CWMG CWMA CWCT QW4 QW2
10.230196 4.676661 2.922914 3.273663 1.169165 0.588698
0.460637
QWT= 0.1521993

NET WING OUTPUT

BWN	CWCB	UWCN	CWMN	SWN	AWN	
9.2610	4.3444	0.2691		2.7568	25.5304	3.3594
fuel vol center sec of the box=				0.418		
BWNF=						
9.261007						
fuel vol ext wing box=				1.788		
TOTAL FUEL VOLUME				2.206		
CWCB= 4.344368						
XWAS= 3.607484						
CWCB= 4.344368						
UWCN= 0.2691221						

FUSELAGE OUTPUT

----- SECTION A-----

OFA= 0.6842388

BFA HFA 0.8897970 0.9449644

FLOOR DEPTH 0.2490435

----- SECTION B-----

BFB HFB 1.100000 0.8649071

FLOOR DEPTH 0.2490435

----- SECTION D-----

XP1= 0.0000000E+00

YIDD 0.0000000E+00

BFDS= 0.0000000E+00

OIDD 0.6206743

OFDS= 1.999447

ROFDN= 0.3422140

BFD= 0.9691886

HFD= 0.3943360

----- SECTION E-----

HFE BFE 2.205600 2.052166

----- SECTION F-----

HFF BFF 1.150748 1.074031

EMPENNAGE OUTPUT

TOTAL FIN AREA= 4.401734

FIN MOMENT ARM LEFCQM= 4.864722

NETT SPAN OF THE FIN, BEFN= 3.925057

FIN MASS, MEF= 105.9392

TAIL AREA, SETN= 6.216321

TAIL MOMENT ARM, LETCQM= 4.217972

NETT SPAN OF TAIL, BETN= 4.664453

CHORD OF TAIL, CETB= 2.132321

TAIL MASS,MET= 256.1703

-----FAIRING CURVE-----

XF1 XF2 XF3 XF4 XF5 XF6

0.993955 2.506222 4.774621 5.656776 12.008293 13.596172

OTM= 2.764063

OTA1K OTA2K OTA3K OTA4K

2.764063 0.0000000E+00 -1.4926374E-02 -3.0436364E-03

OTF1K OTF2K OTF3K OTF4K

2.764063 0.0000000E+00 -0.4172916 6.5556444E-02

ACQUSETION COST OUTPUT

ACU COST= 24.01389

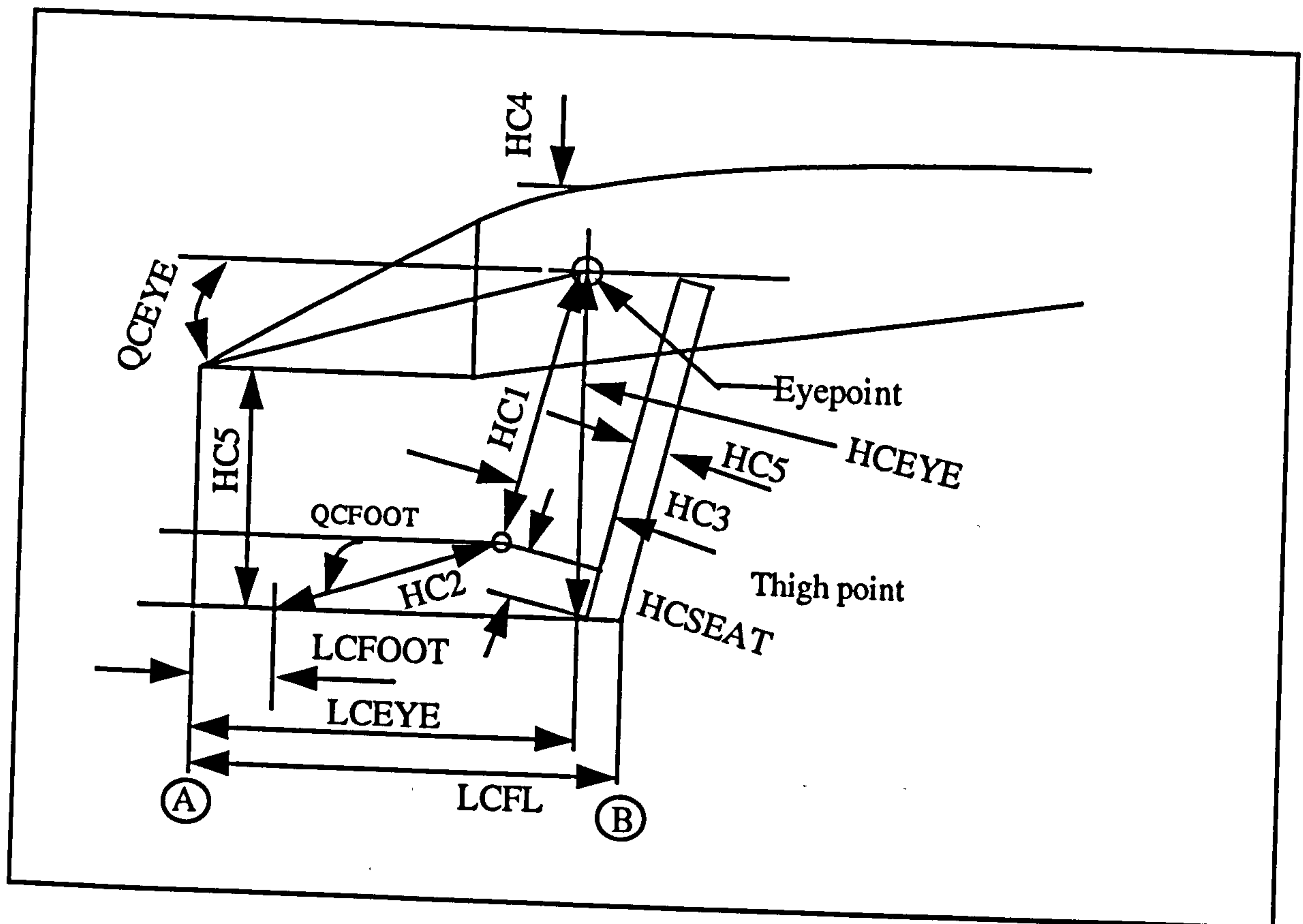


Fig. A.1 Cockpit layout

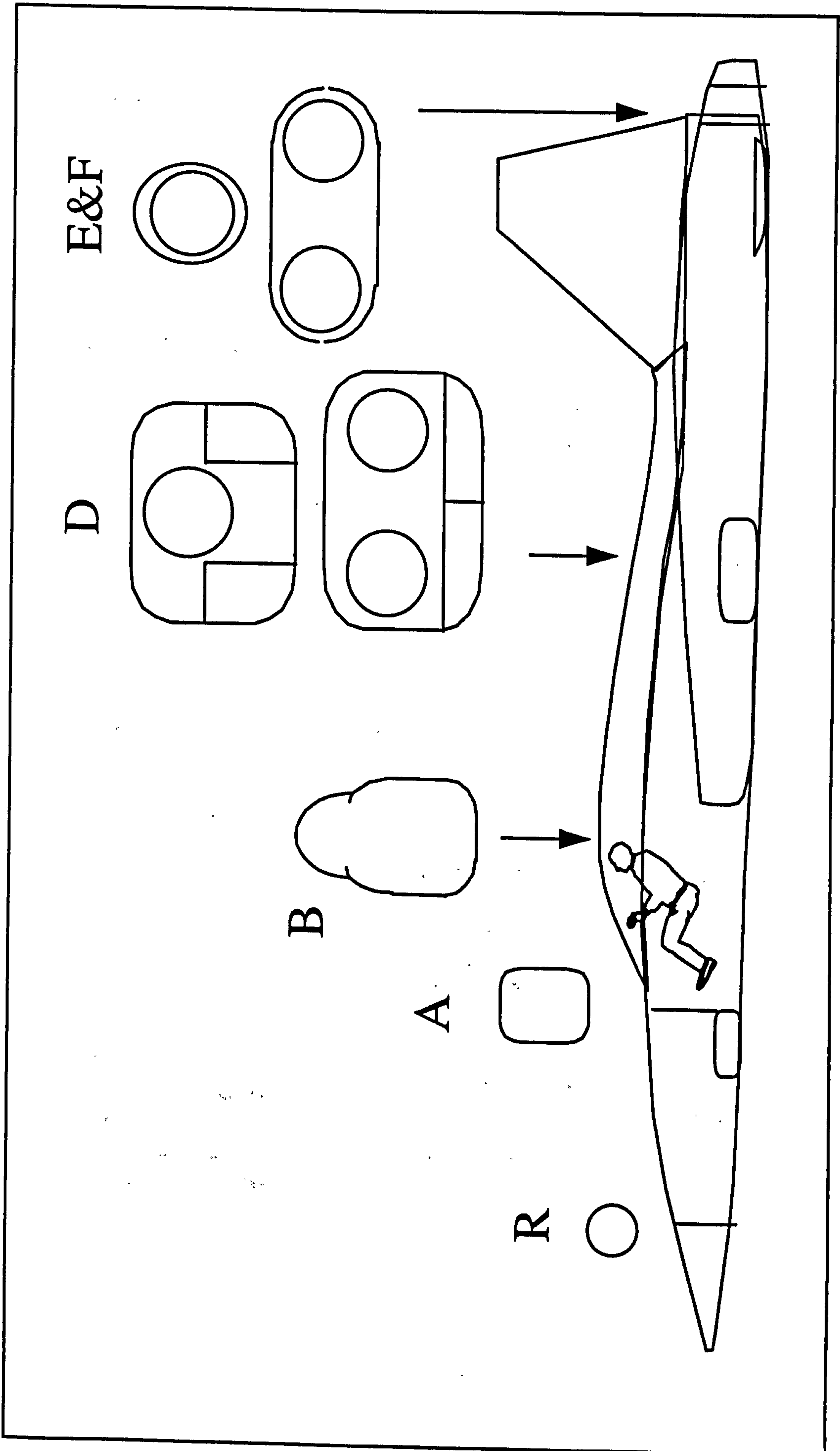


Fig. A.2 Fuselage sections.

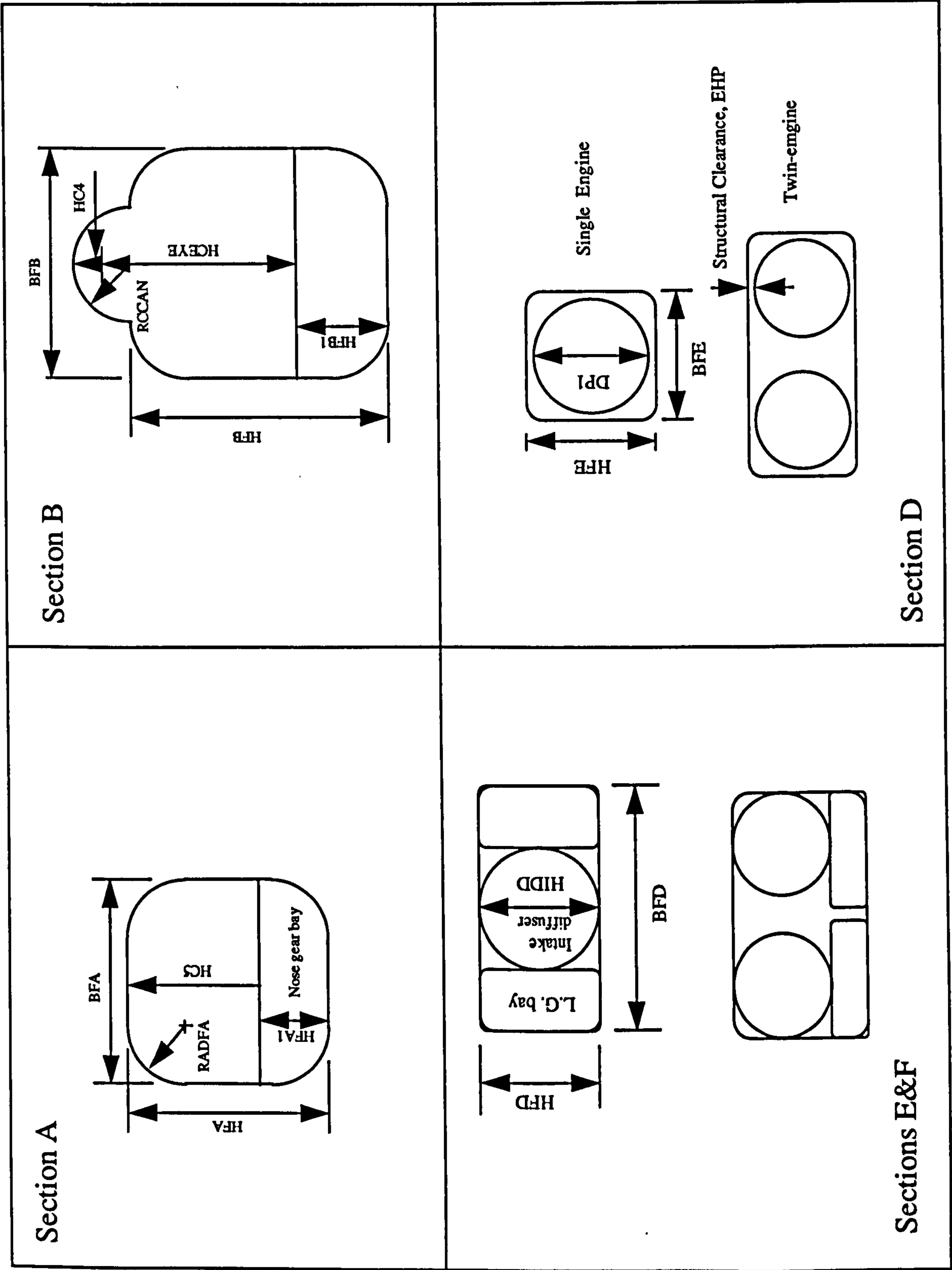


Fig. A.3 Fuselage sections defintion

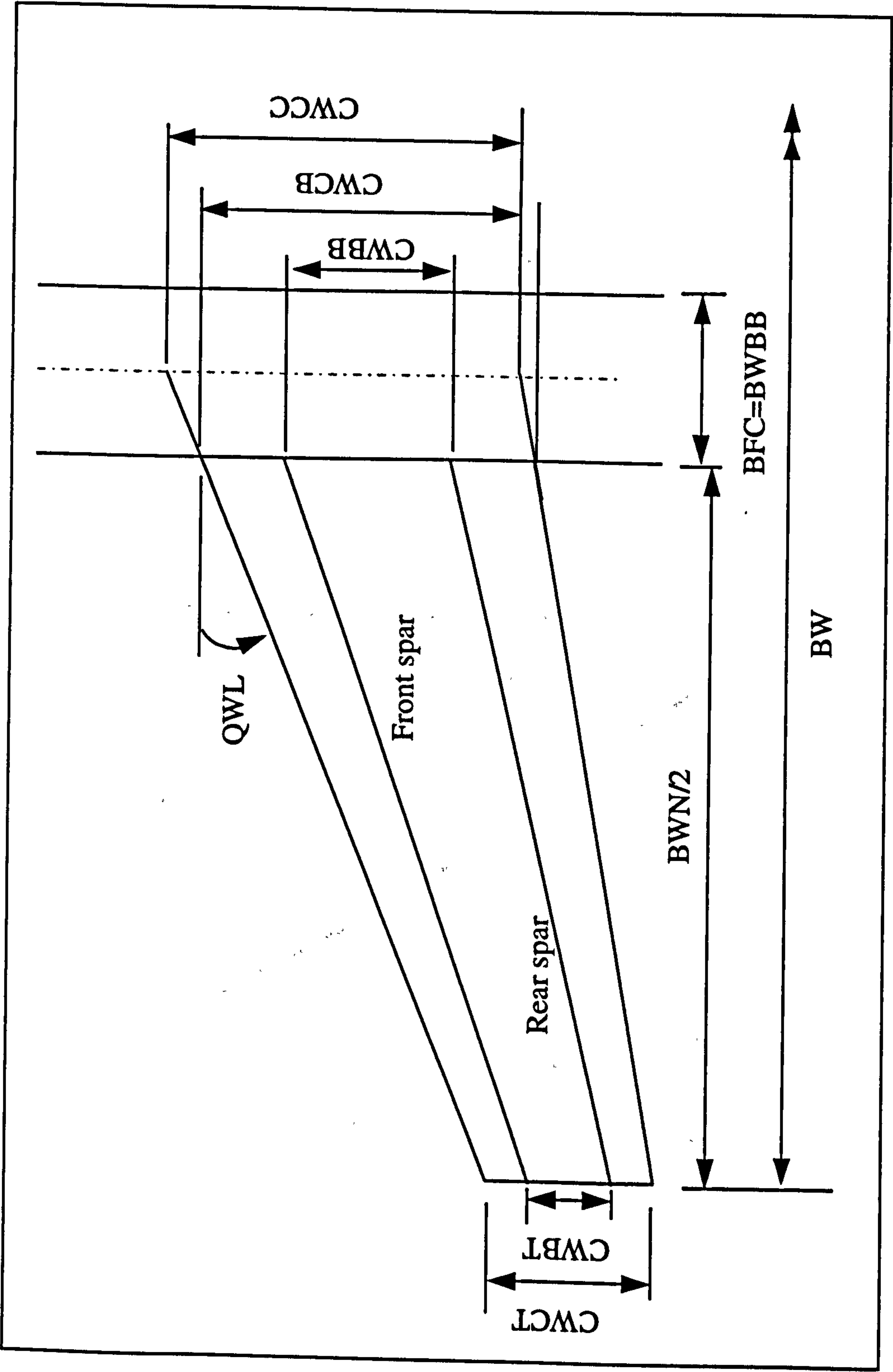


Fig. A.4 Wing geomtery defintion

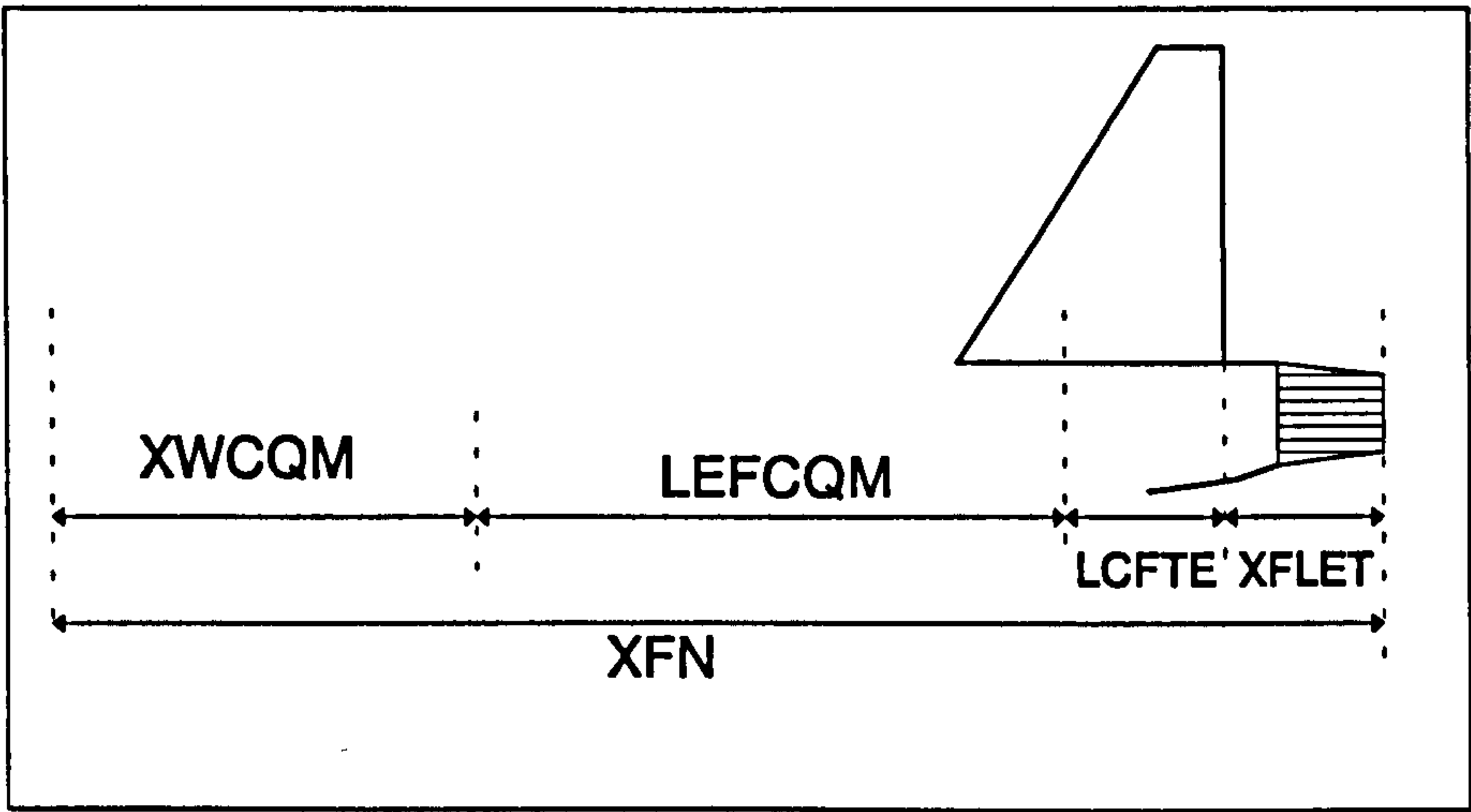


Fig. A.5 Fin postion defintion.

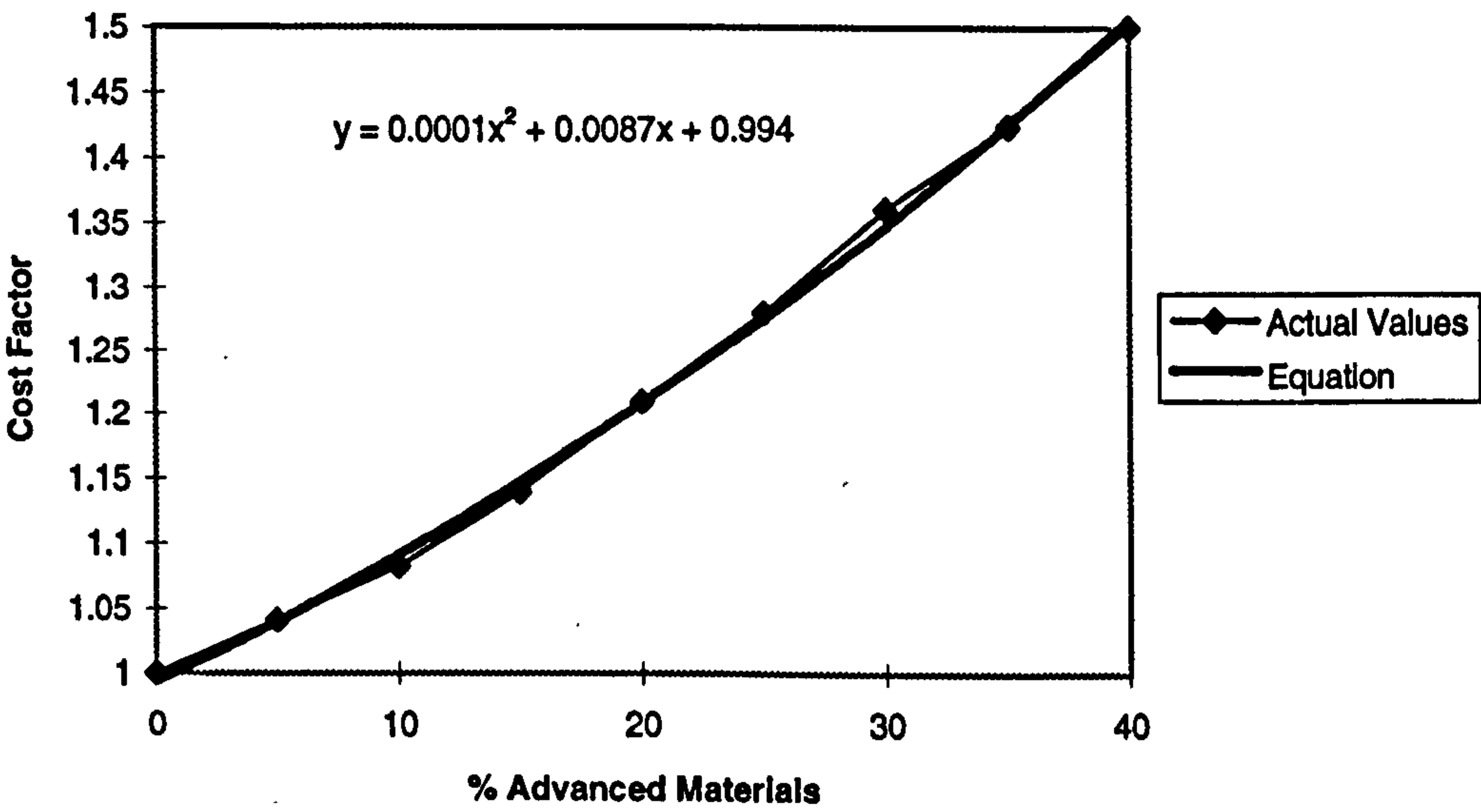


Fig. A6 Advanced Materials Cost Factor

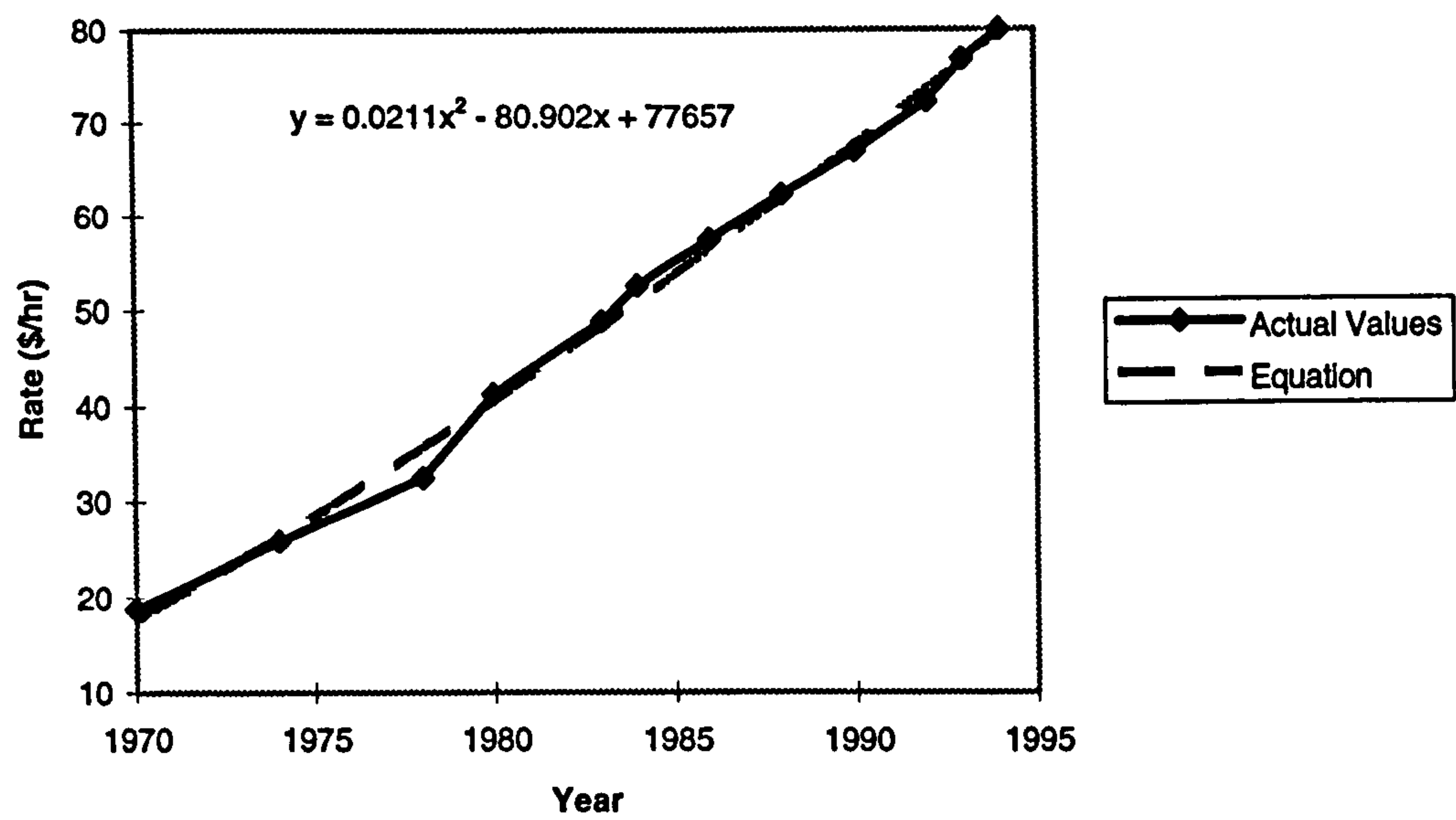


Fig. A7 Engineering Labor Rate

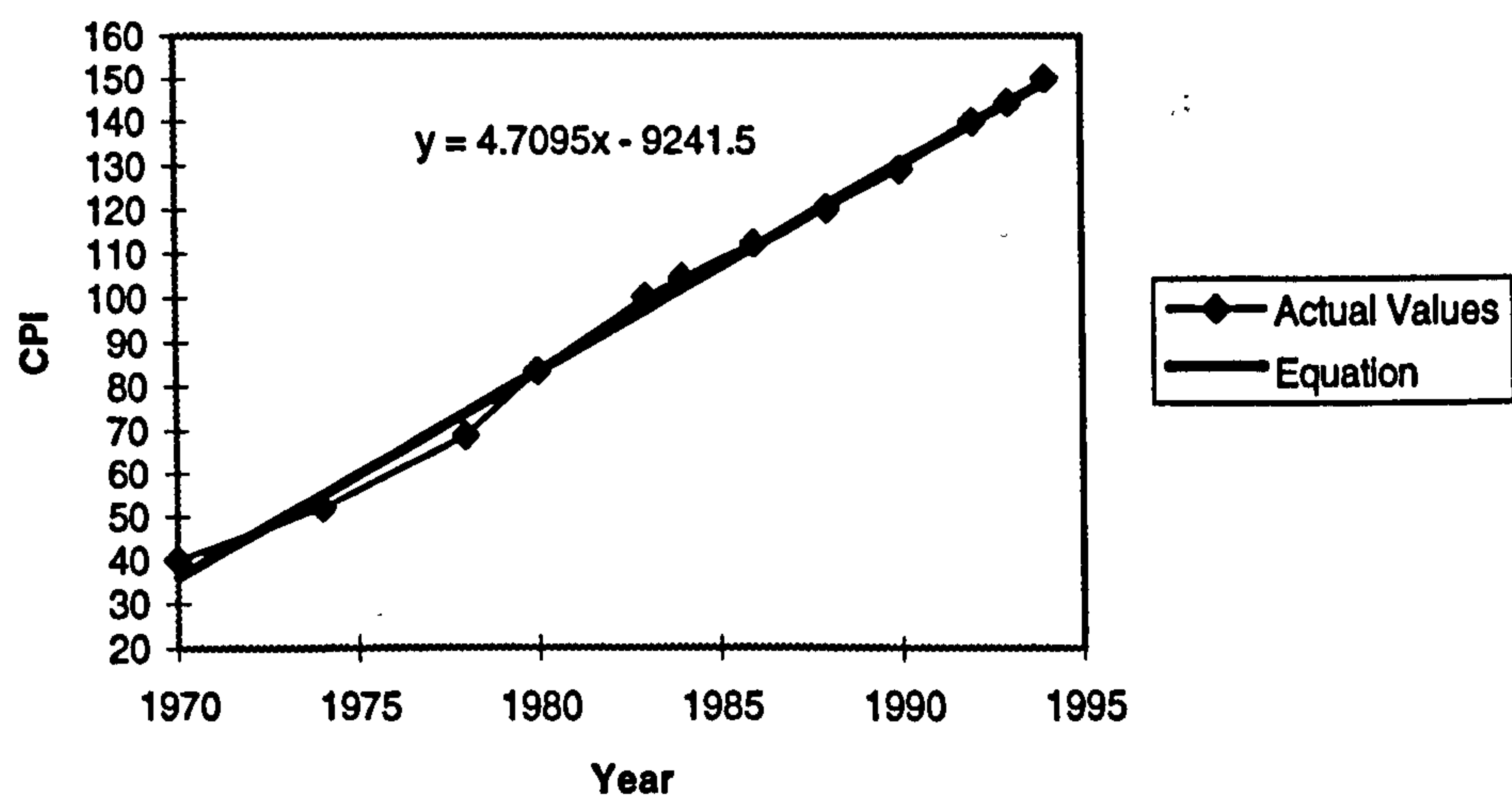


Fig. A8 Consumer Price Index

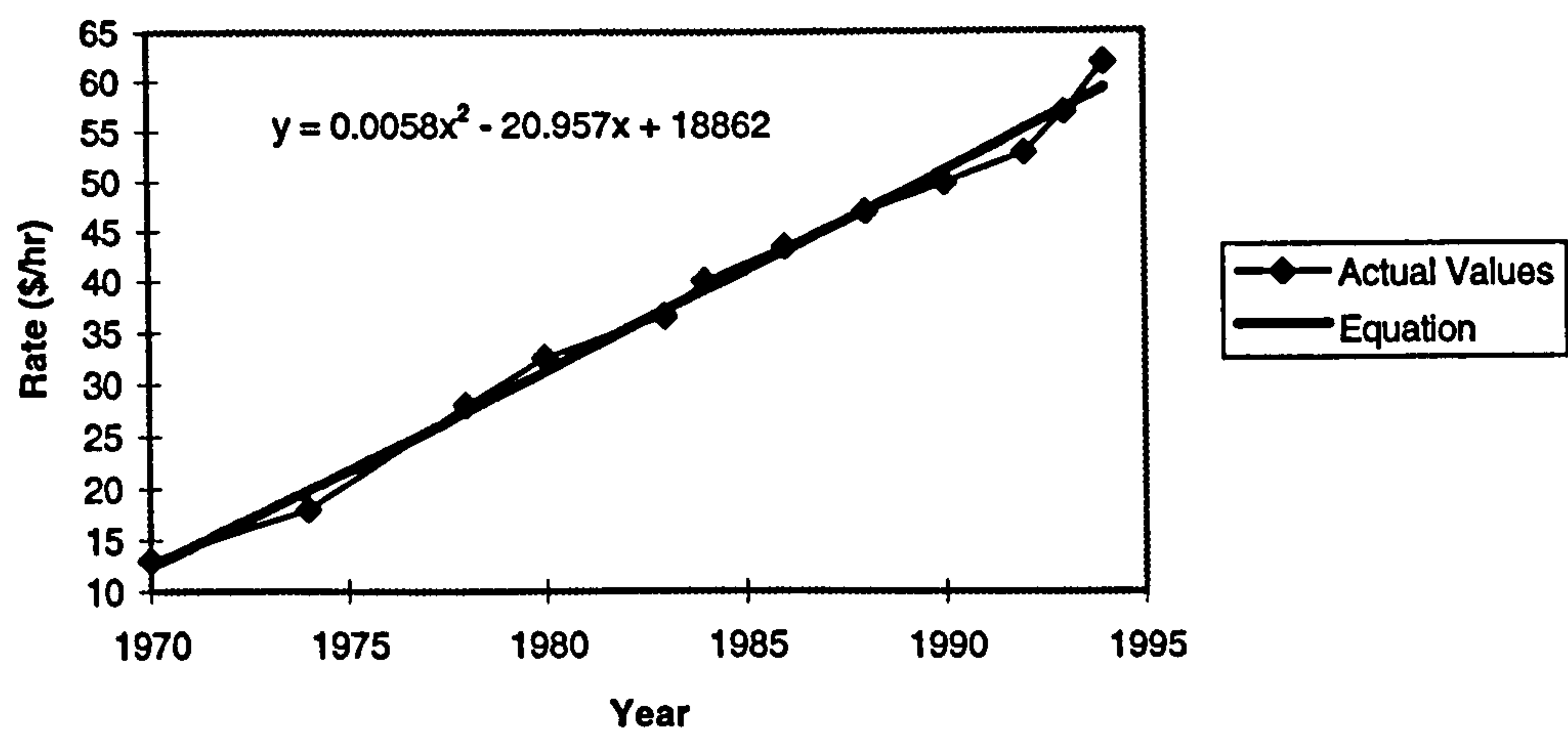


Fig. A9 Tooling & Quality Labor Rate

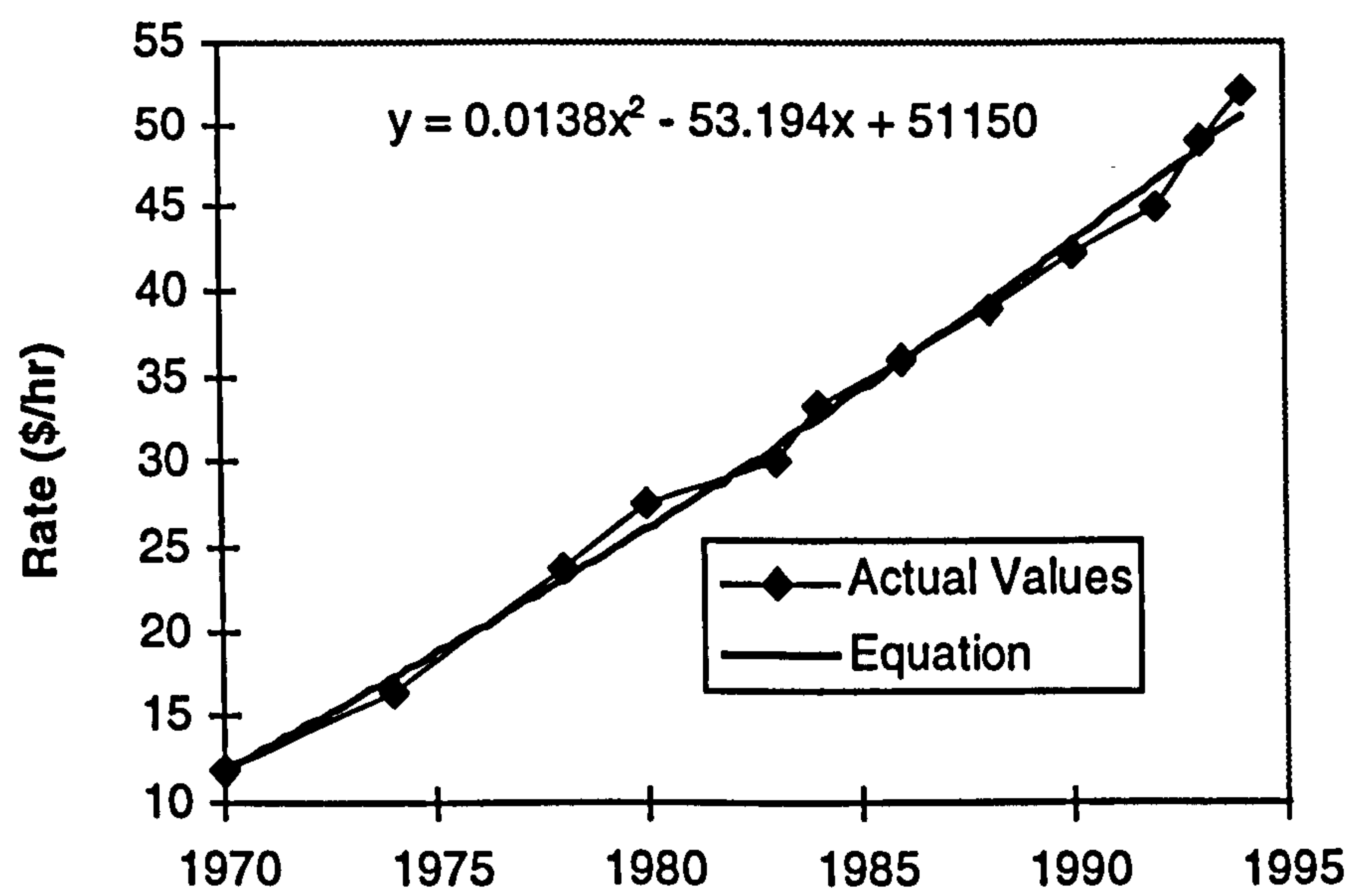


Fig. A10 Manufacturing labor rate

Appendix B

R&M Data and Analysis

B.1 Introduction

This appendix contains the R&M data of the aircraft under investigation. The reliability data are given with the Pareto graphical distribution. The maintainability data did not closely followed the Pareto's distribution. The MTTR value is set to be a user-defined input. The R&M module can generate the MTTR (in terms of man hours) distribution of the aircraft system based on a mean value. Beside the aircraft's design characteristics, the aircraft maintainability depends on other factors such as the maintenance personnel skill and the availability of spare parts.

B.2 Failure Rate Data and Analysis

The following tables contain the FR data for the aircraft under investigations. These aircraft are named by Capital letters for the data security requirements. The collection effort and the data sources has been discussed in Chapter 3. The FR is given for each WUC system for 1,000 flying hours as reported in the Organisational Level.

B.3 Method of Calculating Failure Rate.

The following is an aoutpu from the R&M module. .

INPUT DESIGN PARAMTER

WE=8270.0

NE=1

MACH=1.8

MEAN OF MAINT. TIME=1.5

OUTPUT

NOS= 27

FR1= 43.76600

FR8= 7.721728

<i>Sys. no.</i>	<i>FR</i>	<i>MTTR</i>
1	43.76600	0.77078
2	30.10098	0.26358
3	24.18195	0.46294
4	20.70258	0.80177
5	18.35241	1.42140
6	16.63164	0.25758
7	15.30326	1.05331
8	14.23863	0.33961
9	13.36121	0.74213
10	12.62225	0.18704
11	2.46189	0.12584
12	2.46189	0.58443
13	2.46189	0.41583
14	2.46189	0.55206
15	2.46189	1.47514
16	2.46189	0.80305
17	2.46189	1.14848
18	2.46189	0.96968
19	2.46189	1.15068
20	2.46189	1.17032
21	2.46189	1.23441
22	2.46189	0.22787
23	2.46189	0.93819
24	2.46189	0.47200
25	2.46189	0.52034
26	2.46189	1.37576
27	2.46189	0.77962

WUC	SYSTEM	FR	% OF TOTAL	COMM
13	LANDING GEAR SYSTEM	42.123	13.39670605	13.3967
74	FIRE CONTROL SYSTEM	41.824	13.30145552	26.6982
75	WEAPONS DELIVERY	32.595	10.36629079	37.0645
11	AIRFRAME	25.075	7.974869647	45.0393
23	TURBOFAN POWER PLANT	21.381	6.800038519	51.8394
76	PENETRATION AIDS AND ECM	17.908	5.695519368	57.5349
44	LIGHTING SYSTEM	17.328	5.510965197	63.0458
27	TURBOFAN POWER PLANT	17.218	5.475857464	68.5217
46	FUEL SYSTEM	14.795	4.705397271	73.2271
14	FLIGHT CONTROL SYSTEM	14.245	4.530453013	77.7576
63	UHF COMM	13.581	4.319405154	82.077
42	ELECTRIC			
24	AUX POW			
41	ENVIROM			
51	FLIGHT IN			
12	CREW ST			
65	IFF SYS			
45	HYDRAU			
47	OXYGEN			
71	RADIO NA			
62	VHF COM			
64	INTERPH			
55	MALFUNK			
49	MISC. UT			
96	PERSONNEL & MISC. EQUIP.	0.1425	0.045307112	
97	EXPLOSIVE DEVICES & COMPS	0.095	0.030205889	
91	EMMERGENCY EQUIPMENT	0.0686	0.021814788	
	TOTAL	314.43	100	

Aircraft (F)

System No.	FR
1	42.123
2	41.824
3	32.595
4	25.075
5	21.381
6	17.908
7	17.328
8	17.218
9	14.795
10	14.245
11	13.581

Figure B1.1 FR data for aircraft (F)

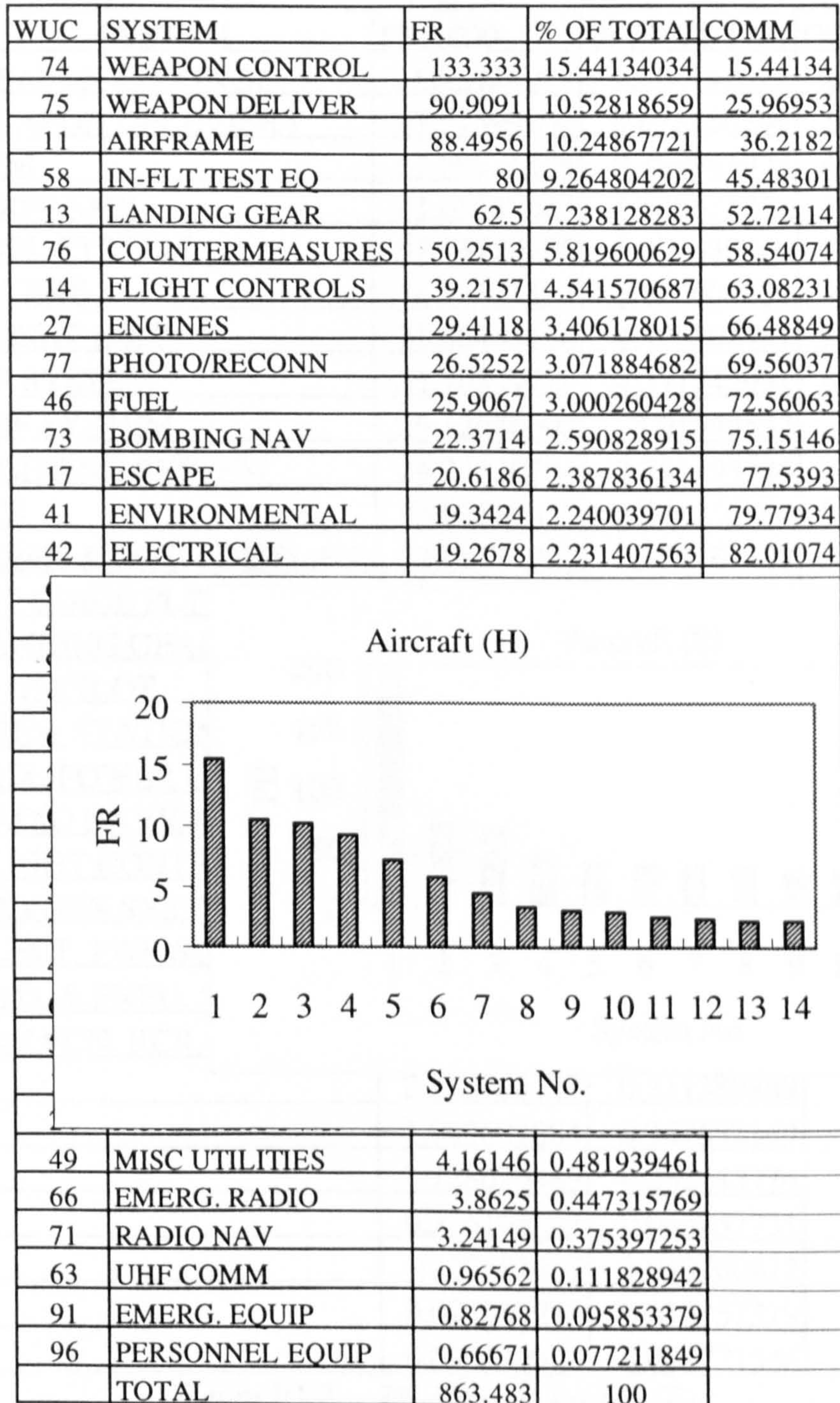


Figure B1.2 FR data for aircraft (H)

WUC	SYSTEM	FR/1000	% OF TOTAL	COMM
74	WEAPON CONTROL	186.2723993	25.04715012	25.04715012
75	WEAPON DELEVIERY	67.51599836	9.078550298	34.12570042
76	ECM	62.39521974	8.389983923	42.51568434
11	AIRFRAME	41.65117387	5.600632237	48.11631658
46	FUEL SYSTEM	37.73720295	5.074339466	53.19065605
23	ENGINE	34.37771124	4.622604838	57.81326088
51	FLIGHT INST.	33.46445136	4.499803191	62.31306408
65	IFF SYSTEM	31.76839729	4.271742991	66.58480707
63	UHF SYSTEM	29.12646692	3.91649537	70.50130244
44	LIGHTING SYSTEM	28.21320704	3.793693724	74.29499616
41	ECS	24.62540037	3.311258684	77.60625484
82	COMP. & DATA DISPLAY	22.08131927	2.969168383	80.57542323
57	INT GUIDE FLT			
13	LANDING GEAR			
52	AUTOPILOT			
12	CREW STATION			
24	AUX. POWER U			
71	RADIO NAVIGA			
14	FLIGHT CONTR			
47	OXYGEN SYST			
42	ELECT. PWR SU			
45	HYD. & PNEU. S			
55	MALFUN. RCR.			
28		2.315766127	0.311389889	
72		1.989601884	0.267532159	
49		1.728670489	0.232445974	
97		0.326164243	0.043857731	
91		0.22831497	0.030700412	
54		0.097849273	0.013157319	
48		0.065232849	0.008771546	

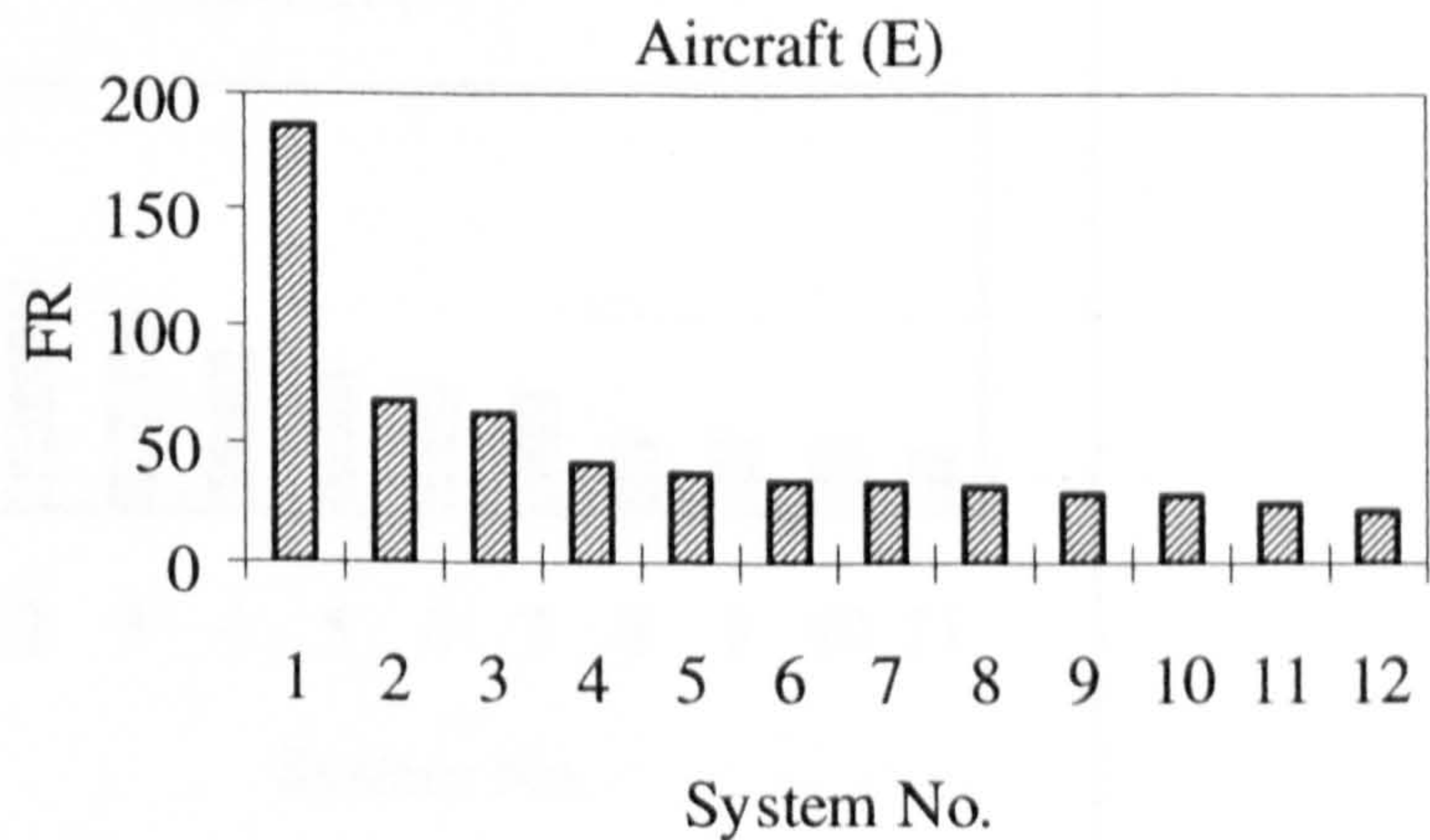


Figure B1.3 FR data for aircraft (E)

SYSTEM	FR	% OF TOTAL	COMM
Airframe	665.9	18.01336327	18.0134
Fire Control	422	11.41558687	29.429
Flight Control	373.6	10.10631103	39.5353
Landing Gear	295	7.980090351	47.5154
Weapon Delivery	255.3	6.906159548	54.4215
Bombing Navigation	227.4	6.151432359	60.5729
Air Crew Compartment	218.4	5.907971975	66.4809
Hydraulic & Pneumatic	137.8	3.727648984	70.2086
Autopilot	137	3.706008061	73.9146
Propulsion System	132.9	3.595098331	77.5097
Instruments	111	3.002678064	80.5123
Radar Navig			
Environment			
ECM			
Fuel System			
Electrical Sy			
Lighting Sys			
IFF			
Oxygen Syst			
UHF Commu			
Misc. Utilitie			
Radio Navig			
Explosive De			
Reconnaissance	15.4	0.416587767	
Drag Chute	14.1	0.381421268	
Intercommunication	11.1	0.300267806	
Personal Equipment	7.6	0.205588768	
Malfunction Analysis	5.4	0.14607623	
Emergency Equipment	3.8	0.102794384	
VHF Communication System	1	0.027051154	
Remote Control System	0	0	
Regency Communication	0	0	
Misc. Communication	0	0	
Total	3696.7	100	

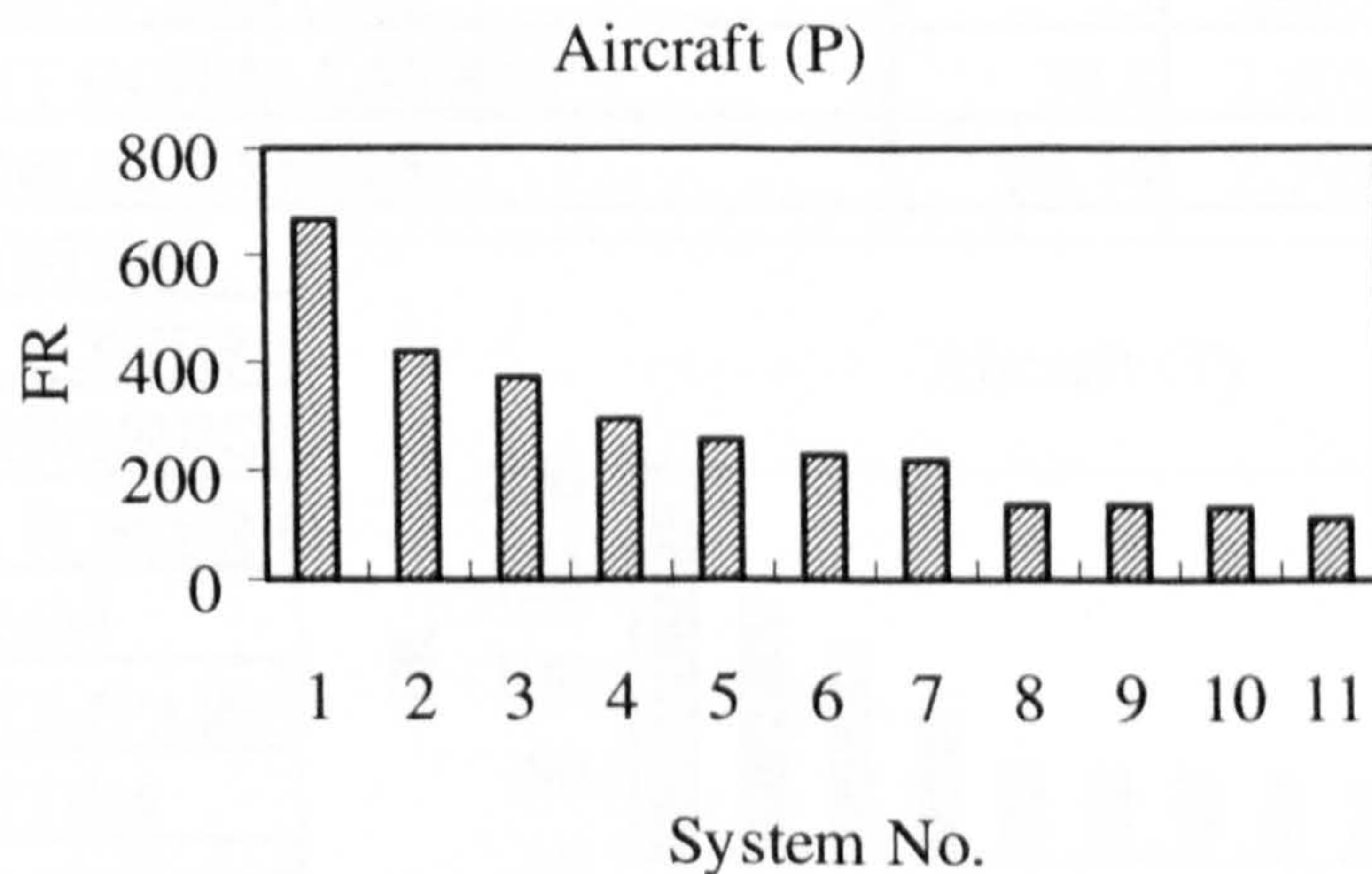


Figure B1.4 FR data for aircraft (P)

SYSTEM	FR	% OF TOTAL	COMM
AIRFRAME	178.91	16.2959522	16.296
LANDING GEAR SYSTEM	133.09	12.12245418	28.4184
FLYING CONTROL SYSTEM	111.35	10.1422742	38.5607
ENGINE	76.62	6.978904798	45.5396
ELECTRONIC COUNTER MEASURES	49.65	4.52235217	50.0619
WEAPON DELIVERY SYSTEM	47.92	4.36477575	54.4267
FUEL SYSTEM	45.78	4.169854629	58.5966
DISPLAYS	42.58	3.878383794	62.475
HYDRAULIC POWER GENERATION	39.91	3.635187817	66.1101
GENERAL NAVIGATION	38.39	3.49673917	69.6069
INSTRUMENTS	34.83	3.172477866	72.7794
WEAPON AIMING SYSTEM	33	3.005792983	75.7851
POWER PLANT INSTALLATION	30.8	2.805406784	78.5906
ENVIRONMENTAL SYSTEM	30.74	2.799941706	81.3905
LIGHTING SYSTEM			
SECONDARY POWER S			
PHOTOGRAPHIC/RECO			
ELECTRICAL POWER C			
UHF/VHF COMM.			
FUSELAGE COMPARTM			
OXYGEN SYSTEM			
MISCELLANEOUS UTIL			
COMPUTING SYSTEM			
EJECTION SEAT EQUIP			
MISCELLANEOUS COM			
IFF SYSTEM	5.71	0.520093271	
GUIDANCE & FLIGHT CONTROL SYSTEM	5.39	0.490946187	
MISCELLANEOUS AVIONICS	5.19	0.47272926	
INTERCOMMUNICATION SYSTEM	5.08	0.46270995	
RADIO NAVIGATION	4.56	0.415345939	
SOFTWARE	4.19	0.381644624	
ALL WEATHER LANDING SYSTEM	3.72	0.338834845	
FLIGHT REFERENCE	3.61	0.328815535	
EXPLOSIVE DEVICES	3.61	0.328815535	
GUN SYSTEM	2.72	0.247750209	
ARRESTOR HOOK SYSTEM	2.41	0.219513972	
EMERGENCY COMMUNICATIONS	0.79	0.071956862	
HF COMM.	0.47	0.042809779	
PERSONNEL EQUIPMENT	0.16	0.014573542	
TOTAL	1097.88	100	

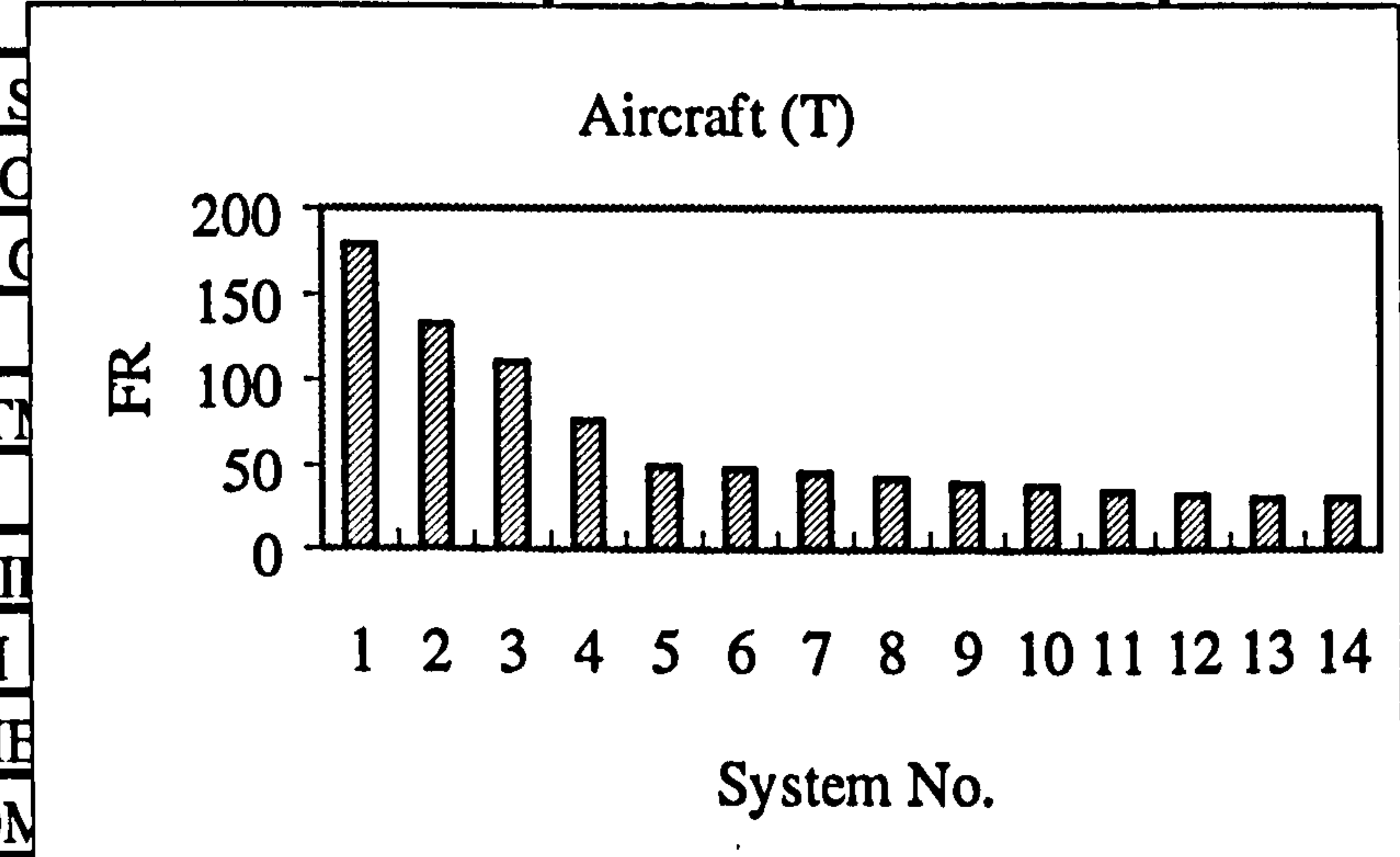


Figure B1.5 FR data for aircraft (P)

B.3 Maintainability Data and Analysis

The following tables contains the Maintainability data of each aircraft. Again the data are for each WUC system. The system MTTR (hours) is for the failures reported in the Organisational Level.

WUC	SYSTEM	MTTR	% OF TOTAL	COMM
27	TURBOFAN POWER PLANT	10.46	12.35369843	12.3537
97	EXPLOSIVE DEVICES & COMPS	6.548	7.733462461	20.0872
46	FUEL SYSTEM	4.927	5.818993516	25.9062
42	ELECTRICAL PWOER SUPPLY	4.664	5.508379492	31.4145
23	TURBOFAN POWER PLANT	4.424	5.224929433	36.6395
75	WEAPONS DELIVERY	3.575	4.222224847	40.8617
13	LANDING GEAR SYSTEM	3.378	3.989559589	44.8512
11	AIRFRAME	3.234	3.819489554	48.6707
74	FIRE CONTROL SYSTEM	3.177	3.752170165	52.4229
91	EMMERGENCY EQUIPMENT	3.019	3.565565542	55.9885
45	HYDRAULIC & PNEUMATICS SY	2.842	3.356521123	59.345
14	FLIGHT CONTROL SYSTEM	2.812	3.321089865	62.6661
41	ENVIROMENTAL CONTROL SYS	2.808	3.316365698	65.9824
24	AUX POWERPLANT/JET FUEL ST	2.783	3.28683965	69.2693
47	OXYGEN SYSTEM	2.717	3.208890884	72.4782
12	CREW STATION SYSTEM	2.435	2.875837063	75.354
49	MISC. UTILITIES	2.426	2.865207686	78.2192
51	FLIGHT INSTRUMENT	2.37	2.799069339	81.0183
76	PENETRATION AIDS AND ECM	2.108	2.489636357	
62	VHF COMM.	2.055	2.427041136	
65	IFF SYS	2.047	2.4175928	
71	RADIO NAVIGATION	1.975	2.332557782	
64	INTERPHONE SYS.	1.722	2.033754178	
63	UHF COMM	1.661	1.961710621	
44	LIGHTING SYSTEM	1.657	1.956986453	
55	MALFUNC ANALY & RECORD E	1.611	1.902658525	
96	PERSONNEL & MISC. EQUIP.	1.236	1.459767807	
	TOTAL	84.67	100	

Figure B2.1 MTTR for Aircraft (F)

WUC	NOMENCLATURE	MTTR	% OF TOTAL	COMM
41	ENVIROMNTAL	3.7	5.573128483	5.57313
14	FLIGHT CONTROLS	3.58	5.39237837	10.9655
27	ENGINES	3.37	5.076065673	16.0416
46	FUEL	3.21	4.835065522	20.8766
45	HYDRAULIC	3.09	4.654315409	25.531
24	AUXILARY PWR	3.02	4.548877843	30.0798
49	MISC UTILITIES	2.84	4.277752674	34.3576
29	PWR PLANT INST.	2.72	4.097002561	38.4546
51	INSTRUMENTS	2.69	4.051815032	42.5064
42	ELCTRICAL	2.62	3.946377466	46.4528
56	FLT REFERENCE	2.24	3.374002109	49.8268
57	INT GUIDE/FLT C	2.1	3.163126977	52.9899
97	EXPLOSIVE DEVIC	2.03	3.057689411	56.0476
47	OXYGEN	2.01	3.027564392	59.0752
65	IFF	1.75	2.635939147	61.7111
44	LIGHTING	1.72	2.590751619	64.3019
72	RADAR NAV	1.72	2.590751619	66.8926
11	AIRFRAME	1.62	2.440126525	69.3327
13	LANDING GEAR	1.59	2.394938997	71.7277
76	COUNTERMEASURES	1.48	2.229251393	73.9569
74	WEAPON CONTROL	1.43	2.153938846	76.1109
62	VHF COMM	1.32	1.988251243	78.0991
67	COM/NAV/IFF INT	1.31	1.973188733	80.0723
12	FUS. COMART	1.3	1.958126224	
71	RADIO NAV	1.29	1.943063714	
64	INTERPHONE	1.25	1.882813677	
73	BOMBING NAV	1.24	1.867751167	
96	PERSONNEL EQUIP	1.24	1.867751167	
91	EMERG. EQUIP	1.19	1.79243862	
63	UHF COMM	1.15	1.732188583	
66	EMERG. RADIO	1.08	1.626751017	
77	PHOTO/RECONN	0.95	1.430938394	
17	ESCAPE	0.87	1.310438319	
75	WEAPON DELIVER	0.86	1.29537581	
58	IN-FLT TEST EO	0.81	1.220063263	
	TOTAL	66.39	100	

Figure B2.2 MTTR for Aircraft (H)

WUC	MTTR	% OF TOTAL	COMM
15	8	11.00479259	11.00479259
46	4.34	5.970099979	16.97489257
78	3.5	4.814596757	21.78948932
24	3.29	4.525720951	26.31521027
14	3.27	4.49820897	30.81341924
42	2.69	3.700361507	30.81341924
45	2.67	3.672849526	38.18663028
13	2.53	3.480265656	41.66689593
49	2.53	3.480265656	45.14716159
97	2.51	3.452753674	48.59991526
12	2.45	3.37021773	51.97013299
23	2.44	3.356461739	55.32659473
52	2.17	2.985049989	58.31164472
41	2.1	2.888758054	61.20040278
47	1.94	2.668662202	63.86906498
11	1.82	2.503590314	66.37265529
55	1.76	2.421054369	68.79370966
75	1.69	2.324762434	71.11847209
76	1.6	2.200958517	73.31943061
51	1.58	2.173446536	75.49287715
71	1.541	2.119798172	77.61267532
82	1.53	2.104666582	79.7173419
72	1.52	2.090910592	81.80825249
94	1.5	2.06339861	
74	1.49	2.049642619	
44	1.3856	1.906030076	
57	1.38	1.898326721	
28	1.35	1.857058749	
91	1.29	1.774522805	
63	1.25	1.719498842	
65	1.079	1.4842714	
85	1	1.375599073	
16	0.75	1.031699305	
56	0.75	1.031699305	
22	0	0	
79	0	0	
96	0	0	
TOTAL	72.6956		

Figure B2.3 MTTR for Aircraft (E)

SYSTEM	MTTR	% OF TOTAL	COMM
ENGINE	56.71430436	13.42157573	13.42157573
WEAPON AIMING SYSTEM	26.3530303	6.236507631	19.65808336
SECONDARY POWER SYSTEM	19.16687422	4.535886613	24.19396997
FLYING CONTROL SYSTEM	16.08819039	3.807308723	28.0012787
GUIDANCE & FLIGHT CONTROL SYSTEM	15.04081633	3.559445146	31.56072384
ENVIRONMENTAL SYSTEM	13.50748211	3.196577937	34.75730178
GENERAL NAVIGATION	13.44490753	3.181769513	37.93907129
INSTRUMENTS	12.79959805	3.029055482	40.96812678
FUEL SYSTEM	12.68283093	3.001422264	43.96954904
RADIO NAVIGATION	12.04166667	2.849689208	46.81923825
UHF/VHF COMM.	11.8400467	2.801975362	49.62121361
COMPUTING SYSTEM	11.7716129	2.78578034	52.40699395
GUN SYSTEM	11.33088235	2.681480401	55.08847435
ELECTRICAL POWER GENERATION	11.31768388	2.678356951	57.7668313
HF COMM.	10.46808511	2.47729737	60.24412867
MISCELLANEOUS AVIONICS	9.973025048	2.360140223	62.6042689
HYDRAULIC POWER GENERATION	9.283137058	2.196876581	64.80114548
AIRFRAME	9.238220334	2.186246931	66.98739241
POWER PLANT INSTALLATION	9.211688312	2.179968064	69.16736047
EMERGENCY COMMUNICATIONS	8.481012658	2.007051924	71.1744124
DISPLAYS	8.377172381	1.982477874	73.15689027
IFF SYSTEM	8.096322242	1.916014017	75.07290429
PHOTOGRAPHIC/RECONNAISSANCE	8.041645505	1.903074636	76.97597892
ARRESTOR HOOK SYSTEM	7.995850622	1.892237168	78.86821609
WEAPON DELIVERY SYSTEM	7.970158598	1.886157089	80.75437318
MISCELLANEOUS COMMUNICATIONS	7.91394148	1.872853174	
ELECTRONIC COUNTER MEASURES	7.905538771	1.870864652	
FLIGHT REFERENCE	7.88365651	1.865686163	
INTERCOMMUNICATION SYSTEM	7.671259843	1.815421984	
FUSELAGE COMPARTMENT	7.543157895	1.785106352	
ALL WEATHER LANDING SYSTEM	7.018817204	1.661019873	
MISCELLANEOUS UTILITIES	6.663316583	1.576889801	
LANDING GEAR SYSTEM	6.653317304	1.574523448	
EJECTION SEAT EQUIPMENT	5.646869984	1.336345283	
PERSONNEL EQUIPMENT	4.6875	1.109308083	
OXYGEN SYSTEM	4.069392813	0.963031539	
EXPLOSIVE DEVICES	3.249307479	0.768956384	
SOFTWARE	2.260143198	0.534868292	
LIGHTING SYSTEM	2.15819209	0.510741318	
TOTAL	422.5606557	100	

Figure B2.4 MTTR for Aircraft (P)

Appendix C

Interactive Vulnerability Assessment

C.1 Introduction

This appendix explains in some detail the interactive solid modelling part and the vulnerability assessment methodology. This appendix can be divided into two parts. The first part contains the modelling process and the second part illustrates the vulnerability analysis with an example.

C.2 Interactive Solid Modelling

The interactive modelling program of a designed aircraft is presented. The solid modeller call functions link with the design synthesis is explained. Because of the thesis size limitation, only components with specific modelling techniques will be presented. For each component a brief description of the modelling methodology, list of the conceptual design variables required (CONCEPT driving parameters) and a graph of the resulting model is given.

C.2.1 Radome Part

The radome is approximated by a conical solid shape. The radome is considered to enclose the radar scanner, radar electronics box and the front avionics bay. The radome structure is approximated by a hollowed cone. A subtraction Boolean operation on two solid cones is used to generate the required shape. The radome length (cone height) and base diameter are variables to be input from the conceptual design part. The radar scanner is represented by a cylinder whose diameter and thickness is that of the radar scanner. Behind the radar scanner is the radar electronic boxes which are in reality of rectangular shapes. The electronics boxes are represented by solid boxes whose size and location are set as input variables. Fig. C.1 shows the 2D layout of the radome and its design parameters. Fig. C.2 shows the solid assembly of the radome part.

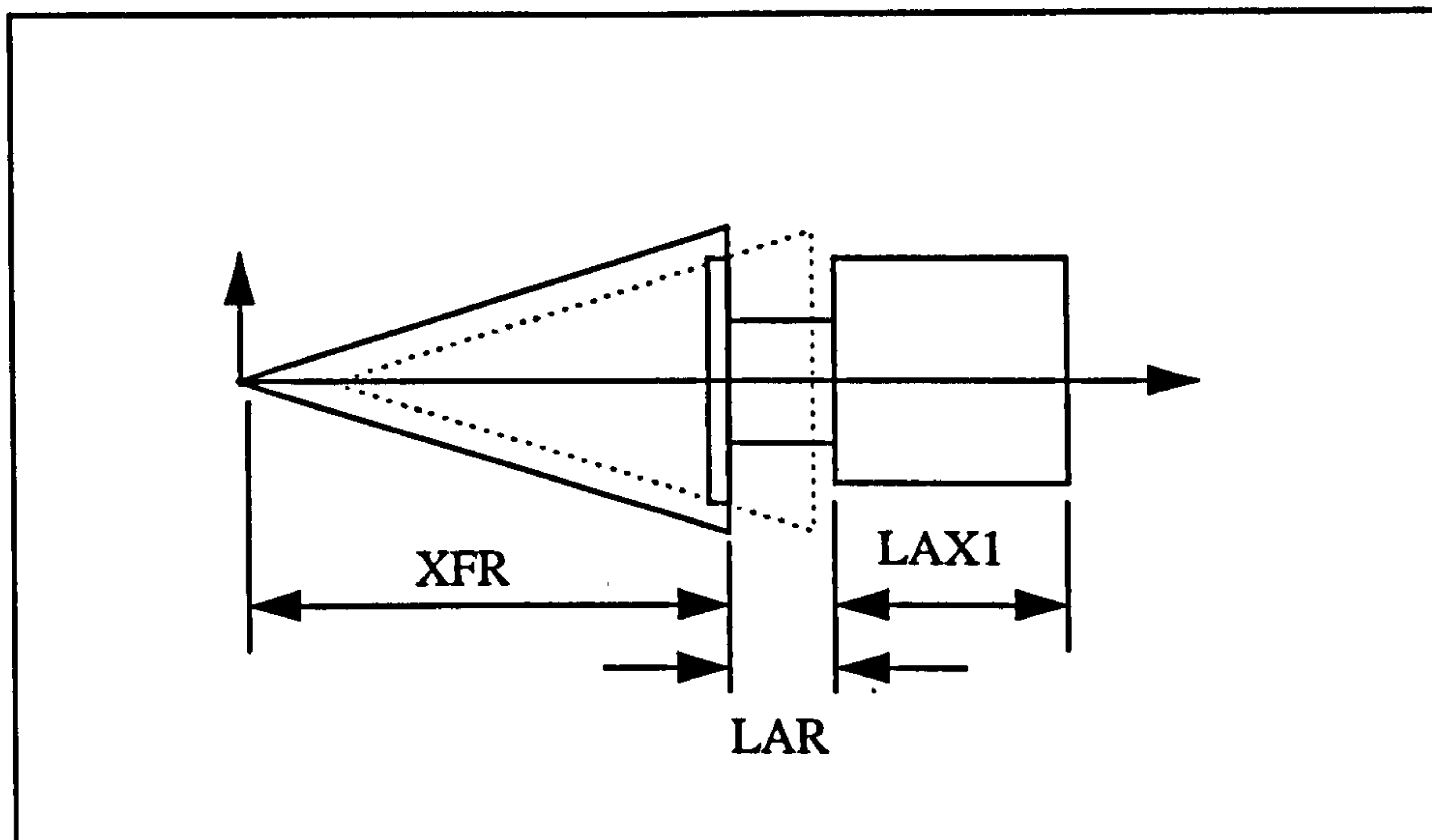


Fig. C.1 Radome modelling variables

Design Variables

DAR	Radius of the radar scanner.
EDAR	Clearance between the radar scanner and radome structure.
XFR	Radome length.
LAR	Radar avionics bay length
LAX1	Front avionics bay length

Modelling Call Sequence

The following sequence of function calls of Parasolid solid modeller is used to create the radome shell solid model.

- *CALL CRCOSO(CEN_VEC,DIR_VEC,RAD,RAD0,HGH,RADOME1,IFAIL)*

A solid cone called *RADOME1* is created at the point *CEN_VEC*(*x,y,z*) with base radius of *RAD* and height *HGH*.

- *CALL CRCOSO(CEN_VEC,DIR_VEC,RAD,RAD0,HGH,RADOME2,IFAIL)*

Another solid cone called *RADOME2* is created.

- *CALL SUBBYS(RADOME1,RADOME2,RADOME3,NBODS,IFAIL)*

Boolean subtraction of *RADOME2* from *RADOME1* gives an assembly *RADOME3* of solid bodies of *NBODS* numbers.

- *CALL IDCOEN(RADOME3,TYTOBY,TBYLI,NBODS,IFAIL)*

This function identifies entities of type *TYTOBY* (solid entities) in the assembly *RADOME3*. The function returns a list *TBYLI* containing *NBODS* number of entities.

- *CALL GTTGLI(TBYLI,POS,NITMS,LBODY,IFAIL)*

This function extracts a list of *NITMS* objects from the list *TBYLI* starting with position *POS* and puts them in the tag list *LBODY*.

- *RADOME=LBODY(1)*

Since only one body is created from subtracting the two cones of Fig. C.1, only one solid object is found in *LBODY* tag list which is placed at the first storage array address. The tag name *RADOME* is given to the resulting conical shell body.

Modelling Parameters

<i>RAD_REFX</i>	X-reference point of the radar scanner
<i>RAD_REFZ</i>	Z-reference point of the radar scanner

Tag Names

<i>RADOME</i>	Radome outer structure
<i>DISH</i>	Radar scanner
<i>RAD_BOX</i>	Radome electronics box
<i>AVN_BOX</i>	Avionics electronics box

C.2.2 Crew

Crew members are of the critical components in the aircraft which has to be protected. The pilot body is modelled using Boolean union set of operations on simple primitive shapes. Dimensions of standard crew size is used to create the simple shapes which are representing parts of the pilot's body. The pilot's body is considered to be assembled from eleven shapes as follows. The head is approximated by a solid sphere, neck by a solid cylinder, torso by a solid box and eight leg and arm parts are approximated as solid cylinders. The reference point of the solid pilot body is selected to be the head center as it represent the eye reference point of the pilot to give the standard visual clearance. The modelling of the pilot's body starts with the head and the rest of the parts are created according to the head's reference point.

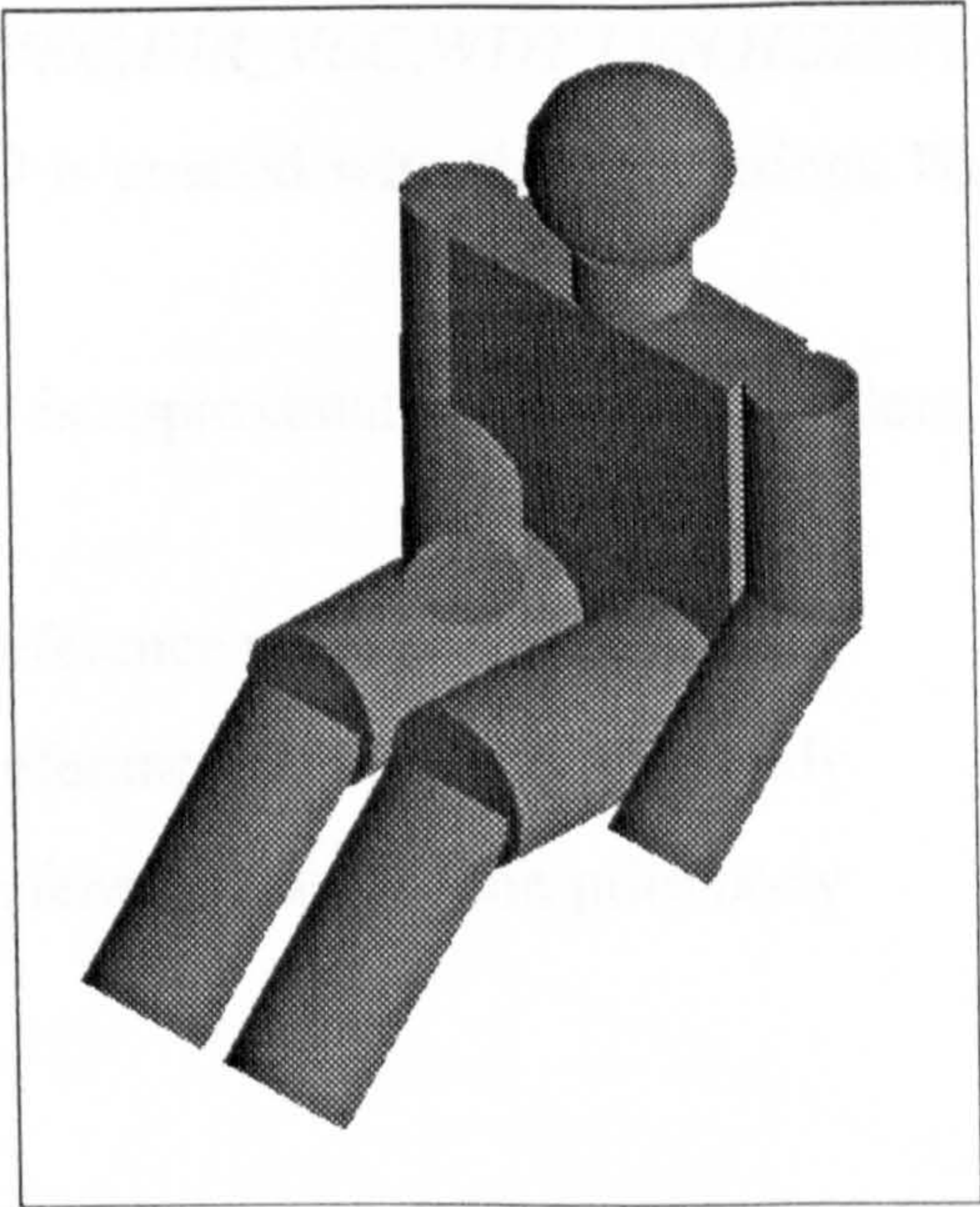


Fig. C.2 Solid model of the pilot

Design Variables

HEAD_RAD	Pilots head radius
NEC_RAD	Neck radius
NEC_HGH	Neck height
CHEST_WDT	Chest width
CHEST_HGH	Chest height
CHEST_LEN	Chest length
ARM_LEN	Arm length
FAC_LEN	Calf length
FAC_RAD	Calf radius
SAG_LEN	Thigh length
SAG_RAD	Thigh radius

Modelling Sequence

- *CALL CRSPSO(CEN_VEC,RAD,HEAD,IFAIL)*

A solid sphere called *HEAD* of radius *RAD* is created at the position *CEN_VEC*.

- *CALL CRCYSO(CEN_VEC,DIR_VEC,RAD,HGH,NEC,IFAIL)*

A solid cylinder called *NEC* of height *HGH* and radius *RAD* is created at the position *CEN_VEC*.

- *CALL CRBXSO(CEN_VEC,DIR_VEC,WDT,LEN,HGH,TORSO,IFAIL)*

A solid box called *TORSO* is created with the dimensions *WDT,LEN,HGH* at the point *CEN_VEC*.

The rest of the pilot's body is approximated by solid cylinders.

Modelling Parameters

PILOT_REFX	X-reference point of the pilot body
PILOT_REFY	Y-reference point of the pilot body
PILOT_REFZ	Z-reference point of the pilot body

Tag Names

HEAD	Pilots head
NEC	Neck
CHEST	Chest
ARM_RHT	Right arm
ARM_LFT	Left arm
FOR_RHT	Left fore arm
FOR_LFT	Right fore arm
SAG_RHT	Right Thigh
SAG_LFT	Left Thigh
FAC_RHT	Right calf
FAC_LFT	Left calf

C.2.3 Wing

The wing structure of most combat aircraft consists of a number of spars along the wing span ribs and the skin structure. The critical components in the wing are the wing spars, control surfaces (ailerons and flaps) and the fuel and hydraulic lines, Fig. C.3. The modeller first creates a solid planform of the nett-wing then places its critical components inside its structure. A solid modelling subroutine creates trapezoidal planforms to be used for modelling the flying surfaces as well other components such as fuel tanks. The spars are modelled as solid boxes whose size are similar of typical combat aircraft

structures. The number of spars per wing can be set as a design parameter. The spars are distributed at equal distances along the wing-root and wing tip.

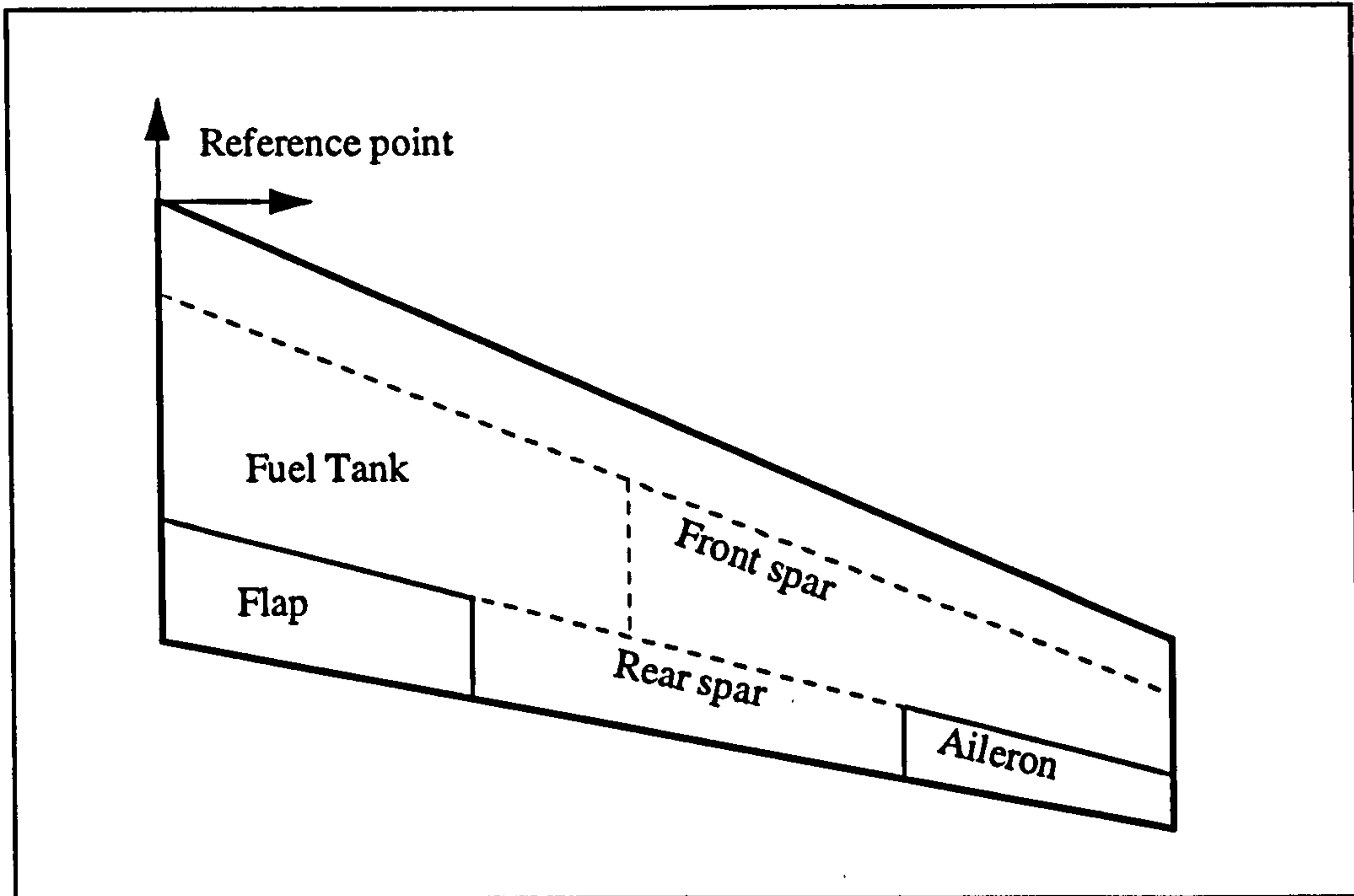


Fig. C.3 Wing nomenclature

Once the wing shape is defined (wing-span, leading-edge angle and taper ratio) the distribution of the selected number of spars is automatically modelled. The reference point of the wing sub-assembly is chosen to be at the leading-edge point at the wing-root junction. The algorithms of the nett-wing of CONCEPT is modified in order to give an expression of the reference point and the dimensions of wing-related components required by the modeller. As defined by CONCEPT, the independent variable $RXWCQM$ defines the position of the mean quarter chord point of the wing from the aircraft nose, as a fraction of the overall fuselage length XFN ,

$$XWCQM = RXWCQM \cdot XFN \quad (C.1)$$

The X-Reference point of the net wing is given by:

$$WNG_REFX = XWXQM - \left(\frac{1}{4} CWMG + XQNWLE \right) \quad (C.2)$$

Where $XQNWLE$ is the distance from the wing leading-edge at the mean quarter chord point and the net-wing root point, Figure C.4, and it is given by:

$$XQNWLE = \frac{0.5BWN \cdot (CWCB - CWMG)}{CWCB(1 - UWCN)} \tan(QWL) \quad (C.3)$$

The Y-Reference point is the half the body width at the wing root.

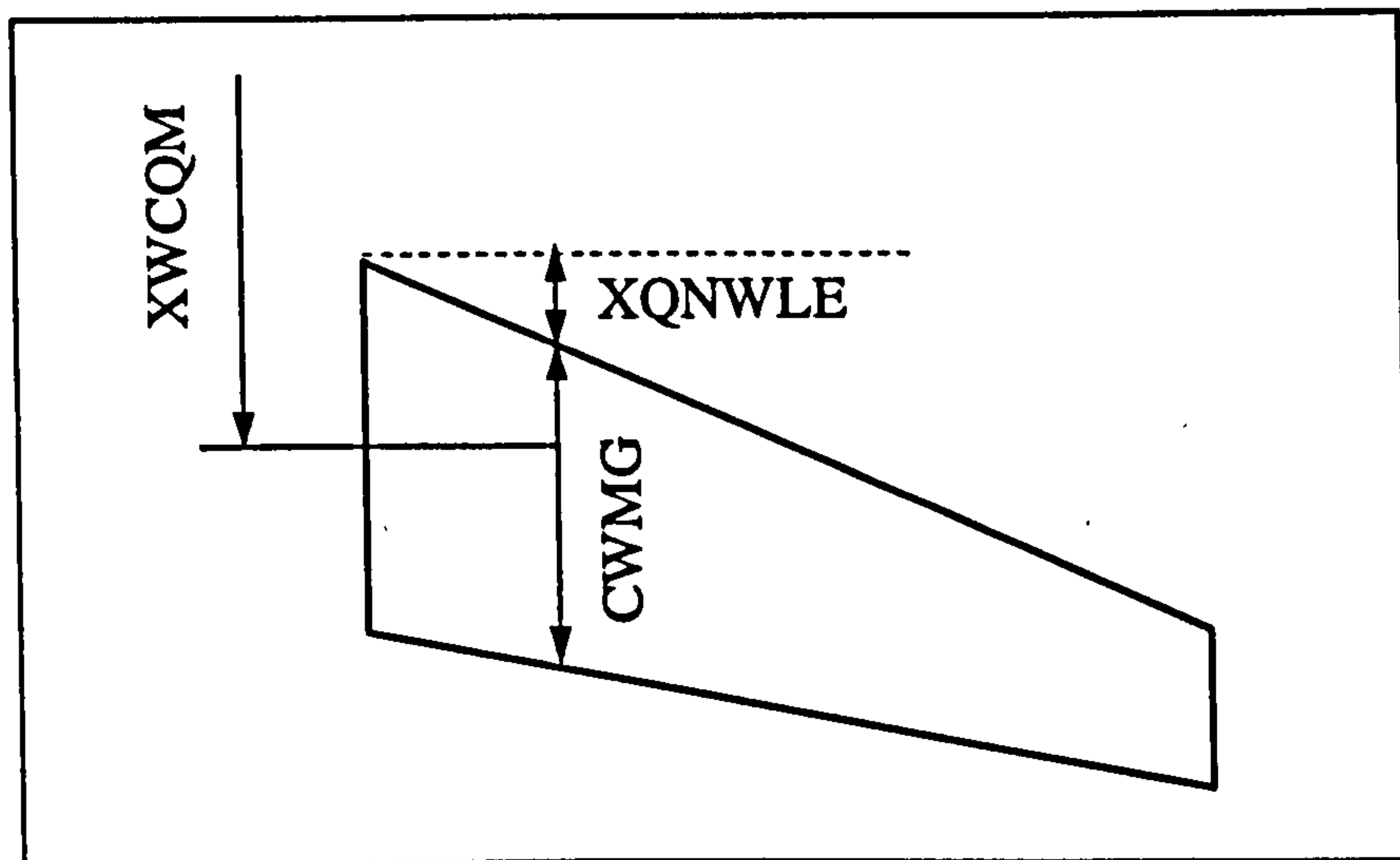


Figure C.4 Net-wing reference points

Modelling the Call Sequence

The following modelling procedure is conducted to create a trapezoidal solid shape.

- CALL

TRAPZ(CEN_VEC,LAMBDA,CROOT,LENGTH,THICK,GAMA,WR_PLAT)

This Call function calls the TRAPZ subroutine. which in tern creates a solid trapezoidal shape at the a point in space defined by the vector CEN_VEC . Given the following inputs (available from CONCEPT)

$LAMBDA$	Nett-wing taper ratio.
$CROOT$	Nett-wing taper ratio.
$LENGTH$	Nett-wing span
$THICK$	Nett-wing average thickness.

GAMA Wing leading-edge sweep

WR_PLAT The tag-name of the created solid trapezoidal shape.

The modelling of a solid trapezoidal shape is done by a series of Boolean and translation operations on a three solid shape as shown in Fig. C.5. The length and width and thickness of the middle box is similar to the trapezoidal shape to be modelled. The two other boxes are rotated according to the leading and trailing angles then used to subtract the intersected area from the middle one to get the required shape.

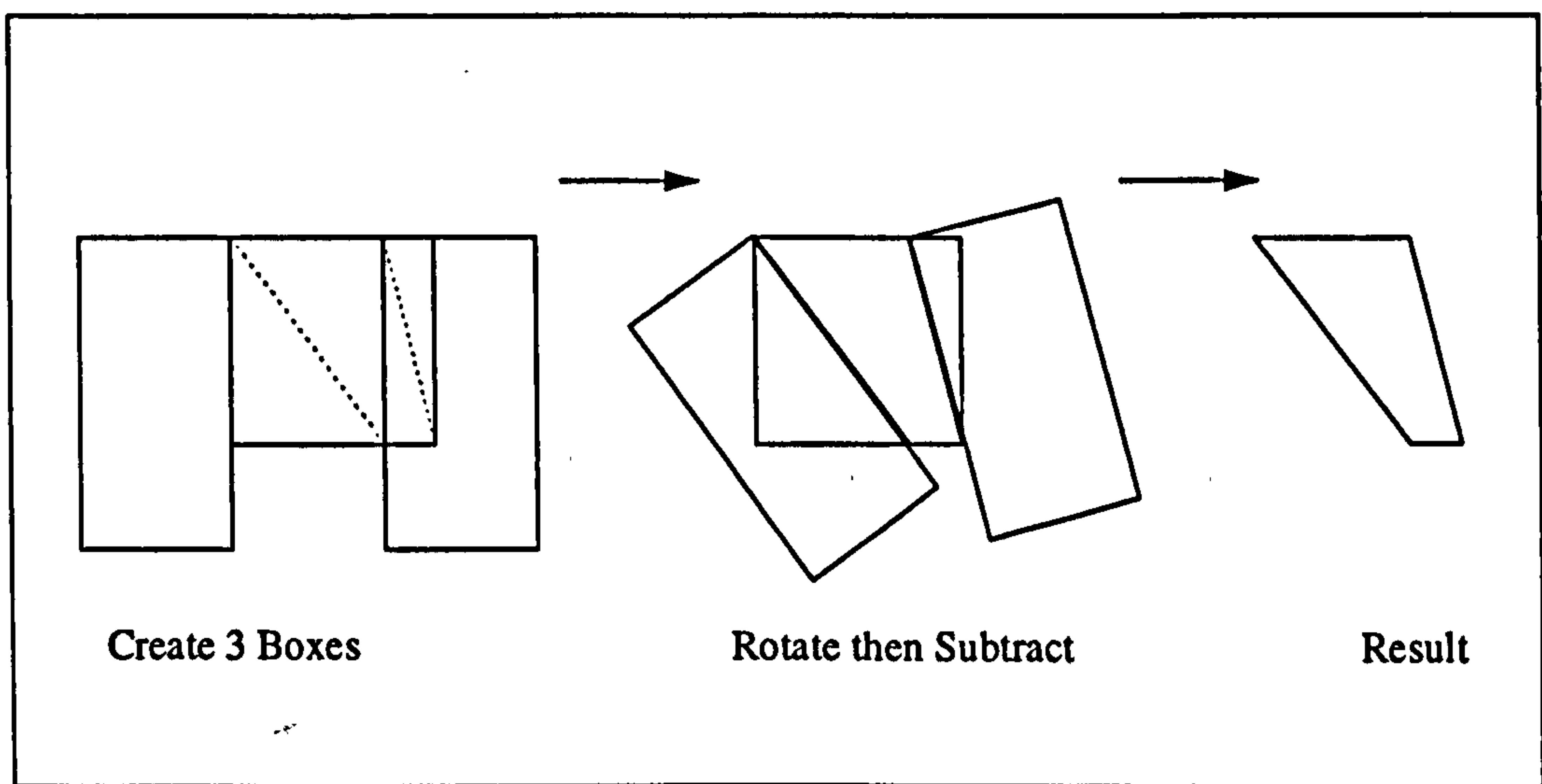


Fig. C.5 Modelling process of a trapezoidal solid shape

Control Surfaces:

The control surfaces in the wing-part are the ailerons and flaps. They are modelled the same way as the wing. Again the location control-surfaces is not very well defined in (Ref. 1). For the ailerons, the X-Reference point, Fig. C.6, is given by:

$$AIL_REFX = WNG_REFX + X1 + X2 - CRA \quad (C.4)$$

Where CRA is the aileron root chord and X1 and X2 are given by:

$$X1 = CWCB + \frac{CWCB \cdot UWCN - CWCB}{0.5BWN} (0.5BWN - 0.5BWA) \quad (C.5)$$

$$X2 = (0.5BWN - 0.5BWA) \tan(QWL) \quad (C.6)$$

The Y-Reference point is given by:

$$AIL_REFY = WNG_REFY + (0.5BWN - 0.5BWA) \quad (C.7)$$

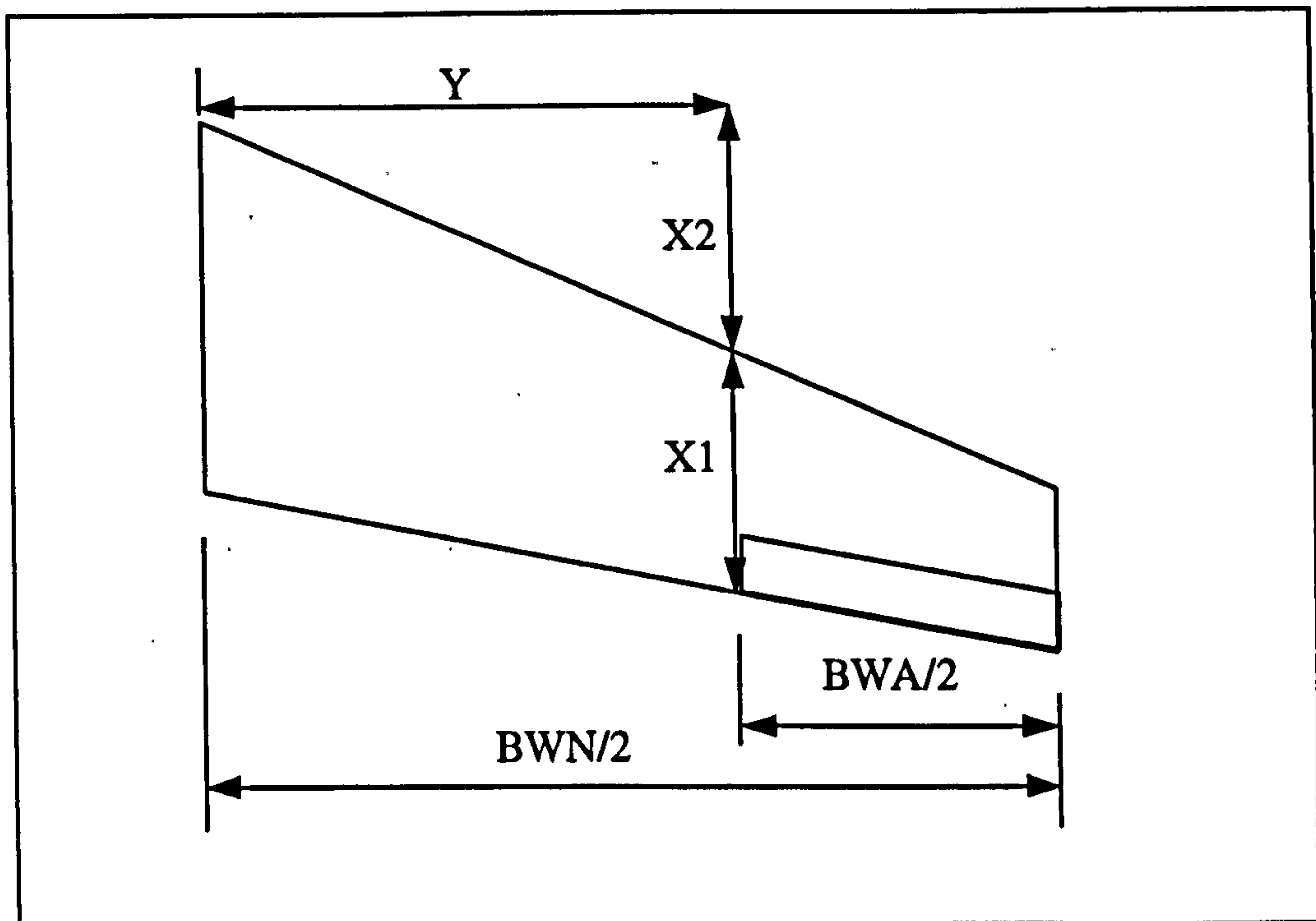


Fig. C.6 Aileron Reference Points

For the flaps, the inboard-edge of the flap coincides with the aircraft centreline. Hence,

$$FLP_REFY = 0.0 \quad (C.8)$$

and the X-Reference point is given by:

$$FLP_REFX = WNG_REFX - 0.5BWDT \cdot \tan(QWL) + CWCC - CRF \quad (C.9)$$

Where CRF is the flap root chord.

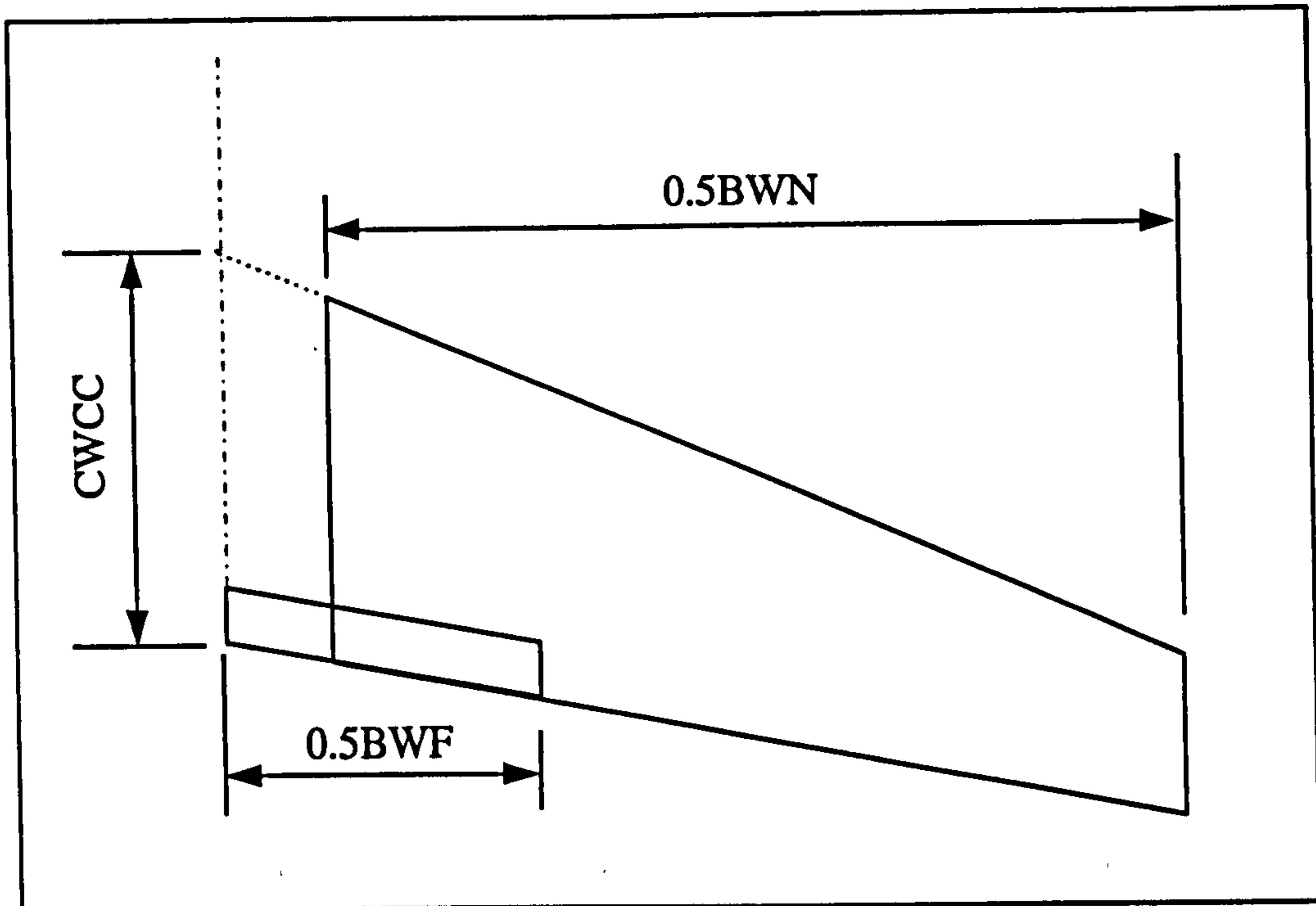


Fig. C.7 Flap Reference points

Design Variables

B2N	Net wing semi span
C_R	Wing chord at the root
GAMA	Wing leading-edge angle
TAP	Wing taper ratio
NSPAR	Number of wing spars
BWDT	Fuselage width at the wing section
WNG_REFX	X-reference point of the wing platform
WNG_REFY	Y-reference point of the wing platform
WNG_REFZ	Z-reference point of the wing platform
FLP_CEN	Flap location along the rear spar
FLP_LEN	Flap length
FLP_CRD	Flap chord
AIL_CEN	Aileron location along the rear spar
AIL_LEN	Aileron length
AIL_CRD	Aileron chord

Tag Names

SPARR(i)	<i>i</i> th spar at the right wing
SPARL(i)	<i>i</i> th spar at the left wing
FLPR	Right wing flap
FLPL	Left wing flap
AILR	Right wing Aileron
AILL	Left wing Aileron

C.2.4 Fuselage

The lofting CAD process was used to model the aircraft fuselage. This process creates a smooth aircraft fuselage solid shape by specially lofting the fuselage sections defined in CONCEPT. Each fuselage section, defined in Fig. A.2, is segmented into eight-curves. For circular cross-sections, such as fuselage section R and section E of a single-engine aircraft, the circle is divided into segments that are 45 degrees circular-arc. For a semi-rectangular curve, the eight-curves consist of four quarter circles at the corners and four straight-line curve segments at the four sides, Fig. C.8. The lofted curve segments are then used in a series of CAD techniques to create a wire-frame body. Another series of CAD solid techniques are then applied to the wireframe body to converted it into a solid one, Fig. C.9 shows a wireframe and a solid model of a lofted fuselage section. A subroutine called LOFT is developed which is used to create the fuselage body and the intake(s). The lofting Parasolid routine alone consists of around 1000 lines of FORTRAN code. The dimensions of each fuselage cross-section are defined by CONCEPT.

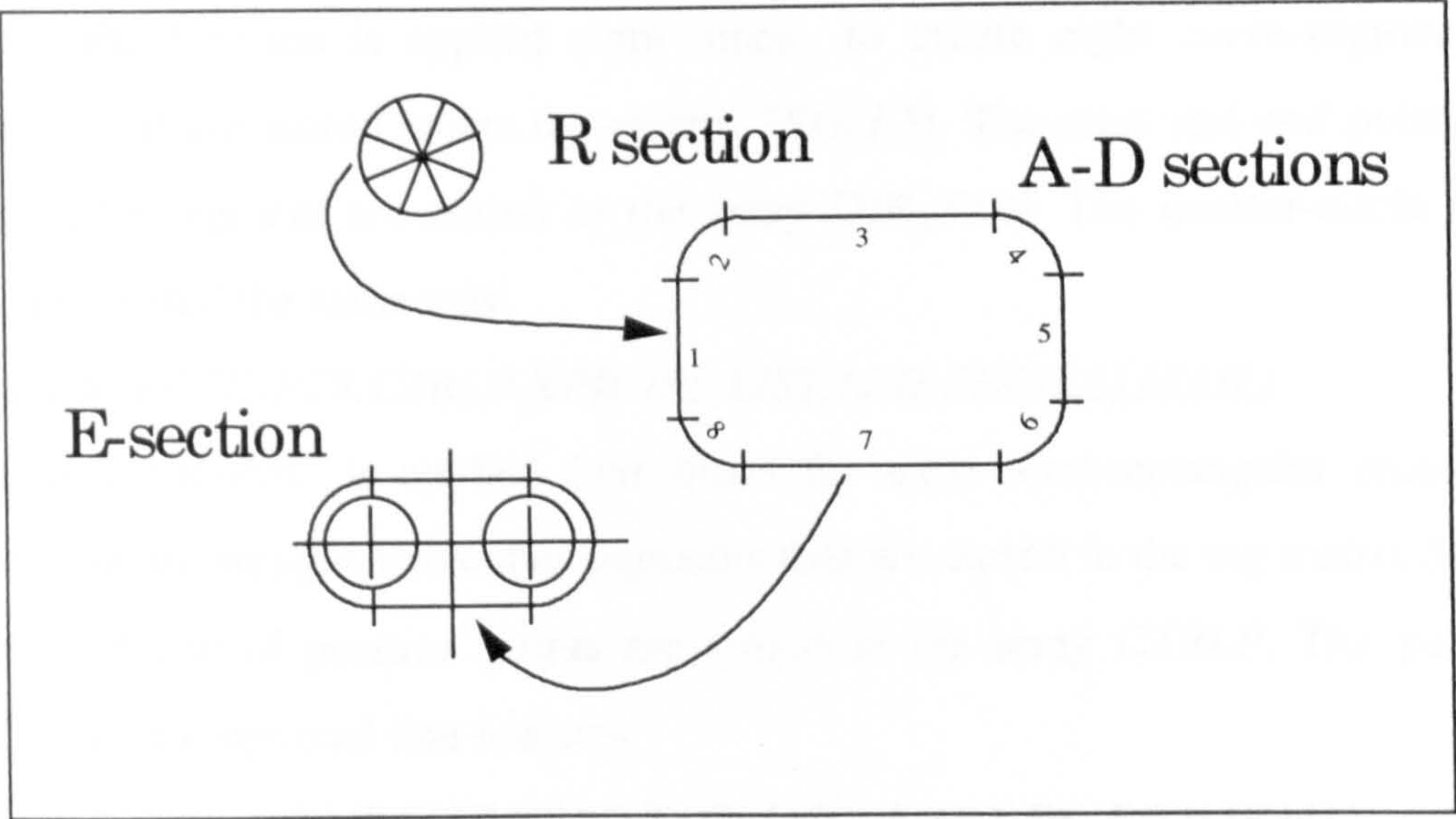


Fig. C.8 Lofted fuselage cross-section's curve segments

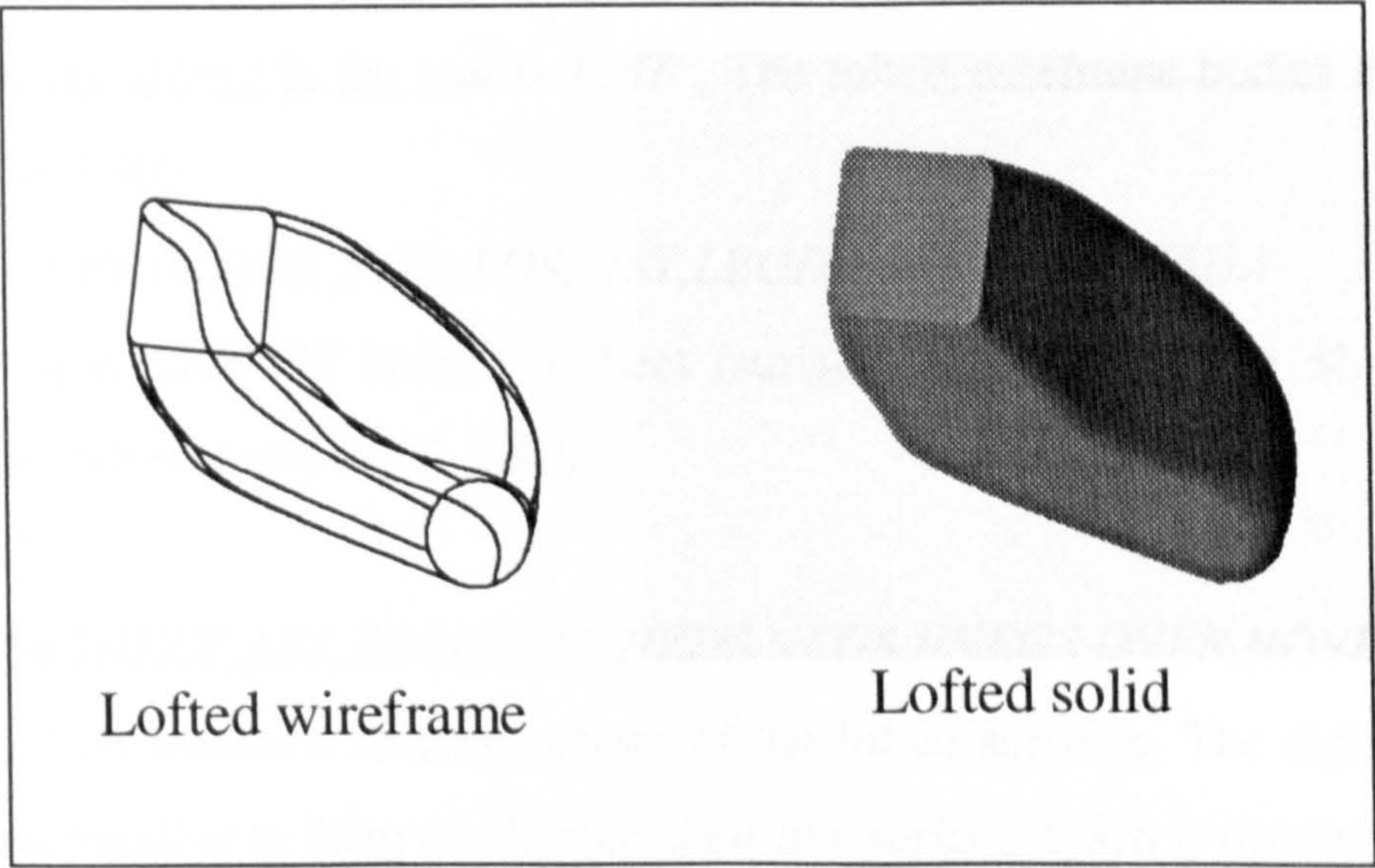


Fig. C.9 Wireframe and solid lofted fuselage shape.

Modelling Sequence

The following Parasolid's Function-Calls are used to generate a lofted solid fuselage.

- *CALL CRCICU(CEN_VEC,DIR_VEC,RAD,RSEC_CIR,IFAIL)*

This *CRCICU* function create a 3D line-circle called *RSEC_CIR* at the point defined by the array *CEN_VEC* and direction defined by the array *DIR_VEC* with radius equals to *RAD*. This circle is created to be matching the contour of the radar section.

- *CALL CRCUPC(RSEC_CIR,DIR_POS,SEG(1,I),NITMS,IFAIL)*

The *CRCUPC* function is applied eight times to create eight curve-segments from *RSEC_CIR* that are stored in the tag-matrix *SEG(I,I)*. The start and end points of the required curve segment are stored in the array *DIR_POS*. The quarter-circle fuselage corners are created the same way.

- *CALL CRSPPC(NPTS,CTRLP,NPROPS,LIST,LIST,SEG(I,I),IFAIL)*

The function *CRSPPC* is applied four times for each semi-rectangular cross-section shape to generate straight-line curve segments that are stored in the tag matrix *SEG(I,I)*. The start and end of position points are stored in the array *CTRLP*. The parameters *LIST,LIST* are for optional line features.

- *CALL CRLFPS(NITMS,LIST,NPRP,TAG_LST,LBODY,BS_FS(I),IFAIL)*

The function *CRLFPS* creates eight-lofted wireframe bodies by lofting each curve segment with its counter one along the fuselage length. The tag names of the curve segments are stored in the matrix *LIST*. The lofted wireframe bodies are stored in the matrix *BS_FS(I)*.

- *CALL CRBYGE(BS_FS(I),POS,LIST,LBODY,SHT_FS(I),IFAIL)*

The function *CRBYGE* creates a sheet (surface) body from each of the eight lofted wireframe bodies stored in *BS_FS(I)*.

- *CALL*

CRKNPA(SHEET_LST,EDS1,EDS2,NEDS,NEGS,NNEGS,OVER,NOVER,IFAIL)

This function creates a knitting pattern of the lofted surfaces. The eight lofted surfaces are joined together to form a hollowed shell-like surface which is opened from both ends. The surfaces to closed the two ends are then created to form a closed surface lofted body. The eight lofted surface segments are stored in the matrix *SHEET_LST*.

Design Variables

<i>RSEC_REFX,Y,Z</i>	X,Y,Z reference point of section R
<i>ASEC_REFX,Y,Z</i>	X,Y,Z reference point of section R
<i>BSEC_REFX,Y,Z</i>	X,Y,Z reference point of section R
<i>CSEC_REFX,Y,Z</i>	X,Y,Z reference point of section R
<i>DSEC_REFX,Y,Z</i>	X,Y,Z reference point of section R
<i>ESEC_REFX,Y,X</i>	X,Y,Z reference point of section R

C.2.5 Landing Gear

A landing gear assembly is assumed to be composed of three parts, tire, tire hub and the gear main leg as shown in Fig. C.10

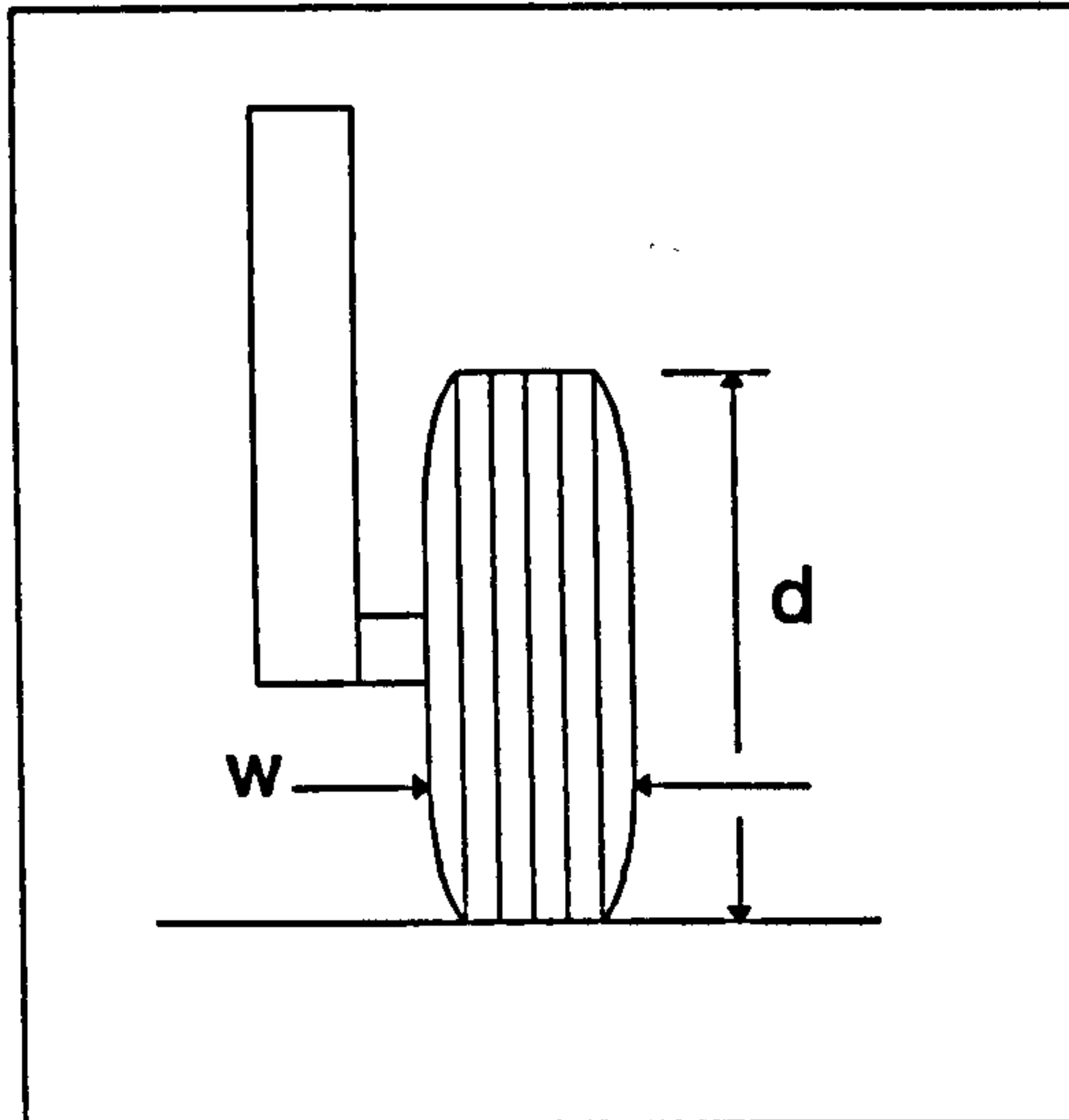


Fig. C.10 Landing-gear assembly

The tire is modelled as a solid torus, the tire hub and leg are modelled as solid cylinders. The landing gear is assembled of these three parts. The reference point lies at the top of the landing gear leg. The dimensions of the landing gear parts are all supplied by CONCEPT.

Modelling Sequence

- *CALL CRCYSO(CEN_VEC,DIR_VEC,RAD,HGH,LEG1R,IFAIL)*

A solid cylinder called *LEG1R* is created at the point defined by the array *CEN_VEC* with the direction defined by the array *DIR_VEC*. The *LEG1R* is the tag name of the right main leg.

- *CALL CRCYSO(CEN_VEC,DIR_VEC,RAD,HGH,LEG2R,IFAIL)*

A solid cylinder called *LEG2R* is created at the point defined by the array *CEN_VEC* with the direction defined by the array *DIR_VEC*. The *LEG1R* is the tag name of the right main leg shaft.

- *CALL CRTOSO(CEN_VEC,DIR_VEC,RAD,RAD0,TIRER,IFAIL)*

A solid torus called *TIRER* is created at the position and direction defined by the arrays *CEN_VEC* and *DIR_VEC* respectively. The *RAD* and *RAD0* defines the radius and width of the wheel.

- *CALL CRCYSO(CEN_VEC,DIR_VEC,RAD,HGH,HUBR,IFAIL)*

A cylinder solid called *HUBR* is created at the position and direction defined by the arrays *CEN_VEC* and *DIR_VEC*. The *HUBR* represents the tire hub of the right main gear.

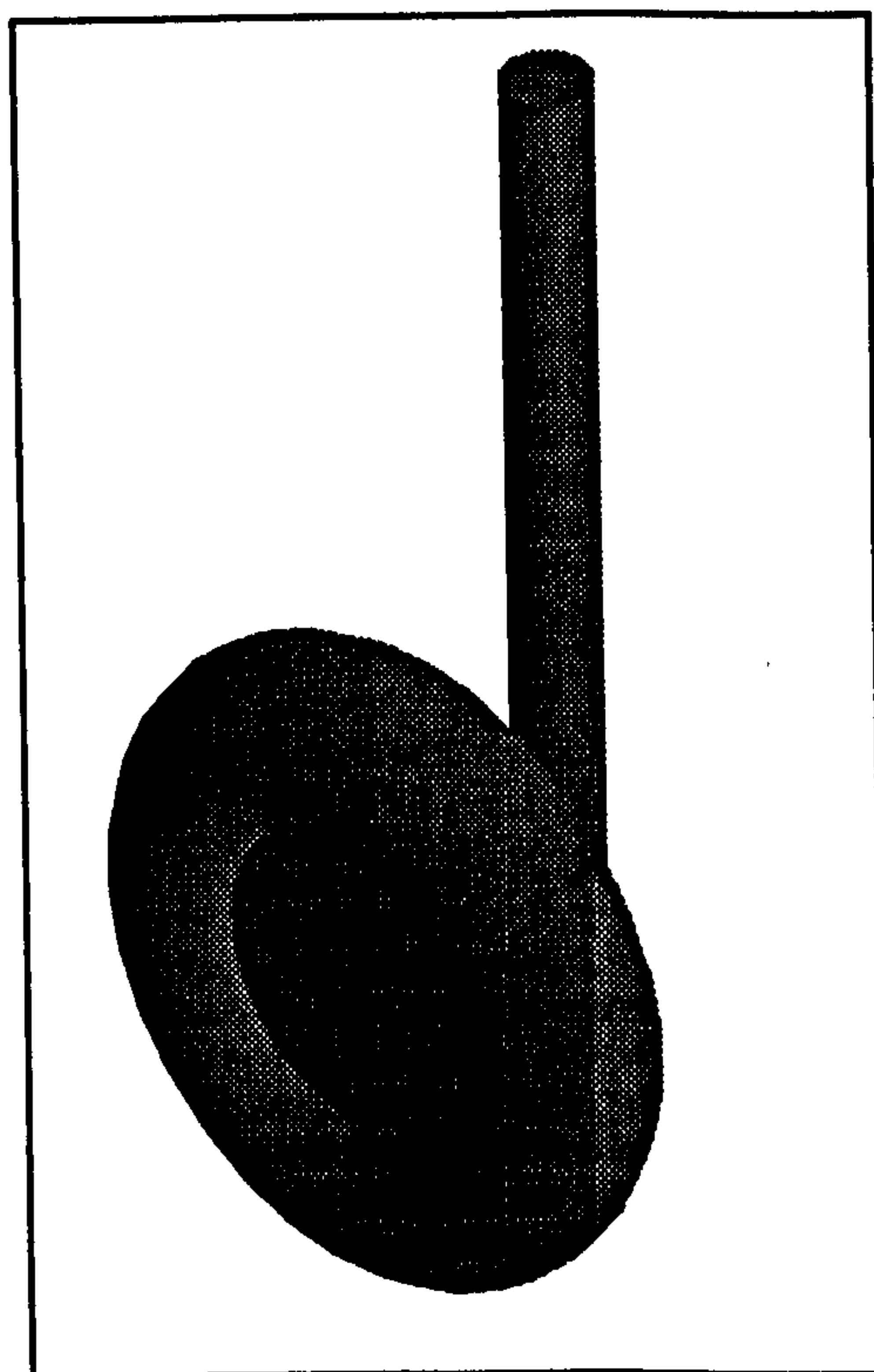


Fig. C.11 Landing-gear solid model

C.2.6 Engine

The engine is modelled using Boolean operations on solid cylinders and cones. The engine is set to be composed of four main parts depending on the part vulnerability. The wireframe picture of the engine shown in Fig. explains the Modelling effort used to create the solid model of the engine which is shown in the same figure. The engine dimensions are again given by the CONCEPT module. The engine reference point is set at the center of the engine circular face.

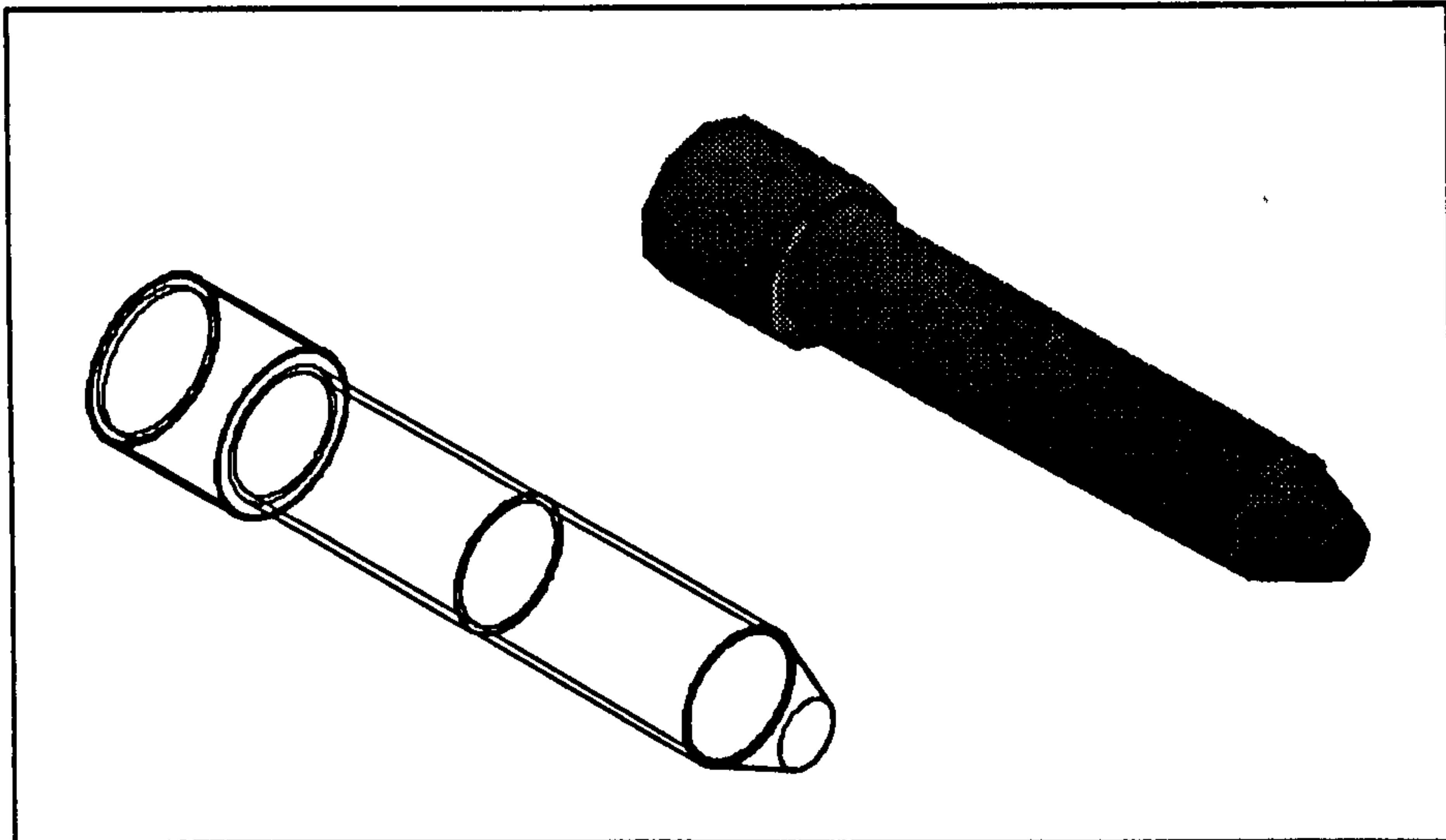


Fig. C.12 Wireframe and solid models of an engine

C.2.7 Aircraft Systems

Having defined major aircraft structural systems and hence defining the internal volume left for aircraft systems, the next step is model the aircraft systems/subsystems which are essential to conduct vulnerability/survivability analysis and assessment. Normally the layout of aircraft systems is conducted at the detail design phase. Exceptions are for the major components which affect the whole aircraft layout such as fuel tanks. The systems chosen for modelling are those which are defined or developed at the conceptual/preliminary design phase. The methodology used to model aircraft systems/subsystems is to:-

- Establish a logic/experience link between the preliminary/conceptual phase and the detail design phase. Such as the location and size of control surfaces actuators and the size and location of these surfaces.
- Make the reference point (location) of these subsystems according to the major systems defined in the conceptual design phase, on which these subsystems are linked with. An example is the accessory gear box and the engine.
- Make it possible for the user do add more systems/subsystems to the whole assembly by common objects such as solid boxes or cylinders to represent another hydraulic bay.

Hydraulic System

The hydraulic system architecture depends on many design factors. The number of engines is a major factor which influences the hydraulic system layout. Following the modelling methodology explained above, modelling of hydraulic system components/subcomponents starts from the engine itself. The following components are modelled:

1. Engine mounted gearbox

The gearbox is usually mounted beneath the jet engine. It is modelled as a solid box. The location (reference point) and size of the box is set to be design variable.

2. Hydraulic pump

The hydraulic system will contain one or more hydraulic pumps, depending on the type of aircraft and the conclusion reached after safety, reliability and survivability requirements. The pump is normally mounted on the engine gearbox. The hydraulic pump is represented as a solid cylinder. Its location and size is set as a design variable.

4. Actuators

On military aircraft, the primary flight control actuators normally consist of two pistons in tandem on a common ram. Each piston acts within its own cylinder and is connected to a different hydraulic system. The arm is connected at a single point to control surface and the actuator itself is connected to a rigid structural member such as a wing spar.

The actuator is modelled as a combination of two cylinders (the cylinder itself and the spool) and a solid box (the actuator control valve). The location of the actuator is normally at the middle of the control surface. However the location and size are set as design variables.

5. Hydraulic lines

The hydraulic pipe layout will take into account the need to separate pipes to avoid common failures as a result of accident damage or the effect of battle damage. In the first attempt to define the layout which happens at the conceptual design phase, it is likely that the first attempt to define a layout will result in straight lines only, but this is adequate for a reasonably accurate initial calculation.

At the wing and tailplane parts, the hydraulic lines can be assumed as straight lines passing behind or inside the spars. It is difficult to define the actuator or the pipes at the fuselage. Because of the big influence of detail definitions of hydraulic lines (as well as fuel lines) a provision is to be made in the program to allow a user friendly modelling capability taking into account the already defined major parts. A collision or intersection check is to be included to check for adequate space for the modelled component.

C.3 Standard Vulnerability Assessment Techniques

The methodology used to develop a vulnerability assessment tool using the solid modelling Cad techniques is illustrated. The two assessment methodologies use the ray tracing technique as the main driver.

C.3.2 Vulnerable Area Routine

The vulnerable area of a critical component is defined as:-

The product of the presented area of the component in the plane normal to the approach direction of the damage mechanism (the shotline) and the probability of kill of the component given a hit on the component.

So in order to compute the vulnerable area of a component from a certain direction it is first required to calculate the 2D area of the 3D solid component at a given direction. The problem of projecting a three dimensional object onto a two dimensional surface has been studied by engineers, architects, and artists for centuries. Computer graphics systems also address problems related to projections. Planer geometric projections are the ones of most interest to engineers. The ray tracing technique is used to develop a methodology by which the presented 2D area of a solid modelled component can be computed. Each solid-modelled component is a set of fine polygon surfaces closing the volume of the component. An array-body intersection is actually based on vector-plane

intersection algorithms (Ref. 31). Parasolid has a general ray-tracing function which is defined as:

- *CALL RAYFIR (tag-lst,transf,no_int,point,dir,nhits,phits,fhits,bhits,ifail)*

This function takes the following variables:

<i>tag-lst</i>	Tag-matrix contains a list of bodies to fire a ray on.
<i>trans</i>	A transformation for the accuracy of the intersection.
<i>no_int</i>	Number of the intersections wanted.
<i>poin</i>	Position array defines point from which ray is fired.
<i>dir</i>	Direction array defines the ray direction.

And the functions returns

<i>nhits</i>	Number of point of intersections.
<i>phits</i>	An array contains the co-ordinates of the <i>nhits</i> points.
<i>fhits</i>	An array containing the tags of faces hit by ray.
<i>bhits</i>	An array containing the tags of bodies hit by ray.
<i>ifail</i>	Failure indicator index.

The following method was developed to calculate the presented area of a 3-D solid body from any direction. The method is illustrated in the following steps:-

1. Find the co-ordinates of the opposite corners of a rectangular box with sides parallel to X, Y, and Z that contains the solid component. This is done by calling the *ENBXEN* Parasolid function. The function will return an array containing the co-ordinates of the two opposite sides of the rectangular box ($x0,y0,z0,x1,y1,z1$) as shown in Fig. C.13

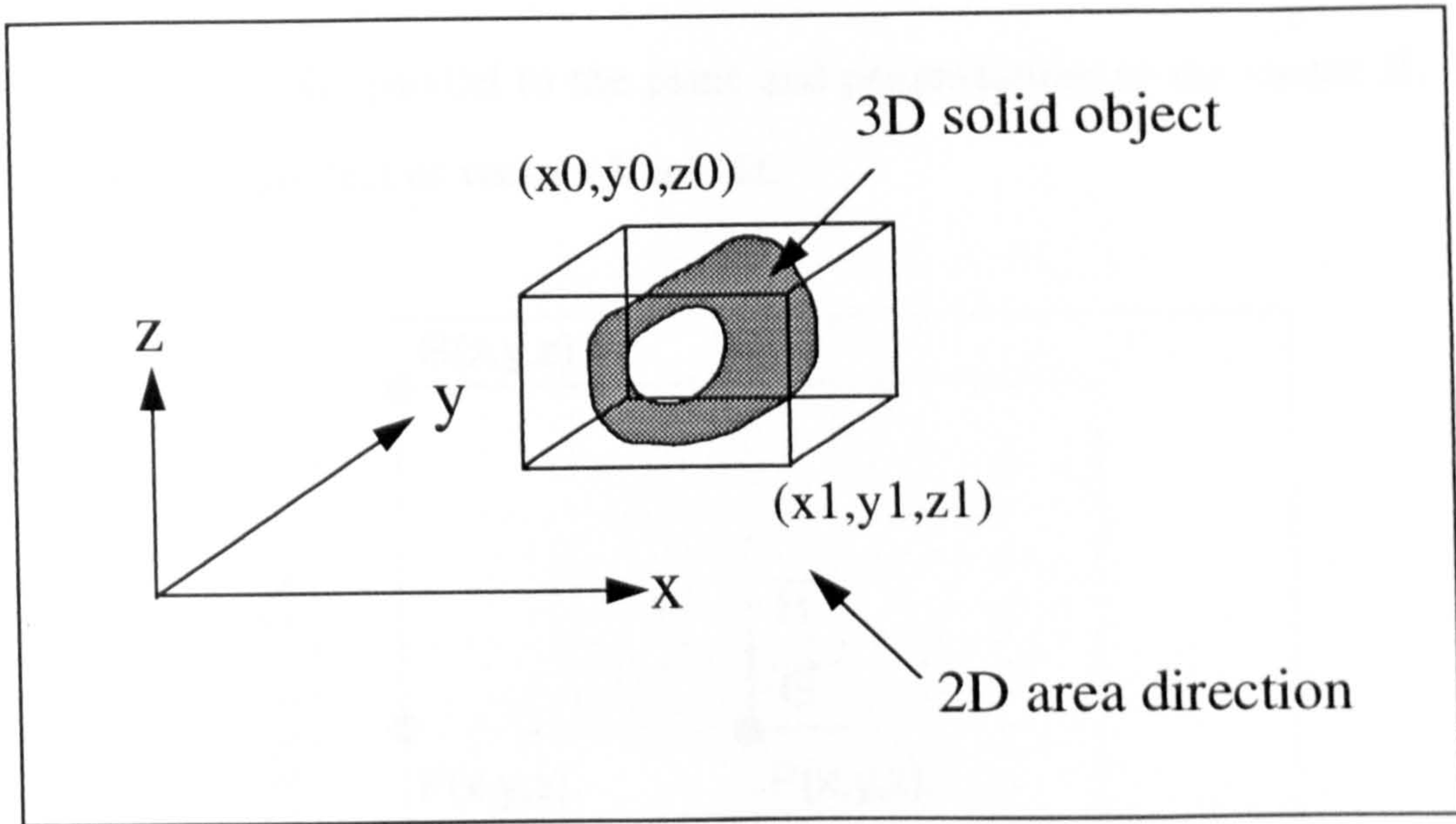


Fig. C.13 Determining the space of the object.

2. Find the co-ordinates of the point centred in the inside box space $O(x2, y2, z2)$, where:

$$\begin{aligned} x2 &= x0 + (x1 - x0) \\ y2 &= y0 + (y1 - y0) \\ z2 &= z0 + (z1 - z0) \end{aligned} \quad (C.10)$$

3. Find the co-ordinates of the start point $P(x3, y3, z3)$ of the vector $V(v1, v2, v3)$ which is parallel to the direction the presented area is to be projected on. The length of the vector is selected such that the point **P** should lie outside the body. A length $MSIDE_LEN$ equal to the maximum side lengths of the enclosed box is selected.
4. Find the equation of the plane perpendicular to the vector **V** and passing through the start point **P**. The equation is:

$$(v1)x + (v2)y + (v3)z = (v1)(x1) + (v2)(x2) + (v3)(x3) \quad (C.11)$$

5. Find another point on the plane. This could be done by finding the intersection of any of the three principle axis with the plane. A unit vector **H** is found by normalising the vector starting at point **P** and ending at the intersection of the principle axis with the plane.

6. Find a vector \mathbf{G} parallel to the plane and perpendicular to the vector \mathbf{H} . This is found by the cross product of vectors \mathbf{V} and \mathbf{H} .

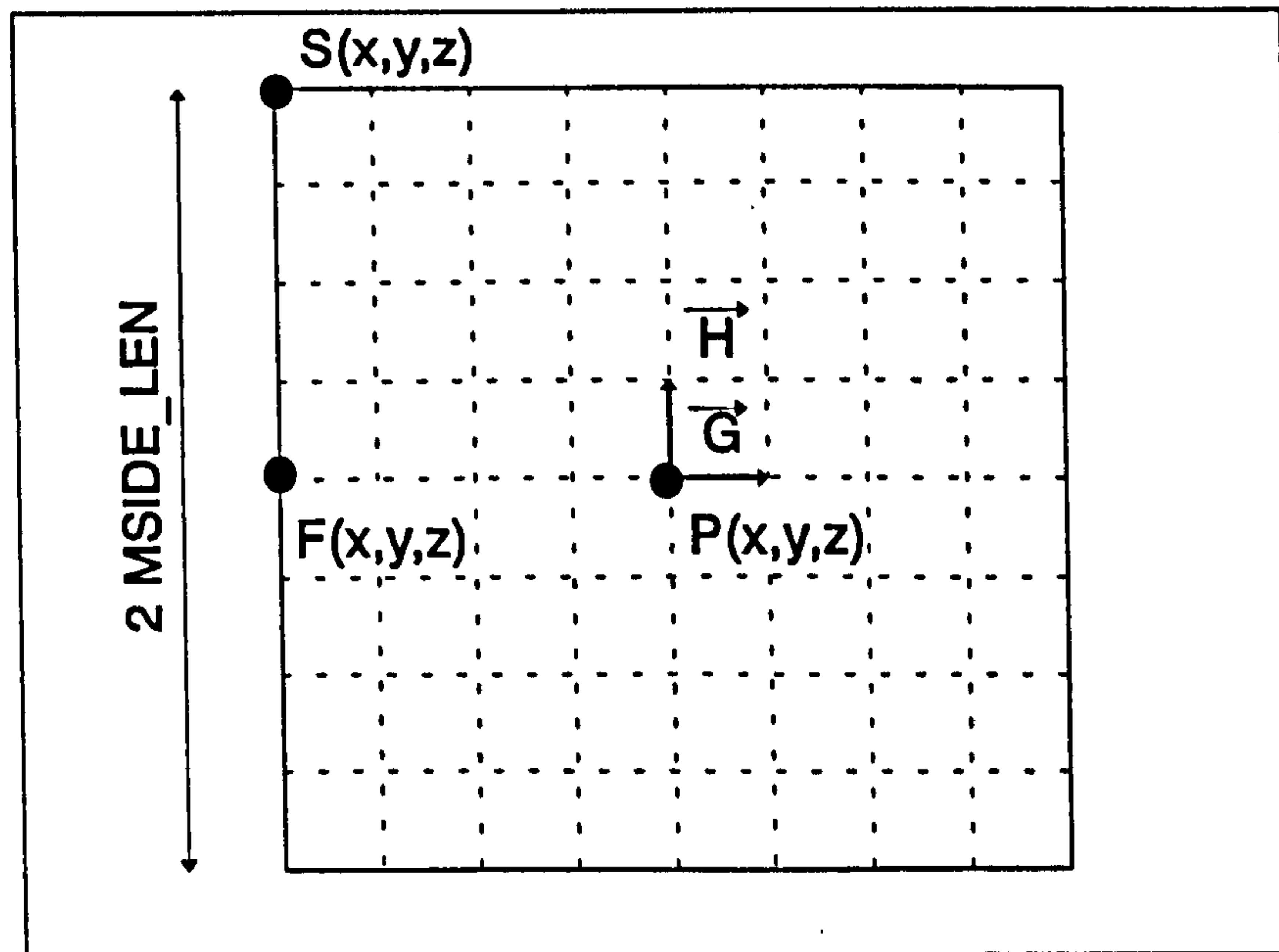


Fig. C.14 Mesh carpet over the body

7. Select a square mesh area on the plane which covers the body. The length of the mesh sides is chosen to be equal to twice of $MSIDE_LEN$. The length of each cell is DG . The edges of the mesh carpet are parallel to the unit vectors \mathbf{H} and \mathbf{G} , where point \mathbf{P} lies in the center of the mesh carpet.

8. Find the co-ordinate of the upper left node, $\mathbf{S}(x,y,z)$. This node is the start of other node co-ordinate calculation. The co-ordinates of point \mathbf{F} is given by:

$$\begin{aligned} x &= (H(1) + F(1)) \cdot MSIDE_LEN + P(1) \\ y &= (H(2) + F(2)) \cdot MSIDE_LEN + P(2) \\ z &= (H(3) + F(3)) \cdot MSIDE_LEN + P(3) \end{aligned} \tag{C.12}$$

8. Find the co-ordinates of the four node points of each cell using the two unit vectors \mathbf{H} and \mathbf{G} and the length of the cell side DG .
9. Use Parasolid function *RAYFIR* to fire rays from each node point on the carpet mesh. Each ray hitting the body returns a value of one in the integer matrix

$COUNT_MAT(GRID_NO, GRID_NO)$, where $GRID_NO$ is number of mesh nodes on the carpet mesh.

10. All the cells which have the integer one in their four corners are counted up. The 2D plane area of the 3D solid body from the direction V is the summation of these cell areas, Fig. C.15

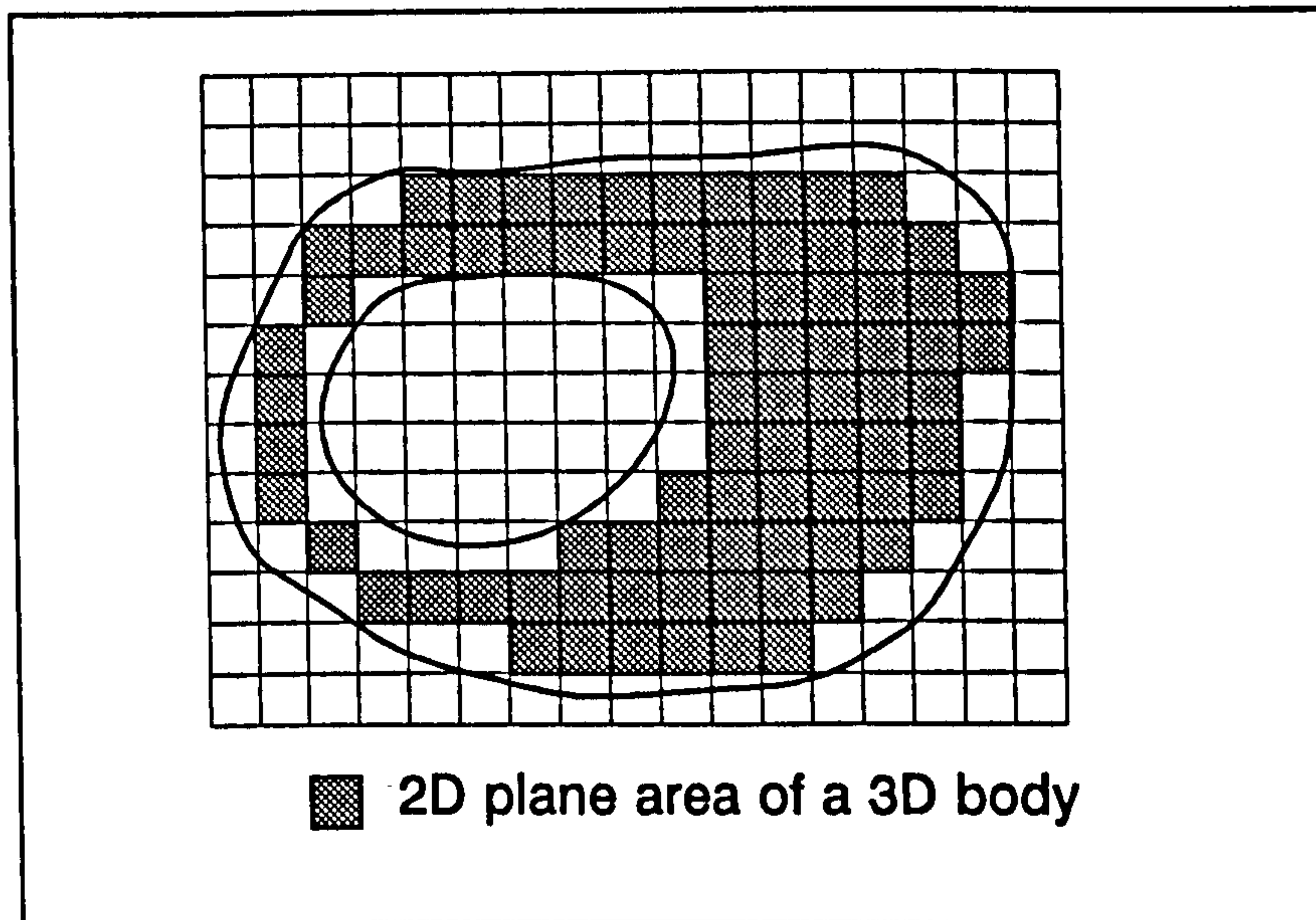


Fig. C.15 Plane Area Approximation

Fig. C.16 shows the solid model of an object test case, a torus, and the rays used to simulate the light source. Only rays that hit the body is counted, since the 2D area generated by the shade of the torus will show a light spot (not counted) generated by the opening in the center of the torus shape.

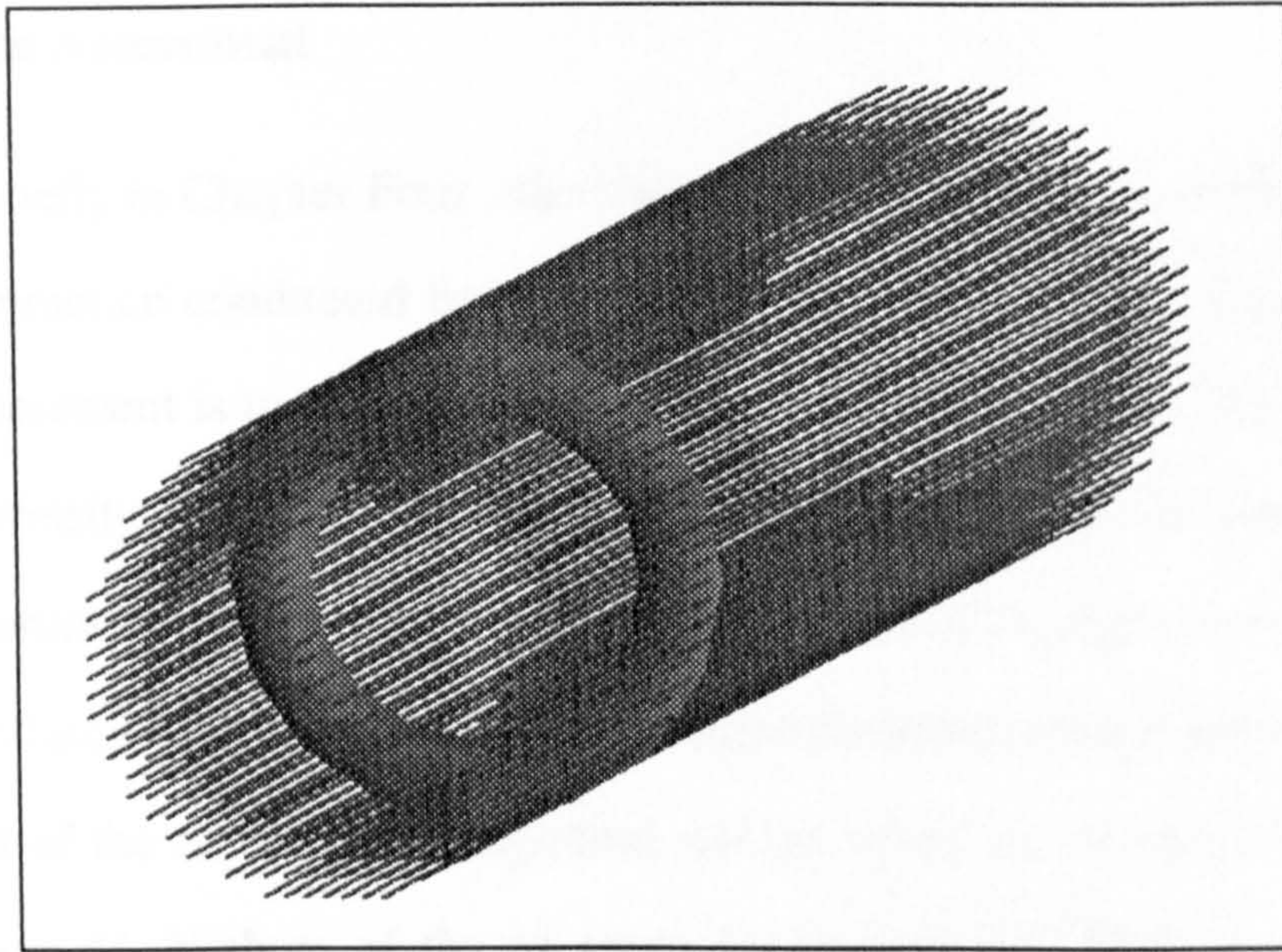


Fig. C.16 Simulating light rays to compute the 2D area of a 3D object

Fig. C.17 shows the result of a test case, An accuracy of 96% compared to the exact one is achieved using a grid of 140 rays and with a computation time of 40 seconds. This method forms a link for future studies on which the computed vulnerable area is linked with the conceptual design for tradeoff studies of internal components location and orientation.

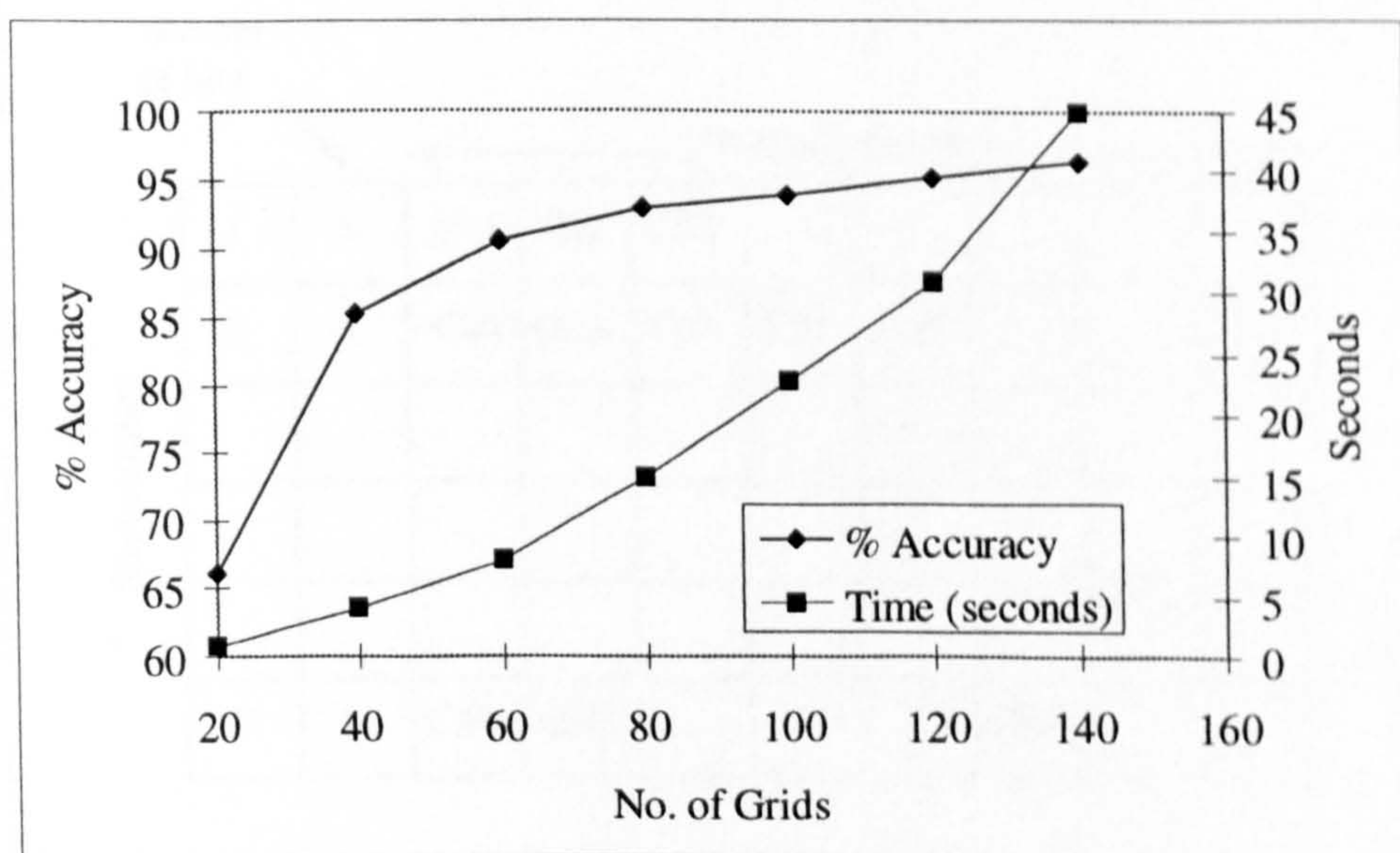


Fig. C.17 Accuracy and computation time.

C.3.3 Shotline Assessment

As discussed briefly in Chapter Four, the shotline assessment is a standard survivability / vulnerability practice conducted by survivability engineers on a designed aircraft. The aim of this assessment is to quantify an aircraft vulnerability undergoing multi-hit attack of variable intensity fragment-type threat. For the shotline assessment methodology, multi hits on aircraft body are simulated by firing a number of rays on the aircraft from a specified direction. Each ray is allowed to go through all the intersected components and to return a list of the component's tags that are hit. When an aircraft is hit by a random number of shots M , N shots of the M shots hit the aircraft. Each ray penetrating the aircraft will provide C number of components before leaving the aircraft body. The number of components that are hit by the N hits depends on the location, size and orientation of the components inside the aircraft body. and the number of the total components that has been penetrated by a single ray C depend on the threat intensity as well as the toughness of the components being hit. An integer matrix called *KILL_TAG* is created which contains a list of killed body's *TAG_NAME*. As shown by Fig. C.18,

	number of hits	components hit							
	1	3	C11	C12	C13				
	2	5	C21	C22	C23	C24	C25		
Shot number	N	h	CN1	CN2	CNh	

Fig. C.18 Kill_TAG matrix

For each row in the matrix, the first cell contains the shot number,(i.e. from 1 to N), the second cell contains the number of components that are penetrated (killed) by that shot, the rest of the cells contains an integer of the *TAG_NAME* of the components. The kill probability of the i th component given a random hit on i th aircraft $P_{k/Hi}$ is the product of the probability the component is hit (given a hit on the aircraft) $P_{h/Hi}$ and the probability the component is killed given a hit on the component $P_{k/hi}$. Thus;

$$P_{k/Hi} = P_{h/Hi} P_{k/hi} \quad (C.13)$$

The probability the component is hit given a random hit on the aircraft can be evaluated in two ways:

1. A matrix of True or False values is created. This matrix is called *KILL_ID(TAG_NAME)* for all the names (components) included in the design. When a ray hits component i , the value of the corresponding field in the *KILL_ID* is set to one, otherwise it is equal to the default value, zero (not hit yet). The multiplication of the *KILL_ID* with the *KILL_TAG* matrix gives the probability of a kill given a random hit on the aircraft. This approach is used in this study.
2. For early analysis during the conceptual design, the vulnerable area of the critical components is a measure of aircraft vulnerability. As illustrated in Chapter 3, for a random hit on the aircraft equation (D1) can be expressed as:

$$P_{k/Hi} = A_{vi} / A_P \quad (C.14)$$

Appendix D

Mission Simulation Model

Subroutines & Algorithms

D.1 Introduction

This Appendix contains the MSM FORTRAN Program and description of its subroutines. A sample of input file and program outputs and results are included. The Program was written in Standard FORTRAN 77 Language.

D.2 Variables List

Variable	Description
AC_SOR_INDX(I)	SORTIES FLOWN BY AIRCRAFT (I)
FAIL_RAT(J)	FAILURE RATE OF SYSTEM (J)
IDAY	SIMULATION DAY COUNTER
IDAY_RET_MIS(I)	RETURN FROM MISSION DAY OF AIRCRAFT (I)
IDAY_RET_MNT(I)	RETURN FROM MAINTENANCE DAY OF AIRCRAFT (I)
IFLG_AVL(I)	AVAILABILITY FLAG OF AIRCRAFT (I)
IFLG_KIL(I)	KILL FLAG OF AIRCRAFT (I)
ILG_LOC(I)	LOCATION FLAG OF AIRCRAFT (I)
IMIN	SIMULATION MINUTE COUNTER
IMIN_DAY	MINUTES PER DAY (=1440)
ISOR	SIMULATION SORTIES COUNTER
ISOR_DAY	NUMBER OF SORTIES PER DAY
MTTR(J)	MEAN TIME TO REPAIR OF SYSTEM (J)
NO_AC	NUMBER OF AIRCRAFT IN SQUADRON
NO_AC_SYS	NUMBER OF SYSTEM IN AN AIRCRAFT
NO_SOR_DAY	NUMBER OF SORTIES PER DAY
NO_SOR_FLR	CUMULATIVE FAILED SORTIES NUMBER
P_DET_AC	PROBABILITY OF DETECTION OF AN AIRCRAFT

P_KIL_AC	KILL PROBABILITY OF AIRCRAFT
P_KIL_RND	RANDOM KILL PROBABILITY FIGURE
SOR_COM	CUMULATIVE LAUNCHED SORTIES COUNTER
SOR_DAY(IDAY)	CUMULATIVE SORTIES OF DAY (IDAY)
TIM_AC(I)	CUMULATIVE FLYING TIME OF AIRCRAFT (I)
TIM_AC_SYS(I,J)	TIME ON SYSTEM (J) OF AIRCRAFT (I)
TIM_CUR	CURRENT TIME BASED ON 24-HOURS/DAY
TIM_MNT(I)	CUMULATIVE MAINTENANCE TIME OF AIRCRAFT (I)
TIM_RET_MIS(I)	RETURN FROM MISSION TIME OF AIRCRAFT (I)
TIM_RET_MNT(I)	RETURN FROM MAINTENANCE TIME OF AIRCRAFT (I)
Variable	Description
TIM_SOR_CAL(ISOR)	CALL TIME OF SORTIE (ISOR)
TIM_SYS_FAIL(I,J)	FAILURE TIME OF SYSTEM (J) OF AIRCRAFT (I)
TIM_TRN	AVERAGE TURNAROUND TIME

D.3 Subroutines

A brief description of some of the main subroutines found in the source code following:

D.3.1 SUBROUTINE MIN_HR(IMIN,TIM_CUR)

This subroutine converts minutes, *IMIN* into clock time based on 24-hours per day system, *TIM_CUR*

D.3.2 SUBROUTINE SCAT(NO_AC)

This subroutine creates a random priority sequence of aircraft ready at the front line. This is used to select an aircraft to fly a mission.

D.3.3 SUBROUTINE GO_MSN(NO_AC,INDX)

This subroutine sends an aircraft to a sortie. The subroutine first checks for all aircraft, *NO_AC*, to isolate those in Front Line. One is then selected randomly, aircraft *INDX*, to fly the sortie. The Logic Flags of the aircraft selected are changed.

D.3.4 SUBROUTINE HR_AD(IDAY,TIM_CUR,T1,DAY,TIME)

This subroutine adds a time, *T1*, to the current day, *IDAY* and current time, *TIM_CUR*, to give the resulting day, *DAY*, and time, *TIME*.

D.3.5 SUBROUTINE

RET_MIS(IDAY,TIM_CUR,NO_AC,P_KIL,P_KIL_AC)

This subroutine returns an aircraft from a mission at the simulation day, *IDAY*, and time *TIM_CUR*, for all aircraft in the squadron, *NO_AC*. The subroutine also withdraw the return aircraft from inventory based on the survivability figures; *P_KIL,P_KIL_AC*. The subroutine then flags the aircraft to return to the front line location.

D.3.6 SUBROUTINE RET_MNT(IDAY,TIM_CUR,NO_AC)

This subroutine checks aircraft, *NO_AC*, at the current simulation day *IDAY* and time *TIM_CUR*, to return aircraft to the front line that finished in maintenance repair.

**D.3.7 SUBROUTINE GO_MNT(IDAY,TIM_CUR,TIM_COM,NO_AC,
NO_AC_SYS)**

This subroutine checks the aircraft at the current simulation day and time for arising failures. Each aircraft's system is checked according to its cumulative time.

D.4 Program Inputs and Outputs

There are two types of input data to the program. The interactive screen input data and a file containing the R&M data. The screen input data are:

NO_SOR_DAY
TIM_SOR
P_DET_AC
P_KIL_AC
P_ABORT
NO_AC
TIM_TRN
IDAY_MAX

The R&M input data file *rm_msm.in* has the following data arrangement

<i>NO_SYS_AC</i>	
<i>FR(1)</i>	<i>MTTR(1)</i>
<i>FR(2)</i>	<i>MTTR(2)</i>
.....
.....
<i>FR(NO_SYS_AC)</i>	<i>MTTR(NO_SYS_AC)</i>

The main program output is the SGR along the simulated days as shown in Fig. C.1. However the program can be used to give more analysis output data. Table C.1 shows each aircraft's performance in terms of sorties flown, hours in the air, and hours in maintenance.

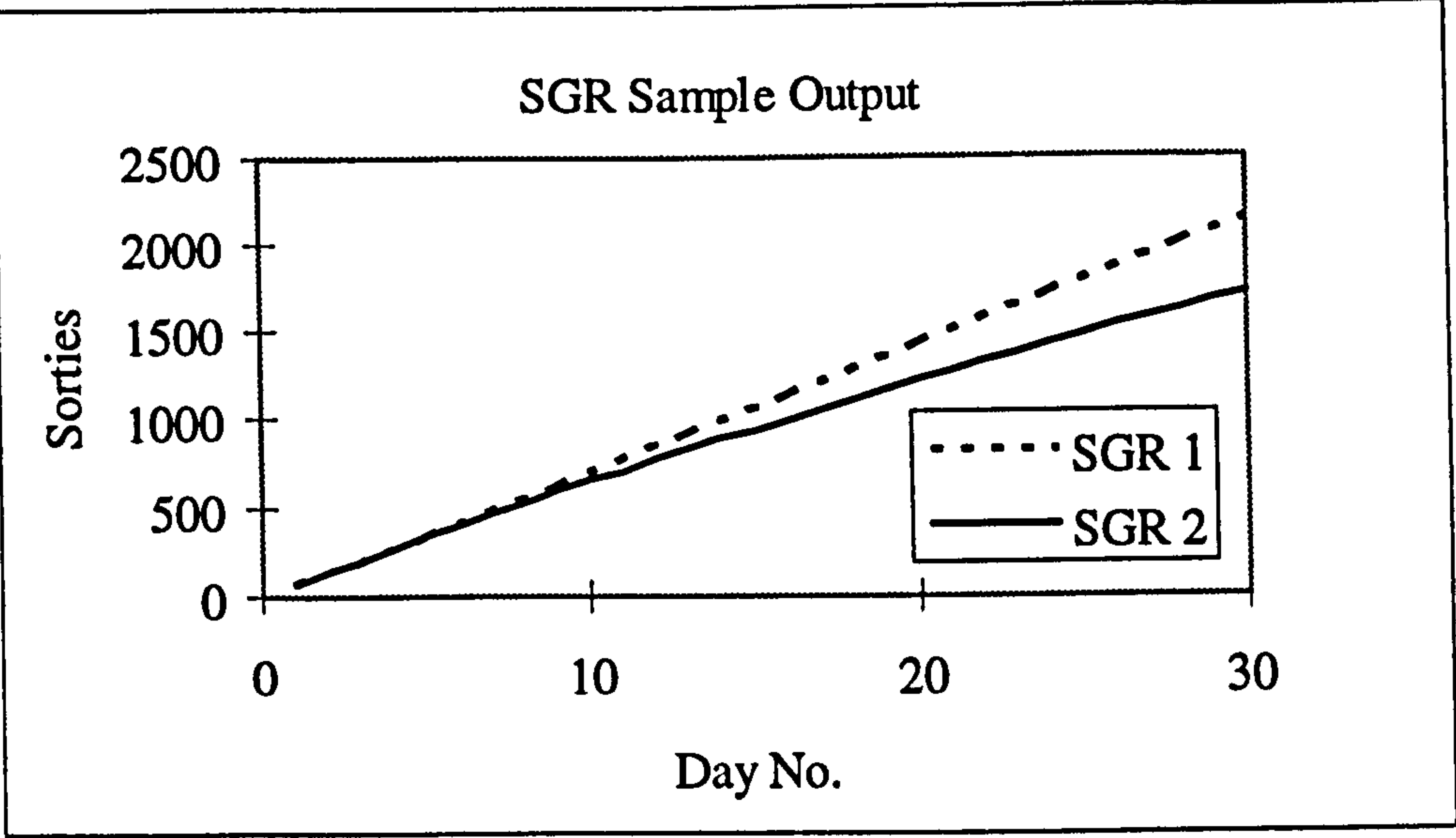


Figure D.1 Sample of MSM SGR.

A/C No.	Sorties Flown	Hours Up	Hours Down
1	30	99.00002	74.48401
2	70	231.0001	112.727
3	30	99.00002	81.998
4	6	19.8	24.673
5	66	217.8001	110.091
6	73	240.9001	137.875
7	71	234.3001	162.676
8	46	151.8001	92.188
9	13	42.89999	33.122
10	71	234.3001	132.349
11	78	257.4001	152.167
12	37	122.1	92.00099
13	72	237.6001	102.271
14	75	247.5002	141.344
15	78	257.4001	111.411
16	76	250.8002	159.973
17	70	231.0001	143.681
18	64	211.2001	121.16
19	48	158.4001	64.67101
20	73	240.9001	118.372
21	78	257.4001	148.564
22	70	231.0001	108.061
23	76	250.8002	168.559
24	64	211.2001	123.241

Table D.1

D.5 Source Code

CHARACTER*64 FILE_NAME

C

DIMENSION TIM_SOR_CAL(1000),IND_SOR(1000),AC_SOR_INDX(300)

C----- VARIABLE DECLARATION -----

INTEGER*4 TIME

INTEGER I,J,SOR_AC,ISEED

INTEGER IDAY_MAX,NO_SOR_DAY,IMIN_DAY,NO_AC_SYS,IFLG_AVL,IFLG_LOC

INTEGER IDAY_RET_MIS,IDAY_RET_MNT,IDAY,IMIN,I_SOR,NO_SOR_FLR

INTEGER IPR_SNO,ICON_FLR,NO_AC,IND_SOR,INDEX,IIDAY,SOR_COM

INTEGER IFLG_KILL,IMIN_COM,AC_SOR_INDX,ID_MF

C-----

REAL*4 TIM_SOR,RTAG,FAIL_RAT,MTTR,TIM_AC_SYS,TIM_RET_MIS,RNDM,

\$ RAND,TIM,TIM_SOR_CAL,TIM_CUR,T3,RELIB,TIM_RET_MNT,TIM_AC,

\$ TT,ALT_CRS,ALT_STR,ALT_ITR,ALT_DSH,V_CRS,V_ITR,V_DSH,

\$ TIME_CO,TIME_LO,W_PAYLOAD,RANGE_CRS,LMDA,RANDOM

REAL*4 P_KILL,TIM_TRN,TIM_SYS_FAIL,TIM_COM,P_ABORT

REAL*4 T_MN,TM_FN,TIM_MN,P_DET

C

COMMON/B1/IDAY_RET_MIS(900),IDAY_RET_MNT(900),TIM_RET_MIS(900),

\$ TIM_RET_MNT(900)

COMMON/B2/IFLG_AVL(900),IFLG_LOC(900),RELIB(300,300),

\$ IFLG_KILL(300)

COMMON/B3/TIM_AC_SYS(300,300),TIM_AC(900),TIM_MN(900)

COMMON/B4/FAIL_RAT(900),MTTR(900),ICON_FLR(300,300)

COMMON/B5/IPR_SNO(300)

COMMON/B6/TIM_SYS_FAIL(300,300)

C

WRITE(*,*) '*****'

WRITE(*,*) ' MSSIONS SIMULATION MODEL '

WRITE(*,*) '*****'

WRITE(*,*)

WRITE(*,*)

WRITE(*,*)

```

WRITE(*,*)
C  WRITE(*,*) 'INPUT FILE NAME='
C  READ(*,12) FILE_NAME
C 12  FORMAT(A)
C
OPEN(UNIT=7,FILE='rm_msm.in',STATUS='OLD')
OPEN(UNIT=10,FILE='des_msm.in',STATUS='OLD')
OPEN(UNIT=8,FILE='msm.out',STATUS='OLD')
OPEN(UNIT=9,FILE='msm1.out',STATUS='OLD')
C
W_PAYLOAD=1440./2.2

C
WRITE(*,*) 'INPUT SORTIES PER DAY'
READ(*,*) NO_SOR_DAY
C
WRITE(*,*) 'SORTIE TIME'
READ(*,*) TIM_SOR
C
WRITE(*,*) 'Pd='
READ(*,*) P_DET
C
WRITE(*,*) 'P_KILL/d='
READ(*,*) P_KILL

C
WRITE(*,*) 'P_ABORT='
READ(*,*) P_ABORT
C
WRITE(*,*) 'NO. OF AIRCRAFT'
READ(*,*) NO_AC

C
WRITE(*,*) 'turnaround time='
READ(*,*) TIM_TRN
C
WRITE(*,*) 'DAYS OF SIMULATION'

```

```

      READ(*,*) IDAY_MAX
C
      TIM_SOR=TIM_SOR+2.*TIM_TRN
C
      IMIN_DAY=24*60
      RTAG=0.45
      DO 9 I=1,NO_AC
9   AC_SOR_INDX(I)=0

C

      READ(7,*) NO_AC_SYS

      DO 7 I=1,NO_AC_SYS
      READ(7,*) FAIL_RAT(I),MTTR(I)

7   CONTINUE
C-----READ CONCEPT OUTPUT
C-----
C  INITILIZE AIRCRAFT FIRST STATUS
C-----
C   IFLG_AVL= 0 for available
C       = 1 for unavailable
C   IFLG_LOC = 0 A/C at maint.
C       = 1 A/C at front line
C       = 2 A/C in a mission
C   IFLG_KILL=0  NO
C       =1  YES
C-----
      DO 8 I=1,NO_AC
      IFLG_AVL(I)=1
      IFLG_LOC(I)=1
      IFLG_KILL(I)=0
8   CONTINUE
C-----
      DO 70 I=1,NO_AC
      DO 70 IJ=1,NO_AC_SYS
      TIM_RET_MIS(I)=0.0

```



```

      IDAY_RET_MIS(I)=0
      IDAY_RET_MNT(I)=0
      TIM_AC(I)=0.0
      TIM_MN(I)=0.0
      TIM_AC_SYS(I,IJ)=0.0
70 CONTINUE
C-----
C  GENERATE RANDOM FAIL TIMES FOR THE AIRCRAFT SYSTEMS
C-----
      DO 71 I=1,NO_AC
      DO 71 IJ=1,NO_AC_SYS
      IF(FAIL_RAT(IJ).EQ.0.) FAIL_RAT(IJ)=0.0001
      LMDA=FAIL_RAT(IJ)/1000.
C
C  ISEED=TIME()
C  CALL SRAND(ISEED)
C
77  RNDM=RAND()
      IF(RNDM.EQ.0.0) GOTO 77
      TIM_SYS_FAIL(I,IJ)=-1./LMDA*ALOG(1.-RNDM)
71 CONTINUE
C
      DO 72 I=1,NO_AC
      DO 72 IJ=1,NO_AC_SYS
72  WRITE(8,*) I,TIM_SYS_FAIL(I,IJ)
C
      IDAY=0
      SOR_COM=0
      IMIN_COM=0
C-----
C  START THE SIMULATION DAYS
C-----
15  IDAY=IDAY+1
      WRITE(*,*) 'SIMULATING DAY=',IDAY
C  WRITE(8,*) 'SIMULATING DAY=',IDAY
C

```

```

      IND_SOR(IDAY)=0
C//
      IF(IDAY.GT.IDAY_MAX) GOTO 51
      GOTO 52
51  WRITE(*,*) 'PROGRAM STOP EXCEEDS MAX DAYS'
      GOTO 99
52  CONTINUE
C-----
C   generate random call times for day sorties
C-----
C   ISEED=TIME()
C   CALL SRAND(ISEED)
C
      DO 1 I=1,NO_SOR_DAY
      RNDM=RAND()
      IMIN=INT(RNDM*IMIN_DAY)
      CALL MIN_HR(IMIN,TIM)
      TIM_SOR_CAL(I)=TIM
1   CONTINUE
C-----
C   sorting call times of day sorties
C-----
6   CONTINUE
      DO 2 I=1,NO_SOR_DAY-1
      IF(TIM_SOR_CAL(I).GT.TIM_SOR_CAL(I+1)) GOTO 3
      GOTO 2
3   TT=TIM_SOR_CAL(I)
      TIM_SOR_CAL(I)=TIM_SOR_CAL(I+1)
      TIM_SOR_CAL(I+1)=TT
      GOTO 6
2   CONTINUE
C
C   DO 501 I=1,NO_SOR_DAY
C 501  WRITE(8,*) 'SORTIE#',I,'AT TIME=',TIM_SOR_CAL(I)
C-----////
C   begin the day operation
C-----

```

```

      IMIN=0
      I_SOR=0
61  I_SOR=I_SOR+1
60  IMIN=IMIN+1
      IMIN_COM=IMIN_COM+1
C
      IF(IMIN.GT.IMIN_DAY) THEN
C                                     write the output of the day here
      WRITE(9,*) IDAY,SOR_COM
      GOTO 15
      ENDIF
C+++++
      CALL MIN_HR(IMIN,TIM_CUR)
      CALL MIN_HR(IMIN_COM,TIM_COM)
C-----
C  TIME FLAGGING PROCESS AS FOLLOWS
C  1. check time to return aircraft from a mission
C  2. check time to return aircraft from maintenance task
C  3. update aircraft/sys reliability figures
C-----
      CALL RET_MIS(IDAY,TIM_CUR,NO_AC,P_KILL,P_DET)
C+++++
      CALL GO_MNT(IDAY,TIM_CUR,TIM_COM,NO_AC,NO_AC_SYS)
C+++++
      CALL RET_MNT(IDAY,TIM_CUR,NO_AC)
C+++++
      IF(I_SOR.GT.NO_SOR_DAY) GOTO 60
      IF(TIM_CUR.LT.TIM_SOR_CAL(I_SOR)) GOTO 60
44  CONTINUE
C+++++
      CALL GO_MIS(NO_AC,INDEX)
C+++++
      IF(INDEX.EQ.0) GOTO 32

C-----
C  AIRCRAFT READY, ABBORT RATE

```



```

C-----
C  ISEED=TIME()
C  CALL SRAND(ISEED)
C
    RANDOM=RAND()
    IF(RANDOM.LE.P_ABORT) THEN
C-----
C  FAILURE FOUND , SEND AIRCRAFT TO MAINTENANCE
C-----
    IFLG_AVL(INDEX)=0
    IFLG_LOC(INDEX)=0

    T_MN=0.5
C*****
    CALL HR_AD(IDAY,TIM_CUR,T_MN,ID_MF,TM_FN)
C*****
    IDAY_RET_MNT(INDEX)=ID_MF
    TIM_RET_MNT(INDEX)=TM_FN
    GOTO 44
    ENDIF
    GOTO 33

32  CONTINUE
C
C  WRITE(8,*) 'AT DAY#  SORTIE #  FAILED, NO A/C AVAILABLE'
C  WRITE(8,*) IDAY,I_SOR
    NO_SOR_FLR=NO_SOR_FLR+1
    GOTO 61
C-----
33  CONTINUE
C----- count the sortie which has been just launched
    SOR_COM=SOR_COM+1
C
    IND_SOR(IDAY)=IND_SOR(IDAY)+1
    TIM_AC(INDEX)=TIM_AC(INDEX)+TIM_SOR
    AC_SOR_INDX(INDEX)=AC_SOR_INDX(INDEX)+1

```

```

DO 19 IJ=1,NO_AC_SYS
19 TIM_AC_SYS(INDEX,IJ)=TIM_AC_SYS(INDEX,IJ)+TIM_SOR
C-----
C compute return day and time of lauched aircraft
C-----
C*****
CALL HR_AD(IDAY,TIM_CUR,TIM_SOR,IIDAY,T3)
C+++++
IDAY_RET_MIS(INDEX)=IIDAY
TIM_RET_MIS(INDEX)=T3
C
IFLG_AVL(INDEX)=0
IFLG_LOC(INDEX)=2
C
C WRITE(8,*) 'AC SENT TO MISSION'
C WRITE(8,*) INDEX
C WRITE(8,*) 'RETURN TIME DAY'
C WRITE(8,*) TIM_RET_MIS(INDEX),IDAY_RET_MIS(INDEX)
C
GOTO 61
C
99 CONTINUE

C
WRITE(9,*) 'TOTAL PAYLOAD DELIVERED=',W_PAYLOAD*SOR_COM
C
C DO 83 I=1,NO_AC
C WRITE(8,*) 'AIRCRAFT #',I
C DO 83 IJ=1,NO_AC_SYS
C WRITE(8,*) 'NO OF FAILURES OF SYSTEM',IJ
C WRITE(8,*) ICON_FLR(I,IJ)
C 83 CONTINUE
C
WRITE(8,*) '-----'
WRITE(8,*) 'AIRCRAFT # HOURS-UP HOURS-DWN'
WRITE(8,*) '-----'
DO 85 I=1,NO_AC

```

```
85 WRITE(8,*) I,TIM_AC(I),TIM_MN(I)
```

```
C
```

```
WRITE(8,*) '-----'
```

```
WRITE(8,*) '    SORTIES FLOWN PER AIRCRAFT    '
```

```
WRITE(8,*) '-----'
```

```
WRITE(8,*) ' AIRCRAFT #          SORTIES  '
```

```
DO 86 I=1,NO_AC
```

```
86  WRITE(8,*) I,AC_SOR_INDX(I)
```

```
STOP
```

```
END
```

```
C*****
```

```
  SUBROUTINE GO_MIS(NO_AC,INDEX)
```

```
C*****
```

```
  INTEGER NO_AC,IK,I,IPR_SNO,IFLG_LOC,IFLG_AVL,INDEX,
```

```
  $ IDAY_RET_MIS,IDAY_RET_MNT,IM,IFLG_KILL
```

```
C
```

```
  REAL*4 TIM_AC_SYS,TIM_AC,RELIB,TIM_RET_MNT,TIM_RET_MIS,TIM_MN
```

```
C
```

```
  COMMON/B1/IDAY_RET_MIS(900),IDAY_RET_MNT(900),TIM_RET_MIS(900),
```

```
  $    TIM_RET_MNT(900)
```

```
  COMMON/B2/IFLG_AVL(900),IFLG_LOC(900),RELIB(300,300),
```

```
  $    IFLG_KILL(300)
```

```
  COMMON/B3/TIM_AC_SYS(300,300),TIM_AC(900),TIM_MN(900)
```

```
  COMMON/B5/IPR_SNO(300)
```

```
C*****
```

```
  CALL SCAT(NO_AC)
```

```
C*****
```

```
  DO 5 IK=1,NO_AC
```

```
  I=IPR_SNO(IK)
```

```
  IF(IFLG_LOC(I).EQ.1) GOTO 13
```

```
  GOTO 7
```

```
13  IF(IFLG_AVL(I).EQ.1) GOTO 15
```

```
  GOTO 7
```

```
15  IF(IFLG_KILL(I).EQ.0) GOTO 14
```

```
  GOTO 7
```



```

14    INDEX=I
      GOTO 12
7     INDEX=0
5     CONTINUE
12 CONTINUE
      RETURN
      END

```

```

C*****

```

```

      SUBROUTINE MIN_HR(IM,H)

```

```

C*****

```

```

      INTEGER IHR,IM

```

```

C

```

```

      REAL*4 RM,HOUR_DEC,RIHR,FRAC,H

```

```

      RM=IM

```

```

      HOUR_DEC=RM/60.

```

```

      IHR=INT(HOUR_DEC)

```

```

      RIHR=IHR

```

```

      FRAC=(HOUR_DEC-RIHR)*60.

```

```

      H=RIHR+FRAC/100.

```

```

      RETURN

```

```

      END

```

```

C*****

```

```

      SUBROUTINE HR_AD(I1,T1,T2,I2,T3)

```

```

C-----

```

```

C I1 current day

```

```

C T1 TIME1

```

```

C T2 TIME2

```

```

C I3 new day

```

```

C T3 TIME3

```

```

C-----

```

```

      INTEGER I1,I2

```

```

C

```

```

      REAL*4 RM1,RM2,RM3,HR1,HR2,HR3,T1,T2,T3

```

```

C

```

```

      RM1=(T1-(FLOAT(INT(T1))))*100.

```

```

      RM2=(T2-(FLOAT(INT(T2))))*100.

```

```

      RM3=RM1+RM2

```

```

HR1=FLOAT(INT(T1))
HR2=FLOAT(INT(T2))
HR3=HR1+HR2
IF(RM3.GT.60.) THEN
HR3=HR3+1.
RM3=RM3-60.
ENDIF
IF(HR3.GE.24.) THEN
I2=I1+1
HR3=HR3-24.
ELSE
I2=I1
ENDIF
T3=HR3+RM3/100.
RETURN
END

```

SUBROUTINE RET_MIS(IDAY,TIM_CUR,NO_AC,P_KILL,P_DET)

C*****

C-----

C return A/C from a mission by flagging IFLG_LOC to 1

C or deleting aircraft from inventory

C-----

INTEGER*4 TIME

INTEGER IDAY_RET_MIS,IDAY_RET_MNT,IFLG_AVL,IFLG_LOC,
\$ I,NO_AC,IDAY,IFLG_KILL,ISEED

C

REAL*4 TIM_RET_MIS,TIM_RET_MNT,RELIB,TIM_AC_SYS,TIM_AC,
\$ TIM_CUR,P_KILL,RANDOM,RAND,TIM_MN,P_DET

C

COMMON/B1/IDAY_RET_MIS(900),IDAY_RET_MNT(900),TIM_RET_MIS(900),
\$ TIM_RET_MNT(900)

COMMON/B2/IFLG_AVL(900),IFLG_LOC(900),RELIB(300,300),
\$ IFLG_KILL(300)

COMMON/B3/TIM_AC_SYS(300,300),TIM_AC(900),TIM_MN(900)

C

C ISEED=TIME()

C CALL SRAND(ISEED)

C

DO 5 I=1,NO_AC

IF(IFLG_LOC(I).EQ.2) GOTO 15

GOTO 5

15 IF(IDAY.GE.IDAY_RET_MIS(I)) GOTO 13

GOTO 5

13 IF(TIM_CUR.GE.TIM_RET_MIS(I)) GOTO 14

GOTO 5

14 IFLG_LOC(I)=1

IFLG_AVL(I)=1

C

P_KILL=P_KILL*P_DET

C

RANDOM=RAND()

IF(RANDOM.LE.P_KILL) THEN

IFLG_KILL(I)=1

WRITE(*,*) ' OUT OF INVENTRORY',I

ENDIF

C WRITE(8,*) 'AT TIME= ',TIM_CUR,' A/C# ',I,' RETURNED FR MS'

5 CONTINUE

RETURN

END

C*****

SUBROUTINE RET_MNT(IDAY,TIM_CUR,NO_AC)

C*****

C-----

C return A/C from maintemance by flaging LOC to 1

C-----

INTEGER IDAY_RET_MIS,IDAY_RET_MNT,IFLG_AVL,IFLG_LOC,

\$ IDAY,I,NO_AC,IFLG_KILL

C

REAL*4 TIM_RET_MIS,TIM_RET_MNT,RELIB,TIM_AC,TIM_AC_SYS,

\$ TIM_CUR,TIM_MN

C

COMMON/B1/IDAY_RET_MIS(900),IDAY_RET_MNT(900),TIM_RET_MIS(900),


```

$      TIM_RET_MNT(900)
COMMON/B2/IFLG_AVL(900),IFLG_LOC(900),RELIB(300,300),
$      IFLG_KILL(300)
COMMON/B3/TIM_AC_SYS(300,300),TIM_AC(900),TIM_MN(900)

```

C

```

DO 5 I=1,NO_AC
  IF(IFLG_LOC(I).EQ.0) GOTO 15
  GOTO 5
15  IF(IDAY.GE.IDAY_RET_MNT(I)) GOTO 12
    GOTO 5
12  IF(TIM_CUR.GE.TIM_RET_MNT(I)) GOTO 10
    GOTO 5
10  IFLG_LOC(I)=1
    IFLG_AVL(I)=1
5   CONTINUE
    RETURN
    END

```

C*****

```

SUBROUTINE GO_MNT(IDAY,TIM_CUR,TIM_COM,NO_AC,NO_AC_SYS)

```

C*****

C-----

C send A/C from maintenance by flaging LOC to 1

C-----

```

INTEGER*4 TIME
INTEGER IDAY_RET_MIS,IDAY_RET_MNT,IFLG_AVL,IFLG_LOC,
$  IDAY,I,NO_AC,ICON_FLR,ID_MF,IJ,NO_AC_SYS,INDEX
INTEGER IFLG_KILL,ISEED

```

C

```

REAL*4 TIM_RET_MIS,TIM_RET_MNT,RELIB,TIM_AC,TIM_AC_SYS,MTTR,
$  RTAG,RR,T_MN,TM_FN,TIM_CUR,FAIL_RAT,TIM_SYS_FAIL,
$  TIM_COM,LMDA,RNDM,RAND,TIM_MN

```

C

```

COMMON/B1/IDAY_RET_MIS(900),IDAY_RET_MNT(900),TIM_RET_MIS(900),
$  TIM_RET_MNT(900)
COMMON/B2/IFLG_AVL(900),IFLG_LOC(900),RELIB(300,300),
$  IFLG_KILL(300)

```

```

COMMON/B3/TIM_AC_SYS(300,300),TIM_AC(900),TIM_MN(900)
COMMON/B4/FAIL_RAT(900),MTTR(900),ICON_FLR(300,300)
COMMON/B6/TIM_SYS_FAIL(300,300)

```

C

```

DO 5 I=1,NO_AC
IF(IFLG_LOC(I).EQ.1) GOTO 6
GOTO 5

```

C

```

6  CONTINUE
DO 9 IJ=1,NO_AC_SYS
IF(TIM_AC_SYS(I,IJ).GE.TIM_SYS_FAIL(I,IJ)) GOTO 10
GOTO 9

```

```

10  CONTINUE

```

C-----

C FAILURE FOUND , SEND AIRCRAFT TO MAINTENANCE

C-----

```

IFLG_LOC(I)=0
IFLG_AVL(I)=0
ICON_FLR(I,IJ)=ICON_FLR(I,IJ)+1

```

C-----

C allocate a random main. time based on the system MTTR

C-----

C ISEED=TIME()

C CALL SRAND(ISEED)

```

20  RNDM=RAND()

```

```

IF(RNDM.EQ.0.0) GOTO 20

```

```

T_MN=MTTR(IJ)

```

```

TIM_MN(I)=TIM_MN(I)+T_MN

```

C*****

```

CALL HR_AD(IDAY,TIM_CUR,T_MN,ID_MF,TM_FN)

```

C*****

```

IDAY_RET_MNT(I)=ID_MF

```

```

TIM_RET_MNT(I)=TM_FN

```

```

TIM_AC_SYS(I,IJ)=0.0

```

C-----

C GENERATE A NEW FAILURE TIME OF THE SYSTEM

```

C-----
  LMDA=FAIL_RAT(IJ)/1000.
C  ISEED=TIME()
C  CALL SRAND(ISEED)
74  RNDM=RAND()
    IF(RNDM.EQ.0.0) GOTO 74
    TIM_SYS_FAIL(I,IJ)=TIM_SYS_FAIL(I,IJ)+(-1./LMDA*ALOG(1.-RNDM))
C  WRITE(8,*) 'AT DAY ',IDAY,' AT TIME ',TIM_CUR
C  WRITE(8,*) 'AIRCRAFT ',I,' SYSTME ',IJ,' FAILED'
C  WRITE(8,*) 'MTTR=',MTTR(IJ)
C  WRITE(8,*) 'DAY AND TIME RETURN FROM MAIN=',IDAY_RET_MNT(I),
C  $      TIM_RET_MNT(I)
C  WRITE(8,*) 'NEW FAIL TIME=',TIM_SYS_FAIL(I,IJ)
9  CONTINUE
C
5  CONTINUE
  RETURN
  END
C*****
  SUBROUTINE SCAT(NO_AC)
C*****
C-----
C  generate random priority proceeding of aircraft
C-----
  INTEGER*4 TIME
  INTEGER I,IPR_SNO,IK,IAC,NO_AC,ISEED
C
  REAL*4 RNDM,RANAC,RAND
  COMMON/B5/IPR_SNO(300)
C
  DO 5 I=1,NO_AC
5  IPR_SNO(I)=0
C
  IK=1
C
C  ISEED=TIME()
C  CALL SRAND(ISEED)

```



```
18  RNDM=RAND()
    RANAC=RNDM*FLOAT(NO_AC)
    IAC=RANAC
    IAC=IAC+1
    IPR_SNO(IK)=IAC
    DO 6 I=1,NO_AC
    IF(I.EQ.IK) GOTO 6
    IF(IPR_SNO(I).EQ.IAC) GOTO 18
6   CONTINUE
    IK=IK+1
    IF(IK.GT.NO_AC) GOTO 20
    GOTO 18
20  RETURN
    END
```